MULTIPLE RECOGNITION BY MODIFIED CYCLODEXTRINS

Carolyn Anne Haskard, B.Sc.(Hons), A.Mus.A

Thesis submitted for the degree of

Doctor of Philosophy

in

The University of Adelaide

Department of Chemistry

JANUARY 1996

CONTENTS

2. Complexation of Amino Acids by the Metallocyclodextrins of βCDpn and βCDtren

3. Cooperative Binding of 6-(*p*-Toluidinyl)naphthalene-2-sulfonate by Linked Cyclodextrin Dimers

4. Complexation of Methyl Orange and Tropaeolin 000 No. 2 by Linked Cyclodextrin Dimers

Abstract

The cavity of a cyclodextrin provides a predominantly hydrophobic recognition site for guest binding. This study focuses on β-cyclodextrins which are modified at the primary rim to incorporate an additional coordination or hydrophobic recognition site.

The modified cyclodextrins 6^A-(3-aminopropylamino)-6^A-deoxy-β-cyclodextrin (βCDpn) and 6^A-(2-(*N*,*N*-bis(2-aminoethyl)amino)ethylamino)-6^A-deoxy-β-cyclodextrin (βCDtren) bind metal ions (M^{2+} = Ni^{2+}, Cu^{2+}, Zn^{2+}), forming metallocyclodextrins which can complex the anions of histidine (His^-), phenylalanine (Phe^-) and tryptophan (Trp^-). The stability order: $[Cu(\beta CDpn)Phe]^+ < [Cu(\beta CDpn)Trp]^+ < [Cu(\beta CDpn)His]^+$, is attributed to the coordination mode of the amino acid and the size of its aromatic side chain. The greater stability of $[M(\beta CDtren)Trp]^+$, by comparison with $[M(\beta CDpn)Trp]^+$, may be attributed to steric, hydrogen bonding and dipole effects influencing cyclodextrin-Trp^- interactions, and the denticity of the coordinating group affecting cyclodextrin-M^{2+} interactions. The ionic radius and d^n electronic configuration of M^{2+} influence the stability of $[M(\beta CDtren)Trp]^+$, which follows the Irving-Williams series ($Ni^{2+} < Cu^{2+} > Zn^{2+}$). Guest interactions with each of the two recognition sites, reinforce each other in $[M(\beta CDtren)Trp]^+$, but not in $[Cu(\beta CDpn)His]^+$. Although $[M(\beta CDpn)]^{2+}$ demonstrates enantioselectivity for (*S*)-Trp^-, no enantioselectivity of $[Cu(\beta CDpn)]^{2+}$ for His^-, nor $[M(\beta CDtren)]^{2+}$ for Trp^-, is found.

The linked cyclodextrin dimers *N*,*N*'-bis-(6^A-deoxy-6^A-β-cyclodextrinyl)-R, where R = urea, oxalamide, malonamide, succinamide and glutaramide ($(\beta CD)_2X$, X = Ur, Ox, Ma, Sc and Gl, respectively), form complexes with guests, possessing two aromatic binding sites. The stabilities increase as follows: $(\beta CD)_2Ma\cdot TNS^- < (\beta CD)_2Gl\cdot TNS^- < (\beta CD)_2Sc\cdot TNS^- < (\beta CD)_2Ox\cdot TNS^- < (\beta CD)_2Ur\cdot TNS^-$, for 6-(*p*-toluidino)naphthalene-2-sulfonate (TNS^-), and $(\beta CD)_2Sc\cdot MO^- < (\beta CD)_2Ur\cdot MO^- < (\beta CD)_2Ox\cdot MO^-$, for methyl orange anion (MO^-), and $(\beta CD)_2Sc\cdot TR^- < (\beta CD)_2Ox\cdot TR^- < (\beta CD)_2Ur\cdot TR^-$, for tropaeolin 000 no. 2 anion (TR^-). The overall trend in stabilities is: $(\beta CD)_2X\cdot TR^- < (\beta CD)_2X\cdot TNS^- < (\beta CD)_2X\cdot MO^-$ (X = Ur, Ox, Sc). These variations reflect differences in

binding mode and stereochemistry. The extent of cooperative binding depends on the βCD separation in $(\beta CD)_2X$, relative to the aromatic separation in the guest. These primary-primary linked cyclodextrin dimers bind TNS^- more strongly than their secondary-secondary and primary-secondary analogous.

This work furthers understanding of the effects of multiple recognition sites on guest binding and selectivity.

Declaration

This work contains no material which has been accepted for the award of any other degree or diploma in any university or other tertiary institution and, to the best of my knowledge and belief, contains no material previously published or written by another person, except where due reference has been made in the text.

I give consent to this copy of my thesis, when deposited in the University Library, being available for loan and photocopying.

SIGNED: DATE: 22/1/96

Acknowledgements

I would like to sincerely thank my supervisor Professor S. F. Lincoln for his guidance and keen interest in this research. His invaluable advice, encouragement and willingness to help me achieve my goal, have been greatly appreciated. Thanks also to Dr. J. H. Coates for his supervision and support prior to retirement.

In addition, I wish to thank Dr. T. Kurucsev for advice on spectroscopic and data fitting aspects of this study. His depth of knowledge and enthusiasm have inspired me.

Financial support from the Australian Government is gratefully acknowledged.

I am indebted to Bruce May and Stella Kassara for the synthesis of the modified cyclodextrins used in this study. Thanks also to Bruce for his helpful suggestions.

My colleagues, especially Sue, Jo and Kym, have shared the highs and lows of research with me, and I thank them for supporting, advising and entertaining me.

I also wish to thank all other members of the Chemistry Department who, in one way or another, have assisted me in the production of this thesis.

Special thanks to my family and friends who, though they may not have fully understood what I have been doing, have prayed for me, encouraged and supported me unwaveringly throughout my studies. In particular, thanks to my parents, whose sacrifice has been appreciated and whose advice, love and understanding have kept me going in the toughest of times.

Abbreviations

en	2-aminoethylamine
pn	3-aminopropylamine
dien	diethylenetriamine
trien	triethylenetetramine
tren	*N*,*N*-bis(2-aminoethyl)amino)ethylamine or 2,2',2''-triaminotriethylamine
Me_6tren	2,2',2''-tri(*N*,*N*-dimethylamino)triethylamine
His^-	histidine anion
Phe^-	phenylalanine anion
Trp^-	tryptophan anion
TNS^-	6-(*p*-toluidino)naphthalene-2-sulfonate
BNS^-	6-(4-*tert*-butylanilino)naphthalene-2-sulfonate
ANS^-	8-(anilino)naphthalene-1-sulfonate
MO^-	*p*-[(*p*-dimethylamino)phenylazo]benzenesulfonate or methyl orange anion or orange III anion
TR^-	*p*-(2-hydroxy-1-naphthylazo)benzenesulfonate or tropaeolin 000 no. 2 anion or orange II anion
αCD	α-cyclodextrin
βCD	β-cyclodextrin
γCD	γ-cyclodextrin
βCDen	6^A-(2-aminoethylamino)-6^A-deoxy-β-cyclodextrin
βCDpn	6^A-(3-aminopropylamino)-6^A-deoxy-β-cyclodextrin
βCDdien	6^A-(2-(2-aminoethylamino)ethylamino)-6^A-deoxy-β-cyclodextrin
βCDtrien	6^A-(2-(2-(2-aminoethylamino)ethylamino)ethylamino))-6^A-deoxy-β-cyclodextrin

βCDtren	6^A-(2-(*N*,*N*-bis(2-aminoethyl)amino)ethylamino)-6^A-deoxy-β-cyclodextrin
M^{2+}	divalent metal ion
$[M(\beta CDtren)]^{2+}$	metallo-6^A-(2-(*N*,*N*-bis(2-aminoethyl)amino)-ethylamino)-6^A-deoxy-β-cyclodextrin
$(\beta CD)_2Ur$	*N*,*N*'-bis-(6^A-deoxy-6^A-β-cyclodextrinyl)-urea
$(\beta CD)_2Ox$	*N*,*N*'-bis-(6^A-deoxy-6^A-β-cyclodextrinyl)-oxalamide
$(\beta CD)_2Ma$	*N*,*N*'-bis-(6^A-deoxy-6^A-β-cyclodextrinyl)-malonamide
$(\beta CD)_2Sc$	*N*,*N*'-bis-(6^A-deoxy-6^A-β-cyclodextrinyl)-succinamide
$(\beta CD)_2Gl$	*N*,*N*'-bis-(6^A-deoxy-6^A-β-cyclodextrinyl)-glutaramide

CHAPTER 1

Introduction

1.1 General

The term "molecular recognition" is used to describe the ability of one molecule to distinguish between slight differences in other molecules. This concept is very important in many areas of science, including such diverse fields as chemistry, pharmacy, medicine, genetics, biochemistry and materials science.

A cavity containing molecule, called a "host", may admit a "guest" molecule into its cavity, without any covalent bonds being formed, to produce what is called a "host-guest" or "inclusion" complex. The host may be able to distinguish between guest shapes, and this is an example of molecular recognition. Inclusion complexes are very appropriate systems for elucidating the nature of molecular recognition, since interactions between the inclusion host and a guest can be measured. They are typical examples of self-assembling supramolecular structures, being held together and organised by intermolecular non-covalent interactions, and demonstrating novel functions only after association of the individual molecular components.[1,2] The physical and chemical properties of inclusion complexes have attracted a great deal of interest over the past 30 years.

There are many known inorganic, organic and biological hosts.[2-6] Some examples are: zeolites, clathrates, coronands, cryptands, cyclophanes, cyclodextrins, calixarenes and enzymes. Hybrid hosts, such as glycophanes which are cyclodextrin-cyclophane hybrids, may posses properties of more than one type of host.[7] Host molecules can be tailored to fit a particular guest and chemical groups can be introduced to enhance the selectivity of binding and the stability of the complexes formed. Natural and synthetic hosts are exploited in a vast number of applications which include sensor technologies, controlled release of drugs, transmission of information, catalysis, separation technologies and transport systems.[2,6]

Analogies between inclusion complex interactions and drug-receptor or enzyme-substrate interactions can be made.[8] The study of inclusion complexes furnishes information about the non-covalent intermolecular forces which are of vital importance to molecular recognition in biological systems.[9] In order to mimic the amazing efficiency of biological systems, an understanding of these intermolecular forces is required. There is a continuing state of uncertainty with respect to the physical principles that dominate molecular recognition,[10] however, non-covalent interactions such as hydrophobic, electrostatic, coordination and hydrogen bonding interactions appear to be involved.

More sophisticated molecular recognition can be achieved using more than one recognition site. The additional recognition interactions may operate simultaneously enabling delicate differences in guest shapes to be distinguished. The term "multiple recognition" is introduced for such recognition of a guest molecule by a host through multiple interactions. Multiple recognition is widely observed in biological systems, permitting the geometry of a reactive guest centre to be optimally positioned relative to catalytic groups.[11] In addition to improvements in molecular recognition (selectivity), complex stability can be enhanced considerably if the recognition sites are able to cooperate in guest binding. It is important to geometrically arrange binding sites in such a way as to enhance complex stability and achieve better molecular recognition.

In this study the natural organic host, cyclodextrin, and its chemically modified derivatives, are utilised as hosts for the inclusion of a range of guests. The modified cyclodextrin hosts consist of either two cyclodextrins linked to one another, or one cyclodextrin which is capable of metal binding to produce a coordination recognition site. This study contributes significantly to understanding the fundamental factors influencing selectivity of binding and the stability of the complexes formed when a guest is bound essentially at two recognition sites. Such information will assist in the design of new hosts with improved properties.

1.2 Properties of Natural Cyclodextrins and their Complexes

1.2.1 Cyclodextrin Structure

Cyclodextrins, also known as cyclomaltopolyoses, are naturally occurring macrocyclic oligosaccharides. They are produced through the degradation of starch by the enzyme cyclodextrin glycosyl transferase which is obtained from *Bacillus macerans* and related bacteria.[3,12-15] Cyclodextrins were first isolated by Villiers in 1891,[16] and were characterised as cyclic oligosaccharides by Schardinger in 1904.[12,13] In 1938 cyclodextrins were reported to be constructed from α(1→4)-linked glucose units by Freudenberg *et al.*,[14] however, the molecular weights of the most common cyclodextrins were not determined until much later.[17-19]

The number of glucose units per cyclodextrin ring vary from 6-13,[20] as the enzyme produces a range of oligosaccharides.[21] A five-membered cyclodextrin is unlikely due to ring strain[22] and has not been observed. The most common cyclodextrins contain 6, 7 and 8 units and are known as α-, β- and γ-cyclodextrin, respectively. The glucose residues are labelled (A-H) in a clockwise direction when facing the primary side.[23,24] This study involves only β-cyclodextrin (βCD) whose structure is shown in Fig 1.1.

X-ray studies reveal that cyclodextrins have a round and slightly conical structure with a narrow opening at the primary O(6)H hydroxyl end and a wide opening at the secondary O(2)H and O(3)H end (Fig. 1.2). Each chiral glucose residue possesses a rigid $^4C_1$ chair conformation. The C(6)—O(6) bonds are preferentially directed away from the centre of the ring (torsion angle O(5)—C(5)—C(6)—O(6) is (–)-*gauche*), however, these bonds can turn inwards (torsion angle O(5)—C(5)—C(6)—O(6) is (+)-*gauche*) after formation of hydrogen bonds between the O(6)H group and the guest molecule.[3]

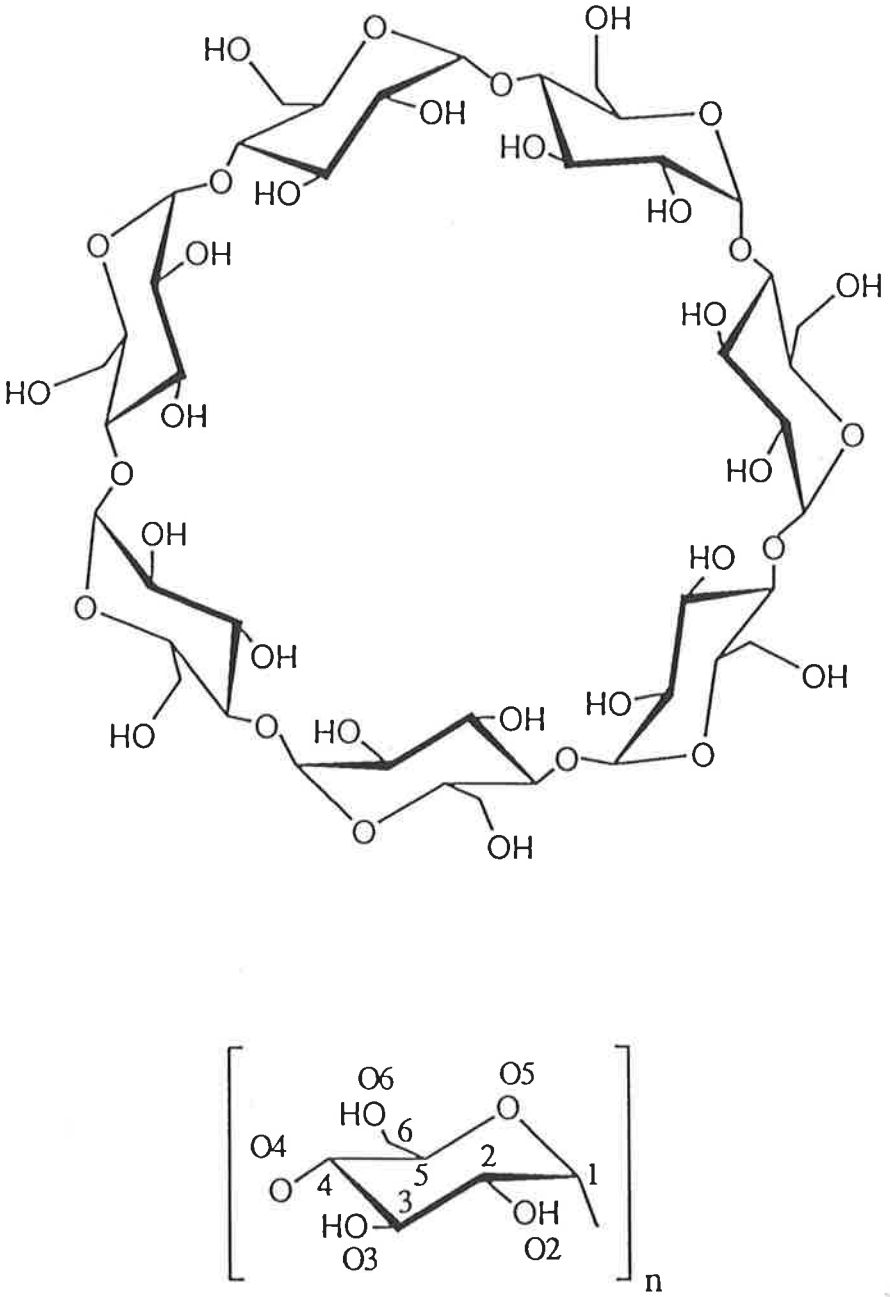

Figure 1.1 *β-cyclodextrin is a cyclic 1,4-linked oligomer of α-D-glucopyranose, where the atoms within the glucose units are numbered as shown.*

Crystallographic studies of cyclodextrins and their inclusion complexes reveal that in the absence of other guest molecules all cyclodextrins include water molecules in their cavities.[25] Expulsion of these water molecules from the "empty" cyclodextrin cavity is one of the important factors in the formation of inclusion complexes (Section 1.2.4). X-ray crystallographic studies show that uncomplexed-hydrated βCD can include twelve largely disordered water molecules, but the average number of water molecules in the cavity is 6.5.[26] If cyclodextrins are crystallised from pure water, they form different hydrates depending on conditions.

There is evidence for polymorphism in empty αCD; an almost ideal round shape cavity structure and a more strained structure, where one glucose unit tilts to form a hydrogen bond with water in the cavity, have been reported.[27] This may suggest conformational variation of cyclodextrins in aqueous solution. Empty βCD and γCD have an almost ideal round shape. The dimensions and properties characterising empty cyclodextrins are listed in Table 1.1.

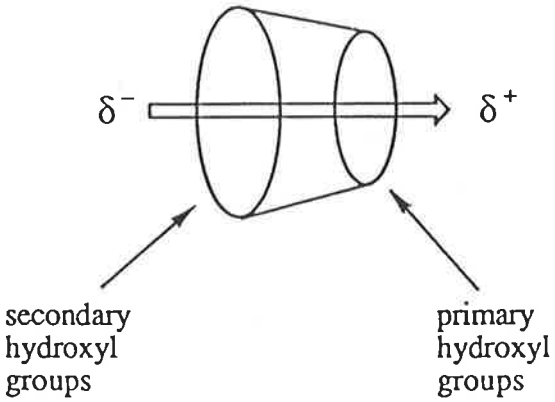

Figure 1.2 *The cyclodextrin annulus is often schematically represented as a truncated cone with the narrow and wide ends representing the circles delineated by primary and secondary hydroxyl groups, respectively. Also shown is the direction of the dipole moment.*

Table 1.1 *Dimensions[a] and properties characterising cyclodextrins.*[3,4,27,28]

Physical Property	αCD	βCD	γCD
Number of Glucose Units	6	7	8
Internal Diameter at Primary Rim (Å)[b]	5.6	6.8	8.0
Internal Diameter at Secondary Rim (Å)[c]	8.8	10.8	12.0
Height of Cavity (Å)	7.8	7.8	7.8
Molecular Weight	973	1135	1297
Solubility in H_2O (g/100 cm^3)[d]	14.5	1.85	23.2

[a] Measured with the aid of CPK models. [b] Measured between C(6) positions. [c] Measured between O(2) positions. [d] At 298.2 K.

While the cyclodextrin cavity is relatively hydrophobic, being lined with O(4) glucosidic linkages and H(3) and H(5) protons, the hydroxyl groups around the rims result in water solubility. Neutron diffraction data reveal the presence of numerous hydrogen bonds in cyclodextrins and their inclusion complexes.[4,29,30] Intramolecular hydrogen bonds, O(3)—H···O(2) and O(3)···H—O(2), exists between the secondary hydroxyl groups of adjacent glucose units, stabilising the circular structure of the cyclodextrin.[3,29] The secondary hydroxyl groups have an unexpectedly low pK_a of *ca.* 12.2,[20,31] probably due to stabilisation of the negative charge by inductive effects and intramolecular hydrogen bonding.[3]

Molecular orbital calculations, based on crystallographic data, reveal that cyclodextrins possess a dipole moment with the positive and negative poles at the centres of the narrow and wide ends of the cyclodextrin annulus, respectively (Fig. 1.2).[32,33] For αCD the magnitude of this dipole moment is 10-20 D (1 D = 3.33564 x 10^{-30} C m).[33] As each glucopyranose unit possesses a dipole moment, and all glucopyranose units are in the same conformation, the individual dipole moments add together to give an overall value, and hence a larger dipole moment is expected for βCD and γCD.

1.2.2 Inclusion Complexes

Freudenberg *et al.* recognised that cyclodextrins could form inclusion complexes[19] and like French *et al.*[14,15] worked out procedures for synthesising pure cyclodextrins. The formation of cyclodextrin inclusion complexes was studied systematically by Cramer *et al.*[34-36]

Cyclodextrins form inclusion complexes with a variety of neutral or ionic molecules which fit, at least partially, into their cavities.[4,20] Inorganic anions,[37-39] various cations,[40] halides,[38] noble gases,[41] alkyl chains,[42] aliphatic molecules,[43] and buckminsterfullerene[44] are all known to form inclusion complexes, but the strongest complexes are usually formed with guests possessing some aromatic character. The complexation of small molecules, such as Cl^-, NO_3^- and ClO_4^-, occurs much quicker than that of larger aromatic molecules, such as azo dyes, as there is no steric hindrance.[3] No obvious correlation has been found between inclusion complex stability and the functional groups of the guest,[3] however, hydrophobic (apolar) guests are generally bound more strongly than hydrophilic (polar) guests.[20,45] Highly hydrophilic molecules complex very weakly or not at all.[20]

Geometric rather than chemical factors are decisive in determining the kind of guest molecules which can penetrate into the cavity.[20] Snugness of fit, which is dependent on the size, shape and rigidity of the guest, is recognised as a major factor in determining the stability of the inclusion complex formed.[43,46] There is, nevertheless, evidence for guest motion within inclusion complexes, although this motion is slow by comparison with that of the free guest.[47,48] It is assumed that only guest rotation about the axis which passes through the centre of the cyclodextrin annulus, remains in the complex.[25,48] In cases where there is a tight fit and close interaction of a guest with the cavity walls, an almost complete "freezing" of the degrees of freedom may result. The complexation of 8-(anilino)naphthalene-1-sulfonate (ANS^-) and 6-(*p*-toluidino)naphthalene-2-sulfonate (TNS^-) by αCD, βCD, and γCD, shows that binding is more effective if there is enough room for high mobility of hydrophobic guest moieties within the cavity.[47] Included

molecules are orientationally disordered to some extent, as evidenced by NMR spectroscopy.[49] Cyclodextrins may also form distinct inclusion complexes with each functional group present within a guest, as exemplified by an electron nuclear double resonance spectroscopic study of the βCD inclusion complexes of a nitroxide spin adduct probe.[50]

Guests are usually considered to be enclosed within the cavity, thus forming an inclusion complex, rather than being merely aggregated to the outside of the cyclodextrin molecule. X-ray crystal structures provide support for formation of a true complex in the solid state, and NMR studies reveal that aromatic guests interact with the H(3) and H(5) atoms inside the cyclodextrins to form a complex which has a similar structure in aqueous solution to that found in the crystalline state.[3] Inclusion complex formation between chiral host cyclodextrins and achiral guest molecules in dilute solution is consistent with the development of extrinsic ellipticity in the absorption bands of the guest.[51] A few examples of complexes where the guest is outside the cavity have been reported.[52,53] The lower stability of these complexes may arise because intermolecular interactions cannot function efficiently between the host and the guest.[52]

Complexes with (host)·(guest) stoichiometry are usually formed, but depending on the size of the guest relative to the size of the cyclodextrin cavity various other stoichiometries, such as (host)·$(guest)_2$,[8,54] $(host)_2$·(guest),[9,42,55-57] and $(host)_2$·$(guest)_2$,[8] may been found. Cyclodextrins can also be threaded like beads onto a linear polymer without forming any covalent bonds with it.[3,58] By attaching two bulky substituents to the ends of the chain, preventing unthreading, a polymeric inclusion complex, known as a polyrotaxane, is created.[58] Rotaxanes are a special type of inclusion complex, where a cyclodextrin is threaded by a linear chain bearing bulky end units, which prevent the complex from dissociating into its cyclic and linear molecular components.[59]

In general the binding of guests by cyclodextrins is largely driven by enthalpy, with a positive or negative entropy contribution.[54,60] The linear relationship between enthalpy and entropy changes in the formation of various cyclodextrin complexes of related guests is known as an enthalpy-entropy compensation effect.[60,61] The slope and intercept of the

$T\Delta S$ versus ΔH plot are characteristic of the guest topology and the complex stoichiometry, and can be used as quantitative measures of the conformational change and the extent of desolvation caused upon complex formation, respectively.[54] The free energy change may be minimised by either increased solvation, which lowers enthalpy at the price of entropy, or diminished solvation, with its entropy advantages arising from the release of solvating water molecules.[60] A positive entropy change is produced when the entropic gain from desolvation of the guest outweighs the entropic loss from molecular association.

Most βCD complexes of organic guests have stabilities in the range 10^2 to 10^4 dm^3 mol^{-1}, characteristic of weak intermolecular interactions.[3,24,45,62,63] Due to the size compatibility of the βCD cavity with a wide variety of guest molecules and for economic reasons, βCD is the cyclodextrin most frequently employed in pharmaceutical and analytical applications, in spite of being the least soluble in water.[64]

1.2.3 Complex Characterisation

As a result of inclusion complex formation, the characteristic properties of the guest, such as solubility, chemical reactivity,[65] pK_a values, diffusion,[66,67] electrochemical properties and spectral properties, are changed.[20] In general, any property of the guest which undergoes a sufficiently large change on complexation may be monitored to obtain information on the inclusion process. Cyclodextrin complexes can be studied by spectroscopic or calorimetric methods. If a guest absorbs light in the visible or ultraviolet range or if it fluoresces, then formation of an inclusion complex can be followed by addition of cyclodextrin. Competitive spectrofluorometry can be used for guests which do not absorb or fluoresce strongly in the region of the probe fluorescence.[68] This method may also be used for studying the complexation of guests which bind either extremely weakly[46] or strongly,[69] as the guest and the probe can be made competitive for the cyclodextrin cavity by changing their concentrations, thus allowing a more accurate determination of stability constants. As cyclodextrins themselves are optically active molecules circular dichroism may be used to study their complexes, and even achiral guests

exhibit a circular dichroic spectrum when included within a chiral cyclodextrin cavity.[23,63] X-ray structure analysis reflects the atomic details of the static complex in the solid state, however, NMR spectroscopy allows its dynamic properties in solution to be studied. From NMR spectra, quantitative statements about the thermodynamic and kinetic parameters of complex formation can be made, and atomic interactions between the guest and host can be identified, permitting geometrical relationships to be established.[3] Inclusion of a guest molecule can also be followed by monitoring apparent changes in its acidity using potentiometric titrations. Conductometric methods may be used to study the inclusion of ionic guests.[68,70,71] Such methods do not require the high cyclodextrin concentrations of spectral methods to produce a significant change.

1.2.4 Driving Force for Inclusion by Cyclodextrins

The inclusion complex formation process in aqueous solution can be divided up into a number of steps:

(i) Approach of the cyclodextrin and guest

(ii) Elimination of water molecules from the cyclodextrin cavity and those surrounding the portion of the guest to be included

(iii) Assimilation of these water molecules by the surrounding water

(iv) Interaction of the cyclodextrin and guest

(v) Reconstitution of the hydrated structure around the finished complex

A variety of interactions have been proposed to play important roles in the complexation process, and they may be summarised as follows:[27]

(i) Hydrophobic interactions, which comprise the following elemental interactions:

  (a) London dispersion forces[45] which require close contact between the cyclodextrin and guest

  (b) Entropy gain due to destruction of the water assembly surrounding the guest molecule

(c) Entropy loss due to restricted motional freedom of the guest in the cyclodextrin cavity

(ii) Expulsion of "high-energy" waters from the cavity of the empty cyclodextrin upon inclusion of the guest, which is dependent on the size of the cyclodextrin cavity and is independent of the guest molecule

(iii) Conformational change in the cyclodextrin upon guest inclusion

(iv) Hydrogen bonding interactions between the cyclodextrin and guest

(v) Polar[45] and ionic[72,73] interactions, including dipole-dipole, dipole-induced dipole and charge-charge interactions

The importance of each of these will now be discussed in more detail.

The hydrophobic interaction, most simply expressed, is the tendency of a hydrocarbon-like molecule to reduce the formation of water assemblies around its exposed surface by making contact with the surface of another hydrocarbon-like molecule.[25] The theory of hydrophobic interaction is based on the large entropy loss and small enthalpy gain observed for a hydrophobic molecule to dissolve in water. In order to recover this entropy loss, molecules having large hydrophobic surfaces tend to associate by themselves in order to minimise surface exposure to water, probably with maximum van der Waals contacts. The entropy loss due to restricted motional freedom of the guest molecule is to a large extent compensated for by the entropy gain of other origin, especially from loss of the water assembly around the guest molecule.

The dependence of complex stability on guest polarisability indicates the general importance of London dispersion forces.[3] Hydrophobic interactions are suggested to be the most important recognition element in binding[45] as apolar guests (aromatic guests in particular) are bound more strongly to cyclodextrin than polar guests. Flexibly and rigidly capped cyclodextrins show a remarkably enhanced binding of hydrophobic guest molecules.[27] The effectiveness of hydrophobic interactions and the significant role of the water structure are also demonstrated by the decrease in inclusion complex formation observed in ethylene glycol,[23,63] ethanol,[74,75] dimethylsufoxide,[76,77] and in the presence

of antihydrophobic agents such as urea and guanidinium chloride.[75] Such antihydrophobic agents may be used to estimate the amount of hydrophobic surface involved in binding.[75]

As inclusion is largely independent of the chemical properties of the guest molecule, it has also been suggested that forces inherent in the cyclodextrin contribute to association.[3] The hydrophobic interior of the cyclodextrin may exert such a force as it prevents the water molecules enclosed within the empty cyclodextrin cavity from exerting their full (tetrahedral) hydrogen bond potential.[25] These water molecules are referred to as "activated" or "high-energy" water by comparison with those in the liquid phase. On expulsion from the cavity, they are taken up by the bulk water, gaining degrees of freedom and favouring complex formation by the resultant gain in entropy and potential energy.[3]

Complex formation may be affected by conformational changes in the cyclodextrin.[27] Despite the apparently rigid skeleton of cyclodextrin, the inclusion of a guest generates conformational changes which may involve the reorganisation of the original hydrogen bond network.[54,78] Rotation of the O(6)H groups about the C(5)-C(6) bonds may be considered as a conformational change.[3] Conformational changes of the glucosidic linkages upon inclusion has also been detected by ^{13}C NMR.[79] X-ray analyses have shown that cyclodextrins take a more symmetrical conformation upon inclusion of a guest than in their hydrated state,[27] although this difference is small, especially for βCD.[25,45] A more substantial conformational change, from circular to ellipsoid shape, has been suggested for the formation of a $\beta CD{\cdot}Cu_2(OH)_2^{2-}$ complex in alkaline solution, where the cyclodextrin ring is cross-linked by a $Cu^{2+}(OH^-)_2Cu^{2+}$ or a $Cu^{2+}(OH^-)(O^{2-})Cu^{2+}$ bridge.[80] The X-ray crystal structures of some inclusion complexes formed by heptakis(2,3,6-tri-*O*-methyl)-βCD have shown elliptical distortion.[81]

The formation of hydrogen bonds between a guest and (preferentially) the O(6)H groups of a cyclodextrin has been demonstrated crystallographically.[3] However, hydrogen bonding interactions do not appear to be of major importance in inclusion complex formation, as guests which are incapable of hydrogen bonding are included relatively strongly.[20,27]

Polar and ionic interactions seem to be important in the inclusion of polar and charged guests by cyclodextrins. The dipole moment of the cyclodextrin may influence the orientation of the included guest. Polar interactions in water are greatest between oppositely charged host-guest pairs.[45] Interestingly, complexation of neutral protonated and anionic deprotonated guests by cationic amino cyclodextrins, may show preferential inclusion of either the neutral[82] or anionic guest,[83] due to the effects of both charge solvation and electrostatic interactions operating.

It appears that the overall driving force which brings a guest molecule into the cavity of a cyclodextrin and drives water molecules out, is a complex composite of a number of forces.[10,25] Although the presence of these forces is generally agreed upon, much debate has surrounded the relative importance of each with respect to the others.

As mentioned in Section 1.2.2, the enthalpy change is always negative whereas the entropy change can be either positive or negative. This indicates that, depending on the guest molecule, several forces are involved in complex formation.[3,10] A comprehensive semiempirical evaluation of the inclusion process thermodynamics has been made,[84] and comparisons between the calculated magnitudes of specific interactions also indicate that there are a number of particularly important interactions.[45] Experiments and theoretical considerations have concluded that the hydrophobic interaction is the major driving force for inclusion. However, other interactions, such as polar, ionic and hydrogen bonding interactions, may also be operative. The extent to which these additional factors contribute is dependent on the nature of the host and guest concerned. When a metal ion is involved, coordination interaction is also possible. The structure of the cyclodextrins is, however, decisive, as inclusion complexes are only formed if there is a good spatial fit between the host and guest components.

1.2.5 Enantioselectivity

Natural and modified cyclodextrins exist only as the (*D*)-enantiomer and thus are chiral hosts. They form two diastereomeric complexes with racemic guest species, often showing selectivity for one enantiomer over the other. The (*R*)- and (*S*)- forms of the guest experience different geometric interactions with the cyclodextrin, which may generate differing stabilities in the two diastereomeric inclusion complexes, and lead to the preferential complexation of one enantiomer. The degree of enantioselectivity varies substantially with the nature of the cyclodextrin and guest. Enantioselectivity may be in favour of either enantiomer, as shown in Section 1.3.3 for some metallocyclodextrin complexes.

It is generally assumed that, for enantioselectivity to occur in solution, the molecular dimensions and shape of the chiral selector have to fit those of the selectand, in such a way that at least three discriminating interactions (either attractive of repulsive) occur.[10] There are a number of requirements for enantioselection by cyclodextrins. Generally an inclusion complex must be formed in which there is a relatively tight fit between the cyclodextrin and guest. The chiral centre, or one substituent of the chiral centre, must be near a rim of the cyclodextrin cavity and must interact with it. The O(2)H and O(3)H groups are thought to be particularly important in chiral recognition.[85] The presence of at least one aromatic ring in the guest structure appears to be of benefit for chiral interaction with cyclodextrins, and the proximity of the ring to the chiral centre of the guest molecule appears to improve chiral resolution, perhaps as a result of less bond rotation than could occur with aliphatic side groups.[85]

Hydrogen bonding interaction between the carboxylate ions of optically active bilirubin and the secondary hydroxy groups of βCD has been shown to be essential for enantioselective complexation, which in this case occurs outside the cyclodextrin cavity.[49] It has been suggested that the enantioselective complexation of tryptophan by metallocyclodextrins requires the indole moiety of the more strongly bound enantiomer to

be inside the cyclodextrin cavity while that of the other enantiomer is excluded from it, as discussed in Section 1.3.3.[86,87] Other types of interactions, such as ionic interactions, may be involved in enantioselection. For example, cyclodextrins bearing a positive and a negative charge on the C(6) carbons of adjacent A and B (or B and A) glucose rings, have been used for the enantioselective recognition of tryptophan, based on triple recognition (two sites for ionic interactions and the hydrophobic cavity).[88]

The replacement of a hydroxyl group by a substituent increases the asymmetry of the cyclodextrin annulus and accordingly the modified cyclodextrin is more likely to show enantioselectivity. Indeed, substituents on a cyclodextrin are known to affect the extent of complexation and enantioselectivity.[89] For example, by comparison with βCD, 6^A-amino-6^A-deoxy-βCD shows greater enantioselectivity in its complexation of sodium 2-phenylpropanoate, favouring the (*R*)- enantiomer, although the complexes with βCD are more stable.[82]

For many drugs, only racemic mixtures are available for clinical use. Numerous examples exist where the undesired effects of one stereoisomer limit the overall effectiveness of the active species because of host toxicities, biodistribution problems, altered metabolism, and unwanted drug interactions.[85] The chiral interactions of cyclodextrins provide a means to measure optical purity and to isolate or produce pure enantiomers of drugs. Since different stereoisomers of drugs often cause different physiological responses, the use of pure isomers could elicit more exact therapeutic effects.[85]

1.2.6 Applications of Natural and Modified Cyclodextrins

The importance of natural and modified cyclodextrins (Section 1.3) in many applications arise from their intrinsic properties. Upon inclusion by a cyclodextrin, the physical and chemical properties of the guest may change significantly. As early as the 1950 s, Cramer discovered that cyclodextrins have a catalytic action in some reactions,[90] and described racemate resolution with cyclodextrins.[91] Since then cyclodextrins have

found many applications in the chemical, pharmaceutical, cosmetics, toiletry, tobacco, food, and agricultural industries, which utilise such changes to their advantage.[20,92,93] Natural and modified cyclodextrins have been used in many diverse applications, some of which are mentioned in the literature.[3,5,28,93,94]

Cyclodextrins can be used to trap certain molecules or for transforming gases or liquids into the solid form, where they are much more easily handled and stored. They can be used to improve guest stability, as encapsulated sensitive, active and aromatic substances are protected from the effects of light and atmosphere. Substances which are not very soluble in water become more soluble upon inclusion by cyclodextrins. Creams and emulsions can also be stabilised by the presence of cyclodextrins. Cyclodextrins can modify the chemical activity of the guest. Undesirable side effects of the guest can be reduced, absorption of the guest molecule through biological membranes can be increased, and the release of the encapsulated guest molecule can be prolonged.

In the food, cosmetics, toiletry, and tobacco industries, cyclodextrins have been widely used either for stabilisation of flavours and fragrances or for the suppression of unpleasant tastes, and elimination of microbiological contaminations, and other undesired components.[20] Cyclodextrins have been utilised in the agricultural industry to increase the growth and yield of grain harvests.

In the laboratory[20] cyclodextrins have found use in electrochemical analysis,[95] spectrometric methods,[96,97] chromatographic separations,[98] stereoselective synthesis[1,8,72,89,99] and catalysis. Recently cyclodextrins have been used in capillary electrophoresis for chiral separations.[100] Cyclodextrins are able to separate compounds with very similar properties, such as molecules with similar molecular weights, structural isomers, geometric isomers, diastereomers and enantiomers,[101] and are used in all types of chromatography to carry out difficult separations.[20] Cyclodextrins are known to catalyse various reaction types, including hydrolysis,[11,102-105] hydration,[106,107] decarboxylation,[108,109] carboxylation,[110] allylation[25] and oxidation.[111,112] They are also useful as novel reaction media.[113] Their ability to accommodate a wide variety of guest compounds has permitted them to be used as potential molecular vessels and containers.[92]

As biological systems are often too complex for direct study, details of their multiple recognition may be elucidated using appropriate simplified model systems, called "biomimetic models", which emphasise certain features of biological systems. Biological systems possess many dersirable characteristics, such as including extraordinarily high stability and rate of catalysis, remarkably sharp substrate selectivities, activity under neutral aqueous conditions and turnover behaviour. The importance of metal ions in biological systems is well known,[114,115] and the first modified cyclodextrin described as an artificial enzyme, in 1970,[102] incorporated a metal ion. Virtually all enzyme mimics studied to date succeed in mimicking only one or two of the desirable properties at a time.[116] An understanding of biological systems may also enable the construction of novel chemical catalysts amongst other applications.[27,117]

Cyclodextrins have been used to model important biological phenomena in which hydrophobic recognition plays a significant role, these include guest binding,[118] enzymatic catalysis,[11,25] and membrane transport.[93] Cyclodextrins have been used to mimic enzymes such as carbonic anhydrase,[107,109] glyoxalase,[119] ribonuclease,[23,24] cytochrome P-450,[120] flavoenzyme,[112] B_6 enzyme,[89] isozyme,[89] and also co-enzymes such as NAD.[121] Artificial analogues of heme-containing proteins have also been prepared by encapsulating porphyrins between the secondary faces of two heptakis(2,6-di-*O*-methyl)-βCDs.[122] Cyclodextrins have been used to model the dimerisation of proteins involved in the DNA transcription process, which is known to occur through non-covalent interactions.[123]

As mentioned in Section 1.2.2, βCD complexes of well-fitting organic guests may have stabilities as high as 10^4 dm^3 mol^{-1}, but this binding strength is not very strong compared with that often displayed by enzymes (10^6 dm^3 mol^{-1} or more) or good antibodies (10^9 dm^3 mol^{-1} or more).[23,24] By suitable molecular design, the enormously large stability constants often encountered in biological recognition by a native receptor, have been achieved (Section 1.3.4).[23,124] In a similar way, rates of catalysis which are comparable to those of biological systems, have also been obtained.[11,27,108]

In order to construct more efficient modified cyclodextrins, a better understanding of the factors influencing the binding, selectivity and catalytic activity of cyclodextrins

incorporating multiple recognition sites is required. Hence the importance of this work, which investigates the binding and selectivity of such cyclodextrins.

1.3 Modified Cyclodextrins

1.3.1 General

Modified cyclodextrins have been prepared for a number of reasons. Firstly, the binding properties of cyclodextrins may be improved by appropriate functionalisation, to improve their affinity for a particular guest. Secondly, although unsubstituted cyclodextrins are well known to catalyse some organic reactions such as ester hydrolysis, their catalytic activities are relatively small.[27] It is possible to enhance the catalytic activity remarkably by the use of appropriately designed modified cyclodextrins. The reactivity of the catalytically active hydroxyl groups of cyclodextrin is low at neutral pH, and the cavity is open to solvent at both ends, so that most cyclodextrin-guest inclusion complexes do not have the well-defined geometry required for great rate acceleration.[111] Thirdly, with suitable functionalisation cyclodextrins provide a promising approach to mimicking biomolecules. In each case the cyclodextrin properties are enhanced by the introduction of additional recognition sites for the guest.

Cyclodextrins can be modified in a number of ways,[92,93,125] the most common being substitution of hydroxyl groups. The hydroxyl groups of cyclodextrin provide opportunities for substitution on either the primary or secondary rim,[116,126,127] or both. In general a less rigid attachment is made on the primary rim, due to the free rotation of the C-CH_2 groups. The stereochemistry is more obviously expressed on the secondary rim, since attachment is directly to an asymmetric carbon atom. Functionalisation of the cyclodextrin annulus may result in modified complexation and solubility characteristics.[28,128] Stability constants may increase with an increase in rigidity[102] or flexibility[45] of the host, depending on the system involved.

As mentioned in Section 1.1, multiple recognition sites may enhance selectivity and stability. The number of non-covalent recognition interactions operating may be increased by the introduction of functional groups onto the cyclodextrin annulus (Fig. 1.3). Selectivity and stability are not only affected by the functional groups chosen, but also on their geometrical arrangement.

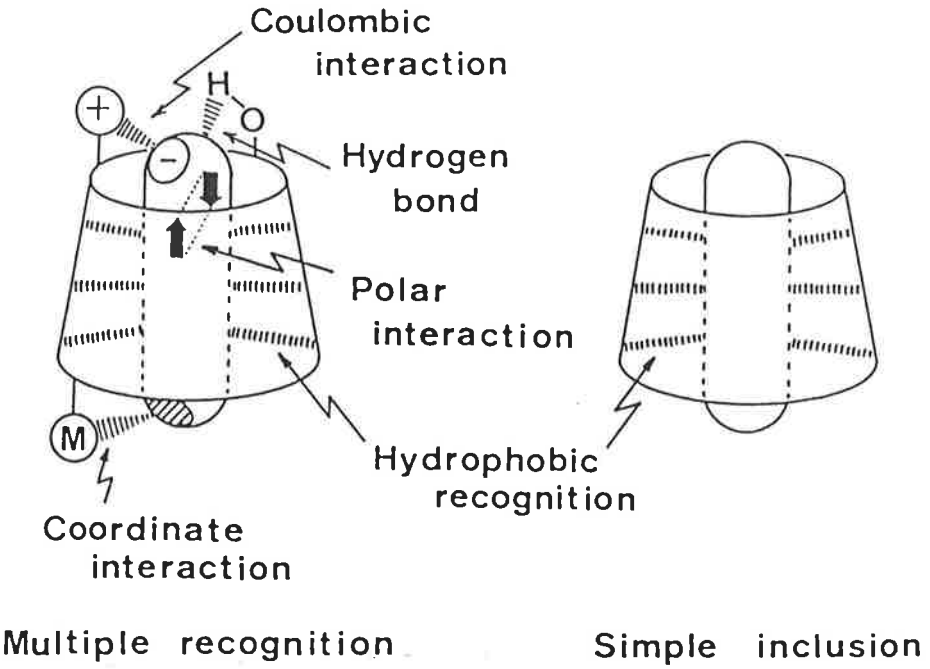

Figure 1.3 *Recognition interactions operating in cyclodextrin inclusion complexes may include hydrophobic, polar, hydrogen bonding, ionic and coordinate interactions.*[27]

In this thesis two types of modified βCDs are considered and the effects of the additional recognition sites on selectivity and stability are discussed. Modified cyclodextrins of the types concerned in this work are introduced in Sections 1.3.3 and 1.3.4, after mentioning some simpler derivatives in Section 1.3.2.

1.3.2 Modified Cyclodextrin Monomers

The X-ray analysis of βCD substituted with a *t*-butyl-thio moiety at the C(6) position was reported as the first example of mono-substituted cyclodextrin.[129] Interestingly, the *t*-butyl moiety of one substituted cyclodextrin was included as the guest in the cyclodextrin moiety of another substituted cyclodextrin. This strongly suggests that the capacity for inclusion is much the same for substituted cyclodextrins as for natural cyclodextrins.

Many modified cyclodextrins have been synthesised which contain functional groups such as amines, esters, ethers, *etc.* in place of their primary or secondary hydroxyl groups. While a single catalytic group mounted on a cyclodextrin generally affords reasonable acceleration and guest selectivity, with the introduction of more functional groups recognition should be much more precise and strict, just like enzyme recognition. Each glucose unit may potentially become tri- substituted, providing many possible derivatives even from a simple functionalisation. In the case of βCD, up to 21 groups may be incorporated. By grafting multiple amphiphilic side chains onto a modified βCD a channel-type molecule, which appears to be suitable for incorporation into lipid bilayer membranes, may be produced.[130]

Particular groups may be introduced onto the cyclodextrin in order to enhance a specific type of interaction. For example, hydrophobic recognition may be enhanced by capping (also known as bridging) one side of the cyclodextrin annulus with an apolar moiety, thus increasing the hydrophobic surface area of the cavity. Interestingly, the complex stability for a round guest molecule like adamantane-1-carboxylate is enhanced 80-fold with a flexibly capped cyclodextrin, whereas, for a flat guest it decreases considerably.[25] However, for rigidly capped cyclodextrins the stabilities of the complexes formed with most hydrophobic guests increase remarkably.[25] Cyclodextrins, such as diphenylmethane-*p*,*p*'-disulfonate capped cyclodextrin, are also very useful in the preparation of difunctionalised cyclodextrins.[27] An increase in the effective cyclodextrin

cavity size may be achieved through preparation of per-methylated or other alkylated cyclodextrins.[46] Di- and tri-*O*-octylated cyclodextrins have also been prepared,[40,131] and these modified cyclodextrins appear suitable for electrochemical sensing of chiral molecules incorporating aryl rings.[95] Electrostatic interaction with an ionic guest can be enhanced by the introduction of oppositely charged groups on the cyclodextrin annulus.[73,82,83] A βCD with seven cationic methyl ammonium groups attached to its primary rim forms a complex with ATP^{4-} characterised by a stability constant of more than 10^6 dm^3 mol^{-1}.[73]

Larger molecules have also been attached to the cyclodextrin rim. Cyclodextrins appended with at least one chromophore or fluorophore, may be useful chemosensors for molecular recognition, allowing detection of various organic compounds by the spectral changes of these modified cyclodextrins.[43,77,96,132-135] In most of these sensoring systems the probe experiences a location change upon inclusion of the guest.[132] Initially the probe is included within the attached cyclodextrin cavity (or the cavity of another cyclodextrin), but upon guest complexation it is displaced from the cavity, resulting in a marked change in the spectrum of the probe-modified cyclodextrin. Conformational changes in these hosts upon guest inclusion may also produce marked spectral changes.[134] Indeed, such probe cyclodextrins exhibit other useful characteristics such as thermochromism[136] and pH sensitivity.[135] Cyclodextrins bearing seven or fourteen naphthyl chromophores are good models for studying energy hopping among chromophores in well-defined positions, as in photosynthetic antennae.[137,138] Photochemical communication between the photoactive unit attached to the cyclodextrin and a guest molecule encapsulated in its cavity may also occur.[138-141]

Molecules, which are in themselves hosts, such as coronands,[140,142] cages,[143] cyclodextrins (see Section 1.3.4), porphyrins,[141,144,145] cyclen,[104] or other coordinating systems have been attached to cyclodextrins. Cooperativity between the two recognition sites of a diaza-coronand capped βCD, tetraoxadiazacyclo-octadecanyl-βCD, results in up to 70-fold enhancement in the binding of alkali metal *p*-nitrophenolates by comparison with βCD, and even more in comparison to diaza-coronand.[142] The coronand moiety acts

as a cation receptor site, while the hydrophobic cavity of the cyclodextrin includes the aromatic portion of the phenolate anion in close proximity, allowing electrostatic interactions.[142] In another example, the conformation of a polypeptide attached to a cyclodextrin seems to determine guest binding capabilities, for instance ANS^- is bound at low pH, but at high pH the βCD is concealed in the random coil of the polypeptide.[146] Coupling of the hydrophobic cyclodextrin cavity to a cyclic peptide (a cation receptor in itself), may afford a molecule with two different recognition sites and the cyclic peptide may also coordinate a metal ion that can work as a third recognition site.[147] This may provide a stepwise approach to the multiple recognition which is very common in biological interactions. Many other cyclodextrins are known to bind metal ions, and are discussed in the following section.

1.3.3 Metallocyclodextrins

Natural cyclodextrins are capable of metal ion complexation under alkaline conditions, where they become negatively charged.[80,148,149] 3,6-Anhydro-cyclodextrins have been reported to selectively bind the alkali metal ions, K^+, Rb^+ and Cs^+, owing to their hydrophilic cavities.[150] The metal binding properties of a cyclodextrin can be improved by substituting hydroxyl groups with coordinating groups.

Included guests which possess coordinating groups may form metal complexes with metal ions present in solution.[151] By substituting one or more coordinating groups onto a cyclodextrin, a metal ion can be coordinated by the cyclodextrin to form a metallocyclodextrin. The coordinated metal ion, held in close proximity to the cavity, may provide an additional anchoring site for a metal binding guest molecule. The ability of metal ions to act as additional recognition and/or catalytic sites has stimulated the investigation of modified cyclodextrins bearing ligand subunits for metal ion complexation.[152]

Modified cyclodextrins which bind metal ions such as: Mg^{2+},[109,153] Al^{3+},[128] Fe^{3+},[128] Co^{2+},[154] Co^{3+},[104,116,149] Ni^{2+},[154-156] Cu^{2+},[109,111,152-154,156-158]

Zn^{2+},[45,109,153,154,156,159] Rh^{+},[126] Pd^{2+},[127] Re^{+},[139] Pb^{2+},[160] and trivalent lanthanides,[140,161,162] have been reported. Cyclodextrins may be designed with multiple ligating sites stereoselectively arranged over the molecular cavity.[163] Bimetallic cyclodextrin complexes of Co^{2+} and Cu^{2+} have been prepared.[163] Ferrocene-appended cyclodextrins have also been reported.[127,164]

Some aspects of metallocyclodextrins will now be discussed in more detail.

i) Binding

Metallocyclodextrins generally behave as double recognition hosts where the specific guest is recognised by the mutually independent elements of hydrophobic interaction with the cyclodextrin cavity and coordination interaction with the metal ion operating additively, resulting in remarkably enhanced binding. However, the presence of two or more recognition sites does not necessarily mean cooperation between them will occur, and in some instances competition arises between recognition sites. This may be explained by taking into account the geometry of binding of the guest.[152]

Cooperativity between the hydrophobic cyclodextrin cavity and the metal ion in binding specific guests has been demonstrated in a number of examples.[45,109,107,142] Cyclodextrins functionalised on their primary rim with diethylenetriamine (βCDdien) and triethylenetetramine (βCDtrien) interact strongly with metal ions such as Cu^{2+}, Zn^{2+} and Mg^{2+}.[109] The modified cyclodextrins which are flexibly capped with Zn^{2+} bind several guests, which contain hydrophobic moieties and anionic $-CO_2^-$, $-SO_3^-$ or $-O^-$ groups, up to 300 times more strongly than βCD or βCDdien and βCDtrien (which are only two to three times more effective than βCD).[109] For guests possessing a carboxylate group, the additivity of the free energies, characterising hydrophobic interaction and metal-ligand coordination (and/or coulombic) interaction, is clearly demonstrated.[109]

Hydrophobic and coordination interactions also operate additively in the inclusion of sodium cyclohexanecarboxylate by the Zn^{2+} complex of $6^A,6^C$-di(1-imidazolyl)-$6^A,6^C$-deoxy-βCD. However, the coordination interaction energy involved for this

metallocyclodextrin is not as large as that for βCDdien, in complexing the same guest, probably as a result of the increased rigidity of this metallocyclodextrin requiring an unfavourable coordination angle.[45] This suggests that stereochemical requirements are important for coordination recognition. The Zn^{2+} metallocyclodextrin of $6^{A},6^{C}$-di(1-imidazolyl)-$6^{A},6^{C}$-deoxy-βCD demonstrated remarkably improved stability and selectivity, by comparison with βCD, in complexing a range of cyclohexane derivatives.

ii) Catalytic Activity

The majority of metallocyclodextrin studies have focused on their catalytic effects. For example, the hydrolysis of activated esters complexed within metallocyclodextrin cavities may be catalysed.[102,104,156,158] A number of factors influence the catalytic enhancement, or lack thereof, and some of these are aptly demonstrated in the following examples.

Comparisons have been made between the rate enhancements exhibited by primary and secondary substituted cyclodextrins, however, no general rule is found. The rate of hydrolysis of *p*-nitrophenylacetate under neutral conditions is substantially enhanced by a primary substituted βCD-cyclen-Co^{3+} complex (1000-fold), whereas the secondary substituted analogue shows less enhancement (4-fold). This rate enhancement of the primary substituted βCD-cyclen-Co^{3+} is not simply due to interaction with βCD-cyclen, which yields a 9-fold increase, nor interaction with cyclen-Co^{3+}, which does not promote hydrolysis of *p*-nitrophenylacetate, but a cooperativity between the two recognition sites.[104,116] The reverse situation is found for the hydrolysis of *p*-nitrophenylphosphate, where a greater rate acceleration is seen with the secondary substituted cyclodextrin (3700-fold) than the primary substituted cyclodextrin (2900-fold), and both are *ca.* 20 times less effective than the cyclen-Co^{3+} complex.[104] The difference in properties of the primary and secondary substituted cyclodextrins may arise, in part, because the primary substituted cyclodextrin is able to involve an adjacent primary hydroxyl group in chelation of the metal ion.[104,116] The rotation of the cyclen-Co^{3+} group is probably hindered in the

secondary substituted cyclodextrin, and the guest may be located too far away from the catalytic site in some cases.[116,152]

The complexation of Cu^{2+} by 6^A-(2-aminoethylamino)-6^A-deoxy-βCD (βCDen) forms a $[Cu(\beta CDen)_2]^{2+}$ complex which significantly accelerates the oxidation of furoin. Only slight acceleration is achieved by βCD, en, $Cu(en)_2^{2+}$ or βCDen.[111] The two cyclodextrin cavities of $[Cu(\beta CDen)_2]^{2+}$ may bind furoin in such a way that its reaction site is located in the vicinity of the Cu^{2+} ion. Interestingly, the deacylation of *p*-nitrophenylbenzoate is accelerated by $[Cu(\beta CDen)_2]^{2+}$ in comparison with βCDen, and yet retarded by $[Cu(H_3CCH_2CH_2\text{-}en)_2]^{2+}$ in comparison with $H_3CCH_2CH_2$-en. Presumably the inhibitory effect of Cu^{2+} is overcome in $[Cu(\beta CDen)_2]^{2+}$ by the advantageous effect of the cyclodextrin cavity.[158] Shorter guests which cannot optimise binding to both cyclodextrin cavities simultaneously, bind less strongly and are catalysed less readily.[158]

iii) Enantioselectivity

In some cases metallocyclodextrins may behave enantioselectively in guest complexation. The following examples illustrate that these cyclodextrins are not always selective for the same enantiomer, and the "cis-effect", which has been proposed to explain this, is also discussed.

Ligand exchange chromatography studies have demonstrated that the Cu^{2+} complex of 6^A-[2-(4-imidazolyl)ethylamino]-6^A-deoxy-βCD shows chiral discriminating ability for the (*R*)- enantiomer of tryptophan.[10,86] The closely related cyclodextrin, 6^A-[4-(2-aminoethyl)imidazolyl]-6^A-deoxy-βCD,[87] shows even greater enantioselectivity, but for the opposite enantiomer, (*S*)-tryptophan. Interestingly, when 6^A-[2-(4-imidazolyl)ethyl-amino)]-6^A-deoxy-βCD is used in the absence of Cu^{2+}, the (*S*)-enantiomer is favoured, suggesting that both inclusion and metal ion coordination are effective in the case of the Cu^{2+} complex of 6^A-[2-(4-imidazolyl)ethylamino]-6^A-deoxy-βCD.[86] The greater discriminating ability of 6^A-[4-(2-aminoethyl)imidazolyl]-6^A-deoxy-βCD may be

ascribed to its greater rigidity, conferred by the direct bonding of imidazole to βCD, which places more stringent conditions on guest binding.[87]

These enantioselectivity results have been accounted for by proposing a "cis-effect",[87] where, in the metallocyclodextrin-guest complexes the Cu^{2+} coordination plane is almost parallel to the cavity and the amino groups of the modified cyclodextrin and the amino acid are forced to bind adjacent to one another in the coordination plane. Both tryptophan and the modified cyclodextrins act as bidentate ligands, with the two amino groups most likely arranged in the *cis* position, as generally observed in the ternary complexes formed by amino acids. The relative stabilities of the metallocyclodextrin-guest complexes are governed by the position of the aromatic side chain of tryptophan relative to the cyclodextrin cavity, so that inclusion may be allowed only for one enantiomer and not the other.[86] Molecular models show that this would result in inclusion of the indole moiety for only the (*R*)- enantiomer in the 6^A-[2-(4-imidazolyl)ethylamino]-6^A-deoxy-βCD cavity, and only the (*S*)- enantiomer in the 6^A-[4-(2-aminoethyl)imidazolyl]-6^A-deoxy-βCD cavity. Hence the higher stability of these diastereomers which can successfully utilise both interactions; coordination to Cu^{2+} and inclusion in the cyclodextrin cavity.[87] A *cis*-complex $\rightleftharpoons$ *trans*-complex equilibrium is proposed to exist in these systems, and the greater the difference between the two donor groups of the cyclodextrin, the more such an equilibrium is shifted towards the left.[10] Consequently it is not surprising that no thermodynamic enantioselectivity is found in the complexation of amino acids by the Cu^{2+} complex of 6^A-(2-aminoethylamino)-6^A-deoxy-βCD.[165]

The overall process for the complexation of an amino acid by the Cu^{2+} complex of 6^A-[2-(4-imidazolyl)ethylamino)]-6^A-deoxy-βCD, is both enthalpically and entropically favoured.[10] The enantioselectivity factors increase in the order tyrosine < phenylalanine < tryptophan, suggesting a dependence on the hydrophobicity and/or the size of the amino acid aromatic side chain, while no significant enantioselectivity is found for histidine and aliphatic amino acids.[10] For the complexes containing aromatic amino acids, the thermodynamic stereoselectivity is due to the more favourable enthalpy contribution in the formation of ternary complexes of the (*R*)-enantiomers, while entropy is less favourable.[10]

Hydrophobic interactions between the cavity and the aromatic side chains of the amino acids seem to be crucial for enantioselectivity, and the less favourable entropy changes for the (*R*)-enantiomers may be interpreted as the result of the loss of internal rotational freedom of the side chain, which predominates over the desolvation effect.[10] The enantioselectivity observed once again supports the "cis-effect", as described above, and no evidence of enantioselective interactions between the cyclodextrin hydroxyl groups and the amino acid coordinating groups is seen. However, the proposed "cis-effect" will not be valid for all metal ions as demonstrated in the next example.

Both the primary and secondary analogues of βCDen have been reacted with diethylenetriaminepentaacetic dianhydride, to form modified cyclodextrins which can coordinate to Dy^{3+} through four oxygen atoms and three nitrogen atoms.[161] These metallocyclodextrins enhance enantiomeric resolution in the ^1H NMR spectra of tryptophan, with the secondary analogue exhibiting more pronounced enhancement than the primary analogue.[161] The lanthanide-induced shifts appear to result from the guest association with the cyclodextrin rather than with the lanthanide, and both enantiomers appear to be included within the cyclodextrin cavity.[161]

iv) System Dependence

As mentioned above, the nature of some amino acid guests influences the enantioselectivity of their complexation by the Cu^{2+} complex of 6^A-[2-(4-imidazolyl)ethylamino)]-6^A-deoxy-βCD. The stabilities of these complexes increase in the order, tyrosine < phenylalanine < tryptophan < histidine, while the aliphatic amino acids have complex stabilities similar to those of tyrosine or phenylalanine. This implies that other factors beside the hydrophobicity and/or size of the amino acid aromatic side chain influence complex formation.[10]

Few reports on metallocyclodextrins have involved a quantitative investigation of the influence of variation in the nature of the metal centre on the complexes formed. The

metal centre chosen may affect the catalytic activity of the metallocyclodextrin, its enantioselectivity and the stability of the complexes formed.

Efficient cleavage of ribonucleoside 2',3'-cyclic monophosphates and ribonucleotide dimers is catalysed by a primary side βCD-diethylenetriamine-Zn^{2+} complex.[153] The importance of both the Zn^{2+} ion and the hydrophobic βCD cavity in the rate enhancement is evident. The analogous Cu^{2+} and Mg^{2+} complexes showed small acceleration, on the cleavage of a ribonucleotide dimer, by comparison with Zn^{2+}. The transacylation of *p*-nitrophenylacetate is catalysed by primary substituted βCD-cyclen-M^{2+} complexes, and the rates of catalysis vary in the order: $Ni^{2+} > Cu^{2+} < Zn^{2+}$.[156] Enhanced rate of catalysis and high stability are not necessarily coincident.[116] The stabilities of some metallocyclodextrins of 6^{A}-(3-aminopropylamino)-6^{A}-deoxy-βCD, and their tryptophan complexes reveal a stability order: $Co^{2+} < Ni^{2+} < Cu^{2+} > Zn^{2+}$.[154] However, the extent of enantioselectivity varies in the order: $Co^{2+} < Ni^{2+} > Cu^{2+}$, and no enantioselectivity is observed for Zn^{2+}.[154] Similar effects are observed for phenylalanine.[166]

Metallocyclodextrins possess a hydrophobic cavity which can encapsulate a guest while it also interacts with the adjacent metal centre, as is observed for some metalloenzymes.[115] Hence, they provide useful models for the mode of action of metalloenzymes, and may also enable extension of the powerful catalytic effects of metals to non-ligand guests. Metalloenzymes are known to be very selective for certain molecules and their mechanism of selectivity arises from multiple recognition sites. It was hoped that a similar selectivity would be acquired from the recognition sites of the metallocyclodextrins used in this study.

1.3.4 Linked Cyclodextrin Dimers

The fact that some guests (usually longer molecules) tend to form (cyclodextrin)$_2$·(guest) complexes[42,56,60,68,122] led to the preparation of what are now known as cyclodextrin dimers, double cyclodextrins, linked cyclodextrins or linked cyclodextrin dimers. Two hydrophobic cyclodextrin cavities are joined by one or more tethers, which are attached to the annuli by substitution of the cyclodextrin hydroxyl groups. Hence, linked cyclodextrin dimers essentially possess two hydrophobic recognition sites. Although (cyclodextrin)$_2$·(guest) complexes only form in the presence of a large excess of cyclodextrin, double capping of a guest by a linked cyclodextrin dimer will occur at low concentrations of linked cyclodextrin dimer due to the close proximity of the second cyclodextrin annulus.[9]

The first linked cyclodextrin dimer, reported in 1972, consisted of two αCDs covalently linked together by their secondary rims by a terephthalate diester link.[167] Subsequently, various disulfide,[11,23,24,60,62,63,124,141,144,168-172] dithiol,[60,62,124,168] diether,[173] diamine,[174] diester,[9,23,63,69] diamide,[144,175-178] imidazole,[24,69,75] tetramine,[174] and tetrasulfide,[23,124] linked cyclodextrin dimers have been synthesised and their binding properties studied. Cyclodextrins have also been linked together by porphyrins.[24,141,144] Generally the two annuli are linked by covalent bonds, however, two cyclodextrin annuli, modified with coordinating groups, have been linked together by coordination to a single metal ion.[23,179] In the last few years, there has been a dramatic increase in the number of papers reporting the synthesis and analysing the behaviour of linked cyclodextrin dimers.[169]

There are three main categories of linked cyclodextrin dimers: those linked by their primary rims (1°,1°-linked), those linked by their secondary rims (2°,2°-linked), and those where the tether joins a primary and a secondary rim (1°,2°-linked). As a consequence of the inherent dipole of a cyclodextrin annulus, 1°,2°-linked cyclodextrin dimers are expected to possess the least dipole repulsion. Potentially, linked cyclodextrin dimers have

improved binding capabilities for guests with two binding sites compared with cyclodextrin monomers. Enzymes and antibodies typically bind several guest segments, and linked cyclodextrin dimers have the potential to do likewise.[63]

Some aspects of linked cyclodextrin dimers will now be discussed in more detail.

i) Binding

Based on statistical factors, the stability constant for a linked cyclodextrin dimer complex should be double that of the native cyclodextrin, without any collaboration occurring between the individual linked cyclodextrin annuli. This is because within every host there are two opportunities for inclusion. If the two cyclodextrin annuli cooperate in guest binding, the stability constants will be significantly greater than this.

The ability of a linked cyclodextrin dimer to complex a guest at two points may increase the stability of the resulting complex, and this may be likened to the chelate effect observed for metal complexes.[180] The chelate effect is classically explained in terms of favourable entropy of binding relative to two independent ligands, as translational entropy does not have to be paid for twice when two ligands are joined to each other.[181] In contrast, the cooperative binding effect of at least some linked cyclodextrin dimers shows an unfavourable entropy, which is compensated for by a favourable enthalpy that is considerably greater than the sum of the enthalpies of binding by two monomeric cyclodextrins.[60] This probably means that there are compensating solvation effects (see Section 1.2.2) whose enthalpy/entropy consequences dominate the thermodynamics.

Guests which have two hydrophobic ends can form complexes of very high stability with linked cyclodextrin dimers, particularly if two tethers are employed.[11] It has been shown that stability constants of more than 10^{11} dm^3 mol^{-1} can be achieved using a doubly-linked cyclodextrin dimer and an appropriately designed guest.[23,24,69] The cooperative action of two covalently linked annuli, in a linked cyclodextrin dimer, provides powerful binding of guests which exploit the extended recognition site, with stability constants of up to 10^9 dm^3 mol^{-1} for a singly-linked cyclodextrin dimer.[23,62,63,69]

However, guests whose geometries do not permit good binding into both cavities show very low stability constants,[69] for example, if the distance between benzene rings of a guest is too small even good binding to a single cavity may not occur.[24]

An effective collaboration of two cyclodextrin moieties, linked by a tether, in guest binding, is demonstrated by disulfide-1°,1°-linked-βCD. Methyl orange (MO^-), ethyl orange and TNS^- are respectively bound 196, 224 and 48 times more strongly by this linked cyclodextrin dimer than by βCD.[171] The cooperation of the two cyclodextrin binding sites may be attributable to the short tether, a disulfide bond, linking them. Although αCD binds the alkyl orange dyes more strongly than βCD, the analogous linked-αCD shows, at most, only slight cooperativity.[171] This implies that the combination of two tight binding sites does not necessarily produce effective collaboration between them.[172] Disulfide-1°,1°-linked-βCD also has the interesting potential to recognise specific amino acid sequences in polypeptides.[23]

Not all linked cyclodextrin dimers bind strongly.[69] Although disulfide-1°,1°-linked-βCD shows strong binding for guests that can occupy both cavities, disulfide-2°,2°-linked-βCD does not, as the two cavities interpenetrate to some extent and this self-binding must be sacrificed when a guest is complexed.[23,63]

Linked cyclodextrin dimers containing cyclodextrin annuli of different sizes are known as heterodimers. Both 1°,1°-linked and 2°,2°-linked cyclodextrin heterodimers containing αCD and βCD have been reported.[176,177] Malonamide-1°,1°-linked-α-βCD binds isoamyl *p*-dimethylaminobenzoate site-specifically, with the alkyl group included in the βCD cavity while the dimethylaminobenzene moiety is partially included in the αCD cavity.[177]

NMR studies on sebacamide-2°,2°-linked-βCD and the analogous αCD-βCD heterodimer, indicate that the long length of the tether enables it to be bound in one of the two cavities of the dimer. This results in a lower affinity of sebacamide-2°,2°-linked-βCD for TNS^-, by comparison with succinamide-2°,2°-linked-βCD, as the octamethylene tether must first be removed from one of the cavities.[176] The first complete NMR characterisation of a linked cyclodextrin dimer was presented by Jiang *et al.*[169] Their

analysis of 3,5-di(thiomethyl)pyridine-2°,2°-linked-βCD suggested that the modified glucose residues of the individual cyclodextrin annuli have undergone a chair inversion.[169] The two βCD halves of the dimer are spectrally indistinguishable, and each of the seven component sugar residues are spectrally unique.[169]

The tether linking the cyclodextrin annuli, may provide an additional recognition site.[170] 3,5-Di(thiomethyl)pyridine-2°,2°-linked-βCD exhibits an enhanced ability, relative to 1,3-di(thiomethyl)benzene-2°,2°-linked-βCD, to encapsulate a diverse assortment of metalated macrocyclic compounds in aqueous solution.[170] The pyridine nitrogen atom of the tether coordinates to the central metal atom of the metalated macrocyclic guest. Evidence of interaction between a cationic tether group and an anionic guest has also been reported.[75]

ii) Catalysis

An important feature of linked cyclodextrin dimers is that a doubly-bound guest is aligned along the tether. Hence, certain tether groups are potential catalysts for reactions of guests that can be held across the catalytic site. For example, the tether of thioanthone-3,6,-dicarboxyl-1°,1°-linked-βCD possesses a catalytic group that can direct chlorination.[182] Some tether groups are capable of binding metal ions, which may in turn be involved in binding and/or catalysis of a guest. Metal ions which have been bound by the tether of a linked cyclodextrin dimer include: Mn^{3+},[24] Fe^{2+},[24] Cu^{2+},[11] Zn^{2+},[11] Rh^{3+},[175] Re^{+},[173] and La^{3+}.[24,69,105] The metal complexes of 5,5'-dithiol-2,2'-dipyridyl-1°,1°-linked-βCD are able to catalyse the hydrolysis of ester guests that bind into both cavities so as to place the ester group next to the metal ion.[11,105] Catalytic hydrolysis occurs with good turnover and striking rate accelerations.[11,105] The effects of the metal centre and the two linked cyclodextrin cavities on the rate of hydrolysis of the *p*-nitrophenyl ester of 3-indolepropionic acid are demonstrated by the 30-fold rate acceleration detected in the presence of βCD, with or without Cu^{2+}, by comparison with the rate in the absence of a catalyst, while the linked cyclodextrin dimer exhibits a rate

enhancement of 80-fold in the absence of Cu^{2+}, and over 10^4-fold in its presence.[11] The additional cyclodextrin cavity more than doubles the rate but the extent to which the metal centre enhances the rate is much greater. Holding a metal ion next to a guest may also be useful for directed oxidation reactions.[24] The metallo-linked cyclodextrin dimer, $[Cu(\beta CDen)_2]^{2+}$, demonstrates catalytic capabilities in accelerating the oxidation of furoin.[111]

Modified cyclodextrins, such as permethylated-βCD, have also been linked together.[173] The 2,2'-bipyridine-1°,1°-linked-permethylated-βCD forms a complex with Re^+ which is electron- and photo-active.[173] Such supramolecular assemblies are of particular interest to study energy transfer communication between an active metal centre and an encapsulated guest.[173]

iii) Singly- and Doubly- Linked Cyclodextrin Dimers

A single flexible tether between cyclodextrin rings permits many conformations which are unsuitable for the binding of a guest to both cavities. Linked cyclodextrin dimers having better defined optimal geometry should exhibit stronger binding. Binding should be increased with more rigid tethers,[63] however, some flexibility is still required, to permit entry and exit of the guest.[23] The amount of free rotation between the two linked cavities of *o*-benzene-disulfide-1°,1°-linked-βCD is restricted by the tether.[62] Twisting around a tether may be prevented by using two tethers to link the cyclodextrin annuli through a hinge. A few doubly-linked cyclodextrin dimers have been reported.[23,24,69,174]

Bis(imidazolium)-1°,1°-linked-βCD has been shown by NMR spectroscopy to exist in two isomeric forms.[23,24,69] Each imidazolium group may be attached to the 6A position of one cyclodextrin and the 6B position of the other, holding the cyclodextrin annuli in occlusive geometry. This is referred to as the *clamshell* isomer as the linked cyclodextrin dimer can exist in an open conformation but binding induces a closing up of the cyclodextrin around the guest to enclose it, in a process analogous to induced fit in enzymes.[23] Alternatively, one imidazolium group may link the 6A positions of the two

cyclodextrins, while the other links the 6B positions, holding the cyclodextrin annuli in aversive geometry. This is referred to as the *loveseat* isomer, where the cyclodextrin annuli are held apart by the hinge and cannot cooperate in guest binding as the two binding sites face in opposite directions.[23] As expected, binding by the *clamshell* isomer is strong, whereas binding by the *loveseat* isomer is only slightly higher than of βCD itself, (presumably because of some extra hydrophobic interaction with the tether).[23,124]

The hinge may restrain bending as well as twisting. For example, the *clamshell* isomer of bis(imidazolium)-1°,1°-linked-βCD has been shown to bind a guest, possessing bent geometry, less strongly than its singly-linked analogue does.[69] Doubly-linked cyclodextrin dimers have also been prepared containing two tethers of different lengths.[69] In this way the *clamshell* linked cyclodextrin dimer has a bent geometry even when it closes up on a guest, and has been shown to preferentially bind a bent guest at least 4000 times more strongly than the linear guest isomer.[69] Such shape recognition may become very useful for selectively binding the shape of the transition state over the shape of the reactant ground state.[23,124] Indeed, many enzymes use shape recognition to help drive their catalysed reactions.

The bis(ethylenediamine)-1°,1°-linked-βCD, which is also known as duplex cyclodextrin (Appendix, (1)), potentially has triple recognition capabilities; having two hydrophobic binding sites and the amine tethers may bind a metal ion creating a third recognition element.[174] This doubly-linked cyclodextrin dimer binds MO^- with a stability constant of K = 3,160 $dm^3\ mol^{-1}$, and comparison with the corresponding stability constant for bis(ethylenediamine)-βCD, K = 520 $dm^3\ mol^{-1}$, demonstrates the additive contribution of the second hydrophobic binding site and multiple recognition is operating.[174]

Linked cyclodextrin dimers are proposed to exhibit simultaneous bifunctional binding, and the best binding occurs when the geometry is optimised to fit the shape of the guest.[23] Where it is geometrically feasible, the binding of a guest by a linked cyclodextrin dimer host occurs through induced fit, in which the host closes around the guest, shielding it from the surrounding aqueous environment.[23] It is unlikely that the guest simply threads

its way into an already closed host structure.[23] In many cases the enzyme-substrate binding process involves induced fit, in which the enzyme folds around the substrate to lock it firmly into position and excludes water from the reaction zone.[23] Linked cyclodextrin dimers may be useful to mimic and explore enzymatic processes or to create supramolecular assemblies by the formation of geometrically well-defined complexes.[23,177] These water-soluble encapsulating agents have an unusually high affinity for hydrophobic molecules[63] and have an apparent ability to serve as membrane-bound receptors.[62] Linked cyclodextrin dimers may also be used to represent the local model of a cyclodextrin polymer (Section 1.3.5).[9] The potential applications of linked cyclodextrin dimers to biomimetic chemistry, drug delivery, and other areas have yet to be fully realised.[169]

Only a limited number of binding studies have been reported in which the effects of variations in the host and/or guest have been considered. The binding of a range of guest molecules, with varied geometries of their hydrophobic segments, to particular linked cyclodextrin dimer hosts,[23,63] have been studied, as has the binding of a particular guest to a range of linked cyclodextrin dimer hosts.[168] These studies, and those reported in this thesis, may further the understanding of the factors influencing optimal binding in such systems.

1.3.5 Cyclodextrin Polymers

The covalent linking of cyclodextrin annuli may be extended to form polymers.[183] The binding of TNS^- by poly(acryloyl-βCD) and the linked cyclodextrin dimers, succinate- and glutarate-2°,2°-linked-βCD, as well as the fluorescence of the resultant complexes, have been compared.[9] In each case, the guest appears to be exclusively bound by two βCD annuli.[9,184] The binding strength of the polymer is intermediate between the dimers, however, the fluorescence enhancement is greatest for the polymer.[9] The large fluorescence enhancement observed for the polymer may arise from a number of factors including a more hydrophobic guest environment and less conformational freedom. The

polymer complex may assume a more rigid conformation than the dimers and may exclude more effectively the solvent relaxation, presumably because of deeper inclusion.[9]

The special properties of cyclodextrins are largely retained in a cyclodextrin polymer, although, if the degree of polymerisation is sufficiently high, the cyclodextrins bound within the matrix become insoluble.[3] The complexation behaviours of monomeric and polymer fixed cyclodextrins may differ. For steric reasons, individual cyclodextrins should bind less strongly in a polymer than as a monomer. Poly(acryloyl-βCD) is more efficient than βCD in binding large guests, which can react with two cyclodextrin annuli, but is less efficient in binding small guests, which can be completely included in a single cavity.[184,185] In the former case, once the guest is bound by one cyclodextrin of the polymer, the extremely high local concentration of cyclodextrin allows an adjacent annulus to bind the guest.[184-186] Hence, poly(acryloyl-βCD) may possess size selectivity even though βCD binds large and small aromatic guests roughly independent of size.

Guest molecules, which can interact with two cyclodextrin annuli, may be included in a number of ways by cyclodextrin polymers: inclusion within a single cyclodextrin annulus, inclusion by two adjacent cyclodextrin annuli on the same polymer chain, inclusion by two non-adjacent cyclodextrin annuli on the same polymer chain, or inclusion by two cyclodextrin annuli on different polymer chains.[186] As the length of the tether increases, the polymer becomes conformationally more flexible and inclusion of the guest by annuli on the same polymer chain is more likely than inclusion by annuli on different polymer chains.[186] Longer guest molecules may interact with more than two cyclodextrin annuli. As many as four cyclodextrins interact with a single molecule of dodecanoic acid.[185]

Glyceryl linked cyclodextrin polymers, poly(glyceryl-XCD) (X = α, β or γ), are water soluble and they appear to bind naphthalene-based fluorescent probes much more strongly than their corresponding monomeric cyclodextrins do.[187] Fluorescence lifetime measurements suggest the presence of more than one type of binding site for the cyclodextrin polymers, and that these are different to the binding site of the monomer. The glyceryl tether itself appears to affect guest binding, providing some non-inclusional

association.[187] One possibility is an expansion of the binding site regions as the tether groups wrap around entrances to the cyclodextrin cavities to maximise hydrogen-bonding interactions between the glyceryl hydroxyl groups and those on the rims of the cyclodextrin cavities. A comparison of fluorescence data using different molecular weight ranges of the cyclodextrin polymer infers that cooperative binding effects between cyclodextrin annuli on the same chain are not significant, rather, cyclodextrin annuli appear to act independently of one another in binding the naphthalene-based guests studied.[187]

It appears that the tethers may serve two functions: as a site for non-inclusional binding and as spacers to hold cyclodextrin annuli in the proper orientation to bind guests.[187] Which of these functions dominates for a given guest may depend on the size, shape and polarity of the guest and the length of the tether chain.[187]

Evidence suggesting the existence of cooperative binding effects between cyclodextrin annuli in poly(glyceryl-βCD) has been reported for some guests.[184,186] Harada *et al.* reported the existence of a poly(glyceryl-βCD)/TNS^- complex in which TNS^- is bound by two cyclodextrin annuli, which may come from the same chain.[188] Szeman *et al.* showed that low molecular weight poly(glyceryl-βCD) fractions form stronger complexes with small guests than do high molecular weight fractions, while the reverse is true for large guests.[189]

Xu *et al.* suggested that the binding of pyrene by two βCD annuli on the same chain occurs with increasing probability as the length of the tethers between the βCD annuli increases.[186] Longer tether lengths permit the greater flexibility required for binding between the secondary faces of cyclodextrins which are attached to a polymer chain by their primary rims.[186] The strength of polymer binding increases with tether length, probably due to this greater ease of binding, as it is not due to a high affinity of pyrene for the tether itself.[186] Presumably, tethers which are too long would reduce the chance of the second cyclodextrin finding the already partially included guest.

The binding sites of poly(glyceryl-XCD) (X = α, β or γ) are much more hydrophobic than those of the corresponding monomers, as evidenced by guest fluorescence behaviour.[187] However, as the tether length of the βCD polymer is

increased, the polymer environment becomes much more hydrophilic than when pyrene is double capped by the βCD monomer.[186] This is possibly due to insertion of the polar tethers or unsubstituted chains into the cavity.

Acryloyl-linked cyclodextrin polymers enhance the fluorescence of TNS^- to a greater extent as the distance between neighbouring cyclodextrin annuli on the polymer chain is decreased.[184] The corresponding monomeric cyclodextrin derivative has similar effects to βCD on the fluorescence of TNS^-, and poly(acrylic acid) has no affect. This indicates the absence of any contribution from substituents, and implies that the hydrophobic environment generated by many cyclodextrins held in close proximity produces the substantial fluorescence enhancement observed for the polymer.[184]

Rates of catalysis and binding strength may be improved when a number of hydrophobic cyclodextrin binding sites are held in close proximity, as in poly(acryloyl-βCD).[185] The rate of ester hydrolysis is accelerated more as the distance between neighbouring cyclodextrin annuli on the polymer chain is decreased.[185] The reactivity of the polymer complex is increased due to catalysis by more than one βCD held in close proximity. Both kinetic and binding studies suggest that a guest may be bound between two neighbouring βCD groups on a polymer chain.[185]

Polymeric cyclodextrins have potential applications in areas such as separations, catalysis, drug delivery and water purification.[186] Cyclodextrin polymers may be effective mobile phase modifiers in high performance liquid chromatography (HPLC) at much lower concentrations than required for the cyclodextrin monomers.[187] A difference in HPLC selectivity for a given guest analyte is also expected between the mobile phases containing monomeric and polymeric cyclodextrins.[187] The enhanced water solubility of poly(glyceryl-βCD) by comparison with βCD, and of the polymer complexes by comparison with the monomer complexes, gives such polymeric cyclodextrins the potential to be very useful encapsulants and promises to assist in designing highly water soluble cyclodextrin carriers for hydrophobic drugs.[186,187]

1.4 Aims of This Research

As outlined in the Section 1.3, a vast number of modified cyclodextrins have been synthesised, studied and used in various applications, hence, the range of modified cyclodextrins considered in this thesis allow only relatively minor contributions to this field. By considering the binding and selectivity of some metallocyclodextrins and linked cyclodextrin dimers, it was hoped that a better understanding of the factors influencing and optimising these two properties would be obtained.

The first section of this thesis is concerned with some simple metallocyclodextrins of 6^A-(3-aminopropylamino)-6^A-deoxy-β-cyclodextrin (βCDpn) and 6^A-(2-(*N*,*N*-bis(2-aminoethyl)amino)ethylamino)-6^A-deoxy-β-cyclodextrin (βCDtren) (Fig. 1.4), and their complexation of amino acids. To determine the factors affecting guest selectivity, the complexation of histidine by the Cu^{2+} metallocyclodextrin of βCDpn was compared with the analogous complexes of phenylalanine and tryptophan, previously reported.

Metalloenzyme activity is very metal centre specific and this may be partly due to the influence of the metal centre on the stability of the metalloenzyme and its efficacy in binding substrates (guests). The influence of the metal centre on the binding of tryptophan by βCDtren is discussed here for Co^{2+}, Ni^{2+}, Cu^{2+} and Zn^{2+}. Similar investigations have been reported for the complexation of tryptophan and phenylalanine by βCDpn.[154,155,166] Such studies may also assist in building an understanding of metalloenzymes.

High guest selectivity with respect to enantiomers is common in biological systems, and in these studies both the (*R*)- and (*S*)-enantiomers of the amino acids were used in the hope of observing enantioselective complexation. An understanding of the factors influencing the stabilities, amino acid selectivities and enantioselectivities of metallocyclodextrins and their complexes, should be furthered by this investigation of the effects that variation in the guest structure and in the nature of the metal centre have on complexation.

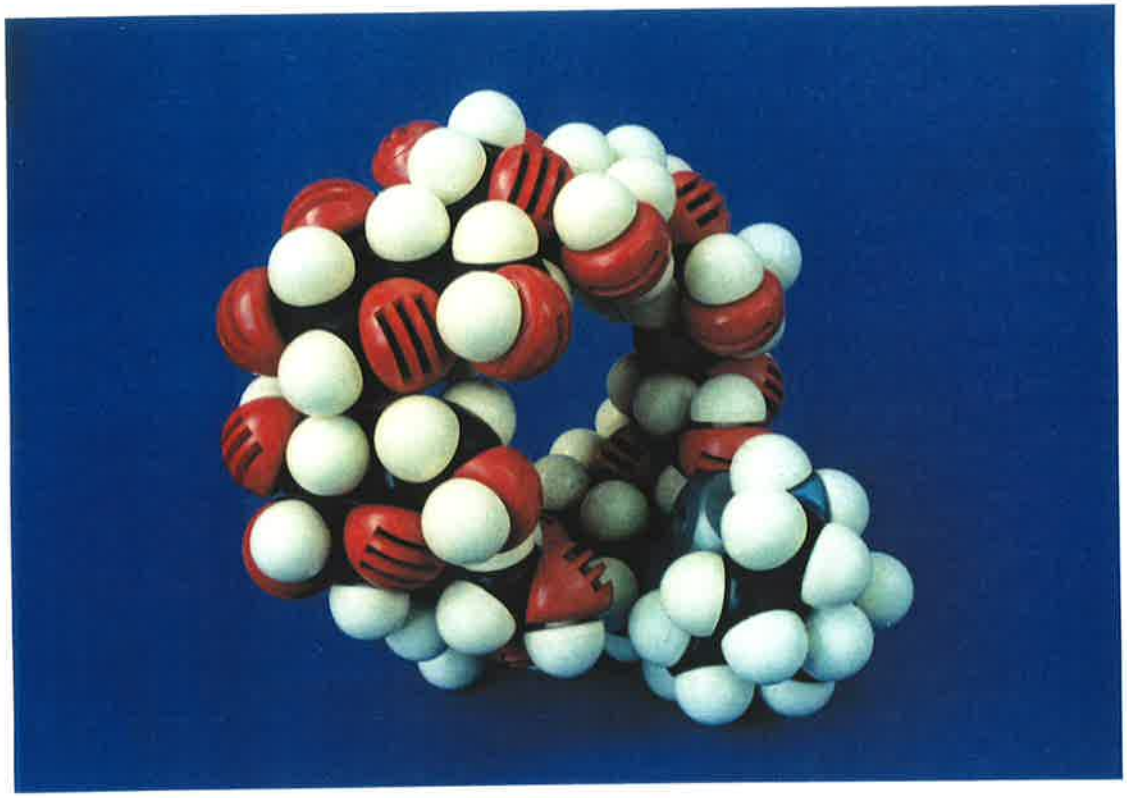

Figure 1.4 *CPK model of a metallocyclodextrin of 6^A-(2-(N,N-bis(2-amino-ethyl)amino)ethylamino)-6^A-deoxy-βCD, $[M(\beta CDtren)]^{2+}$, as discussed in Chapter 2. The colours representing the atoms are black for carbon, red for oxygen, white for hydrogen and silver for the metal ion.*

The second section of this thesis is concerned with some diamide-1°,1°-linked-βCDs. The effects of varying the length of the diamide tether, linking the primary rims of two βCDs, are considered in Chapters 3 and 4. Three guests, each of which possesses two aromatic binding sites, were chosen to study the effects of variation in size and stereochemistry of the aromatic residues. The spectral characteristics of the selected guests allow their complexation by the linked cyclodextrin dimer hosts to be monitored.

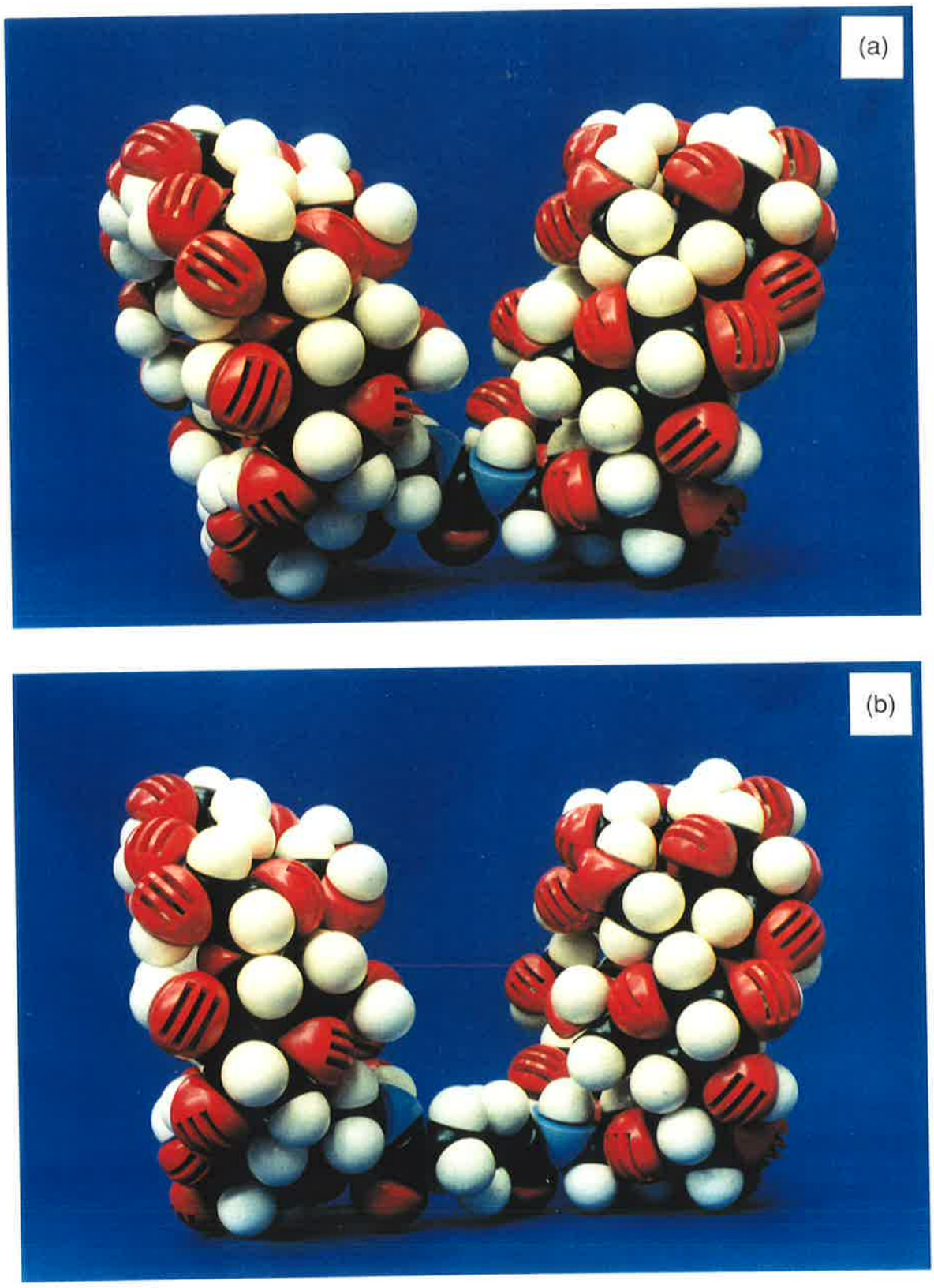

Figure 1.5 *CPK models of some diamide-1°,1°-linked-βCDs discussed in Chapter 3, showing the extent of variation in the tether length, from (a) $(\beta CD)_2Ur$ to (b) $(\beta CD)_2Gl$. The colours representing the atoms are black for carbon, red for oxygen and white for hydrogen.*

The range of tether lengths explored in Chapter 3 are shown in Fig. 1.5, where the βCD annuli are separated by two bond lengths in *N*,*N*'-bis-(6^{A}-deoxy-6^{A}-β-cyclodextrinyl)-urea ((βCD)$_2$Ur), and by six bond lengths in *N*,*N*'-bis-(6^{A}-deoxy-6^{A}-β-cyclodextrinyl)-glutaramide ((βCD)$_2$Gl). The other linked cyclodextrin dimers used; *N*,*N*'-bis-(6^{A}-deoxy-6^{A}-β-cyclodextrinyl)-oxalamide ((βCD)$_2$Ox), *N*,*N*'-bis-(6^{A}-deoxy-6^{A}-β-cyclodextrinyl)-malonamide ((βCD)$_2$Ma) and *N*,*N*'-bis-(6^{A}-deoxy-6^{A}-β-cyclodextrinyl)-succinamide ((βCD)$_2$Sc), have intermediate tether lengths. The complexation of TNS$^-$ by these linked cyclodextrin hosts is considered in Chapter 3. In Chapter 4, the complexation of MO$^-$ and TR$^-$ by (βCD)$_2$Ur, (βCD)$_2$Ox and (βCD)$_2$Ox is discussed.

An understanding of the factors influencing the selectivities of linked cyclodextrin dimers and the stabilities of their complexes, should be furthered by this investigation of the effects that variation in guest structure and tether length have on complexation.

These studies should enable information to be gained on the requirements for multiple recognition sites to reinforce each other. In particular, the additivity of hydrophobic and coordination interactions, in metallocyclodextrin systems, and cooperative binding between the two hydrophobic cavities of linked cyclodextrin dimers are considered.

References

1. R. Ueoka, Y. Matsumoto, K. Harada, H. Akahoshi, Y;. Ihara and Y. Kato, *J. Am. Chem. Soc.*, 1992, **114**, 8339.

2. *Frontiers in Supramolecular Organic Chemistry and Phtotochemistry*, eds. H.-J. Schneider and H. Dürr, VCH Publishers, New York, 1991.

3. W. Saenger, *Angew. Chem. Int. Ed. Engl.*, 1980, **19**, 344 and references therein.

4. *Inclusion Compounds*, eds. J. L. Atwood, J. E. D. Davies and D. D. MacNicol, Academic Press, London, 1984, vol. 2.

5. *Inclusion Compounds*, eds. J. L. Atwood, J. E. D. Davies and D. D. MacNicol, Academic Press, London, 1984, vol. 3.

6. *Inclusion Phenomena and Molecular Recognition*, ed. J. L. Atwood, Plenum Press, New York, 1990.

7. J. M. Coterón, C. Vicent, C. Bosso and W. Penadés, *J. Am. Chem. Soc.*, 1993, **115**, 10066.

8. R. J. Clarke, J. H. Coates and S. F. Lincoln, *J. Chem. Soc., Faraday Trans. 1*, 1986, **82**, 2333.

9. A. Harada, M. Furue and S-I. Nozakura, *Polymer J.*, 1980, **12**, 29.

10. R. Corradini, A. Dossena, G. Impellizzeri, G. Maccarrone, R. Marchelli, E. Rizzarelli, G. Sartor and G. Vecchio, *J. Am. Chem. Soc.*, 1994, **116**, 10267.

11. R. Breslow and B. Zhang, *J. Am. Chem. Soc.*, 1992, **114**, 5882.

12. F. Schardinger, *Wien. Klin. Wochenschr.*, 1904, **17**, 207.

13. F. Schardinger, *Zentralbl. Bakteriol. Parasitenkd. Infektionskr. Hyg. II*, 1911, **29**, 188.

14. K. Freudenberg and M. Meyer-Delius, *Ber. Dtsch. Chem. Ges.*, 1938, **71**, 1596; K. Freudenberg, E. Plankenhorn and H. Knauber, *Chem. Ind. (London)*, 1947, 713; *Justus Liebigs Ann. Chem.*, 1947, **558**, 1.

15. D. French, M. L. Levine, J. H. Pazur and E. Norberg, *J. Am. Chem. Soc.*, 1949, **71**, 353.

16. A. Villiers, *C. R. Acad. Sci.*, 1891, **112**, 536.

17. D. French and M. Levine, J. Pazur, *J. Am. Chem. Soc.*, 1949, **71**, 356.

18. D. French and R. E. Rundle, *J. Am. Chem. Soc.*, 1942, **64**, 1651.

19 K. Freudenberg and F. Cramer, *Z. Naturforsch. B 3*, 1948, 464.

20. S. Li and W. C. Purdy, *Chem. Rev.*, 1992, **92**, 1457 and references therein.

21. A. O. Pulley and D. French, *Biochem. Biophys. Res. Commun.*, 1961, **5**, 11.

22. P. R. Sundarajan and V. S. R. Rao, *Carbohydr. Res.*, 1970, **13**, 351.

23. R. Breslow, *Israel J. Chem.*, 1992, **32**, 23.

24. R. Breslow, *Recl. Trav. Chim. Pays-Bas*, 1994, **113**, 493.

25. I. Tabushi, *Acc. Chem. Res.*, 1982, **15**, 66.

26. K. Linder and W. Saenger, *Angew. Chem. Int. Ed.*, 1978, **17**, 694.

27. I. Tabushi and Y. Kuroda, *Adv. Catal.*, 1983, **32**, 417 and references therein.

28. D. Duchene and D. Wouessidjewe, *J. Coord. Chem.*, 1992, **27**, 223.

29. W. Saenger, C. Niemann, R. Herbst, W. Hinrichs and T. Steiner, *Pure & Appl. Chem.*, 1993, **65**, 809.

30. T. Steiner and W. Saenger, *J. Am. Chem. Soc.*, 1992, **114**, 10146.

31. R. I. Gelb, L. M. Schwartz, J. J. Bradshaw and D. A. Laufer, *Bioorg. Chem.*, 1980, **9**, 299.

32. M. Sakurai, M. Kitagawa, H. Hoshi, Y. Inoue and R. Chûjô, *Chem. Lett.*, 1988, 895.

33. M. Sakurai, M. Kitagawa, H. Hoshi, Y. Inoue and R. Chûjô, *Carbohydr. Res.*, 1990, **198**, 181.

34. F. Cramer, *Einschlussverbindungen*, Springer, Heidelberg 1954.

35. F. Cramer and H. Hettler, *Naturwissenschaften*, 1967, **54**, 625.

36. F. Cramer and F. M. Henglein, *Chem. Ber.*, 1957, **90**, 2561.

37. P. Mu, T. Okada, N. Iwami and Y. Matsui, *Bull. Chem. Soc. Jpn.*, 1993, **66**, 1924.

38. R. P. Rohrbach, L. J. Rodriguez, E. M. Eyring and J. F. Wojcik, *J. Phys. Chem.*, 1977, **81**, 944.

39. Y. Yamashoji, M. Fujiwara, T. Matsushita and M. Tanaka, *Chem. Lett.*, 1993, 1029.

40. P. S. Bates, R. Kataky and D. Parker, *J. Chem. Soc., Chem. Commun.*, 1993, 691.

41. F. Cramer and F. M. Henglein, *Angew. Chem.*, 1956, **68**, 649.

42. T. A. Gadosy and O. S. Tee, *J. Chem. Soc., Perkin Trans. 2*, 1994, 715.

43. L. Tong, Z. Hou, Y. Inoue and A. Tai, *J. Chem. Soc., Perkin Trans. 2*, 1992, 1253.

44. D. Zhang, J. Chen, Y. Yang, R Cai, X. Shen and S. Wu, *J. Inclusion Phenom. Mol. Recognit. Chem.*, 1993, **16**, 245; Z. Yoshida, H. Takekuma, S. Takekuma and Y. Matsubara, *Angew. Chem. Int. Ed. Engl.*, 1994, **33**, 1597.

45. I. Tabushi, Y. Kuroda and T. Mizutani, *Tetrahedron*, 1984, **40**, 545.

46. M. D. Johnson, C. A. McIntosh and V. C. Reinsborough, *Aust. J. Chem.*, 1994, **47**, 187.

47. H-J. Schneider, T. Blatter and S. Simova, *J. Am. Chem. Soc.*, 1991, **113**, 1996.

48. G. Uccello-Barretta, C. Chiavacci, C. Bertucci and P. Salvadori, *Carbohydr. Res.*, 1993, **243**, 1.

49. M. G. Usha and R. J. Wittebort, *J. Am. Chem. Soc.*, 1992, **114**, 1541.

50. Y. Kotake and E. G. Janzen, *J. Am. Chem. Soc.*, 1992, **114**, 2872.

51. V. Crescenzi, A. Gamini, A. Palleschi, and R. Rizzo, *Gazz. Chim. Ital.*, 1986, **116**, 435.

52. K. Kano, K. Yashiyasu, H. Yasuoka, S. Hata and S. Hashimoto, *J. Chem. Soc. Perkin Trans. 2*, 1992, 1265.

53. A. V. Eliseev, G. A. Iacobucci, N. A. Khanjin and F. M. Menger, *J. Chem. Soc., Chem. Commun.*, 1994, 2051.

54. Y. Inoue, T. Hakushi, Y. Liu, L.-H. Tong, B.-J. Shen and D.-S. Jin, *J. Am. Chem. Soc.*, 1993, **115**, 475.

55. S. Das, K. G. Thomas, M. V. George and P. V. Kamat, *J. Chem. Soc. Faraday Trans.*, 1992, **88**, 3419.

56. A. Granados and R. H. de Rossi, *J. Org. Chem.*, 1993, **58**, 1771.

57. K. Harata, *Bull. Chem. Soc. Jpn.*, 1976, **49**, 1493; K. Harata and H. Uedaira, *Nature (London)*, 1975, **253**, 190.

58. G. Wenz and B. Keller, *Angew. Chem. Int. Ed. Engl.*, 1992, **31**, 197.

59. R. S. Wylie and D. H. Macartney, *J. Am. Chem. Soc.*, 1992, **114**, 3136; F. Stoddart, *Angew. Chem. Int. Ed. Engl.*, 1992, **31**, 846.

60. B. Zhang and R. Breslow, *J. Am. Chem. Soc.*, 1993; **115**, 9353.

61. R. I. Gelb, L. M. Schwartz, B. Cardelino, H. S. Fuhrman, R. F. Johnson and D. A. Laufer, *J. Am. Chem. Soc.*, 1981, **103**, 1750.

62. R. C. Petter, C. T. Sikorski and D. H. Waldeck, *J. Am. Chem. Soc.*, 1991, **113**, 2325.

63. R. Breslow, N. Greenspoon, T. Guo and R. Zarzycki, *J. Am. Chem. Soc.*, 1989, **111**, 8296.

64. A. Muñoz de la Peña, F. Salinas, M. J. Gómez, M. I. Acedo and M. Sánchez Peña, *J. Inclusion Phenom. Mol. Recognit. Chem.*, 1993, **15**, 131.

65. H.-J. Buschmann and E. Schollmeyer, *J. Inclusion Phenom. Mol. Recognit. Chem.*, 1992, **14**, 91.

66. A. F. D. de Namor, D. A. P. Tanaka, L. N. Regueira and I. G. Orellana, *J. Chem. Soc., Faraday Trans. 2*, 1992, **88**, 1665.

67. B.-L. Poh and Y. M. Chow, *J. Inclusion Phenom. Mol. Recognit. Chem.*, 1992, **14**, 85.

68. J. W. Park and K. H. Park, *J. Inclusion Phenom. Mol. Recognit. Chem.*, 1994, **17**, 277.

69. R. Breslow, S. Halfon and B. Zhang, *Tetrahedron*, 1995, **51**, 377.

70. K. M. Tawarah and A. A. Wazwaz, *Ber. Bunsenges. Phys. Chem.*, 1993, **97**, 727.

71. K. M. Tawarah and A. A. Wazwaz, *J. Chem. Soc., Faraday Trans.*, 1993, **89**, 1729.

72. K. Hattori, K. Takahashi and N. Sakai, *Bull. Chem. Soc. Jpn.*, 1992, **65**, 2690.

73. A. V. Eliseev and H.-J. Schneider, *Angew. Chem. Int. Ed. Engl.*, 1993, **32**, 1331.

74. R. Breslow, P.J. Duggan and J.P. Light, *J. Am. Chem. Soc.*, 1992, **114**, 3982.

75. R. Breslow and S. Halfon, *Proc. Natl. Acad. Sci. USA*, 1992, **89**, 6916.

76. B. Siegel and R. Breslow, *J. Am. Chem. Soc.*, 1975, **97**, 6869.

77. F. Hamada, Y. Kondo, K. Ishikawa, H. Ito, I. Suzuki, T. Osa and A. Ueno, *J. Inclusion Phenom. Mol. Recognit. Chem.*, 1994, **17**, 267.

78. R. J. Bergeron, M. A. Channing and K. A. McGovern, *J. Am. Chem. Soc.*, 1978, **100**, 2878.

79. M. Suzuki and Y. Sasaki, *Chem. Pharm. Bull.*, 1979, **27**, 609.

80. K. Mochida and Y. Matsui, *Chem. Lett.*, 1976, 963.

81. K. Harata, F. Hirayama, H. Arima, K. Uekama and T. Miyaji, *J. Chem. Soc., Perkin Trans. 2*, 1992, 1159.

82. S. E. Brown, J. H. Coates, P. A. Duckworth, S. F. Lincoln, C. J. Easton and B. L. May, *J. Chem. Soc., Faraday Trans.*, 1993, **89**,1035.

83. T. Yagi, R. Aoshima, M. Kuwahara and H. Shibata, *J. Inclusion Phenom. Mol. Recognit. Chem.*, 1993, **16**, 231.

84. I. Tabushi, Y. Yiyosuke, T. Sugimoto and K. Yamamura, *J. Am. Chem. Soc.*, 1978, **100**, 916.

85. D. W. Armstrong, T. J. Ward, R. D. Armstrong and T. E. Beesley, *Science*, 1986, **232**, 1132.

86. G. Impellizzeri, G. Maccarrone, E. Rizzarelli, G. Vecchio, R. Corradini and R. Marchelli, *Angew. Chem. Int. Ed. Engl.*, 1991, **30**, 1348.

87. V. Cucinotta, F. D'Alessandro, G. Impellizzeri and G. Vecchio, *J. Chem. Soc., Chem. Commun.*, 1992, 1743.

88. I. Tabushi, Y. Kuroda and T. Mizutani, *J. Am. Chem. Soc.*, 1986, **108**, 4514.

89. I. Tabushi, *Pure & Appl. Chem.*, 1986, **58**, 1529.

90. F. Cramer, *Chem. Ber.*, 1953, **86**, 1576.

91. F. Cramer and W. Dietsche, *Chem. Ber.*, 1959, **92**, 378.

92. J. Szejtli, *Cyclodextrin Technology*, Kluwer, Dordrecht, 1988.

93. J. Szejtli, *Cyclodextrins and Their Inclusion Complexes*, Akadémiai Kiadó, Budapest, 1982.

94. J. Szejtli, *J. Inclusion Phenom. Mol. Recognit. Chem.*, 1992, **14**, 25.

95. R. Kataky, P.S. Bates and D. Parker, *Analyst*, 1992, **117**, 1313.

96. A. Ueno, T. Kuwabara, A. Nakamura and F. Toda, *Nature*, 1992, **356**, 136.

97. L. J. Cline-Love, M. L. Grayeski, J. Noroski and R. Weinberger, *Anal. Chim. Acta*, 1985, **170**, 3.

98. *Ordered Media in Chemical Separations*, eds. W. L. Hinze and D. W. Armstrong, American Chemical Society, Washington, D.C., 1987.

99. S. Sawata and M. Komiyama, *J. Phys. Org. Chem.*, 1992, **5**, 502.

100. R. Kuhn and S. Hoffstetter-Kuhn, *Chromatogr.*, 1992, **34**, 505.

101. V. Schurig and H.-P. Nowotny, *Angew. Chem. Int. Ed. Engl.*, 1990, **29**, 939.

102. R. Breslow and L. E. Overman, *J. Am. Chem. Soc.*, 1970, **92**, 1075.

103. E. T. Chen and H. L. Pardue, *Anal. Chem.*, 1993, **65**, 2563; M. Komiyama and Y. Matsumoto, *Chem. Lett.*, 1989, 719; R. Breslow and S. Singh, *Bioorg. Chem.*, 1988, **16**, 408.

104. E. U. Akkaya and A. W. Czarnik, *J. Am. Chem. Soc.*, 1988, **110**, 8553.

105. R. Breslow and B. Zhang, *J. Am. Chem. Soc.*, 1994, **116**, 7893.

106. I. Tabushi, Y. Kuroda and A. Mochizuki, *J. Am. Chem. Soc.*, 1980, **102**, 1152.

107. I. Tabushi and Y. Kuroda, *J. Am. Chem. Soc.*, 1984, **106**, 4580.

108. T. Furuki, F. Hosokawa, M. Sakurai, Y. Inoue and R. Chûjô, *J. Am. Chem. Soc.*, 1993, **115**, 2903.

109. I. Tabushi, N. Shimizu, T. Sugimoto, M. Shiozuka and K. Yamamura, *J. Am. Chem. Soc.*, 1977, **99**, 7100.

110. H. Hirai and H. Mihori, *Chem. Lett.*, 1992, 1523.

111. Y. Matsui, T. Yokoi and K. Mochida, *Chem. Lett.*, 1976, 1037.

112. H. Ye, W. Tong and V. T. D'Souza, *J. Chem. Soc. Perkin Trans. 2*, 1994, 2431.

113. F. M. Menger and M. A. Dulany, *Tetrahedron Lett.*, 1985, **26**, 267; H. Murai, Y. Yamamoto and Y. J. I'Haya, *Can. J. Chem.*, 1991, **69**, 1643.

114. G.L. Eichhorn, *Coord. Chem. Rev.*, 1993, **128**, 167; B. L. Vallee and D. S. Auld, in *Methods in Protein Sequence Analysis*, eds. H. Jörnvall, J.-O. Höög and A.-M. Gustavsson, Birkhäuser Verlag, Basel, 1991, p 363.

115. J. J. R. Frausto da Silva and R. J. P. Williams, *The Biological Chemistry of The Elements*, Oxford University Press, Oxford, 1991.

116. E. U. Akkaya and A. W. Czarnik, *J. Phys. Org. Chem.*, 1992, **5**, 540.

117. R. Breslow, *Cold Spring Harb. Symp. Quant. Biol.*, 1987, **52**, 75.

118. R. Breslow, *Acc. Chem. Res.*, 1991, **24**, 317.

119. S. Tamagaki, A. Katayama, M. Maeda, N. Yamamoto and W. Tagaki, *J. Chem. Soc., Perkin Trans. 2*, 1994, 507.

120. I. Tabushi, *Coord. Chem. Rev.*, 1988, **86**, 1.

121. C.-J. Yoon, H. Ikeda, R. Kojin, T. Ikeda and F. Toda, *J. Chem. Soc., Chem. Commun.*, 1986, 1080.

122. D.L. Dick, T. Venkata, S. Rao, D. Sukumaran and D.S. Lawrence, *J. Am. Chem. Soc.*, 1992, **114**, 2664.

123. M. Ueno, A. Murakami, K. Makino and T. Morii, *J. Am. Chem. Soc.*, 1993, **115**, 12575.

124. R. Breslow and S. Chung, *J. Am. Chem. Soc.*, 1990, **112**, 9659.

125. A. P. Croft and R. A. Bartsch, *Tetrahedron*, 1983, **39**, 1417.

126. M. T. Reetz and J. Rudolph, *Tetrahedron: Asymmetry*, 1993, **4**, 2405.

127. M. Sawamura, K. Kitayama and Y. Ito, *Tetrahedron: Asymmetry*, 1993, **4**, 1829.

128. A.W. Coleman, C. Ling and m. Miocque, *Angew. Chem. Int. Ed. Engl.*, 1992, **31**, 1381.

129. K. Hirotsu, T. Higuchi, K. Fujita, A. Shinoda, T. Imoto and I. Tabushi, *J. Org. Chem.*, 1982, **47**, 1143.

130. J. Canceill, L. Jullien, L. Lacombe and J. Lehn, *Helv. Chim. Acta.*, 1992, **75**, 791.

131. P. S. Bates, R. Kataky and D. Parker, *J. Chem. Soc. Perkin Trans. 2*, 1994, 669.

132. K. Hamasaki, A. Ueno, F. Toda, I. Suzuki and T. Osa, *Bull. Chem. Soc. Jpn.*, 1994, **67**, 516; Y. Wang, T. Ikeda, H. Ikeda, A. Ueno and F. Toda, *Bull. Chem. Soc. Jpn.*, 1994, **67**, 1598; K. Hamasaki, A. Ueno and F. Toda, *J. Chem. Soc., Chem. Commun.*, 1993, 331.

133. T. Kuwabara, A. Matsushita, A. Nakamura, A. Ueno and F. Toda, *Chem. Lett.*, 1993, 2081; I. Suzuki, Y. Sakurai, M. Ohkubo, A. Ueno and T. Osa, *Chem. Lett.*, 1992, 2005; Y. Wang, T. Ikeda, A. Ueno and F. Toda, *Chem. Lett.*, 1992, 863; T. Kuwabara, A. Nakamura, A. Ueno and F. Toda, *J. Phys. Chem.*, 1994, **98**, 6297.

134. I. Suzuki, M. Ohkubo, A. Ueno and T. Osa, *Chem. Lett.*, 1992, 269; A. Ueno, S. Minato and T. Osa, *Anal. Chem.*, 1992, **64**, 2562.

135. Y. Wang, T. Ikeda, A. Ueno and F. Toda, *Tetrahedron Lett.*, 1993, **34**, 4971.

136. T. Kuwabara, A. Nakamura, A. Ueno and F. Toda, *J. Chem. Soc., Chem. Commun.*, 1994, 689.

137. M. N. Berberan-Santos, J. Canceill, J-C. Brochon, L. Jullien, J-M. Lehn, J. Pouget, P. Tauc and B. Valeur, *J. Am. Chem. Soc.*, 1992, **114**, 6427; M. N. Berberan-Santos, J. Pouget, B. Valeur, J. Canceill, L. Jullien and J-M. Lehn, *J. Phys. Chem.*, 1993, **97**, 11376.

138. D. M. Gravett amd J. E. Guillet, *J. Am. Chem. Soc.*, 1993, **115**, 5970.

139. R. Deschenaux, M. M. Harding and T. Ruch, *J. Chem. Soc. Perkin Trans. 2*, 1993, 1251.

140. Z. Pikramenou, J. Yu, R. B. Lessard, A. Ponce, P. A. Wong and D. G. Nocera, *Coord. Chem. Rev.*, 1994, **132**, 181; Z. Pikramenou and D. G. Nocera, *Inorg. Chem.*, 1992, **31**, 532.

141. Y. Kuroda, M. Ito, T. Sera and H. Ogoshi, *J. Am. Chem. Soc.*, 1993, **115**, 7003.

142. I. Willner and Z. Goren, *J. Chem. Soc.*, 1983,1469.

143. B. Siegel, *J. Inorg. Nucl. Chem.*, 1979, **41**, 609.

144. Y. Kuroda, Y. Egawa, H. Seshimo and H. Ogoshi, *Chem. Lett.*, 1994, 2361.

145. L. Weber, I. Imiolczyk, G. Haufe, D. Rehorek and H. Hennig, *J. Chem. Soc., Chem. Commun.*, 1992, 301.

146. Y. Nagata, T. Aso, T. Kinoshita, Y. Tsujita, H. Yoshimizu and N. Minoura, *Bull. Chem. Soc. Jpn.*, 1994, **67**, 495.

147. V. Cucinotta, F. D'Alessandro, G. Impellizzeri, G. Pappalardo, E. Rizzarelli and G. Vecchio, *J. Chem. Soc., Chem. Commun.*, 1991, 293.

148. S. Divakar, *J. Inclusion Phenom. Mol. Recognit. Chem.*, 1994, **17**, 119; R. Fuchs, N. Habermann and P. Klüfers, *Angew. Chem. Int. Ed. Engl.*, 1993, **32**, 852; M. McNamara and N.R. Russell, *J. Inclusion Phenom. Mol. Recognit. Chem.*, 1992, **13**, 145.

149. K. Yamanari, M. Nakamichi and Y. Shimura, *Inorg. Chem.*, 1989, **28**, 248.

150. H. Yamamura, T. Ezuka, Y. Kawase, M. Kawai, Y. Butsugan and K. Fujita, *J. Chem. Soc., Chem. Commun.*, 1993, 636.

151. R. S. Wylie and D. H. Macartney, *Inorg. Chem.*, 1993, **32**, 1830.

152. R. Fornasier, E. Scarpa, P. Scrimin, P. Tecilla and U. Tonellato, *J. Inclusion Phenom. Mol. Recognit. Chem.*, 1992, **14**, 205.

153. M. Komiyama and Y. Matsumoto, *Chem. Lett.*, 1989, 719.

154. S. E. Brown, J. H. Coates, C. J. Easton and S. F. Lincoln, *J. Chem. Soc. Faraday Trans.*, 1994, **90**, 739.

155. S. E. Brown, J. H. Coates, C. J. Easton, S. J. van Eyk, S. F. Lincoln, B. L. May, M. A. Stile, C. B. Whalland and M. L. Williams, *J. Chem. Soc., Chem. Commun.*, 1994, 47.

156. M. I. Rosenthal and A. W. Czarnik, *J. Inclusion Phenom. Mol. Recognit. Chem.*, 1991, **10**, 119.

157. R. P. Bonomo, V. Cucinotta, F. D'Alessandro, G. Impellizzeri, G. Maccarrone, G. Vecchio and E. Rizzarelli, *Inorg. Chem.*, 1991, **30**, 2708.

158. H-J. Schneider and F. Xiao, *J. Chem. Soc. Perkin Trans. 2*, 1992, 387.

159. R. Breslow and S. Singh, *Bioorg. Chem.*, 1988, **16**, 408.

160. P. Klüfers and J. Schuhmacher, *Angew. Chem. Int. Ed. Engl.*, 1994, **33**, 1863.

161. T. J. Wenzel, M. S. Bogyo and E. L. Lebeau, *J. Am. Chem. Soc.*, 1994, **116**, 4858.

162. M. Yashiro, T. Takarada, S. Miyama and M. Komiyama, *J. Chem. Soc., Chem. Commun.*, 1994, 1757.

163. A.W. Coleman, C. Ling and M. Micoque, *J. Coord. Chem.*, 1992, **26**, 137.

164. I. Suzuki, Q. Chen, A. Ueno and T. Osa, *Bull. Chem. Soc. Jpn.*, 1993, **66**, 1472.

165. R.P. Bonomo, V. Cucinotta, F. D'Alessandro, G. Impellizzeri, G. Maccarrone, E. Rizzarelli and G. Vecchio, *J. Inclusion Phenom. Mol. Recognit. Chem.*, 1993, **15**, 167.

166. S. E. Brown, C. A. Haskard, C. J. Easton and S. F. Lincoln, *J. Chem. Soc. Faraday Trans.*, 1995, **91**, 1013.

167. Y. Chao, Ph.D. Thesis, Columbia University, New York, 1972.

168. C. T. Sikorski and R. C. Petter, *Tetrahedron Lett.*, 1994, **35**, 4275.

169. T. Jiang, D. K. Sukumaran, S. Soni and D. S. Lawrence, *J. Org. Chem.*, 1994, **59**, 5149.

170. T. Jiang and D. S. Lawrence, *J. Am. Chem. Soc.*, 1995, **117**, 1857.

171. K. Fujita, S. Ejima and T. Imoto, *J. Chem. Soc., Chem. Commun.*, 1984, 1277.

172. K. Fujita, S. Ejima and T. Imoto, *Chem. Lett.*, 1985, 11.

173. R. Deschenaux, A. Greppi, T. Ruch, H. Kriemler, F. Raschdorf and R. Ziessel, *Tetrahedron Lett.*, 1994, **35**, 2165.

174. I. Tabushi, Y. Kuroda and K. Shimokawa, *J. Am. Chem. Soc.*, 1979, **101**, 1614.

175. F. Venema, C. M. Baselier, E. van Dienst, B. H. M. Ruël, M. C. Feiters, J. F. J. Engbersen, D. N. Reinhoudt and R. J. M. Nolte, *Tetrahedron Lett.*, 1994, **35**, 1773.

176. F. Venema, C. M. Baselier, M. C. Feiters and R. J. M. Nolte, *Tetrahedron Lett.*, 1994, **35**, 8661.

177. Y. Wang, A. Ueno and F. Toda, *Chem. Lett.*, 1994, 167.

178. J. H. Coates, C. J. Easton, S. J. van Eyk, S. F. Lincoln, B. L. May, C. B. Whalland and M. L. Williams, *J. Chem. Soc., Perkin Trans. 1*, 1990, 2619.

179. H-J. Schneider and F. Xiao, *J. Chem. Soc. Perkin Trans.* 2, 1992, 387.

180. D. F. Schriver, P. W. Atkins and C. H. Langford, *Inorganic Chemistry*, 2nd edn., Oxford University Press, Oxford, 1994.

181. L. E. Orgel, *An Introduction to Transition-Metal Chemistry: Ligand-Field Theory*, John Wiley & Sons, New York, 1960, p15.

182. R. Breslow and T. Guo, *Tetrahedron Lett.*, 1987, **28**, 3187.

183. A. Harada, M. Furue and S. Nozakura, *Macromolec.*, 1976, **9**, 701.

184. A. Harada, M. Furue and S. Nozakura, *Macromolec.*, 1977, **10**, 676.

185. A. Harada, M. Furue and S. Nozakura, *Macromolec.*, 1976, **9**, 705.

186. W. Xu, J. N. Demas, B. A. DeGraff and M. Whaley, *J. Phys. Chem.*, 1993, **97**, 6546.

187. T. C. Werner and I. M. Warner, *J. Inclusion Phenom. Mol. Recognit. Chem.*, 1994, **18**, 385.

188. A. Harada, M. Furue and S. Nozakura, *Polymer J.*, 1981, **13**, 777.

189. J. Szeman, H. Ueda, J. Szejtli, E. Fenyvesi, T. Machida and T. Nagai, *Chem. Pharm. Bull.*, 1987, **35**, 282.

CHAPTER 2

Complexation of Amino Acids by the Metallocyclodextrins of βCDpn and βCDtren

2.1 Introduction

A number of metallocyclodextrins have been reported in the literature (Section 1.3.3), and studies on these novel hosts have primarily considered their catalytic activity and use as metalloprotein models. Metallocyclodextrins are also potentially good enantioselective hosts, as a result of the combined effect of the chiral cyclodextrin cavity and the extra recognition point provided by the metal ion. Recently their enantiomeric complexation characteristics have attracted attention.[1-5] The importance of the metal for enantioselection in addition to the chirality of the cyclodextrin is clearly demonstrated in the case of 6^A-(3-aminopropylamino)-6^A-deoxy-βCD (βCDpn), which shows no enantioselectivity in complexing tryptophan, but upon forming a Ni^{2+} complex, shows a 10-fold enantioselectivity in favour of the (*S*)-tryptophan anion.[3,4] This is the highest enantioselectivity reported for a metallocyclodextrin.

Simple metallocyclodextrins and their complexes provide an opportunity to study the factors affecting metallocyclodextrin stability and guest binding in some detail. The interactions of the guest with the metal centre and the hydrophobic cavity may reinforce each other leading to increased complex stability or enantioselection or both. Such reinforcement is sometimes termed cooperative binding.

To further investigate the complexation and enantioselection of guest molecules by metallocyclodextrins, two monosubstituted metal binding cyclodextrins, βCDpn and βCDtren (Fig. 2.1), were chosen. A primary hydroxyl of βCD is replaced by 3-aminopropylamine (pn) to form βCDpn, and by *N*,*N*-bis(2-aminoethyl)aminoethylamine

(tren) (Appendix, (19)) to form βCDtren. These substituents offer structural flexibility for interaction with guests, and provide an opportunity for chelation of metal ions in close proximity to the cavity.

Firstly, the effect of the guest structure was considered by comparing the binding of (*R/S*)-histidine (Fig. 2.1) to the Cu^{2+} metallocyclodextrin derivative of βCDpn, $[Cu(\beta CDpn)]^{2+}$, with that of (*R/S*)-phenylalanine and (*R/S*)-tryptophan previously reported.[3-5] These amino acids all have a chiral centre and are capable of coordinating to a metal ion through at least two binding sites. They all possess an aromatic side chain, which appears to be important for enantioselection,[1,2,6] but the size of the aromatic portion varies. Histidine (His) contains a five-membered polar imidazole ring, whereas phenylalanine (Phe) contains a phenyl ring and tryptophan (Trp) a larger indole moiety (Fig. 2.1). Complexation of phenylalanine and tryptophan by the Co^{2+}, Ni^{2+} and Zn^{2+} metallocyclodextrin derivatives has also been reported,[4,5] however the study of histidine is limited to complexation by the Cu^{2+} metallocyclodextrin derivative. This is because the three titratable protons of $HisH_3^{2+}$ generate more protonic and complexation equilibria which result in more minor species in solution than do phenylalanine or tryptophan, and it was considered that the higher stabilities associated with the Cu^{2+} complexes of amine and amino acid ligands, presented the best opportunity for the detection of these minor species.

Secondly, the influence of the nature of the metal centre was investigated using the metallocyclodextrins formed by βCDtren with four divalent transition metal ions. Metalloenzymes utilise divalent metal ions, typically Zn^{2+},[7] as their metal centres. While Co^{2+}, Ni^{2+} and Cu^{2+} seldom fill this role, they were selected for this study because their closely related size and electronic structure allow an investigation of the effects of variation in metal ion size and *d* electron configuration on the stability and enantioselectivity of these metallocyclodextrins. The guest, (*R/S*)-tryptophan, was chosen as it forms a snug fit in the βCD cavity by comparison with the other amino acids considered above.

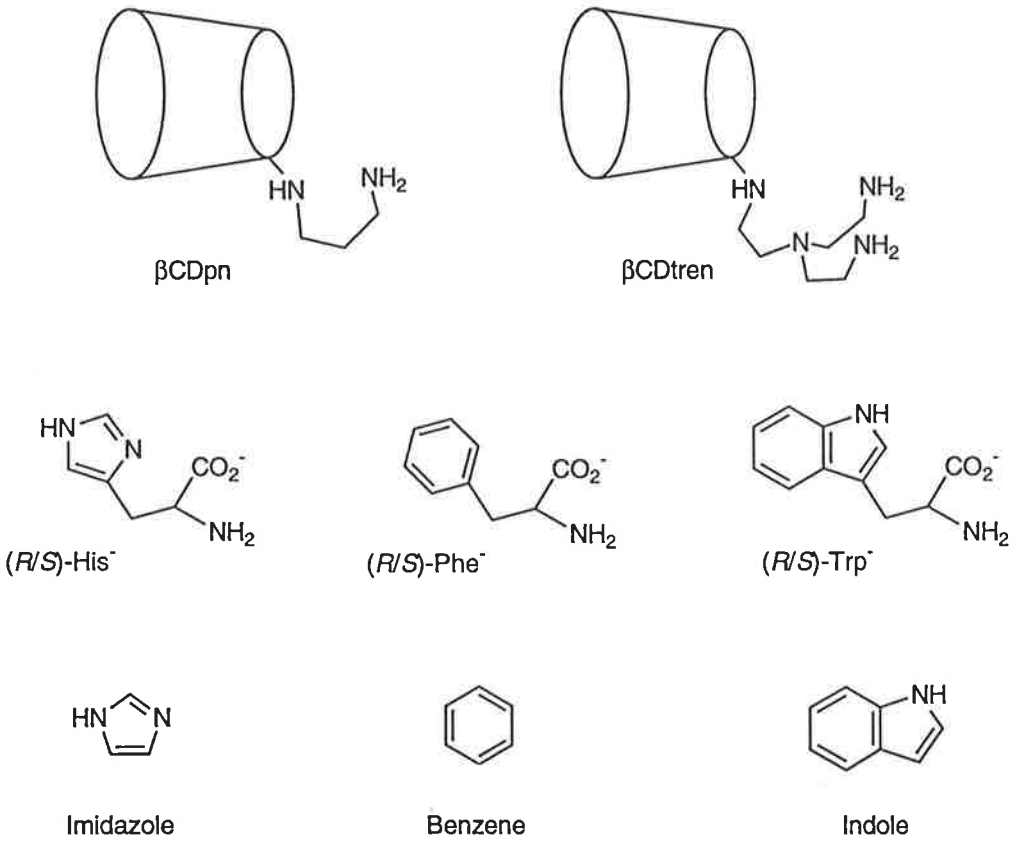

Figure 2.1 *The modified cyclodextrin hosts and amino acid guests studied. Comparisions are made with imidazole, benzene and indole which represent the aromatic portions of histidine, phenylalanine and tryptophan respectively. (Amine substituents of* βCDpn *and* βCDtren *are exaggerated in size by comparison with the* βCD *annulus.)*

Potentiometric titration, commonly used to investigate the binding of metal ions to ligands in solution, can be used to study metallocyclodextrins. The titrimetric technique relies on either the protonation constant of an equilibrium constituent changing on complexation, or the complexation constants for the constituent and its protonated form differing, or both, to produce a pH change (see Fig. 2.6). The differences between the pH profiles arising from titration of acidified solutions, containing various combinations of the complexing species, against NaOH, allows the stabilities of the complexes formed to be calculated using the program SUPERQUAD,[8] which minimises the error-square sum of the differences between measured and calculated electrode potentials.

Here the complexing species are: cyclodextrin (βCD, βCDpn, βCDtren), amino acid (His, Phe, Trp) and metal ion (Co^{2+}, Ni^{2+}, Cu^{2+}, Zn^{2+}). In the pH range 2.0 – 11.5 many complexes of these species are found in aqueous solution and hence it was necessary to independently determine as many stability constants as possible. Protonation constants for the cyclodextrin and the amino acid were determined first, and fixed in the subsequent stability constant determinations. The stability constants for the binary systems: (i) cyclodextrin and either (*R*)- or (*S*)-amino acid, (ii) metal ion and amino acid, and (iii) metal ion and cyclodextrin, were then determined and fixed as constants in the ternary system. Finally the stability constants for the ternary system containing cyclodextrin, metal ion and either (*R*)- or (*S*)-amino acid were determined. All errors quoted for K (the mean of N runs) represent the standard deviation, $\sigma = ((\Sigma(K_i - K)^2)/(N-1))$ where K_i is a value from a single run for the best fit of the variation of pH with added volume of NaOH titrant obtained through SUPERQUAD, and i = 1,2,...,N.

A detailed discussion of the various equilibria now follows.

2.2 Complexation of Histidine, Phenylalanine and Tryptophan by βCDpn and its Cu^{2+} Metallo-cyclodextrin Derivative: Effect of the Amino Acid Structure

2.2.1 Protonation Constants

Successive protonation of the amino acid anion (A^-) results in the formation of a monoprotonated zwitterion (AH), a diprotonated cation (AH_2^+) and in the case of histidine a triprotonated cation (AH_3^{2+}). Protonation constants are derived from titration profiles similar to that shown for histidine in Fig. 2.2.

A tautomeric equilibrium exists for the imidazole ring of histidine.[9,10] The tautomer shown in Fig. 2.1 is the most abundant, especially in the pH region around neutrality.[10] The existence of an intramolecular hydrogen bond between the protonated

amino group and the unprotonated nitrogen of the imidazole ring was proposed to explain the effect ionisation of the amino group had on the tautomeric equilibrium constant.[9] However, thermodynamic parameters obtained through potentiometric measurements of pK_a values did not support this hypothesis and an ion-dipole interaction between the imidazole ring and the positively charged amino group was suggested as an alternative interaction.[10]

The logarithms of the protonation constants in Table 2.1 are equivalent to pK_a values, and compare reasonably well with literature values.[11] The high errors on the lower pK_a values result from the decreased electrode sensitivity at low pH which makes it difficult to determine such low pK_a values.

Table 2.1 *Protonation constants of histidine, phenylalanine and tryptophan in aqueous solution at 298.2 K and I = 0.10 mol dm^{-3} ($NaClO_4$).*

	log (K/dm^3 mol^{-1})		
Equilibrium	A = His[a]	A = Phe[b]	A = Trp[c]
$A^- + H^+ \rightleftharpoons AH$	9.07 ± 0.02	9.08	9.25 ± 0.04
$AH + H^+ \rightleftharpoons AH_2^+$	6.04 ± 0.05	2.3	2.3 ± 0.3
$AH_2^+ + H^+ \rightleftharpoons AH_3^{2+}$	2.1 ± 0.2	—	—

[a] Derived from data in the pH range 2.2 – 11.4. [b] Ref. 5. [c] Derived from data in the pH range 2.1 – 3.9 and 7.8 – 10.2.

A pH titration profile for determination of the protonation constants for βCDpn is shown in Fig. 2.2. The 3-aminopropylamine substituent of βCDpn can be successively protonated to form a monoprotonated cation ($\beta CDpnH^+$) and a diprotonated cation ($\beta CDpnH_2^+$), which are characterised in Table 2.2.

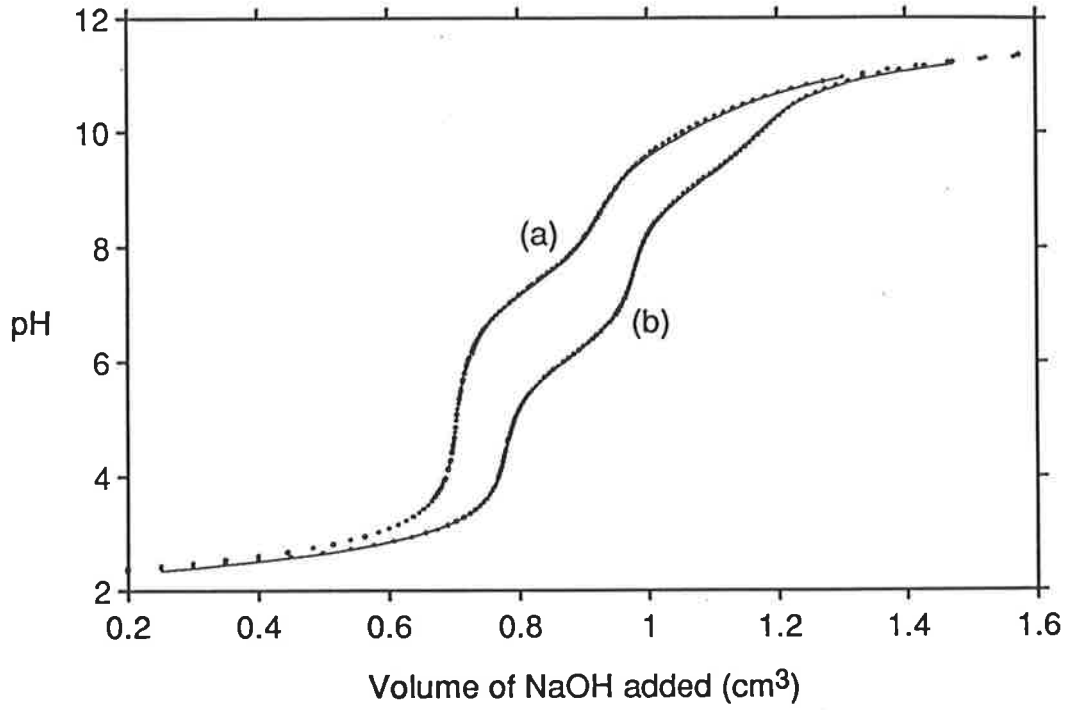

Figure 2.2 *Titration profiles of: (a)* $\beta CDpnH_2^{2+}$ *(2.00 x* 10^{-3} *mol* dm^{-3}*) and (b) (S)-*$HisH_3^{2+}$ *(2.00 x* 10^{-3} *mol* dm^{-3}*), each in aqueous 0.010 mol* dm^{-3} $HClO_4$ *and 0.090 mol* dm^{-3} $NaClO_4$*, against 0.100 mol* dm^{-3} *NaOH. The dots represent data points and the solid line represents the best fit to the algorithm arising from the equilibria shown in Tables 2.2 and 2.1, respectively.*

Table 2.2 *Protonation constants of* βCDpn *and pn in aqueous solution at 298.2 K and* $I = 0.10$ *mol* dm^{-3}.

	log (K/dm^3 mol^{-1})	
Equilibrium	B = βCDpn[a]	B = pn[b]
$B + H^+ \rightleftharpoons BH^+$	9.88 ± 0.01	10.52
$BH^+ + H^+ \rightleftharpoons BH_2^{2+}$	7.34 ± 0.02	8.74

[a] Derived from data in the pH range 6.2 – 10.9. Supporting electrolyte: $NaClO_4$.
[b] Ref. 11.

Over the pH range studied βCD is in the neutral form. The primary amine of βCDpn is more basic than the secondary amine.[12] In comparison with free pn, the basicity of both amines is decreased. A similar phenomenon is observed for 6^A-(2-aminoethylamino)-6^A-deoxy-βCD (Appendix, (2)) and 6^A-(2-(4-imidazolyl)-ethylamino)-6^A-deoxy-βCD (Appendix, (3)).[12,13] The bulky cyclodextrin unit may exert a steric effect on the protonation of the amino groups, interfering with protonation and with stabilisation of the cation by hydration, making these amines less basic. Intramolecular hydrogen bonding between the amino groups of the substituent and between these groups and the adjacent primary hydroxyl groups of the cyclodextrin may also produce a lower basicity as the nitrogen lone pair is less disposed to interact with an incoming proton. The 1D ^1H and ^{13}C NMR spectra of some related amino cyclodextrins[12,13] indicate that an intramolecular hydrogen bond within the substituent group is destroyed upon protonation, thus causing a decrease in basicity of the amine. The effect of amine substitution and of the cyclodextrin cavity are demonstrated by 6^A-(2-aminoethylamino)-6^A-deoxy-βCD, whose stepwise protonation constants, log (K/dm^3 mol^{-1}) = 8.92 and 5.56,[12] are decreased by comparison with 2-aminoethylamine, log (K/dm^3 mol^{-1}) = 9.89 and 7.10,[12] and *N*-methyl-2-aminoethylamine, log (K/dm^3 mol^{-1}) = 10.11 and 7.04.[11]

2.2.2 Complexation of Amino Acids by βCDpn

The log values of the stability constants derived from the best fit of the experimental data, for the complexation of the (*R*)- and (*S*)-amino acids by βCDpn are listed in Table 2.3. The corresponding values for βCD are included for comparison.

The phenyl moieties of Phe$^-$ and Trp$^-$ probably reside largely within the hydrophobic region of the cyclodextrin annulus in the βCD·Phe$^-$ and βCD·Trp$^-$ complexes.[14] Guests with larger hydrophobic surfaces are likely to have more extensive van der Waals interactions leading to increased complex stability, however, in these complexes the reverse is seen. The greater stability of βCD·Phe$^-$ over βCD·Trp$^-$ may indicate that the amino acid moiety of Trp$^-$ extends further from the annulus into the

aqueous environment than does that of Phe^-, such that Trp^- is more hydrated and the stability of βCD·Trp^- is lowered by comparison with that of βCD·Phe^-. No complexation of His^- by βCD was detected. This is consistent with the substantially lower stability constant of 2-7 $dm^3\ mol^{-1}$ reported for the inclusion of imidazole by βCD at pH 9.0,[15] relative to 196 and 184 $dm^3\ mol^{-1}$ reported for the inclusion of benzene[16] and indole,[14] respectively (see Fig. 2.1 for structures). Although the neutral form of imidazole is weakly bound by βCD, histidine would be expected to bind more strongly due to the amino and carboxylate functional groups which may hydrogen bond to the cyclodextrin. It appears that although the His^- ring is flat and possesses aromatic character, the ability of both the ring and the amino acid function of His^- to hydrogen bond with water, and possibly the smaller size of the ring, engender insufficient stability in βCD·His^- for its detection in this study.

Table 2.3 *Stability constants for the complexes of* βCD *and* βCDpn *with the (R)- and (S)-enantiomers of histidine, phenylalanine and tryptophan in aqueous solution at 298.2 K and I = 0.1 mol* dm^{-3} *(*$NaClO_4$*).*

	log (K/$dm^3\ mol^{-1}$)		
Equilibrium	A = His[a]	A = Phe[b]	A = Trp[c]
βCD + (*R*)-A^- ⇌ βCD·(*R*)-A^-	—	2.91 ± 0.08	2.33 ± 0.06
βCD + (*S*)-A^- ⇌ βCD·(*S*)-A^-	—	2.83 ± 0.06	2.33 ± 0.08
βCDpn + (*R*)-A^- ⇌ βCDpn·(*R*)-A^-	—	2.51 ± 0.07	3.41 ± 0.02
βCDpn + (*S*)-A^- ⇌ βCDpn·(*S*)-A^-	—	2.74 ± 0.05	3.40 ± 0.07
βCDpnH^+ + (*R*)-A^- ⇌ βCDpnH·(*R*)-A	2.50 ± 0.02	—	—
βCDpnH^+ + (*S*)-A^- ⇌ βCDpnH·(*S*)-A	2.37 ± 0.09	—	—
βCDpnH^+ + (*R*)-AH ⇌ βCDpnH·(*R*)-AH^+	2.31 ± 0.05	—	—
βCDpnH^+ + (*S*)-AH ⇌ βCDpnH·(*S*)-AH^+	2.18 ± 0.05	—	—

[a] Derived from data in the pH range 6.8 – 11.1. [b] Ref. 5. [c] Refs. 3 and 4.

The absence of protonated βCD complexes is consistent with literature reports which indicate that amino acid zwitterions do not include strongly, as shown by the stability constant of around 10 $dm^3\ mol^{-1}$ for the complexation of tryptophan by βCD at pH 8.9.[17]

The relative stabilities of the βCD and βCDpn complexes decrease in the sequence: βCDpn·Trp^- > βCD·Phe^- > βCDpn·Phe^- > βCD·Trp^-. The most probable structures for βCDpn·Phe^- and βCDpn·Trp^- place the aromatic group inside the cyclodextrin annulus where hydrophobic interactions occur, and the amino acid moiety in the vicinity of the 3-aminopropylamino substituent of βCDpn, where hydrogen bonding interactions with the amino and primary hydroxyl groups may occur. The 10-fold greater stability of βCDpn·Trp^- relative to βCD·Trp^- is consistent with these two interactions being additive in stabilising βCDpn·Trp^-. In contrast, βCD·Phe^- is more stable than βCDpn·Phe^- consistent with these interactions not being additive in their contributions to the stability of βCDpn·Phe^-. This may be attributed to the greater length of Trp^- allowing an optimisation of the two interactions in βCDpn·Trp^- while the shorter Phe^- constrains the interactions in βCDpn·Phe^- to be less favourable. Despite the coexistence of His^- and βCDpn at significant concentrations under the conditions of this study, no βCDpn·His^- complex was detected in the fitting range. This is probably for the same reasons discussed above for βCD·His^-. Nevertheless, protonated complexes, βCDpnH·His and βCDpnH·$HisH^+$, were detected.

Although the equilibria for formation of βCDpnH·His may alternatively be expressed as forming from βCDpn and HisH, and the equilibria for formation of βCDpnH·$HisH^+$ may be expressed as forming from βCDpnH_2^{2+} and His^- or βCDpn and $HisH_2^+$, those in Table 2.3 are considered to be the most likely. As the pK_as of βCDpnH^+ and HisH in the free states are 9.88 and 9.07 respectively, it is probable that the 3-aminopropylamino substituent of βCDpn is protonated in both βCDpnH·His and βCDpnH·$HisH^+$. The greater stability of βCDpnH·His over βCDpn·His^- may arise from the positive charge on βCDpnH^+ producing a greater dipole moment, relative to that of βCDpn, thus providing an increased electrostatic interaction with His^-. This effect

combined with the decreased hydration arising from charge neutralisation within the complex, stabilises βCDpnH·His. The stabilisation of βCDpnH·HisH$^+$ is less readily rationalised. Interestingly, 1D ^{1}H and ^{13}C NMR spectral data for the functionalised cyclodextrin, 6^A-(2-(4-imidazolyl)ethylamino)-6^A-deoxy-βCD (Appendix, (3)), show that interaction of the imidazole ring with the βCD cavity is promoted by an increase in the degree of protonation, resulting in its partial inclusion.[13] Such protonated complexes were not detected in the phenylalanine and tryptophan systems over the fitting range. This difference in behaviour appears to be at least partially associated with the absence of a phenyl ring in histidine as demonstrated by the βCD complexations discussed above.

Within experimental error, βCD does not discriminate thermodynamically between the (*R*)- and (*S*)- enantiomers. There is evidence in the literature for enantioselectivity occurring in the complexation of phenylalanine and tryptophan by αCD but none in the analogous βCD systems.[18] No enantioselectivity is shown by βCDpn for Trp$^-$, but it is slightly enantioselective in complexing (*S*)-Phe$^-$ over (*R*)-Phe$^-$. The enantioselectivity observed for the complexation of Phe$^-$ by βCDpn, despite the lack of enantioselectivity observed for the complexation of this guest by βCD, may be due to a change in orientation of the guest in the cavity due to the presence of the 3-aminopropylamino group. No significant enantioselectivity is seen for histidine.

2.2.3 Complexation of Cu^{2+} by Amino Acids

Complexes formed between Cu^{2+} and the amino acids are characterised by the stability constants listed in Table 2.4, and are in reasonable agreement with those in the literature.[11] An increase in stability constant with the size of the aromatic ring is observed for the mono and bis complexes of Phe$^-$ and Trp$^-$ with Cu^{2+}. Conversely, the analogous complexes of His$^-$ have greater stability, which may indicate a different mode of binding of His$^-$ to Cu^{2+} resulting from its potentially tridentate nature.

Phe$^-$ and Trp$^-$ probably coordinate as a five-membered chelate ring through the amino nitrogen and carboxylate oxygen. This may also occur with His$^-$, as may the

alternative coordination as a six-membered chelate ring through the imidazole nitrogen and the amino nitrogen.[19] Indeed, the most stable ligation for histidine results in a six-membered chelate ring,[20] having greater thermodynamic stability than a five-membered ring as the extra atom in the backbone produces less ring strain and hence enhanced stability. It is possible that all three of these donor groups may coordinate provided that they are not in the same plane.[10,21,22] Within the fitting range there is probably a change in coordinating atoms of histidine, which binds Cu^{2+} through the amino nitrogen and carboxylate oxygen in acidic solution (up to pH 5) but upon approaching neutrality the imidazole nitrogen becomes available for coordination and histidine prefers coordination through the amino and imidazole nitrogens, and hence may become tridentate.[10] However, histidine may be restricted from forming a tridentate complex with Cu^{2+} in the presence of βCDpn.

In all three systems the stability constant for $[Cu(A)]^{+}$ is greater than the stepwise constant for $[Cu(A)_2]$ as anticipated for sequential binding. However, the analogous equilibria for HisH show that the stepwise stability constant for the second binding is greater than the first. This suggests that the coordination geometry of Cu^{2+} may have changed from a six-coordinated tetragonally distorted stereochemistry in $[Cu(HisH)]^{2+}$ to either a four-coordinate square planar or a tetrahedral stereochemistry in $[Cu(HisH)_2]^{2+}$. The lower values of the stability constants for the Cu^{2+} complexes of HisH in comparison with those of His^{-} probably reflect the lesser electrostatic interaction between the metal centre and the uncharged HisH.

The species, [Cu(A)OH], probably corresponds to the deprotonation of an aqua ligand bound to the metal centre in $[Cu(A)H_2O]^{+}$. Dimerisation of the hydroxo species $[Cu(His)OH]^{+}$ to form a dinucleated diolated complex, $[Cu(His)OH]_2$, has previously been reported.[22] The presence of three coordination or protonation sites in histidine leads to formation of Cu^{2+} complexes with many different stoichiometries as seen in Table 2.4. In most cases, these complexes have a tetragonally distorted octahedral structure.[10]

Table 2.4 *Stability constants for the complexes of histidine, phenylalanine and tryptophan with Cu^{2+} in aqueous solution at 298.2 K and I = 0.1 mol dm^{-3} ($NaClO_4$).*

	log (K/dm^3 mol^{-1})		
Equilibrium	A = His[a]	A = Phe[b]	A = Trp[c]
$Cu^{2+} + A^- \rightleftharpoons [Cu(A)]^+$	9.95 ± 0.03	7.8	8.11
$Cu^{2+} + AH \rightleftharpoons [Cu(AH)]^{2+}$	4.78 ± 0.04	—	—
$[Cu(A)]^+ + A^- \rightleftharpoons [Cu(A)_2]$	8.27 ± 0.04	6.9	7.20
$[Cu(AH)]^{2+} + A^- \rightleftharpoons [Cu(AH)(A)]^+$	9.90 ± 0.03	—	—
$[Cu(A)]^+ + AH \rightleftharpoons [Cu(AH)(A)]^+$	4.73 ± 0.04	—	—
$[Cu(AH)]^{2+} + AH \rightleftharpoons [Cu(AH)_2]^{2+}$	4.88 ± 0.04	—	—
$[Cu(A)OH] + H^+ \rightleftharpoons [Cu(A)]^+$	7.92 ± 0.08	7.46	7.28
$2\,[Cu(A)OH] \rightleftharpoons [Cu(A)OH]_2$	3.8 ± 0.1	—	—

[a] Derived from data in the pH range 3.4 – 8.1. [b] Ref. 5. [c] Ref. 4.

Fitting of the experimental data was quite sensitive to the initial ratio of histidine to Cu^{2+}. Titrations were performed using histidine to Cu^{2+} ratios of 1:1, 2:1 and 3:1, and although good fits were obtained for each individual titration, some difficulty was encountered in fitting the same species over this range of reagent concentrations. Remelli *et al.* reported a similar phenomenon[10] with the *N*-methyl-(*S*)-histidine (Appendix, (20)) complexation of Cu^{2+} and, interestingly, Kozlowski *et al.* only used ratios of 2:1 and 3:1 to obtain their values.[19] The hydroxo species, [Cu(His)OH] and $[Cu(His)OH]_2$, which comprise at least 40% of the total histidine concentration at pH 8.0 or higher in the 1:1 ratio, are present in a mere < 10% of the total histidine concentration at pH 11.5 for the 2:1 ratio, and even less for the 3:1 ratio. Consequently, a good fit of the hydroxo species could not be obtained from the data acquired at higher ratios, and this affected the values obtained for the other species present in these systems, causing them to differ from those of the 1:1 ratio. Since the ratio used for the ternary system was

1:1:1 (His:Cu^{2+}:βCDpn) it was of primary importance to accurately characterise the species present at the 1:1 (His:Cu^{2+}) ratio. While the formation of $[Cu(OH)]^{+}$ is negligible at these concentrations,[23] the dimer, $[Cu(OH)]_2^{2+}$, which forms in < 5% had to be taken into account to achieve a good fit. The stability constant for $[Cu(OH)]_2^{2+}$ was fixed to the value, log (K/dm^3 mol^{-1}) = -10.86, obtained from Perrins' data for these conditions.[23] All Cu^{2+}-histidine species were successfully fitted for the 1:1 ratio, and are listed in Table 2.4. These values were used as constants in fitting the ternary system. (The data could also be fitted omitting $[Cu(HisH)_2]^{2+}$ with approximately the same errors, however, since this complex formed in approximately 10% of the total histidine concentration it was retained.) By fixing the formation constants for the hydroxo species to those obtained from the 1:1 ratio, all remaining species could be fitted for the 2:1 and 3:1 data, and the stability constants thus obtained were in reasonable agreement with the 1:1 values.

2.2.4 Complexation of Cu^{2+} by βCDpn

Stability constants for the complexes formed between βCDpn and Cu^{2+} have previously been determined under these conditions and are listed in Table 2.5.[4,5]

The metallocyclodextrin, $[Cu(\beta CDpn)]^{2+}$, is of considerably lower stability than the complex formed by free pn, $[Cu(pn)]^{2+}$, reflecting the decreased basicity of the βCDpn amino groups (Section 2.2.1). This probably arises from a combination of the greater steric hindrance of the bulky cyclodextrin unit attached to the coordinating functional group, and a difference in the electron donating power of the secondary amine group in βCDpn relative to a primary amine group in pn.

A decreased stability of the metallocyclodextrin relative to the metal complex of the free ligand, has been observed for the binding of Cu^{2+} by 6^A-(2-(2-aminoethyl-amino)ethylamino)-6^A-deoxy-β-cyclodextrin (Appendix, (4)),[24] 6^A-(2-aminoethylamino)-6^A-deoxy-βCD (Appendix, (2)),[12] and 6^A-(2-(4-imidazolyl)-ethylamino)-6^A-deoxy-βCD (Appendix, (3)).[13] A bis complex has also been reported for the latter two cyclodextrins,[12,13,25,26] however, no $[Cu(\beta CDpn)_2]^{2+}$ complex was detected at the

concentrations used. The bis complex of 6^A-(2-(4-imidazolyl)ethylamino)-6^A-deoxy-βCD could not be detected by potentiometric titration when using cyclodextrin to Cu^{2+} ratios of up to 2:1, and yet it was observed by EPR.[13] Comparison of the stability constants for the mono and bis complexes of 6^A-(2-aminoethylamino)-6^A-deoxy-βCD, log (K/dm^3 mol^{-1}) = 7.81 and 6.17,[12] with those of 2-aminoethylamine, log (K/dm^3 mol^{-1}) = 10.46 and 9.01,[12] and *N*-methyl-2-aminoethylamine, log (K/dm^3 mol^{-1}) = 10.33 and 8.60,[11] demonstrate the effect of amine substitution and of the cyclodextrin cavity. Furthermore, although the unprotonated Cu^{2+} mono complex of 6^A-(2-(4-imidazolyl)ethylamino)-6^A-deoxy-βCD, log (K/dm^3 mol^{-1}) = 7.26, is drastically less favoured than histamine, log (K/dm^3 mol^{-1}) = 9.57, and *N*-methylhistamine (Appendix, (21)), log (K/dm^3 mol^{-1}) = 8.35, the analogous monoprotonated species have similar stabilities.[13]

Table 2.5 *Stability constants for the complexes of βCDpn and pn with Cu^{2+} in aqueous solution at 298.2 K and I = 0.1 mol dm^{-3}.*

	log (K/dm^3 mol^{-1})	
Equilibrium	B = βCDpn[a]	B = pn[b]
$Cu^{2+} + B \rightleftharpoons [Cu(B)]^{2+}$	7.35	9.75
$Cu^{2+} + BH^+ \rightleftharpoons [Cu(BH)]^{3+}$	3.09	—
$[Cu(B)]^{2+} + H^+ \rightleftharpoons [Cu(BH)]^{3+}$	5.74	—
$[Cu(B)OH]^+ + H^+ \rightleftharpoons [Cu(B)]^{2+}$	7.84	7.66

[a] Refs. 4 and 5. [b] Ref. 11.

The formation of $[Cu(\beta CDpnH)]^{3+}$ is less favoured by comparison with $[Cu(\beta CDpn)]^{2+}$ as anticipated from the charged and monodentate nature of $\beta CDpnH^+$. The pK_a of this species probably characterises the deprotonation of the monoprotonated aminopropylamino substituent of $\beta CDpnH^+$ in the metallocyclodextrin. Comparison of the pK_as of $\beta CDpnH^+$ in the free (Section 2.2.1) and complex states shows that upon

complexation with Cu^{2+} the basicity of the amine decreases as expected. Further deprotonation to form $[Cu(\beta CDpn)OH]^{+}$ probably corresponds to deprotonation of an aqua ligand coordinated to Cu^{2+}.

The primary hydroxyl group of an adjacent glucose unit may also be involved in coordination of the metal ion, as previously postulated.[27,28] Direct coordination of natural cyclodextrins to metal ions has been demonstrated previously for a variety of metal ions including Co^{2+},[29] Ni^{2+},[29] and Cu^{2+},[29-32] under alkaline conditions (Section 1.3.3), where the hydroxyl groups are deprotonated and thus have improved coordinating ability. Within the pH regions used here for fitting, βCD is in the neutral form. However, electron spin resonance measurements on the Cu^{2+} complex of 6^{A}-(2-(4-imidazolyl)ethylamino)-6^{A}-deoxy-βCD provide evidence of cavity interaction with the metal ion at around neutral pH with a consequent "stiffening" effect.[13] The resultant decrease in entropy may explain the lower stability of the metallocyclodextrin complexes compared to those of pn above. Although there is no information about the structure of the $[Cu(\beta CDpn)]^{2+}$ complex in this study, it is most likely that the metal ion has a tetragonally distorted octahedral geometry. Generally, the coordination geometry of a metal ion bound by a ligand attached to a cyclodextrin appears to be similar to that of the same metal ion bound by the free ligand.[2,13]

2.2.5 Complexation of Amino Acids by the Cu^{2+} Metallocyclodextrin Derivative of βCDpn

The difference in shape of the pH titration profiles for the binary cyclodextrin-histidine and Cu^{2+}-histidine systems, and the ternary cyclodextrin-Cu^{2+}-histidine system are shown in Fig. 2.3.

The stability constants for the ternary complexes formed may be found in Table 2.6. These constants, along with the protonation constants for βCDpn and His^{-}, and the stability constants for the binary complexes formed between βCDpn, Cu^{2+} and

histidine (Tables 2.1 - 2.5) were used to derive the variation in major species present with pH, as shown in Fig 2.4.

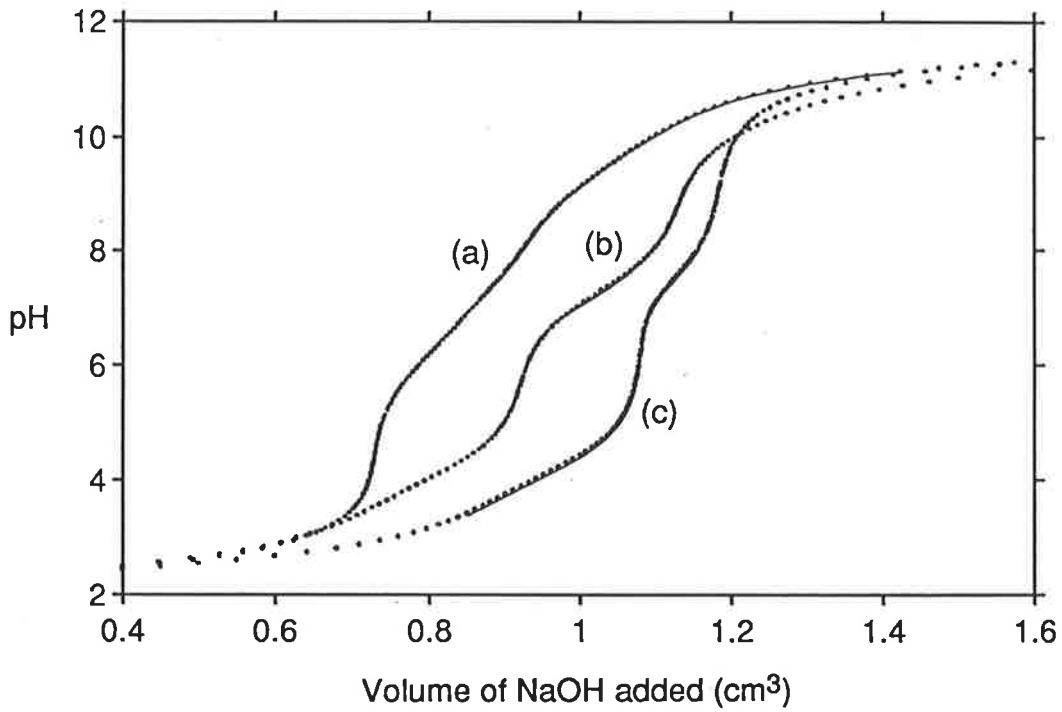

Figure 2.3 *Titration profiles of: (a)* $\beta CDpnH_2^{2+}$ *(1.00 x* 10^{-3} *mol* dm^{-3}*) and (S)-*$HisH_3^{2+}$ *(1.00 x* 10^{-3} *mol* dm^{-3}*), (b)* $\beta CDpnH_2^{2+}$ *(1.00 x* 10^{-3} *mol* dm^{-3}*), (S)-*$HisH_3^{2+}$ *(1.00 x* 10^{-3} *mol* dm^{-3}*) and* $Cu(ClO_4)_2$ *(9.98 x* 10^{-4} *mol* dm^{-3}*), and (c) (S)-*$HisH_3^{2+}$ *(1.00 x* 10^{-3} *mol* dm^{-3}*) and* $Cu(ClO_4)_2$ *(9.98 x* 10^{-4} *mol* dm^{-3}*), each in aqueous 0.010 mol* dm^{-3} $HClO_4$ *and 0.090 mol* dm^{-3} $NaClO_4$*, against 0.101 mol* dm^{-3} *NaOH. The dots represent data points and the solid line represents the best fit to the algorithm arising from the equilibria discussed in Sections 2.2.2 (Table 2.3), 2.2.5 (Table 2.6) and 2.2.3 (Table 2.4), respectively.*

The higher stabilities of $[Cu(\beta CDpn)A]^+$ by comparison with those of $\beta CDpn{\cdot}A^-$ (Table 2.3) demonstrate that Cu^{2+} strengthens the complexation of the amino acid anion. This is consistent with both βCDpn and the amino acid coordinating to Cu^{2+}. Nevertheless, the lower stabilities of $[Cu(\beta CDpn)A]^+$ by comparison with those of $[Cu(A)]^+$ indicate that the conformation required for optimum metal-amino acid

Table 2.6 *Stability constants for the Cu^{2+} complexes of βCDpn with the (R)- and (S)- enantiomers of histidine, phenylalanine and tryptophan in aqueous solution at 298.2 K and I = 0.1 mol dm^{-3} ($NaClO_4$).*

	log (K/dm^3 mol^{-1})		
Equilibrium	A = His[a]	A = Phe[b]	A = Trp[c]
$[Cu(\beta CDpn)]^{2+} + (R)\text{-}A^- \rightleftharpoons [Cu(\beta CDpn)(R)\text{-}A]^+$	8.38 ± 0.04	7.2 ± 0.1	7.85 ± 0.07
$[Cu(\beta CDpn)]^{2+} + (S)\text{-}A^- \rightleftharpoons [Cu(\beta CDpn)(S)\text{-}A]^+$	8.42 ± 0.02	6.9 ± 0.1	8.09 ± 0.05
$[Cu(\beta CDpn)]^{2+} + (R)\text{-}AH \rightleftharpoons [Cu(\beta CDpn)(R)\text{-}AH]^{2+}$	—	—	5.29 ± 0.05
$[Cu(\beta CDpn)]^{2+} + (S)\text{-}AH \rightleftharpoons [Cu(\beta CDpn)(S)\text{-}AH]^{2+}$	—	—	5.4 ± 0.1
$[Cu(\beta CDpn)(R)\text{-}A]^+ + (R)\text{-}A^- \rightleftharpoons [Cu(\beta CDpn)\{(R)\text{-}A\}_2]$	7.75 ± 0.05	—	—
$[Cu(\beta CDpn)(S)\text{-}A]^+ + (S)\text{-}A^- \rightleftharpoons [Cu(\beta CDpn)\{(S)\text{-}A\}_2]$	7.6 ± 0.1	—	—
$[Cu(\beta CDpn)\{(R)\text{-}A\}OH] + H^+ \rightleftharpoons [Cu(\beta CDpn)(R)\text{-}AH]^+$	—	9.56 ± 0.04	9.48 ± 0.07
$[Cu(\beta CDpn)\{(S)\text{-}A\}OH] + H^+ \rightleftharpoons [Cu(\beta CDpn)(S)\text{-}AH]^+$	—	9.6 ± 0.1	9.37 ± 0.04

[a] Derived from data in the pH range 6.7 – 9.3. [b] Ref. 5. [c] Ref. 4.

interaction cannot be achieved. Hence the factors stabilising complexation of the amino acid anion by βCDpn and Cu^{2+} in $[Cu(\beta CDpn)A]^{+}$ do not reinforce each other.

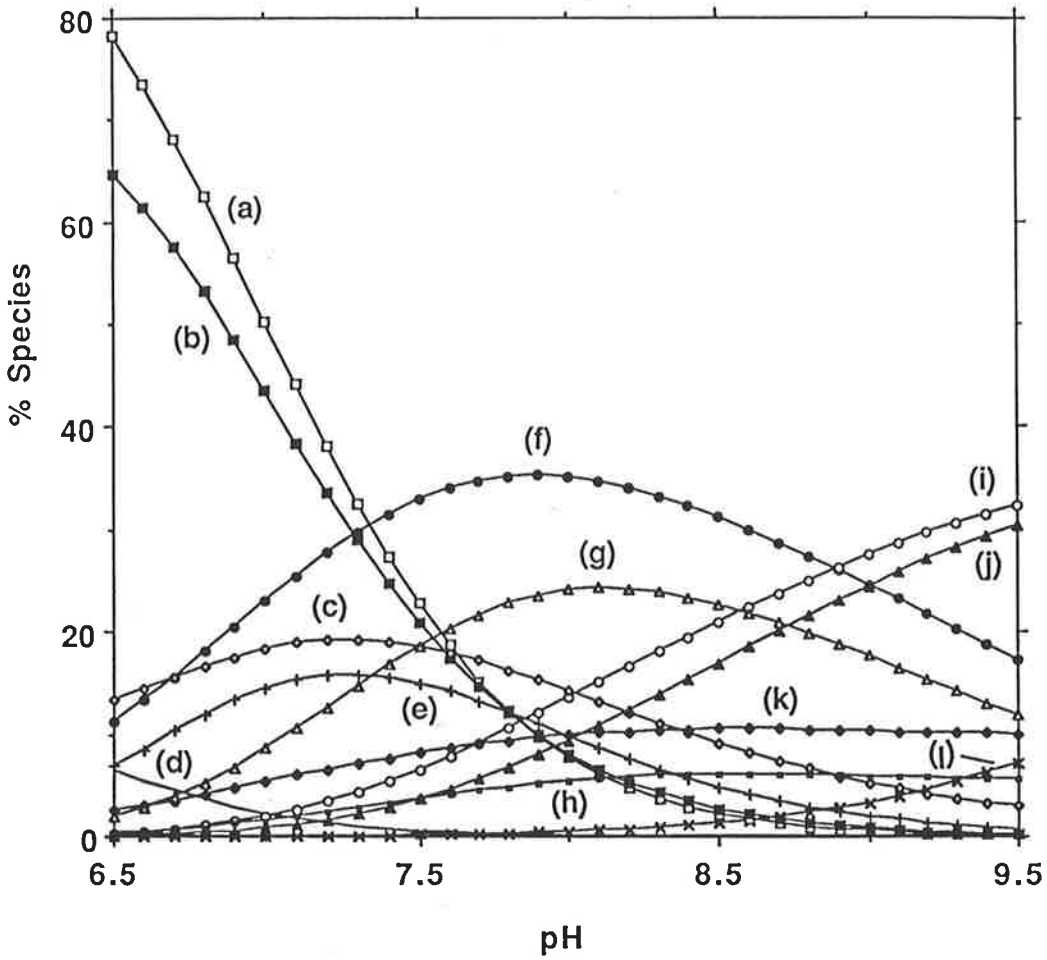

Figure 2.4 *Percentage of species in a solution containing 9.98 x 10^{-4}, 1.00 x 10^{-3} and 1.00 x 10^{-3} mol dm^{-3} total Cu^{2+}, βCDpn and (S)-histidine concentrations, respectively, calculated from the data in Tables 2.1 - 2.6 and plotted relative to total $[\beta CDpn]_{total} = [(S)\text{-histidine}]_{total}$ = 100%. The curves represent: (a) $\beta CDpnH_2^{2+}$, b) $[Cu\{(S)\text{-}His\}]^{+}$, (c) $[Cu\{(S)\text{-}His\}_2]$, (d) Cu^{2+}, (e) $[Cu(\beta CDpn)]^{2+}$, (f) $\beta CDpnH^{+}$, (g) $[Cu(\beta CDpn)(S)\text{-}His]^{+}$, (h) $[Cu\{(S)\text{-}His\}OH]_2$, (i) $[Cu(\beta CDpn)OH]^{+}$, (j) $[Cu(\beta CDpn)\{(S)\text{-}His\}_2]$, (k) $[Cu\{(S)\text{-}His\}OH]$ and (l) βCDpn. No other species are present in greater than 5% in this pH range.*

The closely related Cu^{2+} metallocyclodextrin of 6^A-(2-aminoethylamino)-6^A-deoxy-βCD (Appendix, (2)), forms complexes with (*R*)- and (*S*)-Phe^- and (*R*)- and (*S*)-Trp^- with stability constants of, log (K/dm^3 mol^{-1}) = 7.74 and 7.69, and 8.45 and 8.47, respectively.[12] These are greater than those for the analogous $[Cu(\beta CDpn)]^{2+}$ complexes, and Trp^- is bound more strongly by this metallocyclodextrin than by Cu^{2+} alone (Table 2.4). The Cu^{2+} complex of 6^A-(2-(4-imidazolyl)ethylamino)-6^A-deoxy-βCD (Appendix, (3)) also binds (*R*)- and (*S*)-Phe^- and (*R*)- and (*S*)-Trp^- more strongly than either $[Cu(\beta CDpn)]^{2+}$ or Cu^{2+} alone, log (K/dm^3 mol^{-1}) = 8.59 and 8.42, and 9.21 and 8.86, respectively.[1,6]

The stabilities of $[Cu(\beta CDpn)His]^+$ are greater than for the corresponding Phe^- and Trp^- complexes. This is attributable to bidentate Phe^- and Trp^- coordinating through their carboxylate and amino groups, while His^- may coordinate as a bi- or tridentate ligand as discussed above (Section 2.2.3). A second His^- coordinates to form $[Cu(\beta CDpn)\{His\}_2]$ but formation of complexes with analogous stoichiometry are not observed for Phe^- and Trp^-. This probably reflects the smaller size of His^-, its different coordination mode and its weaker interaction with the βCDpn annulus, all of which should favour the coordination of a second His^- over either a second Phe^- or Trp^-.

The stabilities of $[Cu(\beta CDpn)(R)\text{-}TrpH]^{2+}$ and $[Cu(\beta CDpn)(S)\text{-}TrpH]^{2+}$ are lower than their deprotonated counterparts, probably because (*R*)-TrpH and (*S*)-TrpH act as monodentate ligands. Electrostatic repulsion between the positive charge of the metal ion and the zwitterionic TrpH may also result in destabilisation of the protonated complexes. The pK_as of the ternary metallocyclodextrin may characterise the deprotonation of either the TrpH or the $\beta CDpnH^+$, but an unambiguous assignment is not possible.

The hydroxo species observed for phenylalanine and tryptophan are not detected for histidine, and this probably arises from a lack of coordinated water molecules due to the possible tridentate nature of His^-, and the formation of a bis complex.

The $[Cu(\beta CDpn)A]^+$ complexes show only slight enantioselectivity in favour of (*R*)-Phe^- and (*S*)-Trp^-, and no enantioselectivity is detected for histidine. A slightly greater enantioselectivity is observed by the Cu^{2+} complex of

6^A-(2-(4-imidazolyl)ethylamino)-6^A-deoxy-βCD, favouring (*R*)-Phe$^-$ and (*R*)-Trp$^-$, and once again negligible enantioselectivity is found for histidine.[1,6] The thermodynamic enantioselectivity factor observed for tryptophan (2.2) is greater than for phenylalanine (1.5), suggesting a dependence on the size of the amino acid aromatic side chain.[6] Interestingly, chromatography studies show that the Cu^{2+} complex of the closely related 6^A-(4-(2-aminoethyl)imidazoyl)-6^A-deoxy-βCD (Appendix, (5)) preferentially complexes the opposite tryptophan enantiomer, (*S*)-Trp$^-$.[2] An absence of thermodynamic enantioselectivity is observed for the complexation of (*R*/*S*)-Phe$^-$ and (*R*/*S*)-Trp$^-$ by the Cu^{2+} metallocyclodextrin of 6^A-(2-aminoethylamino)-6^A-deoxy-βCD (Appendix, (2)), which is closely related to [Cu(βCDpn)]$^{2+}$.[12] The enantioselectivity of these complexes is discussed in Section 1.3.3. No significant enantioselectivity is detected for (*R*)-TrpH or (*S*)-TrpH, probably because TrpH acts as a monodentate ligand and is less sterically constrained than its bidentate anions. The lack of enantioselectivity of protonated ternary complexes has been observed previously.[1,6]

No structural studies were made on these complexes. The proposed structure for the [Cu(βCDpn)A]$^+$ complexes has the aromatic moiety of the amino acid anion included inside the cyclodextrin annulus with the chiral centre in the vicinity of the primary hydroxyl groups. The amino acid donor atoms coordinate to the metal ion, which is anchored at the primary end of the cavity by the amines of the coordinating group attached to the cyclodextrin, forming a six-coordinate tetragonally distorted octahedral Cu^{2+} complex. Molecular models show that histidine may behave as a tridentate ligand in the ternary complexes. The high stepwise stability of the bis histidine complex implies that both amino acid anions coordinate to the metal centre. However, for steric reasons only one imidazole ring can interact with the inside of the cyclodextrin annulus. It has been suggested that discrimination between the enantiomers of aromatic amino acids by metallocyclodextrins arises from the aromatic moiety of the more strongly bound enantiomer being included within the cyclodextrin annulus while that of the other enantiomer is excluded from the cavity (Section 1.3.3).[1,2,6] No evidence of such a major structural difference in the βCDpn metallocyclodextrin complexes has been observed.[3-5]

2.3 Complexation of Tryptophan by βCDtren and its Co^{2+}, Ni^{2+}, Cu^{2+} and Zn^{2+} Metallocyclodextrin Derivatives: Effect of the Metal Ion

2.3.1 Protonation Constants

The protonation constants of tryptophan can be found in Table 2.1. The 6^A-(2-(*N*,*N*-bis(2-aminoethyl)amino)ethylamino)- substituent of βCDtren can be successively protonated to form a monoprotonated cation ($\beta CDtrenH^+$), a diprotonated cation ($\beta CDtrenH_2^{2+}$), a triprotonated cation ($\beta CDtrenH_3^{3+}$) and a tetraprotonated cation ($\beta CDtrenH_4^{4+}$), which are characterised in Table 2.7. The pH titration profiles are shown in Fig. 2.5.

The primary amines of βCDtren are probably more basic than the secondary amine.[12] The tertiary amine of βCDtren is probably the least basic; the low basicity arising from the electrostatic repulsion a proton experiences, from other positively charged amino groups present in close proximity, on approach to this amine.

Table 2.7 *Protonation constants of βCDtren and tren in aqueous solution at 298.2 K and* $I = 0.10$ *mol* dm^{-3}.

	log (K/dm^3 mol^{-1})	
Equilibrium	B = βCDtren[a]	B = tren[b]
$B + H^+ \rightleftharpoons BH^+$	9.85 ± 0.02	10.14
$BH^+ + H^+ \rightleftharpoons BH_2^{2+}$	8.99 ± 0.09	9.43
$BH_2^{2+} + H^+ \rightleftharpoons BH_3^{3+}$	6.89 ± 0.05	8.41
$BH_3^{3+} + H^+ \rightleftharpoons BH_4^{4+}$	2.6 ± 0.3	—

[a] Derived from data in the pH range 2.2 – 11.3. Supporting electrolyte: $NaClO_4$. [b] Ref. 11.

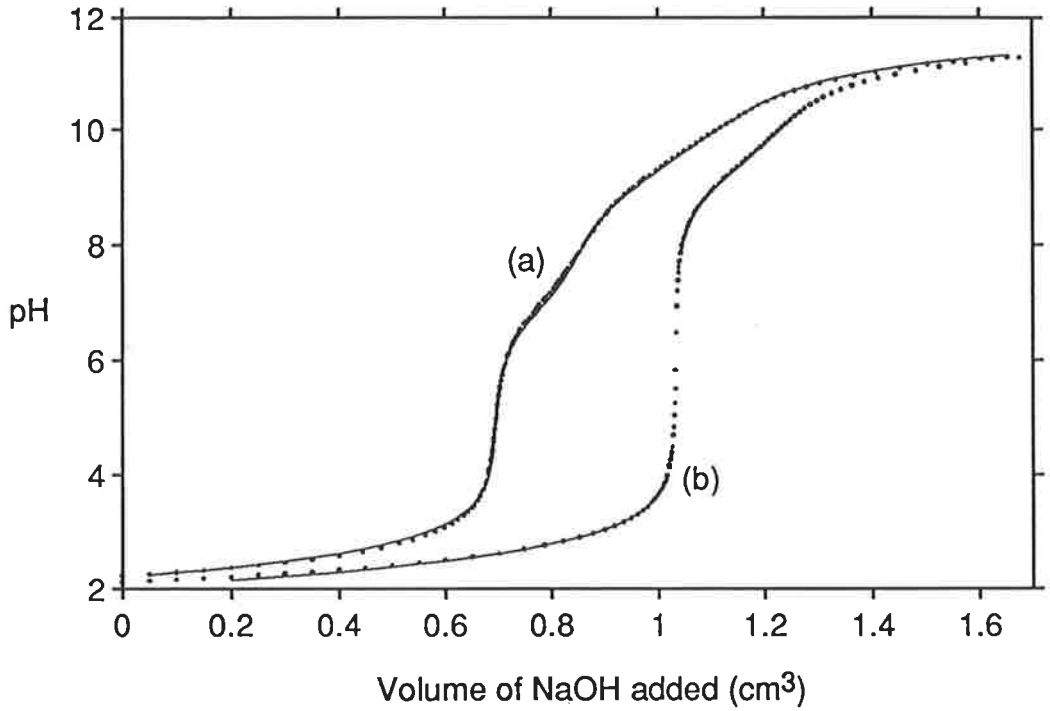

Figure 2.5 *Titration profiles of: (a) βCDtrenH$_4^{4+}$ (1.65 x 10^{-3} mol dm^{-3}) and (b) (R)-TrpH$_2^+$ (2.07 x 10^{-3} mol dm^{-3}), each in aqueous 0.007 mol dm^{-3} HClO$_4$ and 0.090 mol dm^{-3} NaClO$_4$, against 0.101 mol dm^{-3} NaOH. The dots represent data points and the solid line represents the best fit to the algorithm arising from the equilibria shown in Tables 2.7 and 2.1, respectively.*

In comparison with tren, the pK_as are decreased. This is attributed to the effects described in Section 2.2.1. A similar decrease in basicity is seen for 2,2',2''-tri(*N*,*N*-dimethylamino)triethylamine (Me$_6$tren) (Appendix, (22)) in comparison with tren.[33]

2.3.2 Complexation of Tryptophan by βCDtren

The stability constants for βCDtren·Trp$^-$ (Table 2.8) are approximately 10^3 times greater than those for βCDpn·Trp$^-$ and about 10^4 times greater than those for βCD·Trp$^-$ (Table 2.3). As mentioned previously (Section 2.2.2) the phenyl moiety of Trp$^-$ probably resides largely within the hydrophobic region of the cyclodextrin annuli in these

complexes. Polar guests tend to align their dipole moments antiparallel to that of the cyclodextrin. The modified cyclodextrins being discussed are assumed to have a dipole orientation similar to that of the natural cyclodextrin (Section 1.2.1), where the positive and negative poles are adjacent to the centres of the narrow and wide ends of the annulus, respectively. Thus, the increase in stability of the complexes with change in nature of the cyclodextrin in the sequence βCD < βCDpn < βCDtren is largely attributable to the interaction of the Trp^- amino carboxylate group with the narrow end of the cyclodextrin annulus.

Table 2.8 *Stability constants for the complexes of βCDtren with (R)- and (S)-tryptophan in aqueous solution at 298.2 K and I = 0.1 mol dm^{-3} ($NaClO_4$).*

	$\log(K/dm^3\ mol^{-1})^a$	
Equilibrium	A = (*R*)-Trp	A = (*S*)-Trp
βCDtren + A^- ⇌ βCDtren·A^-	6.36 ± 0.01	6.5 ± 0.1
βCDtrenH$^+$ + A^- ⇌ βCDtrenH·A	5.85 ± 0.03	5.9 ± 0.1
βCDtren·A^- + H^+ ⇌ βCDtrenH·A	9.34 ± 0.04	9.3 ± 0.2
βCDtrenH$^+$ + AH ⇌ βCDtrenH·AH$^+$	5.59 ± 0.05	5.61 ± 0.08
βCDtrenH·A + H^+ ⇌ βCDtrenH·AH$^+$	8.99 ± 0.7	8.9 ± 0.2

[a] Derived from data in the pH range 7.0 – 10.6.

The higher stability of the βCDtren complexes may arise because βCDtren either i) has a greater dipole and a consequently stronger interaction with Trp^-, or ii) the greater bulk of the 6^A-(2-(*N*,*N*-bis(2-aminoethyl)amino)ethylamino)- substituent hinders egress more than ingress of Trp^-, or iii) it hydrogen bonds more strongly to Trp^-, or a combination of these factors. As no complexation of Trp^- by *N*,*N*-bis(2-aminoethyl)aminoethylamine (tren) (Appendix, (19)) is detected by the pH titrimetric method employed in this study, it appears that the interaction of the phenyl moiety of Trp^-

with the interior of the cyclodextrin annulus is the essential contribution to complex stability on which the stabilising effect of the 6^A-(2-(*N*,*N*-bis(2-aminoethyl)amino)ethylamino)- substituent is superimposed.

Protonation decreases the stabilities of βCDtrenH·(*R*)-Trp, βCDtrenH·(*S*)-Trp, βCDtrenH·(*R*)-TrpH$^+$ and βCDtrenH·(*S*)-TrpH$^+$ despite an anticipated increase in the dipolar character of βCDtrenH$^+$ and the possibility of charge-charge interactions between the positively charged nitrogen of βCDtrenH$^+$ and the negatively charged carboxylate of Trp$^-$. This may reflect either a decreased ability of βCDtrenH$^+$ to hydrogen bond with Trp$^-$ and TrpH, or the increased hydration of βCDtrenH$^+$, by comparison with that of βCDtren, diminishing the hydrophobic interaction with the aromatic moiety of tryptophan.

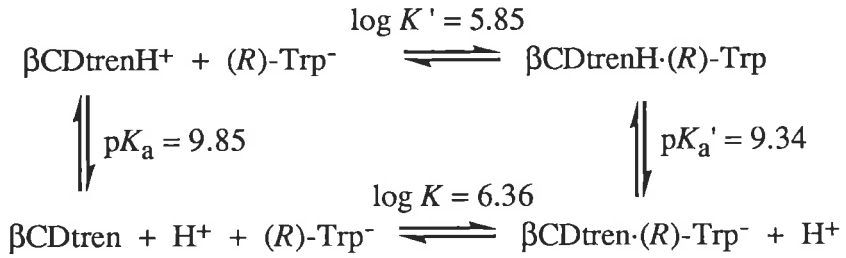

Figure 2.6 *The effect of (R)-Trp$^-$ complexation on the pK_a of βCDtren. Analogous values for (S)-Trp$^-$ may be found in Table 2.8.*

A decrease in the pK_a of βCDtren is seen upon complexation of Trp$^-$ (Fig. 2.6 and Table 2.8), indicating that the conjugate base, βCDtren, is stabilised relative to the conjugate acid, βCDtrenH$^+$, by comparison with the situation in the uncomplexed state. Changes such as this lead to the characteristic shape of the pH titration profile, which, for the complexation of tryptophan by βCDtren, can be seen in Fig. 2.13.

No significant enantioselection of Trp$^-$ or TrpH by βCDtren or βCDtrenH$^+$ is observed. The similarity of the βCDtren·(*R*)-Trp$^-$ and βCDtren·(*S*)-Trp$^-$ stabilities are also consistent with the interaction between the hydrophobic interior of the cyclodextrin annulus and the Trp$^-$ aromatic moiety dominating any free energy differences arising from

interaction of the opposite chiralities of (*R*)-Trp$^-$ and (*S*)-Trp$^-$ with the homochirality of βCDtren. A similar dominance applies for the analogous βCD and βCDpn complexes (Section 2.2.2).

2.3.3 Complexation of Co^{2+}, Ni^{2+}, Cu^{2+} and Zn^{2+} by Tryptophan

The stability constants for the complexation of tryptophan by metal ions have been reported under the same conditions as this study.[4]

Table 2.9 *Stability constants for the complexes of tryptophan with Co^{2+}, Ni^{2+}, Cu^{2+} and Zn^{2+} in aqueous solution at 298.2 K and I = 0.1 mol dm^{-3} ($NaClO_4$).*

	log(K/dm^3 mol^{-1})[a]			
Equilibrium	M = Co	M = Ni	M = Cu	M = Zn
$M^{2+} + Trp^- \rightleftharpoons [M(Trp)]^+$	4.41	5.42	8.11	4.90
$[M(Trp)]^+ + Trp^- \rightleftharpoons [M(Trp)_2]$	4.01	4.67	7.20	—
$[M(Trp)OH] + H^+ \rightleftharpoons [M(Trp)]^+$	—	9.1	7.28	—

[a] Ref. 4.

The stabilities of these tryptophan complexes exhibit the variations anticipated from the Irving-Williams series ($Co^{2+} < Ni^{2+} < Cu^{2+} > Zn^{2+}$).[34] The hydroxo species detected for Ni^{2+} and Cu^{2+} are most likely formed by deprotonation of a coordinated water molecule.

2.3.4 Complexation of Co^{2+}, Ni^{2+}, Cu^{2+} and Zn^{2+} by βCDtren

The stability constants of the metallocyclodextrins formed and related species are listed in Table 2.10. In the subsequent discussion, the values listed for $[Co(\beta CDtren)]^{2+}$,

$[Co(\beta CDtrenH)]^{3+}$ and $[Co(\beta CDtren)OH]^{+}$ are not compared with other stability constants due to possible formation of μ-peroxo species as discussed in Section 2.3.5.

Characteristic pH titration profiles for each metal ion are shown in Fig 2.7. If the offset effect produced by variation in the initial acid concentration is taken into account, the titration profiles for the Ni^{2+} and Zn^{2+} ions are similar up to pH 6. The Ni^{2+} complexes of βCDtren formed quite slowly, leading to the bumpy nature of the corresponding titration curve.

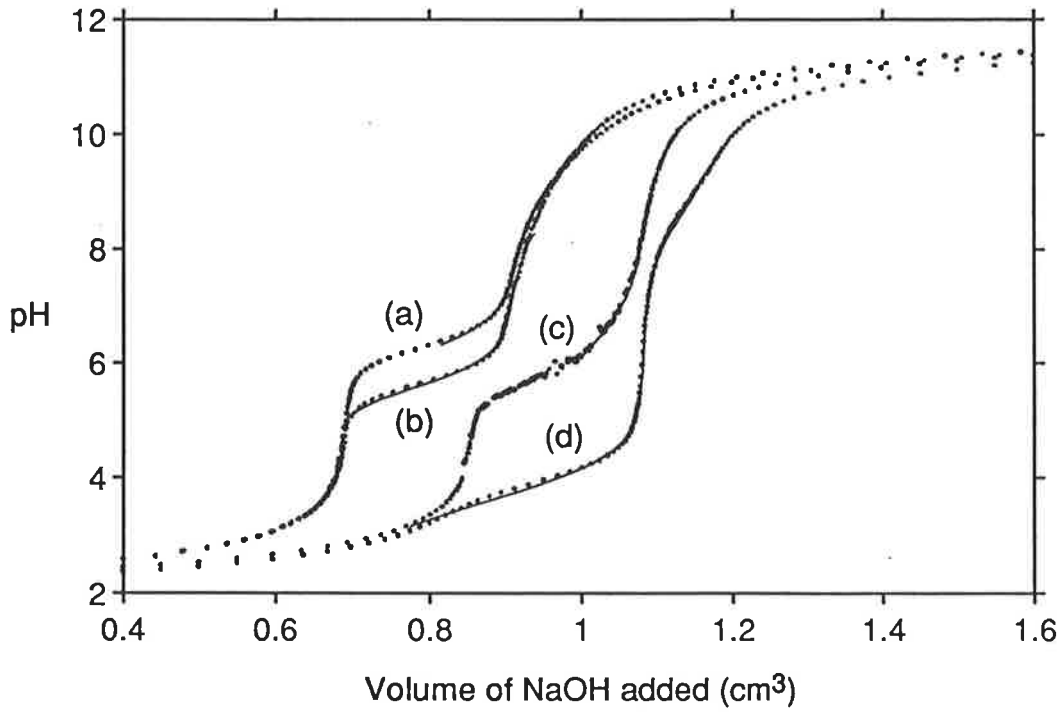

Figure 2.7 *Titration profiles of: (a) $\beta CDtrenH_4^{4+}$ (8.55 x 10^{-4} mol dm^{-3}) and $Co(ClO_4)_2$ (7.52 x 10^{-4} mol dm^{-3}), (b) $\beta CDtrenH_4^{4+}$ (8.55 x 10^{-4} mol dm^{-3}) and $Zn(ClO_4)_2$ (7.52 x 10^{-4} mol dm^{-3}), (c) $\beta CDtrenH_4^{4+}$ (8.25 x 10^{-4} mol dm^{-3}) and $Ni(ClO_4)_2$ (7.52 x 10^{-4} mol dm^{-3}), and (d) $\beta CDtrenH_4^{4+}$ (8.25 x 10^{-4} mol dm^{-3}) and $Cu(ClO_4)_2$ (7.64 x 10^{-4} mol dm^{-3}), each in aqueous 0.007 ((a) and (b)) or 0.009 ((c) and (d)) mol dm^{-3} $HClO_4$ and 0.090 mol dm^{-3} $NaClO_4$, against 0.100 mol dm^{-3} NaOH. The dots represent data points and the solid line represents the best fit to the algorithm arising from the equilibria shown in Table 2.10.*

Table 2.10 Stability constants for the complexes of βCDtren, tren, βCDpn and pn with Co^{2+}, Ni^{2+}, Cu^{2+} and Zn^{2+} in aqueous solution at 298.2 K and I = 0.1 mol dm^{-3}.

	log (K/dm^3 mol^{-1})			
Equilibrium	M = Co	M = Ni	M = Cu	M = Zn
M^{2+} + βCDtren ⇌ $[M(βCDtren)]^{2+}$ [a]	10.50 ± 0.05[d]	11.65 ± 0.06	17.29 ± 0.05	12.25 ± 0.03
M^{2+} + βCDtrenH$^+$ ⇌ $[M(βCDtrenH)]^{3+}$ [a]	6.91 ± 0.03[d]	8.46 ± 0.06	11.56 ± 0.02	7.92 ± 0.02
$[M(βCDtren)]^{2+}$ + H^+ ⇌ $[M(βCDtrenH)]^{3+}$ [a]	6.26 ± 0.06[d]	6.65 ± 0.09	4.11 ± 0.05	5.51 ± 0.04
$[M(βCDtren)OH]^+$ + H^+ ⇌ $[M(βCDtren)]^{2+}$ [a]	9.06 ± 0.01[d]	9.68 ± 0.09	8.48 ± 0.04	8.9 ± 0.6
M^{2+} + tren ⇌ $[M(tren)]^{2+}$ [b]	12.7	14.6	18.5	14.5
$[M(tren)OH]^+$ + H^+ ⇌ $[M(tren)]^{2+}$ [b]	—	—	4.65	—
M^{2+} + βCDpn ⇌ $[M(βCDpn)]^{2+}$ [c]	4.22	5.2	7.35	4.96
M^{2+} + βCDpnH$^+$ ⇌ $[M(βCDpnH)]^{3+}$ [c]	2.5	3.1	3.09	3.0
$[M(βCDpn)]^{2+}$ + H^+ ⇌ $[M(βCDpnH)]^{3+}$ [c]	8.3	7.83	5.74	8.1
$[M(βCDpn)OH]^+$ + H^+ ⇌ $[M(βCDpn)]^{2+}$ [c]	—	9.20	7.84	—
M^{2+} + pn ⇌ $[M(pn)]^{2+}$ [b]	—	6.31	9.75	—
$[M(pn)OH]^+$ + H^+ ⇌ $[M(pn)]^{2+}$ [b]	—	—	7.66	—

[a] Derived from data in the pH ranges 6.3 – 10.1, 6.1 – 8.9, 3.0 – 9.3 and 5.0 – 8.6 for Co^{2+}, Ni^{2+}, Cu^{2+} and Zn^{2+} respectively. Supporting electrolyte: $NaClO_4$. [b] Ref. 11. [c] Refs. 4 and 5. [d] These values may be affected by the formation of a μ-peroxo species (see Section 2.3.5).

The stabilities of the binary metallocyclodextrins, $[M(\beta CDtren)]^{2+}$, relative to the analogous $[M(tren)]^{2+}$ complexes, are several orders of magnitude lower (Table 2.10). This probably reflects a difference in the electron donating powers of the secondary amine group in βCDtren and a primary amine group in tren. The bulky cyclodextrin unit attached to the coordinating group of βCDtren may also produce substantial steric hindrance to metal binding. Similar effects are responsible for the decreased metal binding of Me_6tren (Appendix, (22)) relative to tren (Appendix, (19)).[33,35] Although in most metallocyclodextrins the cyclodextrin can be considered to act as a second-sphere ligand,[36] the possibility of the cyclodextrin itself interacting with the metal ion, as mentioned in Section 2.2.4, should not be dismissed.

The stabilities of $[M(\beta CDtren)]^{2+}$ are substantially greater than those of $[M(\beta CDpn)]^{2+}$ because of the tetradentate nature of βCDtren. The variation in $[M(\beta CDtren)]^{2+}$ and $[M(\beta CDpn)]^{2+}$ stabilities with the nature of M^{2+} is as anticipated from the Irving-Williams series ($Ni^{2+} < Cu^{2+} > Zn^{2+}$),[34] which arises through a combination of the variation of M^{2+} size and ligand-field effects.

The formation of $[M(\beta CDtrenH)]^{3+}$ is less favoured, by comparison with $[M(\beta CDtren)]^{2+}$, as anticipated from the charge repulsion between M^{2+} and $\beta CDtrenH^{+}$. In the $[M(\beta CDtrenH)]^{3+}$ complexes, a nitrogen atom of the tren substituent is presumed to be protonated. Hence the denticity of the substituent is restricted to three rather than its maximum of four, which may account for the lower stability of these complexes.

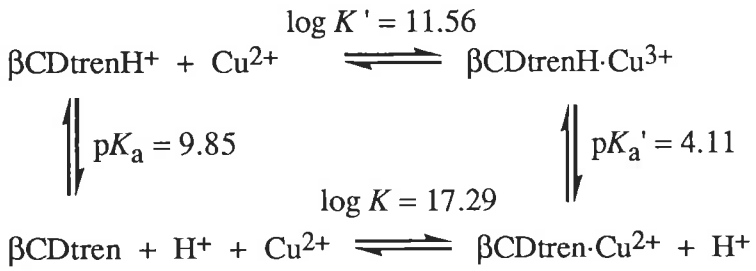

Figure 2.8 *The effect of Cu^{2+} complexation on the pK_a of βCDtren. Analogous values for Co^{2+}, Ni^{2+} and Zn^{2+} may be found in Table 2.10.*

The acidity of $[M(\beta CDtrenH)]^{3+}$ is markedly increased, by comparison with that of $\beta CDtrenH^{+}$ (Fig. 2.8 and Table 2.10), because of the coordination to M^{2+}. This change in acidity upon complexation is substantially greater than that observed in βCDtrenH·Trp (Section 2.3.2). The most acidic binary metallocyclodextrin is $[Cu(\beta CDtrenH)]^{3+}$, coincident with it being the most stable of the protonated binary metallocyclodextrins (Table 2.10).

The $[M(\beta CDtren)H_2O]^{2+}$ complexes can act as monoprotonic acids leading to the formation of hydroxo species, $[M(\beta CDtren)OH]^{+}$, and are characterised by the pK_as listed in Table 2.10.

Titrations were performed using M^{2+} to βCDtren ratios of 1:1, 1:2 and 2:1. The fitted values obtained for the $[M(\beta CDtren)]^{2+}$ and $[M(\beta CDtren)OH]^{+}$ species vary significantly for the three reagent concentrations. This variation appears to be due to the close proximity of the higher βCDtren pK_as permitting the formation of a number of minor species at higher pH. These additional species form in varying amounts for each ratio used, and whilst they are not formed in sufficient concentrations for their stability constants to be obtained, they affect the fitted values of the more significant species. This is consistent with the fact that stability constants for $[M(\beta CDtrenH)]^{3+}$ and $[M(\beta CDtren)]^{2+}$, obtained by fitting data in the lower pH region, are consistent over the range of reagent concentrations used. However, since all species could not be fitted within this restricted range, the values obtained from the 1:1 ratio were selected, since these most closely represented the ratio used in the ternary system.

2.3.5 Binary and Ternary Metallocyclodextrin Structure

The transition metal ions Co^{2+}, Ni^{2+} and Cu^{2+}, exhibit *d-d* transitions in the visible region of the electromagnetic spectrum, due to their partially filled *d* orbitals. Since the geometry and electronic spectra of the $[M(tren)]^{2+}$ complexes is well known, information on the geometry of the $[M(\beta CDtren)]^{2+}$ (Section 2.3.4) and $[M(\beta CDtren)Trp]^{+}$ (Section 2.3.6) complexes may be obtained by spectral comparisons. A change in metal

coordination number has a substantial effect on the electronic spectrum of the complex. Consequently any change in coordination number upon complexation of Trp^- by the binary metallocyclodextrin, to form the ternary metallocyclodextrin, should be observable in the electronic spectra.

In aqueous solution, tren forms five-coordinate complexes, $[M(tren)H_2O]^{2+}$, with M^{2+} = Co^{2+}, Cu^{2+} and Zn^{2+}, and a six-coordinate complex with Ni^{2+}, $[Ni(tren)(H_2O)_2]^{2+}$.[33,35,37-42] Trigonal bipyramidal and cis-diaquo-octahedral geometries are most probable for these five and six-coordinate complexes, respectively, in which tren acts as a tetradentate ligand.[37,38,41-43]

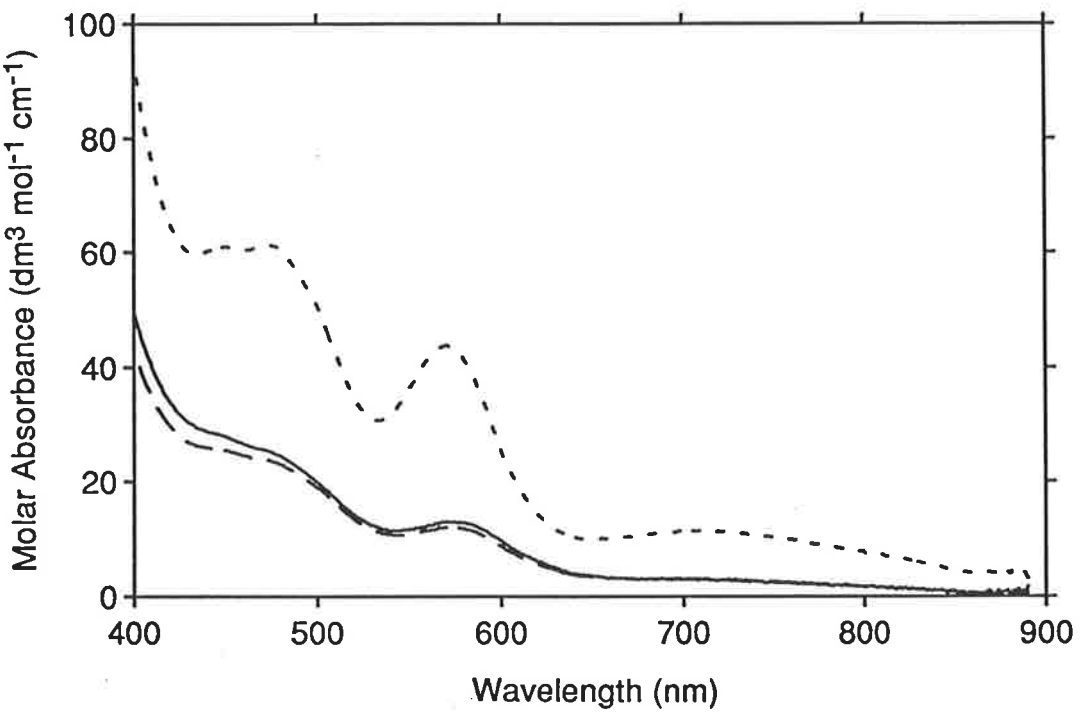

Figure 2.9 *Molar absorbance of $[Co(tren)H_2O]^{2+}$ (----), $[Co(\beta CDtren)H_2O]^{2+}$ (– – –) and $[Co(\beta CDtren)R\text{-}Trp]^{2+}$ (——) at pH 7.0 (0.025 mol dm^{-3} NaPIPES buffer) in aqueous solution at 298.2 K and I = 0.10 mol dm^{-3} ($NaClO_4$).*

The spectra of the Co^{2+} complexes, recorded under the same saturating nitrogen conditions as those applying in the titrations, are shown in Fig. 2.9. The spectrum of the

high-spin complex, $[Co(tren)H_2O]^{2+}$, is characterised by peaks at (λ_{max} nm (ε dm^3 mol^{-1} cm^{-1})) 480 (47), 570 (42), and 732 (12), in the range 350-1000 nm.[38] These bands are assigned to the $^4A_2' \rightarrow {}^4E''$, $^4A_2'(1) \rightarrow {}^4A_2'(3)$, and $^4A_2' \rightarrow {}^4E'$ transitions, respectively.[43,44]

Upon inspection of the spectra in Fig. 2.9, an additional band at 450 nm (ε = 61 dm^3 mol^{-1} cm^{-1}) can be seen, with other strongly absorbing bands apparent at shorter wavelengths. These charge transfer bands, which are absent from the spectra of completely oxygen free solutions of $[Co(tren)H_2O]^{2+}$, probably arise from the formation of μ-peroxo complexes and give the solutions their intense brown colour. Such binuclear peroxo-bridged complexes are well established for tetra- and pentaaminecobalt(II) complexes.[45,46]

The same bands are present for the metallocyclodextrin complexes, suggesting the formation of μ-peroxo metallocyclodextrin complexes, and probably the same geometry as the tren complex. The lower intensity of the charge transfer bands may indicate that the μ-peroxo species does not form as readily with the metallocyclodextrins as it does with the tren complex. In addition, the decreased absorbance at longer wavelengths may reflect a change in stereochemistry in the metallocyclodextrin complexes relative to the tren complex, as octahedral complexes are typically weakly absorbing.

Since the above spectra most closely represent the situation present in the titration vessel, no attempt to eliminate the μ-peroxo species in the spectral solutions was made. While the proportion of the complex existing as the μ-peroxo form is probably small, the effect of this on the measured stability constants is uncertain and accordingly the stability constants for the Co^{2+} system listed in Table 2.10 and 2.11 cannot be reliably compared with those of related species.

Spectra for the complexes formed by Ni^{2+} with tren, βCDtren and both βCDtren and tryptophan can be seen in Fig. 2.10. Over the wavelength range 400-900 nm, $[Ni(tren)(H_2O)_2]^{2+}$ exhibits a major absorbance maximum at 560 nm (ε = 10 dm^3 mol^{-1} cm^{-1}), assigned to the $^3A_{2g} \rightarrow {}^3T_{1g}(F)$ transition,[40,44] in reasonable agreement with the literature.[41]

The spectra of $[Ni(\beta CDtren)(H_2O)_2]^{2+}$ and $[Ni(\beta CDtren)Trp]^{+}$ differ only slightly in molar absorbance within this spectral range, exhibiting maxima at 567 nm (ε = 6 dm^3 mol^{-1} cm^{-1} for both complexes). The spectral similarity between the metallocyclodextrin complexes and the tren complex is consistent with the metallocyclodextrins also being six-coordinate.

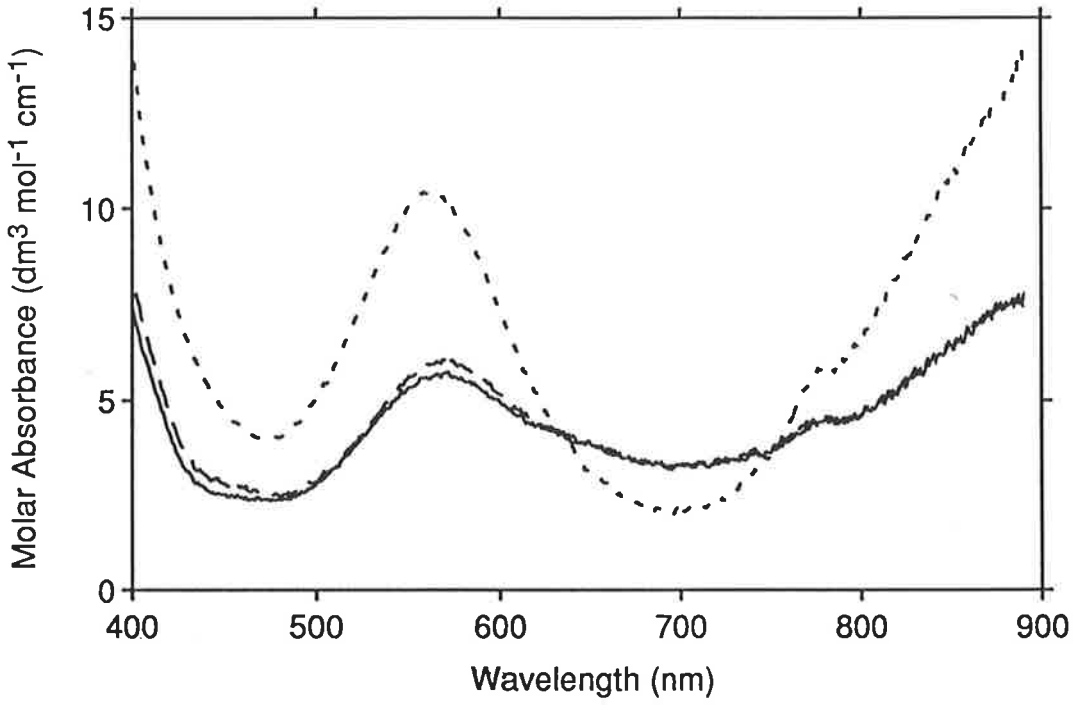

Figure 2.10 *Molar absorbance of $[Ni(tren)(H_2O)_2]^{2+}$ (----), $[Ni(\beta CDtren)(H_2O)_2]^{2+}$ (– – –) and $[Ni(\beta CDtren)(R\text{-}Trp)]^{2+}$ (——) at pH 7.0 (0.025 mol dm^{-3} NaPIPES buffer) in aqueous solution at 298.2 K and I = 0.10 mol dm^{-3} ($NaClO_4$).*

Spectra for the complexes formed by Cu^{2+} with tren, βCDtren and both βCDtren and tryptophan can be seen in Fig. 2.11. The spectrum of $[Cu(tren)H_2O]^{2+}$ shows a shoulder at *ca.* 720 nm and a maximum at 847 nm (ε = 142 dm^3 mol^{-1} cm^{-1}), assigned to the $^2A_1' \rightarrow {}^2E''$ and $^2A_1' \rightarrow {}^2E'$ transitions, respectively,[43] in reasonable agreement with the literature.[41]

The spectra of $[Cu(\beta CDtren)H_2O]^{2+}$ and $[Cu(\beta CDtren)Trp]^{+}$ exhibit shoulders at *ca.* 698 and *ca.* 690 nm, respectively, and maxima at 841 nm (ε = 131 and 128 $dm^3\ mol^{-1}\ cm^{-1}$, respectively). These metallocyclodextrin spectra closely resemble that of the tren complex, consistent with Cu^{2+} also being five-coordinate in these metallocyclodextrins.

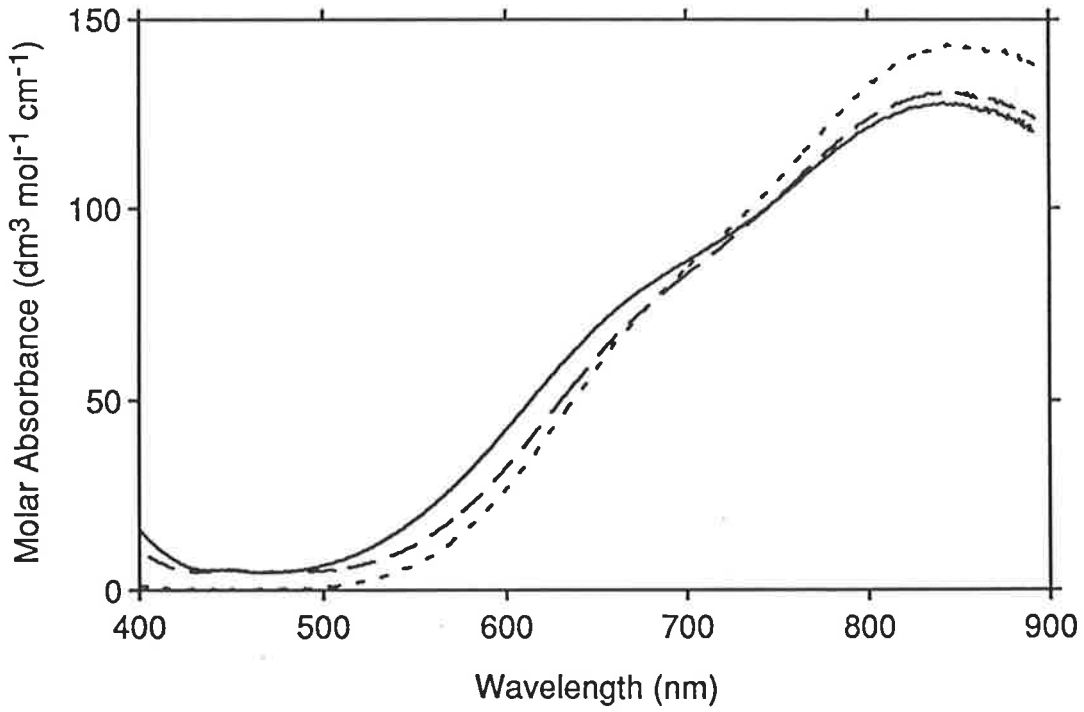

Figure 2.11 *Molar absorbance of $[Cu(tren)H_2O]^{2+}$ (----), $[Cu(\beta CDtren)H_2O]^{2+}$ (– – –) and $[Cu(\beta CDtren)(R\text{-}Trp)]^{2+}$ (——) at pH 7.0 (0.025 mol dm^{-3} NaPIPES buffer) in aqueous solution at 298.2 K and I = 0.10 mol dm^{-3} ($NaClO_4$).*

U/v-visible spectroscopy provides little information about the environment of Zn^{2+} because its d^{10} electronic configuration results in no *d-d* bands. While the formation of five-coordinate $[Zn(tren)H_2O]^{2+}$ in solution[38] indicates the possibility of five-coordinate $[Zn(\beta CDtren)H_2O]^{2+}$ and $[Zn(\beta CDtren)Trp]^{+}$ forming, an analysis of stability data indicates that six-coordination is more probable.

On comparison of the $\log(K/dm^3\ mol^{-1})$ values for $[M(\beta CDtren)]^{2+}$ with those of $[M(tren)]^{2+}$, differences of 2.95, 1.21 and 2.25 are found when M^{2+} = Ni^{2+}, Cu^{2+} and

Zn^{2+}, respectively (Table 2.10). The first difference corresponds to the effect of the βCD substituent on a six-coordinate metal centre, whereas the second corresponds to its effect on a five-coordinate metal centre. The difference when $M^{2+} = Zn^{2+}$ is intermediate between the other two values, which may result from the βCD substituent causing a change from five to six-coordination.

The differences between the $\log(K/dm^3\ mol^{-1})$ values for $[M(\beta CDtren)(R)\text{-}Trp]^+$ and $[M(\beta CDtren)]^+$ are 3.45, 7.79 and 4.15, and the analogous data for the (*S*)-Trp^- analogue are 3.55, 7.89 and 3.95 when $M^{2+} = Ni^{2+}$, Cu^{2+} and Zn^{2+}, respectively (Tables 2.10 and 2.11). In both cases the first and third values are quite similar, whereas the difference is about double in the case of Cu^{2+}. This is consistent with similar coordination changes occurring for $[Ni(\beta CDtren)]^+$ and $[Zn(\beta CDtren)]^+$ on complexation of Trp^-, and both metal centres being six-coordinate. Similar comparisons may be made with the binary and ternary metallocyclodextrins of βCDpn (Table 2.10 and 2.11).

The changes in band position and intensity, observed between the $[M(tren)]^{2+}$ and $[M(\beta CDtren)]^{2+}$ spectra, indicate that the presence of βCD does perturb the binding ability of the tren substituent. The similarity of the binary and ternary metallocyclodextrin spectra suggest negligible perturbation is induced by the amino acid. The formation of $[Ni(\beta CDtren)Trp]^+$ whose structure is probably cis-diaquo-octahedral, is outlined in Fig. 2.12.

In the metallocyclodextrin complexes a cyclodextrin primary hydroxy group may coordinate to the metal centre, which is bound by the polyamine substituent in close proximity (Section 2.2.4 and 2.3.4), but it is not possible to distinguish between such coordination and that of a water molecule from this data. Hence, the stoichiometries of the binary five and six-coordinate metallocyclodextrins may be $[M(\beta CDtren)]^{2+}$ and $[M(\beta CDtren)H_2O]^{2+}$, respectively, and a similar situation may arise in the ternary complexes.

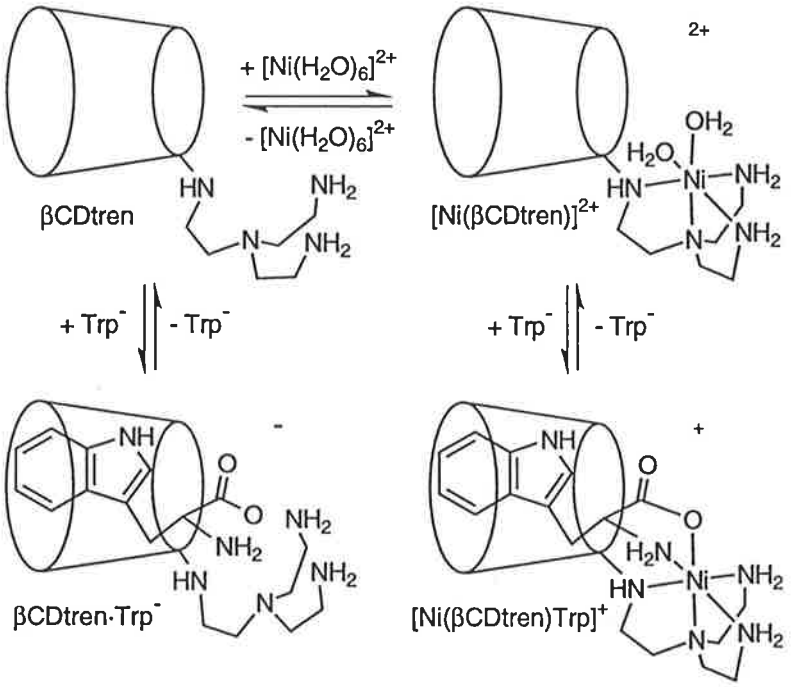

Figure 2.12 *Proposed structure and formation of the six-coordinate binary and ternary metallocyclodextrins, [Ni(βCDtren)(H$_2$O)$_2$]$^{2+}$ and [Ni(βCDtren)Trp]$^+$.*

The substantial increase in stability of the ternary metallocyclodextrin complexes (Table 2.11) relative to [βCDtren·Trp]$^-$ (Table 2.8), indicates interaction of tryptophan with the metal centre. This is consistent with the amino acid moiety facing the primary end of the cyclodextrin cavity. Coordination through the amino or the carboxylate group of Trp$^-$, or both may occur, although in the five-coordinate complexes a second coordination would require displacement of a coordinating group other than water. The nature of the coordinating atoms (oxygen or nitrogen) cannot be determined from these spectra, as a change in donor atom may not produce a detectable spectral change. Consequently the number of coordinated water molecules displaced by tryptophan upon formation of the ternary complex cannot be deduced, and the stoichiometry of the six-coordinate ternary complexes may in fact be [M(βCDtren)(H$_2$O)Trp]$^+$ rather than [M(βCDtren)Trp]$^+$. Structural changes may also occur with a change in pH as donor atoms become deprotonated.

2.3.6 Complexation of Tryptophan by the Co^{2+}, Ni^{2+}, Cu^{2+} and Zn^{2+} Metallocyclodextrin Derivatives of βCDtren

The formation of the ternary metallocyclodextrins, as exemplified by [Ni(βCDtren)Trp]$^+$ in Fig. 2.12, are now discussed in detail.

The [M(βCDtren)Trp]$^+$ stabilities are greater than those of either βCDtren·Trp$^-$ or [M(Trp)]$^+$ (Table 2.8 and Table 2.9). This is consistent with the binding of the Trp$^-$ amino acid moiety by M^{2+} and the hydrophobic interaction between the Trp$^-$ aromatic moiety and the hydrophobic interior of the cyclodextrin annulus reinforcing each other to stabilise [M(βCDtren)(*R*)-Trp]$^+$ and [M(βCDtren)(*S*)-Trp]$^+$. Characteristic pH titration profiles for the βCDtren/Trp, βCDtren/Cu^{2+} and βCDtren/Cu^{2+}/Trp systems are compared in Fig. 2.13.

The stability constants, for the binding of Trp$^-$ by the metallocyclodextrins of βCDtren (Table 2.11), reveal a departure from the Irving-Williams series ($Co^{2+} < Ni^{2+} < Cu^{2+} > Zn^{2+}$) for Co^{2+}. This may arise from the formation of a μ-peroxo species as mentioned in Section 2.3.5, and consequently the Co^{2+} system is not further discussed. For the other three metal ions, the relative stabilities of the ternary metallocyclodextrins reflect the variation in ionic radii of six-coordinate Ni^{2+}, five-coordinate Cu^{2+} and six-coordinate Zn^{2+}, which are 0.69, 0.65 and 0.74 Å, respectively,[47] and the geometric constraints arising from ligand-field effects in Ni^{2+} and Cu^{2+}.[46] This variation in stability with the nature of M^{2+} in the sequence $Ni^{2+} < Cu^{2+} > Zn^{2+}$ is similar to that for the formation of [MTrp]$^+$ (Table 2.9), and is consistent with the size[47] and electronic configuration[48] of M^{2+} exerting a major influence in the complexation of tryptophan.

The stability of the analogous ternary complexes formed with βCDpn vary with the nature of M^{2+} in the sequence, $Co^{2+} \leq Ni^{2+} < Cu^{2+} > Zn^{2+}$.[4,5] The influence of the nature of M^{2+} on the stabilities of the ternary complexes reflects the variation in the ionic radii of six-coordinate Co^{2+}, Ni^{2+}, Cu^{2+} and Zn^{2+}, which are 0.745, 0.69, 0.73 and 0.74 Å,[47] respectively, and the geometric constraints arising from ligand-field effects in

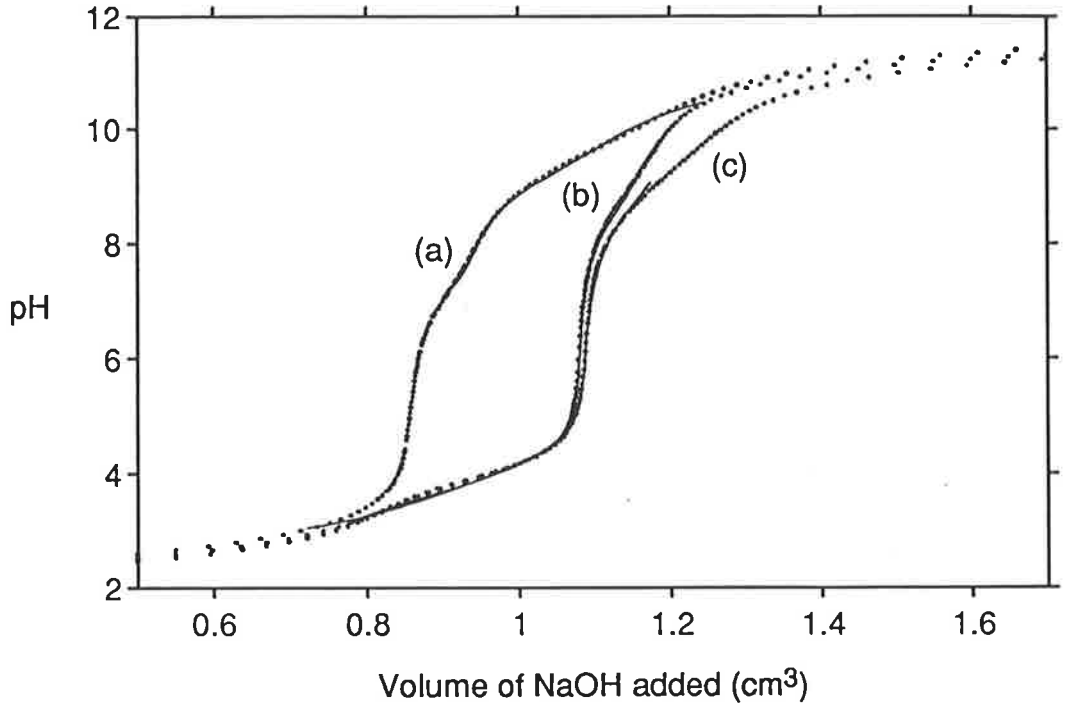

Figure 2.13 *Titration profiles of: (a) $\beta CDtrenH_4^{4+}$ (8.25 x 10^{-4} mol dm^{-3}) and (R)-$TrpH_2^+$ (1.03 x 10^{-3} mol dm^{-3}), (b) $\beta CDtrenH_4^{4+}$ (8.25 x 10^{-4} mol dm^{-3}) and $Cu(ClO_4)_2$ (7.64 x 10^{-4} mol dm^{-3}), and (c) $\beta CDtrenH_4^{4+}$ (8.25 x 10^{-4} mol dm^{-3}), (R)-$TrpH_2^+$ (1.03 x 10^{-3} mol dm^{-3}) and $Cu(ClO_4)_2$ (7.64 x 10^{-4} mol dm^{-3}), each in aqueous 0.009 mol dm^{-3} $HClO_4$ and 0.090 mol dm^{-3} $NaClO_4$, against 0.101 mol dm^{-3} NaOH. The dots represent data points and the solid line represents the best fit to the algorithm arising from the equilibria discussed in Sections 2.3.2 (Table 2.8), 2.3.4 (Table 2.10) and 2.3.6 (Table 2.11), respectively.*

Co^{2+}, Ni^{2+} and Cu^{2+}.[46] The stepwise stability constants for the formation of the ternary metallocyclodextrins, $[M(\beta CDtren)(R)\text{-}Trp]^+$ and $[M(\beta CDtren)(S)\text{-}Trp]^+$, from $[M(\beta CDtren)]^{2+}$ and (*R*)- and (*S*)-Trp^-, are substantially greater than the analogous stability constants for the formation of $[M(\beta CDpn)(R)\text{-}Trp]^+$ and $[M(\beta CDpn)(S)\text{-}Trp]^+$ (Table 2.11). This reflects the differing interactions of Trp^- with βCDpn and βCDtren that produced the *ca.* 10^3 fold greater stability of βCDtren·(*R*)-Trp^- and βCDtren·(*S*)-Trp^- by comparison with that of βCDpn·(*R*)-Trp^- and βCDpn·(*S*)-Trp^-, as discussed in

Table 2.11 Stability constants for the Co^{2+}, Ni^{2+}, Cu^{2+} and Zn^{2+} complexes of βCDtren and βCDpn with (R)- and (S)-tryptophan in aqueous solution at 298.2 K and I = 0.1 mol dm^{-3} ($NaClO_4$).

	log (K/dm^3 mol^{-1})			
Equilibrium	M = Co	M = Ni	M = Cu	M = Zn
$[M(\beta CDtren)]^{2+} + (R)\text{-}Trp^- \rightleftharpoons [M(\beta CDtren)(R)\text{-}Trp]^{+}$ [a]	12.2 ± 0.2[c]	8.2 ± 0.2	9.5 ± 0.3	8.1 ± 0.1
$[M(\beta CDtren)]^{2+} + (S)\text{-}Trp^- \rightleftharpoons [M(\beta CDtren)(S)\text{-}Trp]^{+}$ [a]	12.6 ± 0.1[c]	8.1 ± 0.2	9.4 ± 0.2	8.3 ± 0.1
$[M(\beta CDtren)]^{2+} + (R)\text{-}TrpH \rightleftharpoons [M(\beta CDtren)(R)\text{-}TrpH]^{2+}$ [a]	8.9 ± 0.2[c]	4.6 ± 0.2	4.3 ± 0.3	—
$[M(\beta CDtren)]^{2+} + (S)\text{-}TrpH \rightleftharpoons [M(\beta CDtren)(S)\text{-}TrpH]^{2+}$ [a]	9.2 ± 0.2[c]	4.3 ± 0.2	4.2 ± 0.2	—
$[M(\beta CDtren)(R)\text{-}Trp]^{+} + H^+ \rightleftharpoons [M(\beta CDtren)(R)\text{-}TrpH]^{2+}$ [a]	6.0 ± 0.4[c]	5.6 ± 0.3	4.0 ± 0.5	—
$[M(\beta CDtren)(S)\text{-}Trp]^{+} + H^+ \rightleftharpoons [M(\beta CDtren)(S)\text{-}TrpH]^{2+}$ [a]	5.8 ± 0.3[c]	5.4 ± 0.3	4.0 ± 0.3	—
$[M(\beta CDtrenH)]^{3+} + (R)\text{-}TrpH \rightleftharpoons [M(\beta CDtrenH)(R)\text{-}TrpH]^{3+}$ [a]	9.5 ± 0.2[c]	3.56 ± 0.07	4.4 ± 0.2	4.82 ± 0.06
$[M(\beta CDtrenH)]^{3+} + (S)\text{-}TrpH \rightleftharpoons [M(\beta CDtrenH)(S)\text{-}TrpH]^{3+}$ [a]	9.73 ± 0.06[c]	3.6 ± 0.3	4.4 ± 0.2	4.96 ± 0.05
$[M(\beta CDtren)(R)\text{-}TrpH]^{2+} + H^+ \rightleftharpoons [M(\beta CDtrenH)(R)\text{-}TrpH]^{3+}$ [a]	6.9 ± 0.4[c]	5.6 ± 0.3	4.3 ± 0.4	—
$[M(\beta CDtren)(S)\text{-}TrpH]^{2+} + H^+ \rightleftharpoons [M(\beta CDtrenH)(S)\text{-}TrpH]^{3+}$ [a]	6.8 ± 0.3[c]	6.0 ± 0.4	4.3 ± 0.3	—
$[M(\beta CDtren)((R)\text{-}Trp)OH] + H^+ \rightleftharpoons [M(\beta CDtren)(R)\text{-}Trp]^{+}$ [a]	6.78 ± 0.02[c]	7.86 ± 0.02	8.58 ± 0.02	8.7 ± 0.3
$[M(\beta CDtren)((S)\text{-}Trp)OH] + H^+ \rightleftharpoons [M(\beta CDtren)(S)\text{-}Trp]^{+}$ [a]	6.6 ± 0.1[c]	7.77 ± 0.03	8.53 ± 0.08	8.76 ± 0.08
$[M(\beta CDpn)]^{2+} + (R)\text{-}Trp^- \rightleftharpoons [M(\beta CDpn)(R)\text{-}Trp]^{+}$ [b]	4.04 ± 0.03	4.1 ± 0.2	7.85 ± 0.07	5.3 ± 0.1
$[M(\beta CDpn)]^{2+} + (S)\text{-}Trp^- \rightleftharpoons [M(\beta CDpn)(S)\text{-}Trp]^{+}$ [b]	4.32 ± 0.05	5.1 ± 0.2	8.09 ± 0.05	5.3 ± 0.1

[a] Derived from data in the pH ranges 4.3 – 7.0, 5.1 – 9.0, 2.9 – 8.9 and 4.9 – 9.2 for Co^{2+}, Ni^{2+}, Cu^{2+} and Zn^{2+} respectively. [b] Refs. 3 and 4.
[c] These values may be affected by the formation of a μ-peroxo species (see Section 2.3.5).

Section 2.3.2. The probability of Trp^- coordinating to the metal ion should be greater for $[M(\beta CDpn)]^+$ than $[M(\beta CDtren)]^{2+}$ on a statistical basis, as there are four coordinated water molecules available for substitution in the former case, compared with one or two in the latter, depending on the identity of M^{2+}. However, this is insufficient to offset the differences in the contributions to ternary metallocyclodextrin stability arising from the interaction of Trp^- with βCDpn and βCDtren.

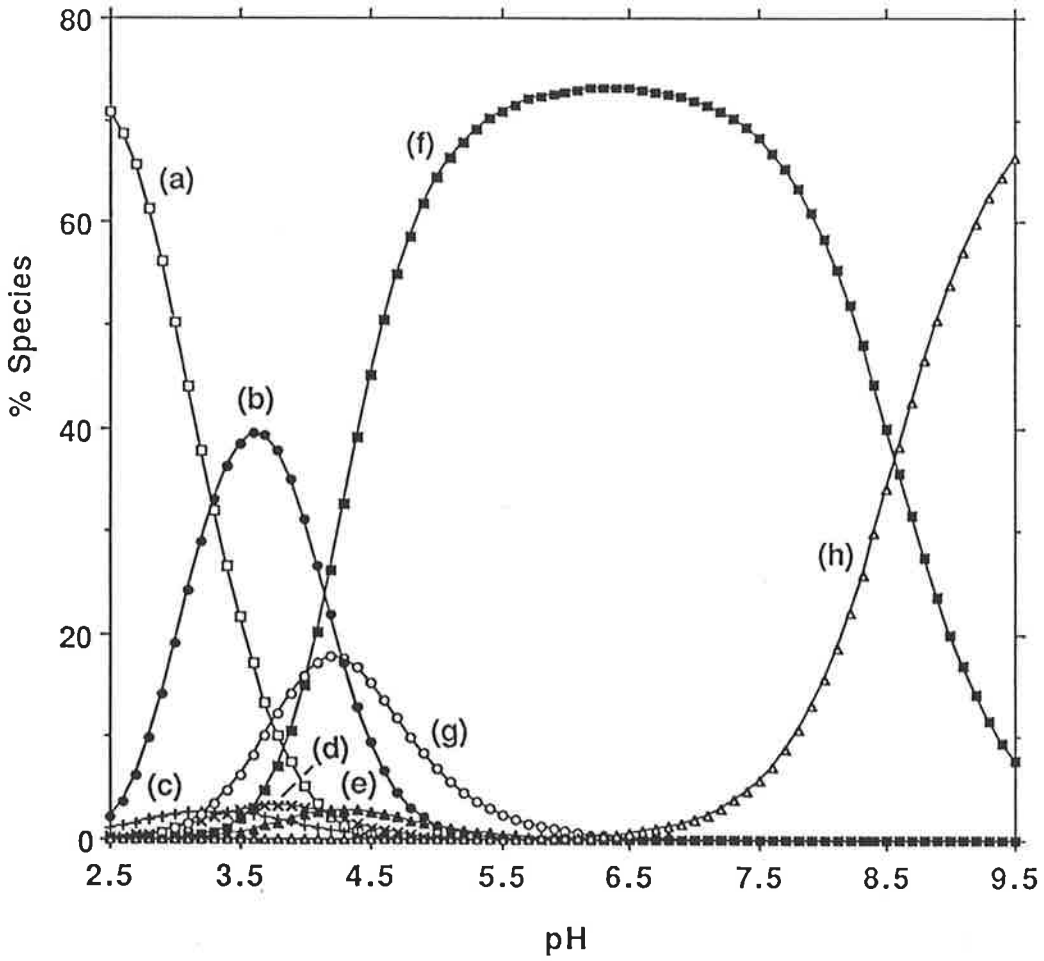

Figure 2.14 *Percentage of Cu^{2+} species in a solution 7.64 x 10^{-4}, 8.25 x 10^{-4} and 1.03 x 10^{-3} mol dm^{-3} in total Cu^{2+}, βCDtren and (R)-tryptophan concentrations, respectively, calculated from the data in Tables 2.1, 2.7 - 2.11 and plotted relative to $[(R)\text{-tryptophan}]_{total}$ = 100%. The curves represent: (a) Cu^{2+}, b) $[Cu(\beta CDtrenH)\text{-}(R)\text{-}TrpH]^{3+}$, (c) $[Cu\{(R)\text{-}Trp\}]^+$, (d) $[Cu(\beta CDtrenH)]^{3+}$, (e) $[Cu(\beta CDtren)]^{2+}$, (f) $[Cu(\beta CDtren)(R)\text{-}Trp]^+$, (g) $[Cu(\beta CDtrenH)(R)\text{-}Trp]^{2+}$ and (h) $[Cu(\beta CDtren)\text{-}\{(R)\text{-}Trp\}OH]$. No other Cu^{2+} species are present at greater than 5% in this pH range.*

The stability constants listed in Table 2.1 and Tables 2.7 to 2.11 were used to derive the variation in major species present with pH for the Cu^{2+}/βCDtren/-(*R*)-tryptophan system, as shown in Figs. 2.14 and 2.15.

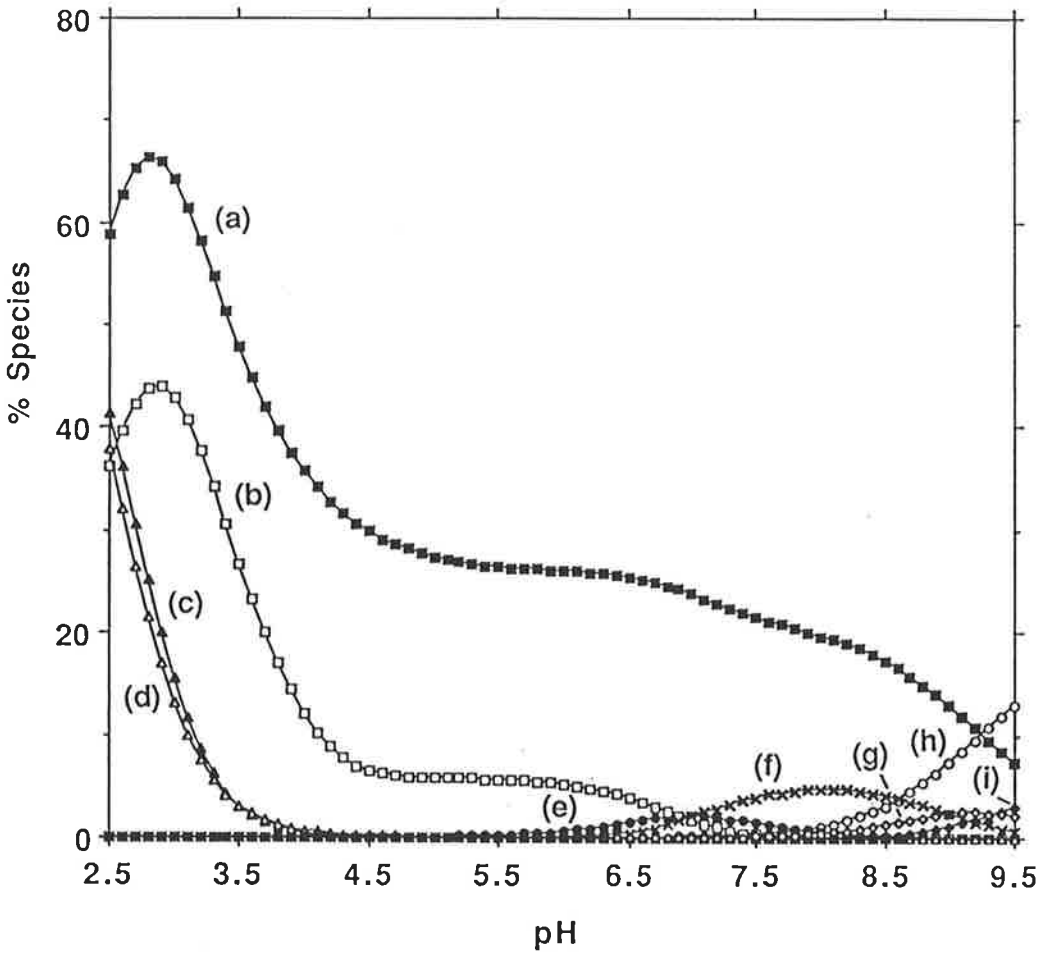

Figure 2.15 *Percentage of non-Cu^{2+} species in a solution 7.64 x 10^{-4}, 8.25 x 10^{-4} and 1.03 x 10^{-3} mol dm^{-3} in total Cu^{2+}, βCDtren and (R)-tryptophan concentrations, respectively, calculated from the data in Tables 2.1, 2.7 - 2.11 and plotted relative to $[(R)\text{-tryptophan}]_{total}$ = 100%. The curves represent: (a) (R)-TrpH, (b) $\beta CDtrenH_3^{3+}$, (c) $\beta CDtrenH_4^{4+}$, (d) $(R)\text{-}TrpH_2^{+}$, (e) $\beta CDtrenH_2^{2+}$, (f) $\beta CDtrenH\cdot(R)\text{-}TrpH^{+}$, (g) βCDtrenH·(R)-Trp, (h) $(R)\text{-}Trp^{-}$ and (i) $\beta CDtren\cdot(R)\text{-}Trp^{-}$. No other non-$Cu^{2+}$ species are present at greater than 5% in this pH range.*

The pairs of protonated species, [M(βCDtren)(*R*)-TrpH]$^{2+}$ and [M(βCDtren)(*S*)-TrpH]$^{2+}$, and [M(βCDtrenH)(*R*)-TrpH]$^{3+}$ and [M(βCDtrenH)-(*S*)-TrpH]$^{3+}$, are of similar stabilities which are substantially decreased by comparison with those of [M(βCDtren)(*R*)-Trp]$^{+}$ and [M(βCDtren)(*S*)-Trp]$^{+}$. This similarity probably arises because TrpH acts as a monodentate ligand in both pairs and the major contribution to stability arises from the interaction of the Trp^{-} aromatic moiety with the hydrophobic interior of the cyclodextrin annulus. (Once again the hydroxo species probably corresponds to the deprotonation of a coordinated water molecule.)

No enantioselectivity is found in the formation of [M(βCDtren)(*R*)-Trp]$^{+}$ and [M(βCDtren)(*S*)-Trp]$^{+}$. This contrasts with the closely related [M(βCDpn)(*R*)-Trp]$^{+}$ and [M(βCDpn)(*S*)-Trp]$^{+}$ complexes, where a 10-fold enantioselectivity for (*S*)-Trp^{-} is found when $M^{2+} = Ni^{2+}$, and a moderate enantioselectivity is also seen when $M^{2+} = Co^{2+}$ or Cu^{2+} (Table 2.11). A similar variation has been found in the enantioselective complexation of (*R*)- and (*S*)-Phe^{-} by [M(βCDpn)]$^{2+}$, which shows an enantioselectivity of greater than 6-fold when $M^{2+} = Ni^{2+}$, favouring the (*S*)-Phe^{-} enantiomer.[5] Evidently the size of Ni^{2+} and its octahedral stereochemistry are particularly appropriate in engendering enantioselectivity for (*S*)-Trp^{-} over (*R*)-Trp^{-} and for (*S*)-Phe^{-} over (*R*)-Phe^{-} resulting from the interaction of their chiral centres with βCDpn in the metallocyclodextrin. No enantioselectivity is observed for Zn^{2+} (d^{10}), suggesting that the absence of ligand-field-generated geometric constraints allows more flexibility in the structures of its ternary complexes and the stabilising effects of βCDpn are more easily accommodated.[4] In contrast, the d^{9} electronic configuration of the similar sized Cu^{2+} imposes a tetragonally distorted octahedral geometry which may place greater constraints on the interaction of the chiral centres of (*R*)-Trp^{-} and (*S*)-Trp^{-} with the βCDpn moiety, and decrease the stability of [Cu(βCDpn)(*R*)-Trp]$^{+}$ by comparison with that of [Cu(βCDpn)(*S*)-Trp]$^{+}$. Similar arguments may be applied in the cases of d^{7} Co^{2+} and d^{8} Ni^{2+} whose six-coordinate geometries more closely approach regular octahedrons. The smaller enantioselectivity observed in the more stable complexes of Cu^{2+} demonstrate that increasing complex stability does not necessarily induce a corresponding increase in

enantioselectivity. The enantioselectivity observed for βCDpn is coincident with the weaker interaction of Trp^- with βCDpn, by comparison with βCDtren, allowing M^{2+} to exert more influence on the binding of Trp^-.

The absence of enantioselectivity in the $[M(\beta CDtren)]^{2+}$ complexation of Trp^-, appears to be correlated with the strength of the diastereomeric ternary complexes formed. The existence of enantioselectivity requires the difference in the free energy contributions arising from interaction of the (*R*)- and (*S*)- chiral centres of the guests with the homochirality of the metallocyclodextrin to be significant compared with the total free energy for guest binding. Despite the higher stabilities of $[M(\beta CDtren)(R)\text{-}Trp]^+$ and $[M(\beta CDtren)(S)\text{-}Trp]^+$, by comparison with those of $[M(\beta CDpn)(R)\text{-}Trp]^+$ and $[M(\beta CDpn)(S)\text{-}Trp]^+$, the opposed chiralities of (*R*)-Trp^- and (*S*)-Trp^- generate too small a free energy difference for this requirement to be satisfied, and hence no thermodynamic enantioselectivity is observed. Thermodynamic enantioselectivity may also reverse to favour (*R*)-Trp^- and (*R*)-Phe^- with a change in the metal binding group, as is discussed in Section 2.2.5 (and Section 1.3.3). Although the potentiometric titration method did not detect a significant thermodynamic enantioselectivity, discrimination may still be detectable by other methods such as ^1H NMR spectroscopy for the diamagnetic systems.[49]

2.4 Summary and Conclusions

Substitution of a primary hydroxyl group with a coordinating group produces modified cyclodextrins capable of binding metal ions to form metallocyclodextrins whose variation in stability, with the nature of M^{2+}, follows the Irving-Willams series.[34]

The binary metallocyclodextrin may bind a guest, thus producing a ternary metallocyclodextrin. These ternary complexes also appear to follow the Irving-Williams series.[34] The metallocyclodextrin/amino acid ternary complex is stabilised, relative to that of the cyclodextrin/amino acid complex, by the coordination interactions between the guest and the additional binding site introduced by the metal ion. However, the ternary metallocyclodextrin complex stability may be lower or higher than that of the M^{2+}/amino

acid complex, implying that in some instances competition between the binding sites occurs, whilst in others the guest interactions with the cyclodextrin annulus and the metal centre reinforce each other. Such reinforcement of the binding interactions is observed for the complexation of tryptophan by the Ni^{2+}, Cu^{2+} and Zn^{2+} metallocyclodextrins of βCDtren and the Zn^{2+} metallocyclodextrin of βCDpn.

The variation in ternary metallocyclodextrin complex stability with the nature of the amino acid reflects the different coordination mode of histidine by comparison with phenylalanine and tryptophan, and the variation in size of the amino acid aromatic side chain.

The proposed general structure of these complexes has the aromatic moiety of the amino acid included inside the cyclodextrin annulus with the chiral centre in the vicinity of the primary hydroxy groups, where the amino acid donor atoms can coordinate to the metal ion which is anchored at the primary end of the cavity by the amines of the coordinating group attached to the cyclodextrin.

No evidence of a change in coordination number upon formation of a ternary metallocyclodextrin from its binary metallocyclodextrin precursor, $[M(\beta CDtren)]^{2+}$, is found. The binary and ternary metallocyclodextrins appear to be six-coordinate for Ni^{2+} and Zn^{2+}, but five coordinate for Cu^{2+}, probably with cis-diaquo-octahedral and distorted trigonal bipyramidal geometry, respectively. The binary and ternary Cu^{2+} metallocyclodextrins of βCDpn probably have six-coordinate tetragonally distorted octahedral geometry around the metal centre.

Although the Cu^{2+} metallocyclodextrin of βCDpn demonstrates enantioselectivity for Phe^- and Trp^-,[3,4,5] no significant enantioselectivity is seen for histidine. The complexation of tryptophan by $[M(\beta CDtren)]^{2+}$, where $M^{2+} = Ni^{2+}$, Cu^{2+} and Zn^{2+}, also showed no thermodynamic enantioselectivity, despite the greater stability of these complexes by comparison with those of βCDpn. The free energy difference for complexation of the tryptophan enantiomers by the metallocyclodextrin must be significant relative to the total free energy of ternary metallocyclodextrin formation, if enantioselectivity is to be observed. In this case the free energy contributions arising from

selective interactions of (*R*)- and (*S*)-Trp^- enantiomers with the cyclodextrin homochirality are not significant compared with the free energy contributions arising from the non-selective interactions of the amino acid with the cyclodextrin annulus and M^{2+}. However, the closely related metallocyclodextrins, $[M(\beta CDpn)]^+$, bind (*S*)-Trp^- enantioselectively over (*R*)-Trp^- when M^{2+} = Co^{2+}, Ni^{2+} and Cu^{2+}. This enantioselectivity is coincident with the weaker interaction of Trp^- with βCDpn, by comparison with βCDtren, allowing M^{2+} to exert more influence on the binding of Trp^-.

These observations indicate the subtle relationship between the nature of the cyclodextrin and M^{2+} in guest binding in ternary metallocyclodextrins. The interplay of chiralities of host and guest in the ternary complexes can be strongly influenced by small changes in M^{2+} ionic radius and d^n electronic configuration, which affect the preferred geometry about the M^{2+} centre. Similarly, subtle relationships are probably partly responsible for the high degree of metal ion specificity observed for metalloenzyme activity.

The metallocyclodextrins studied here are also potential catalysts for ester hydrolysis, and rate studies could comprise some interesting comparisons with the work discussed in Section 1.3.3, and provide more information on the effect of the metal centre. By suitable adjustment of the ligand-metal orientation, taking into account the angles and distances between the coordinating groups, enhancement of the coordination recognition interactions and stricter binding constraints may be achieved in the future.

References

1. G. Impellizzeri, G. Maccarrone, E. Rizzarelli, G. Vecchio, R. Corradini and R. Marchelli, *Angew. Chem. Int. Ed. Engl.*, 1991, **30**, 1348.

2. V. Cucinotta, F. D'Alessandro, G. Impellizzeri and G. Vecchio, *J. Chem. Soc., Chem.Commun.*, 1992, 1743.

3. S. E. Brown, J. H. Coates, C. J. Easton, S. J. van Eyk, S. F. Lincoln, B. L. May, M. A. Stile, C. B. Whalland and M. L. Williams, *J. Chem. Soc., Chem. Commun.*, 1994, 47.

4. S. E. Brown, J. H. Coates, C. J. Easton and S. F. Lincoln, *J. Chem. Soc. Faraday Trans.*, 1994, **90**, 739.

5. S. E. Brown, C. A. Haskard, C. J. Easton and S. F. Lincoln, *J. Chem. Soc. Faraday Trans.*, 1995, **91**, 1013.

6. R. Corradini, A. Dossena, G. Impellizzeri, G. Maccarrone, R. Marchelli, E. Rizzarelli, G. Sartor and G. Vecchio, *J. Am. Chem. Soc.*, 1994, **116**, 10267.

7. B. L. Vallee and D. S. Auld, in *Methods in Protein Sequence Analysis*, eds., H. Jörnvall, J.-O. Höög and A.-M. Gustavsson, Birkhäuser Verlag, Basel, 1991, p. 363.

8 P. Gans, A. Sabatini and A.Vacca, *J. Chem. Soc., Dalton Trans.*, 1985, 1195; A. Sabatini, A. Vacca and P. Gans, *Coord. Chem. Rev.*, 1992, **120**, 389.

9. S. Farr-Jones, W.Y.L. Wong, W. G. Gutheil and W. W. Bachovchin, *J. Am. Chem. Soc.*, 1993, **115**, 6813.

10. M. Remelli, C. Munerato and F. Pulidori, *J. Chem. Soc. Dalton Trans.*, 1994, 2049.

11. *Critical Stability Constants*, ed., R. M. Smith and A. E. Martell, Plenum Press, New York, 1975.

12. R. P. Bonomo, V. Cucinotta, F. D'Alessandro, G. Impellizzeri, G. Maccarrone, E. Rizzarelli and G. Vecchio, *J. Inclusion Phenom. Mol. Recognit. Chem.*, 1993, **15**, 167.

13. R. P. Bonomo, V. Cucinotta, F. D'Alessandro, G. Impellizzeri, G. Maccarrone, G. Vecchio and E. Rizzarelli, *Inorg. Chem.*, 1991, **30**, 2708.

14. Y. Inoue and Y. Miyata, *Bull. Chem. Soc. Jpn.*, 1981, **54**, 809; A. Örstan, J. B. A. Ross, *J. Phys. Chem.*, 1987, **91**, 2739.

15. M. D. Johnson, C. A. McIntosh and V. C. Reinsborough, *Aust. J. Chem.*, 1994, **47**, 187.

16. M. Hoshino, M. Imamura, K. Ikehara and Y. Hama, *J. Phys. Chem.*, 1981, **85**, 1820.

17. I. Tabushi, Y. Kuroda and T. Mizutani, *J. Am. Chem. Soc.*, 1986, **108**, 4514; I. Tabushi, Y. Kuroda, M. Yamada and T. Sera, *J. Inclusion Phenom.*, 1988, **6**, 599.

18. D. W. Armstrong, X. Yang, S. M. Han and R. A. Menges, *Anal. Chem.*, 1987, **59**, 2594; K. B. Lipkowitz, S. Raghothama and J. Yang, *J. Am. Chem. Soc.*, 1992, **114**, 1554.

19. H. Kozlowski, A. Anouar, T. Kowalik-Jankowska, P. Decock, J. Swiatek-Kozlowska and L. D. Pettit, *Inorg. Chim. Acta.*, 1993, **207**, 223.

20. P. Gockel, H. Vahrenkamp and A. D. Zuberbühler, *Helv. Chim. Acta.*, 1993, **76**, 511.

21. V. J. Montesinos, A. Terrón, J. J. Fiol, V. Moreno and A. Caubet, *Synth. React. Inorg. Met.-Org. Chem.*, 1993, **23**, 937.

22. D. D. Perrin and V. S. Sharma, *J. Chem. Soc. (A)*, 1967, 724.

23. D. D. Perrin, *J. Chem. Soc.*, 1960, 3189.

24. I. Tabushi, N. Shimizu, T. Sugimoto, M. Shiozuka and K. Yamamura, *J. Am. Chem. Soc.*, 1977, **99**, 7100.

25. H-J. Schneider and F. Xiao, *J. Chem. Soc. Perkin Trans. 2*, 1992, 387.

26. Y. Matsui, T. Yokoi and K. Mochida, *Chem. Lett.*, 1976, 1037.

27. E. U. Akkaya and A. W. Czarnik, *J. Phys. Org. Chem.*, 1992, **5**, 540.

28. E. U. Akkaya and A. W. Czarnik, *J. Am. Chem. Soc.*, 1988, **110**, 8553.

29. M. McNamara and N. R. Russell, *J. Inclusion Phenom. Mol. Recognit. Chem.*, 1992, **13**, 145.

30. K. Mochida and Y. Matsui, *Chem. Lett.*, 1976, 963.

31. S. Divakar, *J. Inclusion Phenom. Mol. Recognit. Chem.*, 1994, **17**, 119.

32. R. Fuchs, N. Habermann and P. Klüfers, *Angew. Chem. Int. Ed. Engl.*, 1993, **32**, 852.

33. G. Anderegg and V. Gramlich, *Helv. Chim. Acta*, 1994, **77**, 685.

34. H. Irving and R. J. P. Williams, *J. Chem. Soc.*, 1953, 3192.

35. J. H. Coates, G. J. Gentle and S. F. Lincoln, *Nature*, 1974, **249**, 775.

36. K. Yamanari, M. Nakamichi and Y. Shimura, *Inorg. Chem.*, 1989, **28**, 248.

37. M. Ciampolini and N. Nardi, *Inorg. Chem.*, 1966, **5**, 41.

38. P. Paoletti, M. Ciampolini and L. Sacconi, *J. Chem. Soc.*, 1963, 3589.

39. M. Ciampolini and P. Paoletti, *Inorg. Chem.*, 1967, **6**, 1261.

40. R. J. West, PhD Thesis, The University of Adelaide, 1973.

41. C. K. Jørgensen, *Acta Chem. Scand.*, 1956, **10**, 887.

42. D. P. Rablen, H. W. Dodgen and J. P. Hunt, *J. Am. Chem. Soc.*, 1972, **94**, 1771.

43. M. Ciampolini, *Struct. Bonding*, 1969, **6**, 52.

44. D. B. Lever, *Studies in Physical and Theoretical Chemistry 33: Inorganic Electronic Spectroscopy*, 2nd edn., Elsevier, Amsterdam, 1984, p. 491 & 507.

45. M. Mori and J. A. Weil, *J. Am. Chem. Soc.*, 1967, **89**, 3732. M. Mori, J. A. Weil and M. Ishiguro, *J. Am. Chem. Soc.*, 1968, **90**, 615.

46. F. A. Cotton and G. Wilkinson, *Advanced Inorganic Chemistry*, 5th edn., Wiley-Interscience, New York, 1988.

47. R. D. Shannon, *Acta Crystallogr., Sect. A*, 1976, **32**, 751.

48. D. F. Shriver, P. W. Atkins and C. H. Langford, *Inorganic Chemistry*, 2nd edn., Oxford University Press, Oxford, 1994.

49. S. E. Brown, J. H. Coates, P. A. Duckworth, S. F. Lincoln, C. J. Easton and B. L. May, *J. Chem. Soc., Faraday Trans.*, 1993, **89**,1035.

CHAPTER 3

Cooperative binding of 6-(p-Toluidinyl)-naphthalene-2-sulfonate by Linked Cyclodextrin Dimers

3.1 Introduction

Several linked cyclodextrin dimers have been reported in the literature and some studies on the combined effect of the two cyclodextrin hydrophobic binding sites have been made (Section 1.3.4). If each cyclodextrin annulus of a linked cyclodextrin dimer behaves as a separate entity in complexing a guest molecule, the (host)·(guest) complex stability constant is expected to be double that of the corresponding cyclodextrin monomer complex, on statistical grounds. However, if the stability of the linked cyclodextrin dimer complex exceeds this value, and any interactions with the tether are assumed not to stabilise the complex significantly, cooperative binding between the two cyclodextrin hydrophobic recognition sites is operating.

Although complexation studies have been undertaken for particular hosts with a range of guests, few comparisons of the binding properties of a range of hosts for a particular guest have been made. The linked cyclodextrin dimers reported in the literature are connected by several different types of linking groups, and the distance between the cyclodextrin annuli is also quite variable. The constraint this inter-cavity distance poses on the complexation of guests which contain two aromatic binding sites, as in TNS^- (Fig. 3.1), is of interest, since each aromatic moiety is expected to maximise interaction with a hydrophobic cyclodextrin cavity.

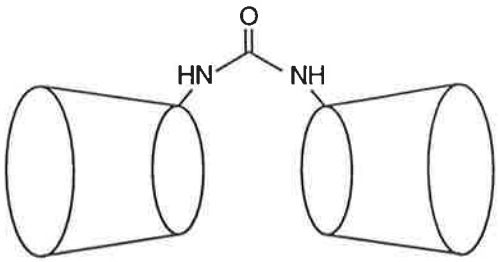

$(\beta CD)_2Ur$

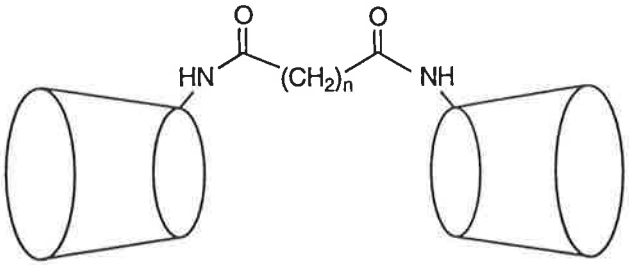

n=0 : $(\beta CD)_2Ox$
n=1 : $(\beta CD)_2Ma$
n=2 : $(\beta CD)_2Sc$
n=3 : $(\beta CD)_2Gl$

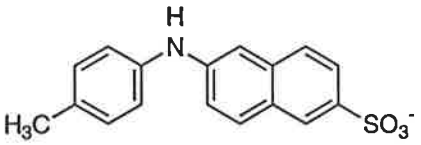

6-(*p*-Toluidino)naphthalene-2-sulfonate (TNS^-)

Figure 3.1 *The linked cyclodextrin dimer hosts,* $(\beta CD)_2Ur$, $(\beta CD)_2Ox$, $(\beta CD)_2Ma$, $(\beta CD)_2Sc$ *and* $(\beta CD)_2Gl$, *and the guest molecule studied,* TNS^-. *(The tethers of the linked cyclodextrin dimers are exaggerated in size by comparison with the* βCD *annuli.)*

To further investigate the complexation properties of linked cyclodextrin dimers, a range of diamide-1°,1°-linked-βCDs ($(\beta CD)_2X$, X = Ur, Ox, Ma, Sc, Gl) were selected, and their complexation of the anionic fluorophore, TNS^-, was compared with that of βCD. The term diamide-1°,1°-linked-βCD is used here to refer to two βCD units which are connected by a diamide group which joins their primary rims (Fig. 3.1). The linked cyclodextrin dimers utilised in this study are generally referred to as diamide-1°,1°-linked-

βCDs, although the tether in $(\beta CD)_2Ur$ (Fig 3.1) is not strictly a diamide. In each linked cyclodextrin dimer a primary hydroxyl of each annulus is replaced by the amine portion of an amide group. The cyclodextrin annuli are separated by two bonds length in $(\beta CD)_2Ur$, which has urea as the linking group, and this is the shortest tether used in this study. The length of the tether is increased to oxalamide in $(\beta CD)_2Ox$, separating the annuli by three bonds. In $(\beta CD)_2Ma$, the malonamide link separates the annuli by four bonds. Methylene groups continue to be added within the tether for $(\beta CD)_2Sc$ and $(\beta CD)_2Gl$, producing annuli separations of five and six bonds, respectively. Diamide-linked cyclodextrin dimers were selected as they are more resistant to hydrolysis than esters and hence are more stable on storage.[1] The guest, TNS^- (Fig. 3.1), was chosen as its fluorescent properties are extremely sensitive to the immediate local environment (Section 3.2) and it possesses two aromatic rings, which can each potentially fit into the hydrophobic cavity of a cyclodextrin host and may behave as two hydrophobic recognition sites for complexation by a linked cyclodextrin dimer. The size of the βCD annulus is most appropriate for the inclusion of TNS^-, as evidenced by the greater fluorescence enhancement and the higher stability constants for inclusion of TNS^- by βCD (Table 3.1) compared with those of αCD or γCD. The stability constants for the inclusion complexes of TNS^- formed with αCD and γCD have been reported as < 50 and 110-1500 $dm^3\ mol^{-1}$, respectively.[2-4] Both βCD and γCD form $(host)_2 \cdot TNS^-$ complexes, whereas αCD, which is known not to include a naphthalene ring, forms only an $\alpha CD \cdot TNS^-$ complex.[2]

The complexation of TNS^- by various linked cyclodextrin dimers has been reported, as discussed in Section 3.4.6. During the course of this work Petter *et al.*[5] reported the complexation of 6-(4-*tert*-butylanilino)naphthalene-2-sulfonate (BNS^-) (Appendix, (23)), whose structure is closely related to TNS^-, by a range of dithiol-1°,1°-linked-βCDs. The variation in stability of the linked cyclodextrin dimer complex with BNS^- upon increasing the tether length from a disulfide (-S-S-) to $-S(CH_2)_nS-$ (n = 2,3,4,5,6) was investigated. The optimum length tether was $-S(CH_2)_2S-$, and as the tether length was increased beyond this, the free energy of binding dropped by *ca.* 1.0 kJ mol^{-1} per methylene group added.[5] Linked cyclodextrin dimers with longer tethers are

expected to undergo more negative entropy changes upon forming a highly ordered complex, which is consistent with the observed trend.

Before discussing the complexation of TNS^- by βCD and its linked cyclodextrin dimers, it is essential to understand the origin of the TNS^- fluorescence itself, and this is now discussed.

3.2 Properties of TNS^-

The absorption spectrum of TNS^- possesses bands centred at 223 nm ($\varepsilon = 4.70 \times 10^4$ dm^3 mol^{-1}), 263 nm ($\varepsilon = 2.45 \times 10^4$ dm^3 mol^{-1}), 317 nm ($\varepsilon = 1.89 \times 10^4$ dm^3 mol^{-1}) and a broad less intense amine band at 366 nm ($\varepsilon = 4.08 \times 10^3$ dm^3 mol^{-1}).[6] Although the absorbance spectra of TNS^- in water and ethanol are very similar, the quantum yields of TNS^- in these two solvents are very different.[6] This suggests that ground state interactions play only a small role in determining the width and maximum of the TNS^- fluorescence peak.

The dependence of TNS^- fluorescence wavelength and intensity on the local molecular environment is well known, exhibiting blue shifts and intensification in less polar environments. In water TNS^- is barely fluorescent, with emission maxima at *ca.* 400 and 490 nm, whereas in organic solvents of low polarity or when bound to the hydrophobic environment of a macromolecule, it fluoresces much more strongly, with a λ_{max} of *ca.* 420-460 nm.[6,7] Accordingly, TNS^- has been widely used as a microenvironmental probe in studying the structure, conformational changes, interactions and dynamics of macromolecules, such as proteins[6,8,9] and membranes.[10] Although TNS^- is charged, the charged group does not appear to play a large role in binding. Generally TNS^- is bound to sites which are hydrophobic in nature.[6]

The variation in TNS^- fluorescence with a change in polarity of the local environment may arise partially from general solvent effects. A change in dipole moment of TNS^- upon excitation from the ground to the excited state, leads to reorientation of the surrounding solvent molecules, which is known as solvent relaxation. Polar solvents

interact more strongly with the more polar state, and thus, stabilise one state more than the other. This induces a change in energy difference between the ground and excited states and a concomitant shift in emission wavelength. The quantum yield of TNS^- is also related to the extent of solvent interactions, as the likelihood of nonradiative transitions increases with increasing interactions of the solvent with the excited fluorophore.

The solvent dependence of TNS^- emission has been studied[6,7,11,12] in an effort to analyse the mechanism of fluorescence. A number of factors are known to influence the fluorescence of TNS^- besides environmental polarity. Fluorescence intensity is enhanced by solvents of low dielectric constant and, to a lesser extent, by solvents of high viscosity.[6] Microscopic, rather than macroscopic, viscosity appears important, as TNS^- fluorescence is unchanged in the presence of high molecular weight sugars at high concentrations.[13] The fluorescence of TNS^- is also affected by temperature.[6] Interestingly, the fluorescence in ice, where the fluorophore is surrounded by polar molecules, is similar to that in nonpolar solvents and in the presence of cyclodextrin.[14] This may be due to a slowing of solvent relaxation, such that it does not occur within the fluorescence lifetime of the fluorophore, or a reduction in the intramolecular freedom of TNS^-. Specific chemical groupings can also affect fluorescence by solvent-fluorophore interactions such as hydrogen bonding, charge-transfer interactions, acid-base chemistry, and complexation.[6,7] These effects are determined by the chemical nature of the solvent and fluorophore. For instance, the emission maximum of TNS^- is shifted to longer wavelengths by hydrogen bonding (probably to the sulfonate oxygens) in hydrogen bond donor solvents, but to shorter wavelengths as a consequence of hydrogen bonding (probably from the toluidino proton) to hydrogen bond acceptor solvents.[15]

The effect of solvents on the fluorescence of TNS^- has previously been interpreted in terms of conformation and rigidity of the fluorophore, solvent relaxation, and the existence of one[6] or two[12] excited singlet species. However, a trilinear analysis of TNS^- fluorescence in various solvents recently led to the proposal of a third distinct excited state.[7]

This recently proposed model for TNS^- fluorescence (Fig. 3.2) incorporates excitation (λ_{max} = 290 nm) of a S_0 ground state, in which the bridging nitrogen is either protonated or hydrogen bonded, and subsequent emission from a charge-transfer excited state ($S_{1\text{-ct,perp}}$, λ_{max} emission = 400 nm). Also incorporated is excitation (λ_{max} *ca.* 330 nm) of a S_0 ground state in which hydrogen bonding and protonation are absent. Subsequent emission occurs from a conventional π^* excited state ($S_{1,np}$, λ_{max} emission *ca.* 453 nm) and a charge-transfer excited state ($S_{1\text{-ct,np}}$, λ_{max} emission *ca.* 490 nm), which is generated by an intramolecular electron transfer from the phenyl to the naphthyl ring.

Both ground states possess a nonplanar orientation of the phenyl and naphthyl rings (Fig. 3.2) as free rotation is permitted by the tetrahedral geometry about the bridging nitrogen. This nonplanar orientation of the rings is maintained in the $S_{1,np}$ excited state and conjugation of the nitrogen lone pair with the rings can occur to an extent in some conformations. The $S_{1\text{-ct,perp}}$ excited state is stabilised by an essentially perpendicular orientation of the phenyl and naphthyl moieties (Fig. 3.2), and the extent of conjugation is either reduced or absent, in the presence of hydrogen bonding or protonation, respectively. The extent of conjugation is greatest for the $S_{1\text{-ct,np}}$ excited state, which is stabilised by a close to coplanar orientation of the phenyl and naphthyl rings, and the geometry about the bridging nitrogen atom may become trigonal planar (Fig. 3.2).

Using the model outlined in Fig. 3.2, the variation in TNS^- fluorescence may be interpreted in terms of solvent effects which induce changes in molecular conformation and promote an equilibrium between the conventional and charge-transfer excited states. The contribution of each of the three distinct excited states to the overall observed fluorescence is sensitive to the microenvironment of TNS^-. Charge-transfer excited states are stabilised by highly polar environments, with emission from the $S_{1\text{-ct,perp}}$ and $S_{1\text{-ct,np}}$ excited states dominating in protic and aprotic polar solvents, respectively. The relative emission of the $S_{1\text{-ct,perp}}$ state also increases with decreasing pH of aqueous solutions. As solvent polarity is decreased, the contribution to overall fluorescence from $S_{1,np}$ increases dramatically.

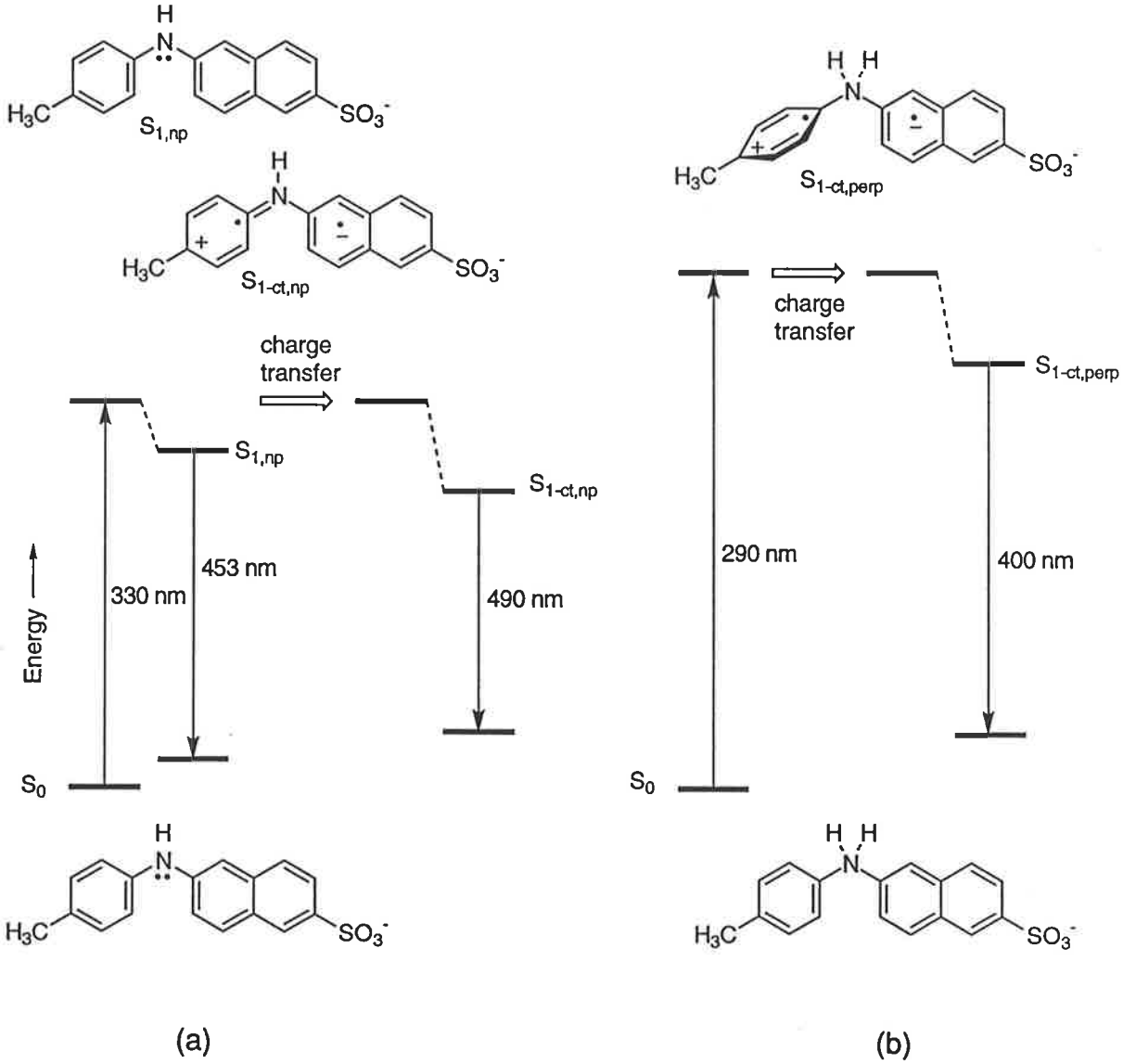

Figure 3.2 *Energy level diagram showing the excitation and emission of TNS^- when (a) the amino group is unprotonated and not hydrogen bonded, and (b) when the amino group is either protonated or hydrogen bonded. The ground states are denoted by S_0, and the conventional π^* excited state is represented by $S_{1,np}$. The charge-transfer excited states are denoted $S_{1\text{-}ct,np}$ and $S_{1\text{-}ct,perp}$. Proposed molecular species are drawn near their corresponding states and dashed lines represent solvent relaxation of the excited state energy levels.*

The decrease in quantum yield of emission with a increase in solvent polarity arises from a slight decrease in the radiative rate and a dramatic increase in the nonradiative rate.[11,16] A number of mechanisms of nonradiative deactivation of the excited state may occur, but the main nonradiative pathway[16] involves intramolecular charge-transfer. A rapid equilibrium between the conformations of the conventional and charge-transfer excited states, and the accompanying electron-transfer reaction, lead to fluorescence quenching. The charge-transfer process is extremely fast in highly polar solvents and the short fluorescence lifetimes of the resultant $S_{1\text{-ct,perp}}$ and $S_{1\text{-ct,np}}$ excited states produce a low quantum yield in polar solvents. Molecular degrees of freedom also provide modes for radiationless transitions between electronic states. The increase in quantum yield with increasing solvent viscosity strengthens the hypothesis that intramolecular rotation between the phenyl and naphthyl rings of TNS^- causes internal losses of energy.[6] Nonradiative deactivation may also occur through collisional quenching with the solvent, and through chemical quenching by specific functional groups in the solvent. In general, solvents possessing delocalised electrons are fairly effective as quenching agents.[6] Intersystem crossing from an excited singlet state to an excited triplet state has been excluded as a likely quenching mechanism, as the yield of triplet state molecules decreases sharply with increasing solvent polarity.[11]

Although the solvent dependence of the TNS^- emission spectrum indicates the existence of three distinct excited states, no emission from the $S_{1,np}$ state is observed in aqueous solution due to the rapid rate of intramolecular charge-transfer.[7] The $S_{1\text{-ct,np}} \rightarrow S_0$ transition is red shifted by comparison with the $S_{1\text{-ct,perp}} \rightarrow S_0$ transition, as expected from the increased planarity and π-conjugation.[17,18] Emission from the $S_{1\text{-ct,perp}}$ state predominates in neutral aqueous solution as a result of the protic nature of water (Fig. 3.3). However, the emission maximum of TNS^- in water is usually quoted as being 480-500 nm[13,19-21] since the extent of blue shift from the 490 nm band is used as a measure of hydrophobicity. The emission spectrum of TNS^- in aqueous phosphate buffer (Fig. 3.3), was fitted to two gaussian curves giving rise to band centres at 408 and 489 nm, and the quantum yield of TNS^- under these conditions was determined to be 0.0008. Both

the emission maxima and quantum yield are in good agreement with literature values.[2,7,16] Emission from the third excited state, $S_{1,np}$, appears in solvents of lower polarity and higher viscosity.

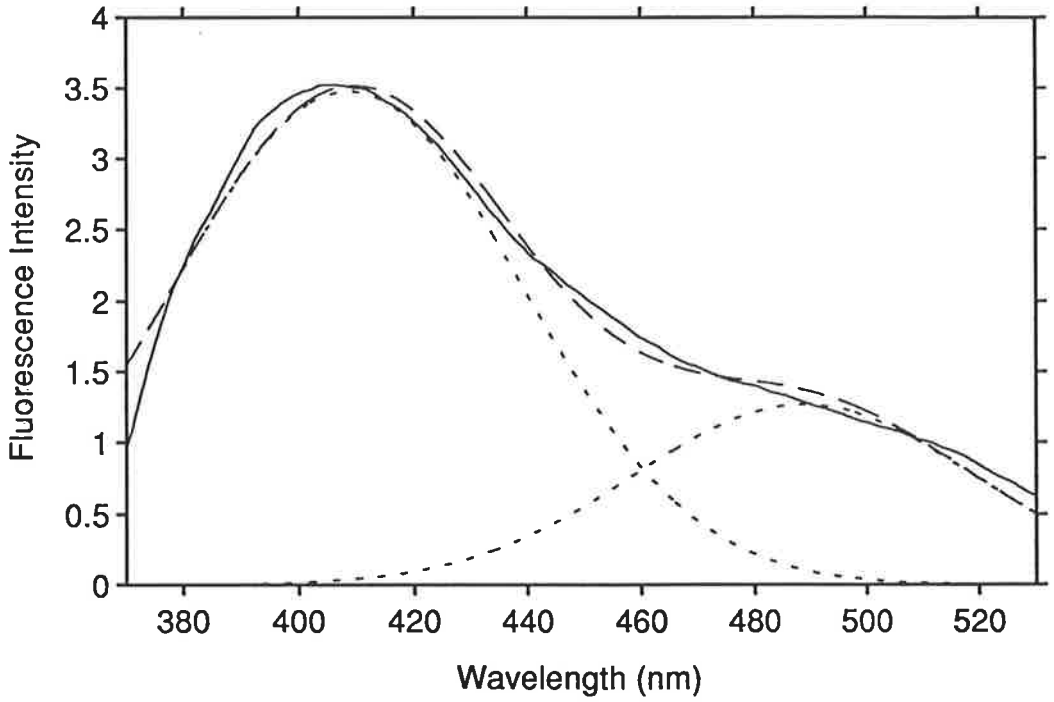

Figure 3.3 *Emission spectrum of TNS^- (1.00×10^{-6} mol dm^{-3}) in aqueous phosphate buffer (pH 7.0, I = 0.10 mol dm^{-3}) at 298.2 K, when excited at 353 nm with excitation and emission slit widths of 5 and 10 nm, respectively. Dotted lines show the fit to two Gaussians having maxima at 408 and 489 nm.*

The effect of different environments on the fluorescence spectrum of TNS^- allowed the stability constants, of the inclusion complexes formed with various cyclodextrins, to be determined. The concentration of TNS^- was fixed at 1.0×10^{-6} mol dm^{-3} and the effect of increasing cyclodextrin concentration on the fluorescence of aqueous solutions was monitored. As mentioned above, TNS^- fluorescence is affected by temperature[6] and pH. Consequently, all solutions were maintained at 298.2 ± 0.1 K and pH 7.0 (phosphate

buffer). Under these conditions the fluorescence of TNS^- was low (Fig. 3.3), and TNS^- was in the anionic form where the sulfonate group is strongly solvated.

In each experiment the excitation wavelength was chosen from within the longest wavelength absorption band to reduce the possibility of reabsorption. Excitation was made at either the isosbestic point, or in its absence, at the wavelength where the least change in absorption occurred upon addition of cyclodextrin to the TNS^- solution. Since the difference in absorbance of TNS^- in the absence and presence of cyclodextrin was known, the relative fluorescence emission could be calculated (Section 6.2.3).

3.3 Complexation of TNS^- by βCD

3.3.1 Stoichiometry

The complexation of TNS^- by βCD has previously been studied by a number of workers,[2-5,13,16,19,20,22-26] and the formation of complexes with up to two different stoichiometric ratios, as outlined in Eqns. 3.1 and 3.2, have been proposed.

$$\beta CD + TNS^- \overset{K_1}{\rightleftharpoons} \beta CD \cdot TNS^- \qquad (3.1)$$

$$\beta CD \cdot TNS^- + \beta CD \overset{K_2}{\rightleftharpoons} (\beta CD)_2 \cdot TNS^- \qquad (3.2)$$

Schneider *et al.*[24] found a poor fit and a strong dependence of the stability constant values on the emission wavelength if the variation in TNS^- fluorescence with addition of βCD was analysed on the basis of $\beta CD \cdot TNS^-$ formation only. This indicated the presence of another complex besides $\beta CD \cdot TNS^-$.

The additional complex was proposed to be $(\beta CD)_2 \cdot TNS^-$. When spectral data analysis was based on the formation of both $\beta CD \cdot TNS^-$ and $(\beta CD)_2 \cdot TNS^-$ an excellent fit resulted.[24] Molecular models indicate that TNS^- is too large to be completely included in a single βCD annulus, however, the cavity of βCD is sufficiently large to enable

accommodation of the naphthyl group or the toluidinyl group. This provides two opportunities for inclusion, at first one of these groups can be included by a βCD cavity, and then the other can associate with a second βCD molecule to form $(\beta CD)_2 \cdot TNS^-$. The formation of a $(\beta CD)_2 \cdot TNS^-$ complex is also supported by the deviation from linearity of double reciprocal plots of fluorescence versus βCD concentration at high concentrations, where the large excess of βCD permits formation of such a complex.[2,13,20]

The generation of two distinct $\beta CD \cdot TNS^-$ complexes, one with the phenyl and one with the naphthyl group in the cavity, has also been suggested.[24-26] The rationalisation of NOE and complex induced shift NMR data suggest that this is more likely than formation of a $(\beta CD)_2 \cdot TNS^-$ complex.[24] The ^1H NMR shift data yield stability constants of 2040 and 1520 $dm^3\ mol^{-1}$, for the formation of two $\beta CD \cdot TNS^-$ complexes.[24] However, the NMR data do not rule out the possibility of $(\beta CD)_2 \cdot TNS^-$ complex formation.

Multiple fluorescence lifetimes for TNS^- in βCD solutions show that TNS^- occupies a number of different sites. Fluorescence decay traces have been analysed in accordance with the formation of three inclusion sites.[25] The first represents the formation of an encounter complex, as previously postulated,[27] in which the forward rate constant is presumed to be close to the diffusion-controlled limit and TNS^- is placed in a slightly more hydrophobic environment than in water. This is followed by a deeper penetration of TNS^- into the much more hydrophobic environment of the βCD cavity, with a concomitant expulsion of water, thus forming the second inclusion site. The third, less populated and most hydrophobic site, is consistent with a deeper penetration of TNS^- into the βCD cavity, or the formation of a $(\beta CD)_2 \cdot TNS^-$ complex, where both ends of the TNS^- molecule are included by βCD annuli. The formation of $(\beta CD)_2 \cdot TNS^-$ as the third inclusion site appeared to be more consistent with fluorescence and conductance data.[25]

More recent fluorescence lifetime distribution measurements indicate that the conformation or depth of insertion of an excited TNS^- molecule in a βCD cavity may be distributed within a wide range, leading to the co-existence of multiple $\beta CD \cdot TNS^-$ complexes with different fluorescence lifetimes, in addition to $(\beta CD)_2 \cdot TNS^-$.[26] A continuous lifetime distribution model has been proposed for the βCD complexation of a

closely related guest, 6-(anilino)naphthalene-2-sulfonate (Appendix, (24)), using frequency domain phase-and-modulation fluorometry.[28]

In summary, complexes with both βCD·TNS$^-$ and (βCD)$_2$·TNS$^-$ stoichiometry appear to form, and it is also quite likely that more than one complex exists with the same stoichiometry.

3.3.1 Stability

The variation in TNS$^-$ fluorescence upon addition of βCD is shown in Fig. 3.4. The data obtained from 46 solutions, of TNS$^-$ with varying βCD concentrations, were fitted to the algorithm arising from the equilibria shown in Eqns. 3.1 and 3.2. The use of matrices permitted simultaneous fitting of the data at 0.5 nm intervals over the wavelength range 410-520 nm, in which a significant change in fluorescence intensity was observed (Fig. 3.4). Accordingly, the derived stability constants of K_1 = 3,140 ± 20 mol dm^{-3} and K_2 = 86 ± 5 mol dm^{-3} (Eqn. 3.1 and 3.2) were based on over 10,000 data points. Due to the errors involved in spectral measurement and solution preparation, the actual errors on these stability constants are greater than the non-weighted standard deviations quoted (but they are unlikely to exceed the non-weighted standard deviation by a factor of ten in this system). The best fit of the variation in fluorescence emission at 453 nm, with added βCD, to this model is shown in Fig. 3.5. Two phases are recognisable in the binding curve, corresponding to the formation of the βCD·TNS$^-$ and (βCD)$_2$·TNS$^-$ complexes.

The same data could also be fitted to the formation of βCD·TNS$^-$ only, yielding K_1 = 1,851 ± 8 mol dm^{-3} (Eqn. 3.1). The visual fit of the data was not as good as that shown in Fig. 3.5. An increase in the sum of squared deviations is expected when the number of fitting parameters is decreased. However, the magnitude of the difference between the sum of squared deviations for this fit (1.6 x 10^4) and that of the fit shown in Fig. 3.5 (3.7 x 10^3), implies that the formation of both βCD·TNS$^-$ and (βCD)$_2$·TNS$^-$ is more likely.

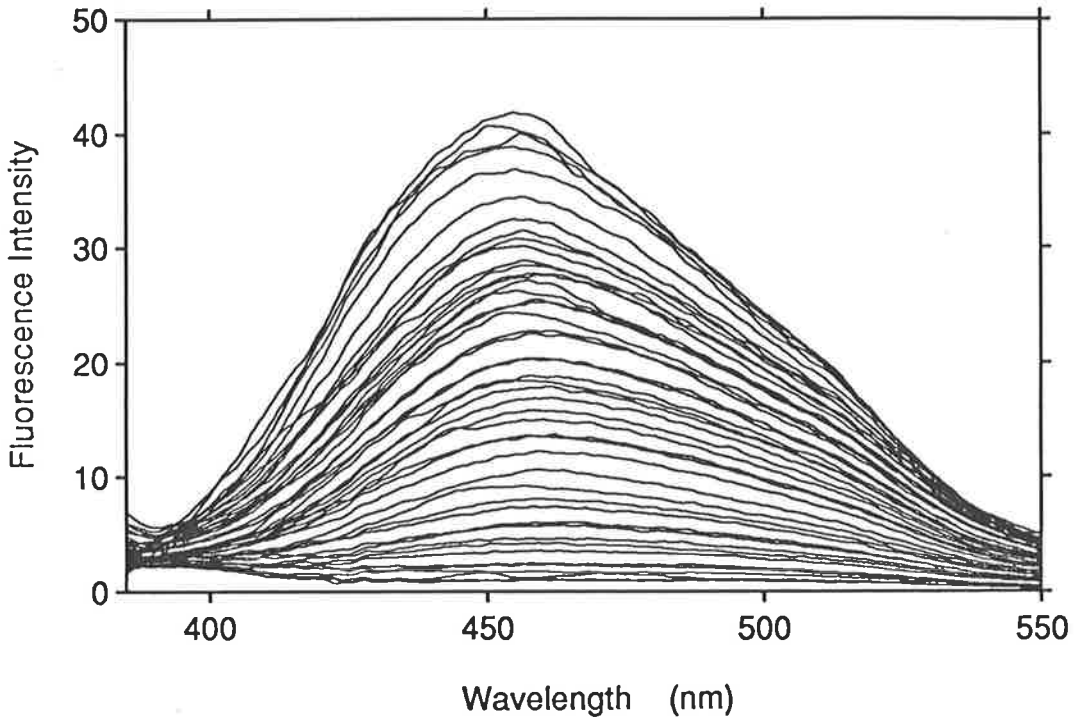

Figure 3.4 *Emission spectrum of TNS^- alone (1.04×10^{-6} mol dm^{-3}) and in the presence of increasing concentrations of βCD (ranging from 1.50×10^{-6} to 5.50×10^{-3} mol dm^{-3}) in aqueous phosphate buffer (pH 7.0, I = 0.10 mol dm^{-3}) at 298.2 K, when excited at 369 nm with excitation and emission slit widths of 5 and 10 nm, respectively. The emission of TNS^- alone is the lowest intensity curve in the montage.*

Stability constants for the complexation of TNS^- by βCD have previously been determined from fluorescence,[2,3,5,13,16,19,22-25] circular dichroism,[4] conductance,[25] and NMR[24] measurements. The stability constants characterising the equilibria in Eqn. 3.1 and 3.2 are reported in Table 3.1. Several studies have only detected formation of $βCD{\cdot}TNS^-$, and yield K_1 values ranging from 1,200 to 3,950 dm^3 mol^{-1}, while others have detected both $βCD{\cdot}TNS^-$ and $(βCD)_2{\cdot}TNS^-$, and yield values of K_1 and K_2 ranging from 970 to 6,650 and from 1.4 to 600 dm^3 mol^{-1}, respectively. This variation probably arises for a number of reasons, as the experimental conditions, measurement methods and data treatments vary considerably (see footnote Table 3.1).

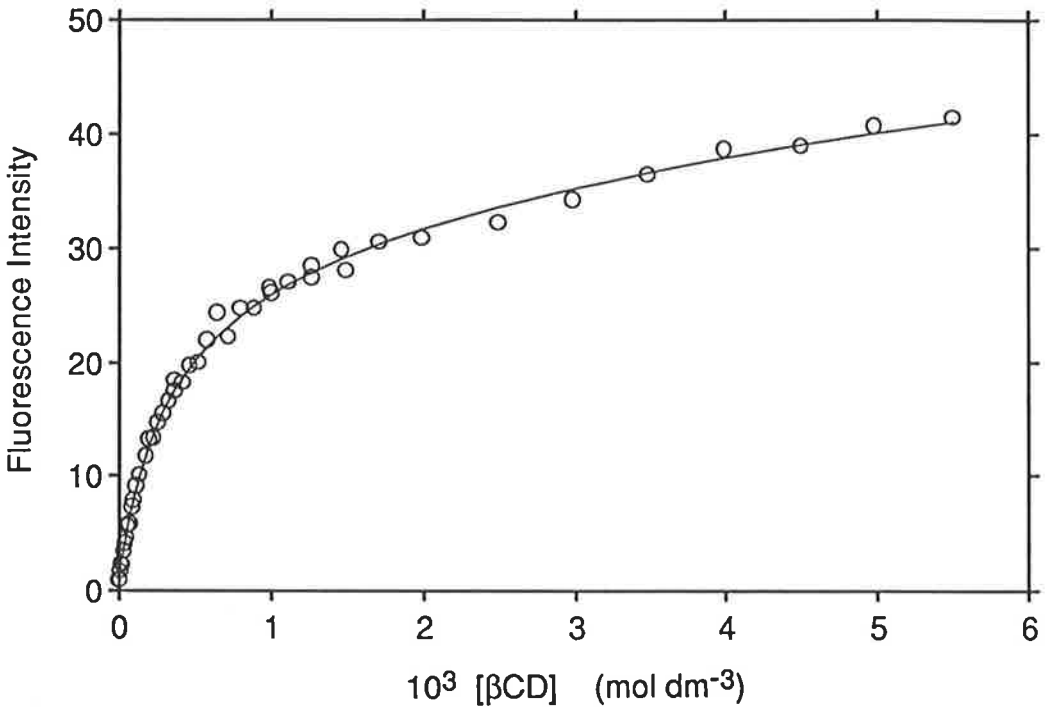

Figure 3.5 *Emission of TNS^- (1.04×10^{-6} mol dm^{-3}) at 453 nm in the presence of increasing concentrations of βCD (ranging from 1.50×10^{-6} to 5.50×10^{-3} mol dm^{-3}) in aqueous phosphate buffer (pH 7.0, I = 0.10 mol dm^{-3}) at 298.2 K, when excited at 369 nm with excitation and emission slit widths of 5 and 10 nm, respectively. The circles represent data points and the solid line represents the best fit to the algorithm arising from the equilibria shown in Eqns. 3.1 and 3.2.*

The seemingly conflicting nature of the values in Table 3.1 may arise partially from complexes other than a simple βCD·TNS^- complex being ignored in some cases.[24] Although only small amounts of $(\beta CD)_2 \cdot TNS^-$ may be present at the concentrations used, this complex is probably strongly fluorescent, and thus, may cause a significant error when fitting for βCD·TNS^- only. Surprisingly, an even greater variation in stability constant is found when the formation of $(\beta CD)_2 \cdot TNS^-$ is also considered. This is possibly due to insufficient $(\beta CD)_2 \cdot TNS^-$ complex formation for reliable stability constant determination. The concentrations of TNS^- and βCD used in these studies determine the relative amounts of each complex forming, and thus the reliability of their respective derived constants.

Table 3.1 *Values of the stability constants defined in Eqns. 3.1 and 3.2 for the complexes formed between βCD and TNS⁻ in aqueous solution.*[a]

K_1 (dm^3 mol^{-1})	K_2 (dm^3 mol^{-1})
1,200[b]	—
1,400[c]	—
1,800[d]	—
3,500[e]	—
3,950[f]	—
9,70[g]	28[g]
1,270[h]	3.3[h]
1,540[i]	14[i]
1,650[g]	57[g]
1,980[j]	600[j]
2,200[k]	68[k]
2,290[g]	91[g]
2,400[l]	1.4[l]
3,140 ± 20 [m]	86 ± 5 [m]
4,000[n]	20[n]
6,650[o]	310[o]

[a] Fluorometrically determined unless indicated otherwise. Linear and non-linear fitting methods are denoted by *l* and *nl*, respectively. [b] Ref. 5 ([TNS⁻] = 3.33 x 10^{-6} mol dm^{-3}, [βCD] ≤ 2.66 x 10^{-6} mol dm^{-3}, 0.01 mol dm^{-3} phosphate buffer, pH 7.0, 296.2 K). [c] Ref. 4 (*l*, [TNS⁻] = 1 x 10^{-4} mol dm^{-3}, [βCD] ≤ 2.0 x 10^{-3} mol dm^{-3}, circular dichroism measurements). [d] Ref. 19 (carbonate buffer, pH 10.60, I = 0.05 mol dm^{-3}, 298.2 K). [e] Ref. 22 ([TNS⁻] = 1 x 10^{-5} mol dm^{-3}, [βCD] ≤ 5 x 10^{-4} mol dm^{-3}, 0.1 mol dm^{-3} phosphate buffer, pH 7.0, 298.2 K). [f] Ref. 3 (*l*, [TNS⁻] = 1 x 10^{-5} mol dm^{-3}, 0.1 mol dm^{-3} $NaHCO_3$, pH 9.0, I = 0.30 mol dm^{-3}). [g] Ref. 25 ([TNS⁻] = (1.0-4.0) x 10^{-3} mol dm^{-3}, [βCD] ≤ 1.3 x 10^{-2} mol dm^{-3}, 298.2 K, these conductometrically determined values decrease with increasing TNS⁻ concentration). [h] Ref. 25 (*nl*, [TNS⁻] = 2 x 10^{-5} mol dm^{-3}, [βCD] ≤ 1.4 x 10^{-2} mol dm^{-3}). [i] Ref. 2 (*nl*, [TNS⁻] = 2.57 x 10^{-5} mol dm^{-3}, [βCD] ≤ 1.3 x 10^{-2} mol dm^{-3}, 0.08 mol dm^{-3} sodium acetate buffer, pH 5.3, I = 0.08 mol dm^{-3}, 298.2 K). [j] Ref. 23 (*nl*, [TNS⁻] = 1.0 x 10^{-5} mol dm^{-3}, [βCD] ≤ 1.0 x 10^{-2} mol dm^{-3}, 0.1 mol dm^{-3} phosphate buffer, pH 7.0, 298.2 K). [k] Ref. 16 (*l*, [TNS⁻] = 1 x 10^{-5} mol dm^{-3}, [βCD] ≤ 1.5 x 10^{-2} mol dm^{-3}). [l] Ref. 24 (*nl*, [TNS⁻] = (1.1-10) x 10^{-4} mol dm^{-3}, [βCD] = (5.0-8.9) x 10^{-4} mol dm^{-3}, fluorometric and NMR measurements). [m] This work (*nl*, [TNS⁻] = 1.0 x 10^{-6} mol dm^{-3}, [βCD] ≤ 5.50 x 10^{-3} mol dm^{-3}, 0.046 mol dm^{-3} phosphate buffer, pH 7.0, I = 0.10 mol dm^{-3}, 298.2 K). [n] Ref. 13 ([TNS⁻] = 1.0 x 10^{-5} mol dm^{-3}, [βCD] ≤ 1.0 x 10^{-2} mol dm^{-3}, 0.1 mol dm^{-3} phosphate buffer, pH 5.9). [o] Ref. 24 (*nl*, [TNS⁻] = (3.3-10) x 10^{-5} mol dm^{-3}, [βCD] = (2.0-6.7) x 10^{-4} mol dm^{-3}).

In the literature it appears that any scattering or fluorescence arising from βCD itself has not been considered, and this may also cause significant variation in the reported stability constants as different βCD concentration ranges were used. Some constants were obtained by linear fitting methods such as double reciprocal plots, and whilst these give good estimates, they place more weight on the lower concentration values than on the higher ones.[23,29] Values obtained from non-linear regression methods are more reliable.

The fluorescence intensity of TNS^- in the presence of βCD is unaffected by a change in ionic strength within the range 0.04-0.64 mol dm^{-3}.[2] This is consistent with the absence of strong electrostatic (dipole-dipole or ion-dipole) interaction in the formation of the inclusion complexes. Within the pH range 4-11 the fluorescence intensity of TNS^- in the presence of βCD is unaffected,[2] and no clear trend is observed in the stability of the complexes formed.[23]

It was due to this substantial variation in literature values, that the excited state stability constants were redetermined, as reported above, under the specific conditions used in the linked cyclodextrin dimer study (Section 3.4). These stability constants were based on a much larger number of data points than those reported in the literature, and the data were fitted using a non-linear least-squares regression routine (Section 6.2.5). The formation of complexes besides $\beta CD \cdot TNS^-$ were considered, and $(\beta CD)_2 \cdot TNS^-$ formed in up to 30% within the concentration range used. The effect of free βCD on the fluorescence spectrum was also taken into account.

The rate of interaction of βCD with TNS^- has been shown by the stopped-flow method to be rapid, essentially being completed within the dead-time of the instrument (*ca.* 1 msec).[2] As the excited state lifetime of TNS^- is much shorter than the mean residence time of a molecule in the βCD cavity (*ca.* 10^{-4} s),[30] the complexation equilibria do not change appreciably during the excited lifetime of the fluorophore. Hence, the excited state stability constants obtained from TNS^- fluorescence enhancement upon addition of βCD, reflect the ground state stability constants.

Thermodynamic quantities for the stepwise formation of $(\beta CD)_2 \cdot TNS^-$ have been determined from conductometric[25] and steady-state fluorescence measurements,[23] and the

reported values vary considerably. The values determined in the latter study were $\Delta H_1° = -9.3$ kJ mol^{-1} and $\Delta S_1° = 31.4$ J mol^{-1} K^{-1} for the first binding, and $\Delta H_2° = 29.9$ kJ mol^{-1} and $\Delta S_2° = 63.6$ J mol^{-1} K^{-1} for the second. These correspond to values of $K_1 = 1860$ dm^3 mol^{-1} and $K_2 = 0.01$ dm^3 mol^{-1} at 298.2 K. Upon binding, the ordered solvent shell surrounding TNS$^-$ is broken up, and the entropy increase for this process is great enough to offset the entropy loss associated with the binding itself.

The dependence of the (βCD)$_2$·TNS$^-$ stability constant on temperature is not as great as that of the βCD·TNS$^-$ complex. For this reason hydrogen bonding is believed to be less important in stabilising (βCD)$_2$·TNS$^-$ than it is in stabilising βCD·TNS$^-$.[23] Hydrogen bonding may occur between the amine group of TNS$^-$ and the hydroxyl groups at the rim of the βCD cavity in both complexes. Hydrogen bonding of the sulfonate group to the βCD hydroxyl groups may also assist in stabilising the complex upon inclusion of the naphthyl moiety, however, when the toluidinyl moiety is included this effect is absent, since the methyl group is only weakly hydrogen bonding at best. This leads to discussion of the most likely complex structures.

3.3.3 Structure

The structures of βCD·TNS$^-$ and (βCD)$_2$·TNS$^-$ are proposed to have either a phenyl or a naphthyl moiety included within each cyclodextrin annulus, with a nonplanar orientation between these aryl rings.

From Corey-Pauling-Kolton (CPK) space filling molecular models, the dimensions of the *p*-toluidinylamino moiety are approximately 6.1 by 7.8 Å, with a thickness of around 3.1 Å. The phenyl group shows at least as much intracavity immersion as the larger naphthyl residue.[24] 2D ROESY spectra and ^{1}H NMR complex induced shifts imply that the phenyl ring of the closely related fluorophore, 8-(anilino)-naphthalene-1-sulfonate (ANS$^-$) (Appendix, (25)), is preferentially included within βCD.[24,31] However, the inclusion of naphthalene derivatives is highly sensitive to substituent position.[32] The presence of a substituent in the 1-position prevents deep penetration into the cyclodextrin

cavity, and naphthalene derivatives substituted at the 2-position produce more stable inclusion complexes with βCD, as they do not experience hindrance from the substituted group.[33] Since TNS^- is 6,2-substituted the naphthyl moiety is more able to be immersed in the cavity than the napthyl group of 8,1-substituted ANS^-.[24]

From CPK molecular models, the dimensions of the naphthalene moiety are approximately 6.8 by 8.4 Å.[29] Accordingly, only a partial inclusion is expected if the naphthyl moiety is included with its long axis perpendicular to the C_7 symmetry axis of βCD (Table 1.1). In the energetically favoured orientation, the long axis of the naphthyl moiety is included parallel to the C_7 symmetry axis of βCD.[29] Circular dichroism and life-time measurements support the almost total inclusion of 2-substituted naphthalenes in this orientation.[29,32] The naphthyl group probably adopts a position in the cavity which allows for maximal solvation of charge on the sulfonate group. The pK_a of 2-naphthyloxyacetic acid (Appendix, (26)) is unaffected by the addition of βCD, to form a βCD·(2-naphthyloxyacetic acid) complex with a stability constant of 560 dm^3 mol^{-1}.[29] This suggests that the acid group protrudes from the cavity. The sulfonate group of TNS^-, which is in the 2-position of the naphthyl ring, is likely to protrude from the cavity into the hydrophilic aqueous region outside, in a similar manner. The inclusion of naphthalene derivatives is highly sensitive to the number of substituents, as well as their position.[32] The decrease in stability with increasing number of hydrophilic substituents is shown by the stability constants of 234,000 and 1,950 dm^3 mol^{-1}, characterising the βCD complexes of 2-naphthalenesulfonate (Appendix, (27)) and 2,6-naphthalenedisulfonate (Appendix, (28)), respectively.[32]

The amine group is apparently important for a marked fluorescence enhancement upon inclusion.[34] The addition of an amine group to the 2-position of the naphthalene ring also enhances βCD binding with an increase in stability constant from 608 dm^3 mol^{-1}, for naphthalene,[35] to 6430 dm^3 mol^{-1}, for 2-aminonaphthalene (Appendix, (29)).[33] The significantly lower stability constant for the complexation of aniline (Appendix, (30)) by βCD, 50 dm^3 mol^{-1},[34] supports the preferential inclusion of the naphthyl, rather than the phenyl, moiety of TNS^- within the βCD annulus. Admittedly, the toluidinyl group of

TNS^- is likely to bind more strongly than aniline due to additional hydrophobic interactions with the methyl group. The effect of a hydrophobic substituent is clearly demonstrated by stability constants of *ca.* 2000 $dm^3\ mol^{-1}$,[36] and 55,700 $dm^3\ mol^{-1}$,[37] for the βCD complexes of 6-(anilino)naphthalene-2-sulfonic acid (Appendix, (31)) and BNS^- (Appendix, (23)), respectively.

Which of the aromatic rings is involved in the first binding is not agreed upon. It has been suggested that solvation of the sulfonate group decreases the hydrophobicity of the naphthalenesulfonate moiety with respect to the toluidinyl moiety and the first binding of TNS^- to βCD may occur with the toluidinyl group, leaving the naphthalene group still exposed to solvent molecules.[2,13] However, comparisons between the βCD complexes of various anilinonaphthalenesulfonates suggest that inclusion of TNS^-, to form $\beta CD{\cdot}TNS^-$, occurs by complexation of the naphthyl moiety, and this is followed by inclusion of the toluidinyl group, to yield $(\beta CD)_2{\cdot}TNS^-$.[23] On the basis of the evidence submitted in Section 3.3.1, the inclusion of either aryl group or any portion of TNS^- between these extremes, may occur in the $\beta CD{\cdot}TNS^-$ complex.

Complexation studies in the presence of urea, an antihydrophobic agent, reveal that in the $(\beta CD)_2{\cdot}TNS^-$ complex the TNS^- molecule is totally shielded by the two βCD molecules, whereas in the $\beta CD{\cdot}TNS^-$ complex part of the TNS^- molecule projects out of the cavity.[16] The approach of TNS^- is generally considered to occur from the wider end of the cavity, as the greater width of secondary rim permits more facile inclusion. This is consistent with NMR studies.[24,31] Hence, in the $(\beta CD)_2{\cdot}TNS^-$ complex the two βCD molecules probably have their secondary rims facing each other. A more hydrophobic environment for TNS^- may be achieved by this orientation, in which the cyclodextrin dipole moments are opposed, compared with the situation when dipoles are aligned.

3.3.4 Spectroscopic Aspects

Both the blue shift and pronounced increase in quantum yield of TNS^- emission observed upon addition of βCD (Fig. 3.4) are analogous to the observations made with TNS^- on reducing the polarity of the medium (Section 3.2).

The emission maxima, λ_{max}, of βCD·TNS^- and $(\beta CD)_2$·TNS^- were determined to be 463 and 446 nm, respectively, in good agreement with the literature values of 457-462 nm and 444-447 nm, respectively.[13,19,20,21] These blue shifts can be explained in terms of the relative contributions of the three excited states (Section 3.2) to the overall fluorescence spectrum. Upon inclusion, TNS^- is transfered from the hydrophilic aqueous medium to the hydrophobic βCD cavity, resulting in a decrease in intramolecular charge-transfer and a dramatic increase in emission from the $S_{1,np}$ excited state. The dominance of the $S_{1,np} \rightarrow S_0$ transition is also consistent with a nonplanar orientation of the phenyl and naphthyl rings in the inclusion complexes. The λ_{max} of βCD·TNS^- and $(\beta CD)_2$·TNS^- are shifted to higher and lower wavelengths, respectively, compared with the previously observed λ_{max} at *ca.* 453 nm for the $S_{1,np} \rightarrow S_0$ transition of TNS^- (Section 3.2), and these shifts may arise from environmental effects. The encapsulation of TNS^- by two βCDs may restrict the rotational motion of the aromatic rings possibly leading to a less conjugated arrangement in the $(\beta CD)_2$·TNS^- complex, whereas a greater degree of conjugation may be achieved in the βCD·TNS^- complex. The blue shift of the emission maximum relative to the 490 nm ($S_{1\text{-}ct,np} \rightarrow S_0$) band is also generally accepted as a measure of hydrophobicity. The blue shift for βCD·TNS^- is less than that of $(\beta CD)_2$·TNS^-, indicating that TNS^- is in a more hydrophobic environment in the $(\beta CD)_2$·TNS^- complex.

Since the isosbestic wavelength in the absorption spectrum of TNS^- upon addition of βCD was used in excitation, TNS^-, βCD·TNS^- and $(\beta CD)_2$·TNS^- were all absorbing the same number of photons. Hence, the relative fluorescence of these species could be determined from the areas under the derived emission spectra for the complex species and

the previously determined emission spectrum of TNS^-. The emissions of $\beta CD \cdot TNS^-$ and $(\beta CD)_2 \cdot TNS^-$ were determined to be 12 and 24 times greater than that of TNS^-, respectively, implying that the $(\beta CD)_2 \cdot TNS^-$ complex is twice as fluorescent as the $\beta CD \cdot TNS^-$ complex. Previous reports have claimed the $(\beta CD)_2 \cdot TNS^-$ complex to be 1.4,[16] 3,[13,20,24] and 5.7[2] times more fluorescent than the $\beta CD \cdot TNS^-$ complex.

The entire emission spectra of TNS^-, $\beta CD \cdot TNS^-$ and $(\beta CD)_2 \cdot TNS^-$ were not encompassed by the 385-550 nm wavelength range over which the spectra were recorded, hence, the above relative emissions are only approximate. To obtain a more accurate measure of the fluorescence enhancement on complexation, quantum yield measurements were made. These yielded a value of 0.024 for the $\beta CD \cdot TNS^-$ complex, which is in excellent agreement with the value reported by Kondo *et al.*[2] This is 30-fold greater than the quantum yield of TNS^- (0.0008, Section 3.2) determined in this study.

Kondo *et al.* used a least-squares fitting method in determining their quantum yields, and reported a value of 0.136 as the quantum yield of $(\beta CD)_2 \cdot TNS^-$.[2] The quantum yield of emission of TNS^- bound to βCD has also been estimated from the intercept of a double reciprocal plot of the change in emission yield versus concentration of βCD, yielding values of 0.053 and 0.074 for $\beta CD \cdot TNS^-$ and $(\beta CD)_2 \cdot TNS^-$, respectively.[16] The variation in experimental conditions in each of these studies results in different proportions of the $(\beta CD)_2 \cdot TNS^-$ complex being formed, and this, along with the differences in data treatment, may be responsible for the significant variation in the values determined. However, the increase in fluorescence emission in the order: $TNS^- < \beta CD \cdot TNS^- < (\beta CD)_2 \cdot TNS^-$, is unequivocal.

The pronounced increase in lifetime of TNS^- emission observed upon addition of βCD, also shows the same trend. The fluorescence lifetimes of the loose encounter complex (Section 3.3.1), $\beta CD \cdot TNS^-$ and $(\beta CD)_2 \cdot TNS^-$, are reported to be 100-500 ps, 1.5 ns and 3-5 ns, respectively, whereas the lifetimes of TNS^- in water and ethanol are 60 ps and 8.7 ns, respectively.[25] The microviscosities around these sites are 0.0019, 0.0043 and 0.030 kg m^{-1} s^{-1}, respectively, in accordance with increasing hydrophobicity.

The marked increase in TNS^- emission yield and lifetime upon formation of βCD inclusion complexes may arise from several factors, which are considered to suppress the radiationless deactivation of the excited state occurring in solution. Firstly, the hydrophobic environment surrounding the included TNS^- molecule results in a decrease in population of the $S_{1\text{-ct,perp}}$ and $S_{1\text{-ct,np}}$ excited states, which decay more rapidly than the $S_{1,np}$ excited state.[7,16] Secondly, the isolation of TNS^- within a βCD cavity protects the fluorophore from collisional quenching by water and dissolved oxygen.[9,29,34] Thirdly, the rotational degrees of freedom, which provide a path for energy transfer from the excited state, are reduced upon inclusion.[13] Often an increase in planarity and rigidity is associated with a decrease in intersystem crossing, and a concomitant increase in quantum yield.[18] The extent of fluorescence enhancement arising from each of these factors is expected to be greater for $(\beta CD)_2 \cdot TNS^-$ than $\beta CD \cdot TNS^-$, due to the more hydrophobic environment surrounding TNS^-, the greater protection from solvent quenching and more restricted movement of TNS^- when completely encapsulated.

Comparison of the quantum yields for the (host)·TNS^- complexes (host = αCD, βCD and γCD), shows a decrease with increasing cavity size.[2] This is consistent with the assumption that water molecules can more easily enter the space between the cyclodextrin and the aromatic group of TNS^- as the internal diameter of cyclodextrin increases, and consequently the environment of the group becomes somewhat more hydrophilic. Kondo *et al.* found that non-cyclic dextrins show much smaller fluorescence enhancement than cyclodextrins, though the effect is appreciable for longer chain amyloses.[2] The relative TNS^- fluorescence intensity per glucose residue is 30,000-fold greater for βCD than for glucose.[2] The quantum yield of TNS^- in 60% sucrose is 0.015, with a λ_{max} of 486 nm.[6] This quantum yield is lower than that of $\beta CD \cdot TNS^-$, and the λ_{max} is higher, exemplifying less hydrophobic interaction in the 60% sucrose solution compared with βCD.

3.4 Complexation of TNS^- by Linked Cyclodextrin Dimers

Only (host)·(guest) stoichiometries have been reported for the complexation of TNS^- by linked cyclodextrin dimers, and most studies have involved cyclodextrins which are linked through their secondary rims (see Section 3.4.6). The complexation of TNS^- by cyclodextrin dimers which are linked through their primary rims now follows. A systematic increase in the length of the tether is made to determine its influence on binding.

The excited state stability constants reported in the following sections were determined by simultaneously fitting the variation in fluorescence emission with added cyclodextrin, over a range of wavelengths where significant spectral change occurred, to a particular algorithm using non-linear least-squares regression (Section 6.2.5). Due to the errors involved in spectral measurement and solution preparation, the actual errors on the stability constants are greater than the non-weighted standard deviations quoted (but they are unlikely to exceed the non-weighted standard deviation by a factor of ten in these TNS^- systems).

3.4.1 Complexation of TNS^- by $(\beta CD)_2Ur$

The variation in TNS^- fluorescence upon addition of $(\beta CD)_2Ur$ (Fig. 3.6) is readily fitted to the algorithm arising from the equilibrium shown in Eqn. 3.3. The data obtained at 0.5 nm intervals in the wavelength range 400-500 nm were used to determine the value of $K_1 = (4.523 \pm 0.007) \times 10^4$ dm^3 mol^{-1}. This reveals that TNS^- forms a very strong complex with the dimeric host, $(\beta CD)_2Ur$, binding TNS^- over 14 times more strongly than βCD does. The binding curve for the complexation of TNS^- by $(\beta CD)_2Ur$ at 434 nm is shown in Fig. 3.7.

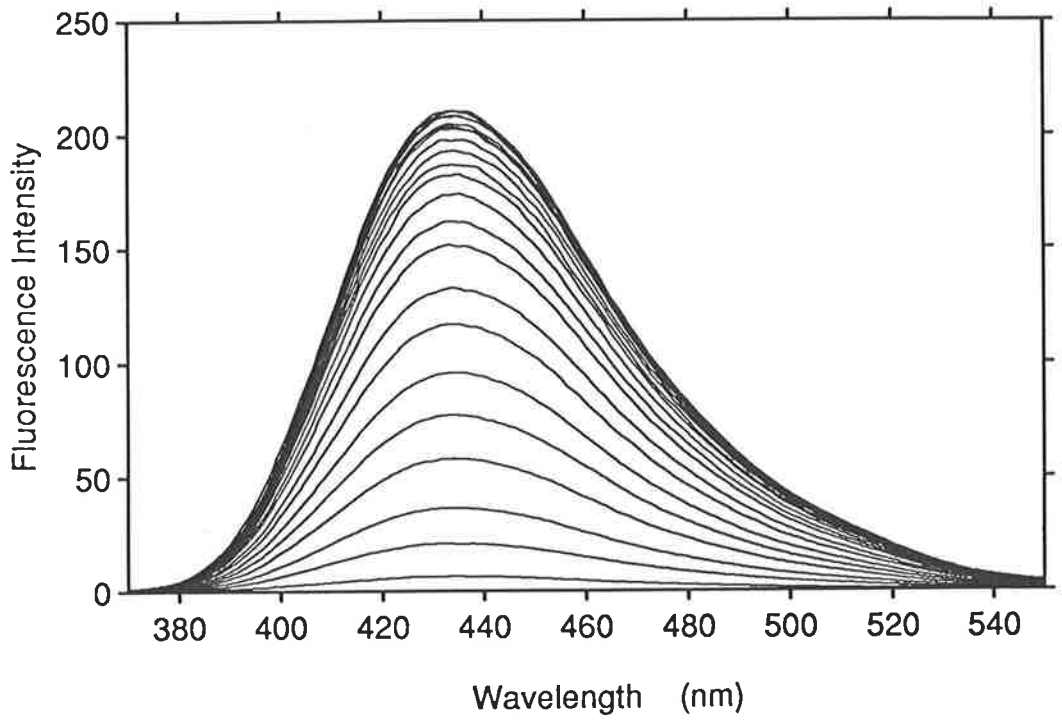

Figure 3.6 *Emission of TNS^- (1.00×10^{-6} mol dm^{-3}) alone and in the presence of increasing concentrations of $(\beta CD)_2Ur$ (ranging from 8.32×10^{-7} to 3.07×10^{-4} mol dm^{-3}) in aqueous phosphate buffer (pH 7.0, $I = 0.10$ mol dm^{-3}) at 298.2 K, as a function of wavelength when excited at 354 nm with excitation and emission slit widths of 5 and 5 nm, respectively. The emission of TNS^- alone is barely visible above the baseline in the montage.*

$$(\beta CD)_2Ur + TNS^- \overset{K_1}{\rightleftharpoons} (\beta CD)_2Ur{\cdot}TNS^- \tag{3.3}$$

$$(\beta CD)_2Ur{\cdot}TNS^- + (\beta CD)_2Ur \overset{K_2}{\rightleftharpoons} ((\beta CD)_2Ur)_2{\cdot}TNS^- \tag{3.4}$$

No TNS^- dimer complex, $(\beta CD)_2Ur{\cdot}(TNS)_2^{2-}$, was detected over the concentration range studied. However, the data could be fitted to the algorithm arising from the two step formation of $((\beta CD)_2Ur)_2{\cdot}TNS^-$ (Eqns. 3.3 and 3.4). Due to the many possible conformations of $(\beta CD)_2Ur$ where the two annuli are not aligned, if $(\beta CD)_2Ur$ is

present in sufficiently high concentrations, TNS^- may be included by a single βCD annulus of each of two $(\beta CD)_2Ur$ molecules. Simultaneous competition between the binding of a guest molecule by a βCD annulus of each of two linked cyclodextrin dimers, to form a ternary complex, and by two βCD annuli of the same linked cyclodextrin dimer, to form a binary complex, has previously been suggested.[38] The driving force for the latter is the high local concentration of cyclodextrin once the guest is included by the first cyclodextrin annulus. Analogous $(host)_2 \cdot TNS^-$ complexes are not detected for the following diamide-1°,1°-linked-βCDs with longer tethers. This is possibly due to increased flexibility and greater separation of the opposed βCD dipole moments facilitating the binding of TNS^- by the two βCD annuli of a single linked cyclodextrin dimer molecule.

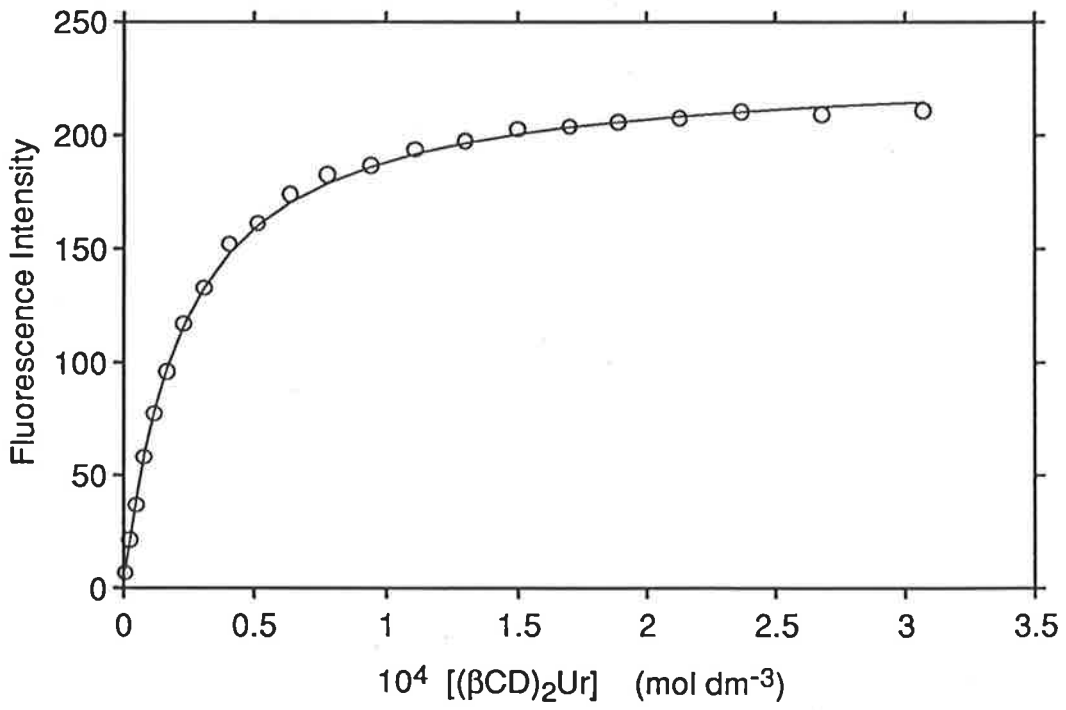

Figure 3.7 *Emission of TNS^- (1.00×10^{-6} mol dm^{-3}) at 434 nm in the presence of increasing concentrations of $(\beta CD)_2Ur$ (ranging from 8.32×10^{-7} to 3.07×10^{-4} mol dm^{-3}) in aqueous phosphate buffer (pH 7.0, $I = 0.10$ mol dm^{-3}) at 298.2 K, when excited at 354 nm with excitation and emission slit widths of 5 and 5 nm, respectively. The circles represent data points and the solid line represents the best fit to the algorithm arising from the equilibrium shown in Eqn. 3.3.*

When the data were fitted to the algorithm arising from the equilibria shown in Eqns. 3.3 and 3.4, this yielded K_1 = (4.57 ± 0.03) x 10^4 dm^3 mol^{-1} and K_2 = (9.3 ± 0.4) x 10^3 dm^3 mol^{-1}. The sum of squared deviations for this fit was 2.8 x 10^3, which is substantially less than the value of 1.1 x 10^4 obtained for fitting the data to the formation of a single $(\beta CD)_2Ur{\cdot}TNS^-$ complex. However, the large errors on the stability constants when the additional complex, $((\beta CD)_2Ur)_2{\cdot}TNS^-$, is incorporated, favour acceptance of the model outlined in Eqn. 3.3 alone.

The extent of fluorescence enhancement with increasing $(\beta CD)_2Ur$ concentration (Fig. 3.7) is greater than that expected from the difference in absorption of free and complexed TNS^- at the excitation wavelength (Section 6.2.3). The fluorescence intensity shows saturation with an increase in $(\beta CD)_2Ur$ concentration indicating that the fluorescence change is caused by formation of a complex, as virtually all the TNS^- molecules added become bound to $(\beta CD)_2Ur$. The normalised fluorescence of the $(\beta CD)_2Ur{\cdot}TNS^-$ complex is 197 times greater than that of TNS^- in buffer alone under the same conditions, and its maximal emission is at 434 nm.

Both the blue shift in emission and remarkable increase in quantum yield of TNS^- emission upon interaction with $(\beta CD)_2Ur$ can reasonably be assumed to be due to the formation of an inclusion complex. These observations can be explained in the same way as those discussed in Section 3.3.4. The greater blue shift of the emission maximum for $(\beta CD)_2Ur{\cdot}TNS^-$, compared with $(\beta CD)_2{\cdot}TNS^-$, is possibly due to a reduction in conjugation which may arise from greater restriction in rotational motion of the aromatic rings when the βCD annuli are connected. As mentioned previously (Section 3.3.4) the blue shift of the emission maximum relative to the 490 nm ($S_{1\text{-}ct,np} \rightarrow S_0$) fluorescence band is generally accepted as a measure of hydrophobicity. This implies that TNS^- is in a more hydrophobic environment in $(\beta CD)_2Ur{\cdot}TNS^-$ than in $(\beta CD)_2{\cdot}TNS^-$. The anticipated difference in orientation of the βCD annuli in these two complexes, with secondary rims adjacent in $(\beta CD)_2{\cdot}TNS^-$ and primary rims adjacent in $(\beta CD)_2Ur{\cdot}TNS^-$, may affect the hydrophobicity of the environment surrounding TNS^-.

The presence of nitrogen atoms or keto groups in the solvent molecule has been associated with low quantum yields, despite low λ_{max} and narrow band width, as these groups appear to be effective quenchers.[6] The amide group in the tether may have a similar effect, but if so, it is swamped by other factors which enhance fluorescence, such as the hydrophobicity of the environment.

3.4.2 Complexation of TNS⁻ by (βCD)$_2$Ox

The variation in TNS^- fluorescence upon addition of $(\beta CD)_2Ox$ is shown in Fig. 3.8. The data obtained at 0.5 nm intervals in the wavelength range 400-500 nm were successfully fitted to the algorithm arising from the equilibrium in Eqn. 3.5, yielding $K_1 = (3.264 \pm 0.009) \times 10^4$ dm^3 mol^{-1} for the formation of $(\beta CD)_2Ox \cdot TNS^-$. Once again the linked cyclodextrin dimer bound TNS^- over 10 times more strongly than βCD does. The binding curve for the complexation of TNS^- by $(\beta CD)_2Ox$ at 433 nm is shown in Fig. 3.9.

$$(\beta CD)_2Ox + TNS^- \overset{K_1}{\rightleftharpoons} (\beta CD)_2Ox \cdot TNS^- \qquad (3.5)$$

If any complexes other than $(\beta CD)_2Ox \cdot TNS^-$ are present, the spectral character of the fluorophore in such a complex must not be sufficiently different from that of either $(\beta CD)_2Ox \cdot TNS^-$ or free TNS^-, to allow its detection. As demonstrated by a related guest, 6-(*p*-anisidinyl)naphthalene-2-sulfonic acid (Appendix, (32)), it is possible for the fluorophore to be bound by βCD, as evidenced by a change in fluorescence anisotropy, without any change being induced in the emission spectrum of the fluorophore.[23]

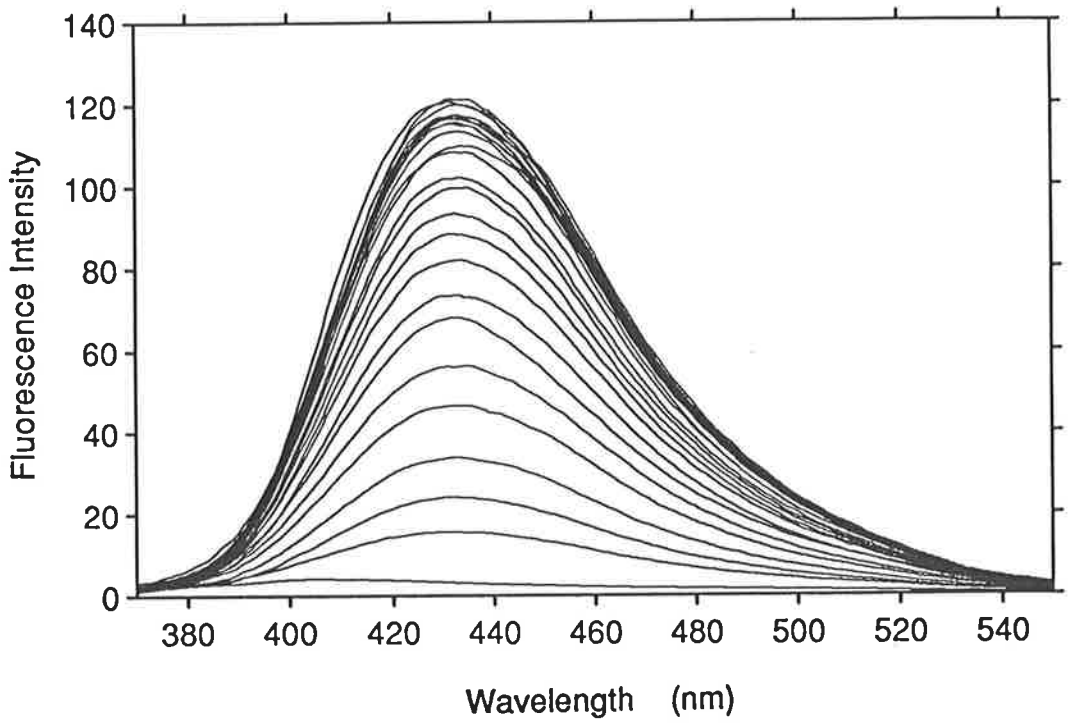

Figure 3.8 *Emission of TNS^- (1.01×10^{-6} mol dm^{-3}) alone and in the presence of increasing concentrations of $(\beta CD)_2Ox$ (ranging from 3.98×10^{-6} to 6.03×10^{-4} mol dm^{-3}) in aqueous phosphate buffer (pH 7.0, I = 0.10 mol dm^{-3}) at 298.2 K, as a function of wavelength when excited at 346 nm with excitation and emission slit widths of 5 and 10 nm, respectively. The emission of TNS^- alone is the lowest intensity curve in the montage.*

The fluorescence enhancement upon addition of $(\beta CD)_2Ox$ (Fig. 3.9) is greater than expected from the difference in absorption of free and complexed TNS^- at the excitation wavelength (Section 6.2.3), and the saturation of fluorescence intensity is consistent with complex formation. The normalised fluorescence of the $(\beta CD)_2Ox \cdot TNS^-$ complex is 23 times greater than that of TNS^- in buffer alone under the same conditions, and its maximal emission occurs at 433 nm. This increase in the fluorescence of TNS^- and blue shift in λ_{max} observed upon addition of $(\beta CD)_2Ox$ can be explained in the same way as those discussed in Sections 3.3.4 and 3.4.1.

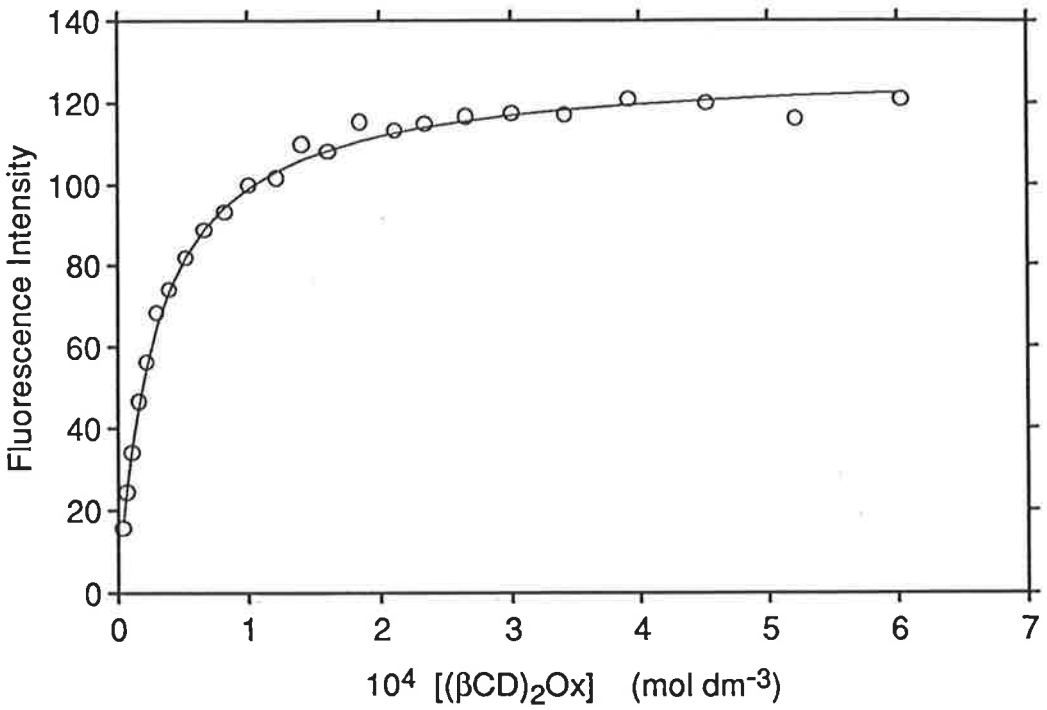

Figure 3.9 *Emission of TNS^- (1.01×10^{-6} mol dm^{-3}) at 433 nm in the presence of increasing concentrations of $(\beta CD)_2Ox$ (ranging from 3.98×10^{-6} to 6.03×10^{-4} mol dm^{-3}) in aqueous phosphate buffer (pH 7.0, I = 0.10 mol dm^{-3}) at 298.2 K, when excited at 346 nm with excitation and emission slit widths of 5 and 10 nm, respectively. The circles represent data points and the solid line represents the best fit to the algorithm arising from the equilibrium shown in Eqn. 3.5.*

3.4.3 Complexation of TNS^- by $(\beta CD)_2Ma$

The variation in TNS^- fluorescence upon addition of $(\beta CD)_2Ma$ is shown in Fig. 3.10. The data obtained at 0.5 nm intervals in the wavelength range 400-500 nm were successfully fitted to the algorithm arising from the equilibrium in Eqn. 3.6, yielding $K_1 = (1.100 \pm 0.001) \times 10^4$ dm^3 mol^{-1} for the formation of $(\beta CD)_2Ma \cdot TNS^-$. No other complexes were detected. The binding curve for the complexation of TNS^- by $(\beta CD)_2Ma$ at 441 nm is shown in Fig. 3.11.

$$(\beta CD)_2Ma + TNS^- \overset{K_1}{\rightleftharpoons} (\beta CD)_2Ma{\cdot}TNS^- \qquad (3.6)$$

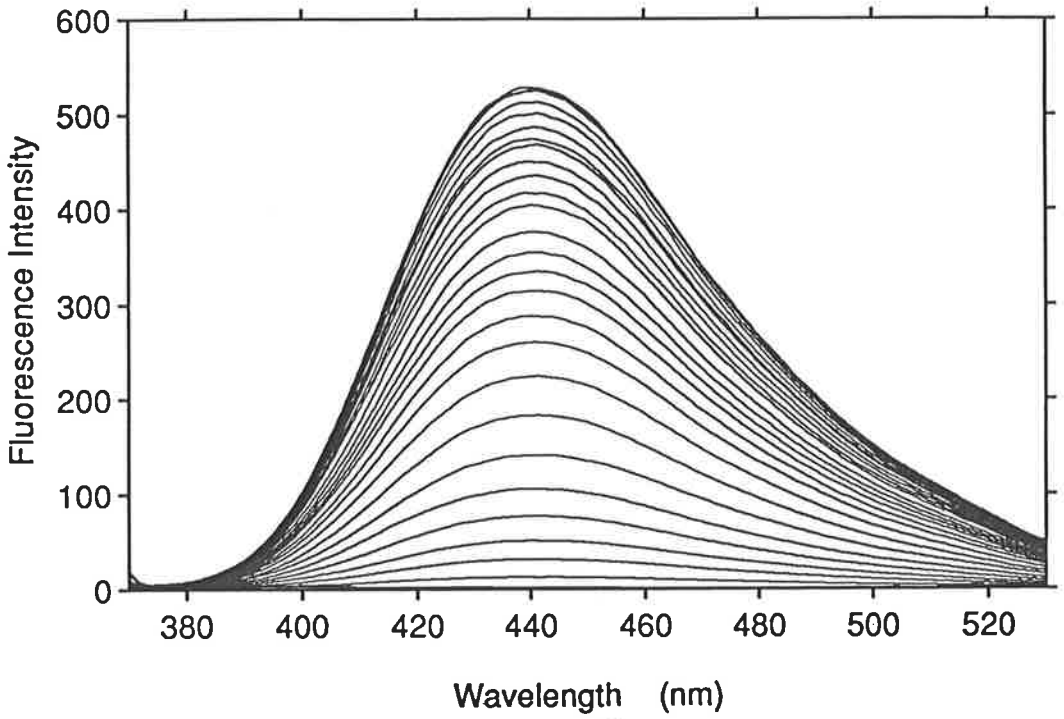

Figure 3.10 *Emission of TNS^- (1.01×10^{-6} mol dm^{-3}) alone and in the presence of increasing concentrations of $(\beta CD)_2Ma$ (ranging from 2.51×10^{-6} to 9.00×10^{-4} mol dm^{-3}) in aqueous phosphate buffer (pH 7.0, I = 0.10 mol dm^{-3}) at 298.2 K, as a function of wavelength when excited at 357 nm with excitation and emission slit widths of 5 and 10 nm, respectively. The emission of TNS^- alone is barely visible above the baseline in the montage.*

The fluorescence enhancement upon addition of $(\beta CD)_2Ma$ (Fig. 3.11) is greater than expected from the difference in absorption of free and complexed TNS^- at the excitation wavelength (Section 6.2.3), and the saturation of fluorescence intensity is consistent with complex formation. The normalised fluorescence of the $(\beta CD)_2Ma{\cdot}TNS^-$ complex is 133 times greater than that of TNS^- in buffer alone under the same conditions, and its maximal emission occurs at 441 nm. These observations can be explained in the same way as those discussed in Sections 3.3.4 and 3.4.1. The extent of blue shift of the

emission maximum for $(\beta CD)_2Ma{\cdot}TNS^-$ is intermediate between that of $(\beta CD)_2Ur{\cdot}TNS^-$ and $(\beta CD)_2{\cdot}TNS^-$. This is possibly due to greater flexibility of the longer tether permitting more movement within the complex compared with $(\beta CD)_2Ur{\cdot}TNS^-$, but less compared with $(\beta CD)_2{\cdot}TNS^-$.

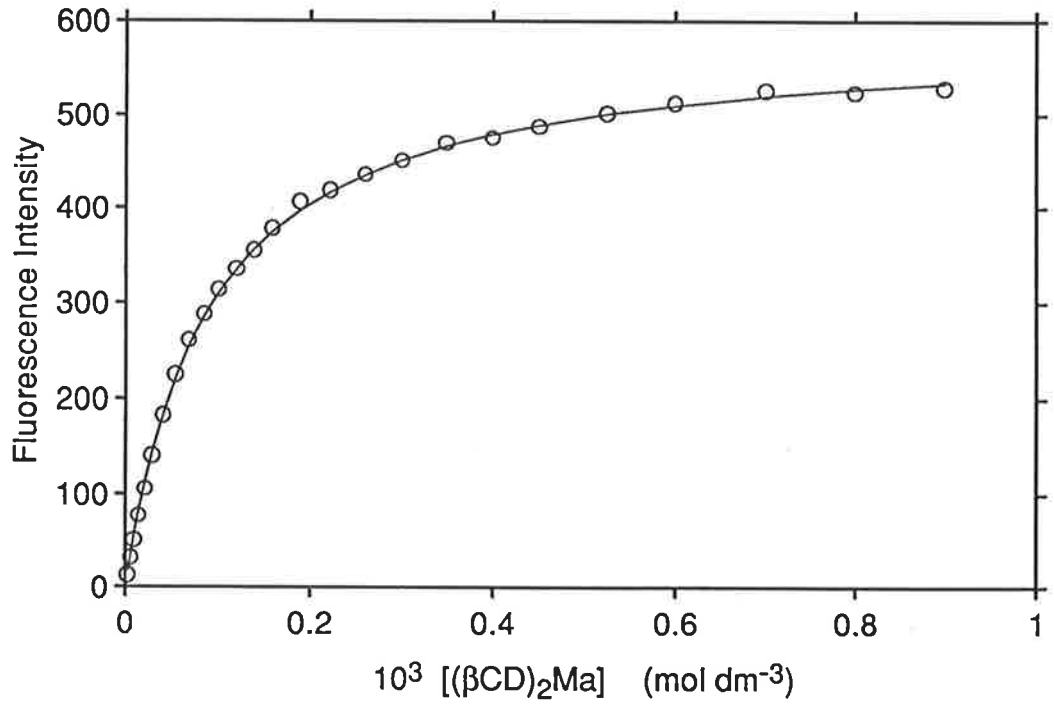

Figure 3.11 *Emission of TNS^- (1.01×10^{-6} mol dm^{-3}) at 441 nm in the presence of increasing concentrations of $(\beta CD)_2Ma$ (ranging from 2.51×10^{-6} to 9.00×10^{-4} mol dm^{-3}) in aqueous phosphate buffer (pH 7.0, I = 0.10 mol dm^{-3}) at 298.2 K, when excited at 357 nm with excitation and emission slit widths of 5 and 10 nm, respectively. The circles represent data points and the solid line represents the best fit to the algorithm arising from the equilibrium shown in Eqn. 3.6.*

3.4.4 Complexation of TNS^- by $(\beta CD)_2Sc$

The variation in TNS^- fluorescence upon addition of $(\beta CD)_2Sc$ is shown in Fig. 3.12. The data obtained at 0.5 nm intervals in the wavelength range 400-500 nm were successfully fitted to the algorithm arising from the equilibrium in Eqn. 3.7, yielding

$K_1 = (1.670 \pm 0.002) \times 10^4$ dm^3 mol^{-1} for the formation of $(\beta CD)_2Sc{\cdot}TNS^-$. Once again no other complexes were detected. The binding curve for the complexation of TNS^- by $(\beta CD)_2Sc$ at 440 nm is shown in Fig. 3.13.

$$(\beta CD)_2Sc + TNS^- \overset{K_1}{\rightleftharpoons} (\beta CD)_2Sc{\cdot}TNS^- \qquad (3.7)$$

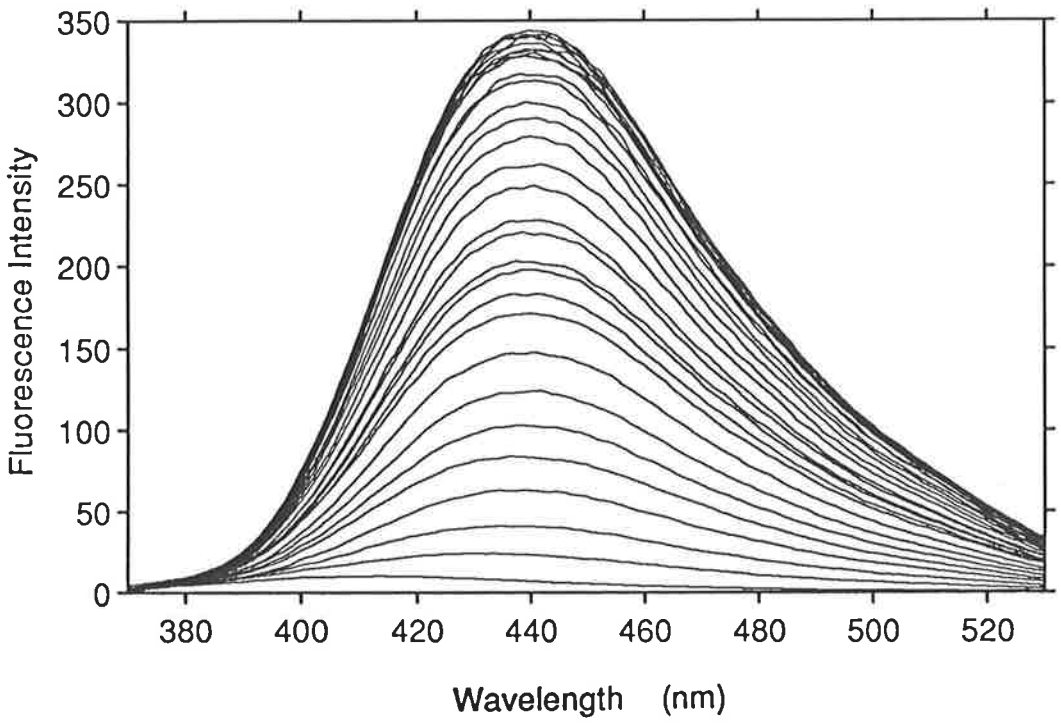

Figure 3.12 *Emission of TNS^- (1.00×10^{-6} mol dm^{-3}) alone and in the presence of increasing concentrations of $(\beta CD)_2Sc$ (ranging from 3.00×10^{-6} to 1.00×10^{-3} mol dm^{-3}) in aqueous phosphate buffer (pH 7.0, $I = 0.10$ mol dm^{-3}) at 298.2 K, as a function of wavelength when excited at 353 nm with excitation and emission slit widths of 5 and 10 nm, respectively. The emission of TNS^- alone is the lowest intensity curve in the montage.*

The fluorescence enhancement upon addition of $(\beta CD)_2Sc$ (Fig. 3.13) is greater than expected from the difference in absorption of free and complexed TNS^- at the excitation wavelength (Section 6.2.3), and the saturation of fluorescence intensity is

consistent with complex formation. The normalised fluorescence of the $(\beta CD)_2Sc{\cdot}TNS^-$ complex is 84 times greater than that of TNS^- in buffer alone under the same conditions, and its maximal emission occurs at 440 nm. These observations can be explained in the same way as those discussed in Sections 3.3.4, 3.4.1 and 3.4.3.

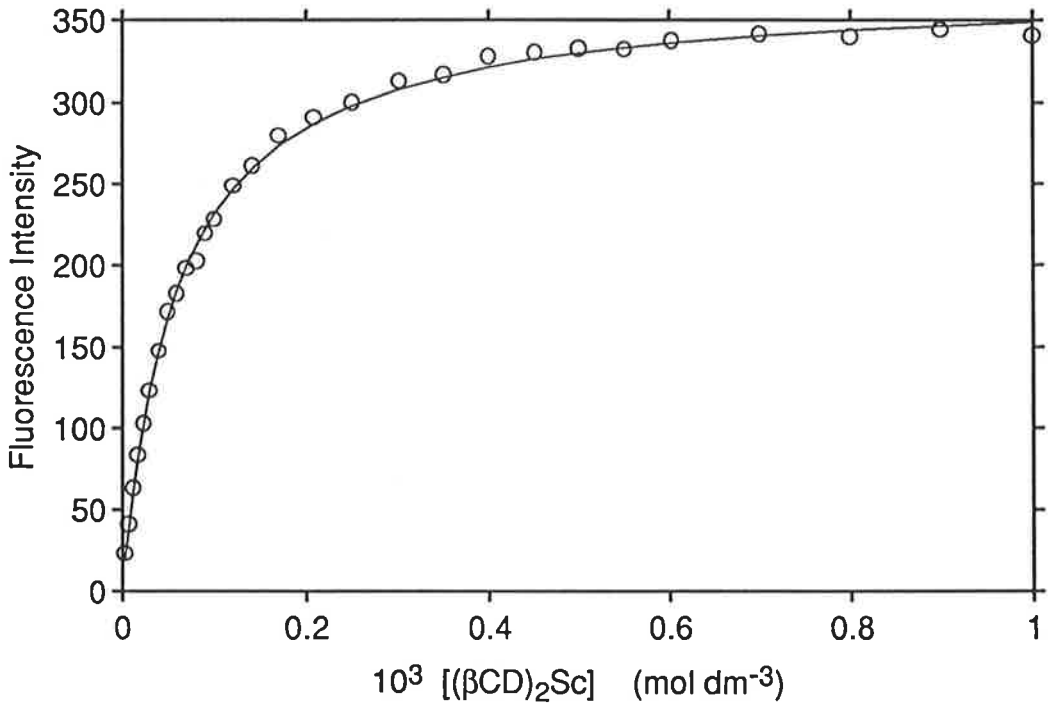

Figure 3.13 *Emission of TNS^- (1.00×10^{-6} mol dm^{-3}) at 440 nm in the presence of increasing concentrations of $(\beta CD)_2Sc$ (ranging from 3.00×10^{-6} to 1.00×10^{-3} mol dm^{-3}) in aqueous phosphate buffer (pH 7.0, I = 0.10 mol dm^{-3}) at 298.2 K, when excited at 353 nm with excitation and emission slit widths of 5 and 10 nm, respectively. The circles represent data points and the solid line represents the best fit to the algorithm arising from the equilibrium shown in Eqn. 3.7.*

3.4.5 Complexation of TNS^- by $(\beta CD)_2Gl$

The variation in TNS^- fluorescence upon addition of $(\beta CD)_2Gl$ is shown in Fig. 3.14. The data obtained at 0.5 nm intervals in the wavelength range 400-500 nm were successfully fitted to the algorithm arising from the equilibrium in Eqn. 3.8, yielding

$K_1 = (1.301 \pm 0.002) \times 10^4$ dm^3 mol^{-1} for the formation of $(\beta CD)_2Gl{\cdot}TNS^-$. Once again, no other complexes were detected. The binding curve for the complexation of TNS^- by $(\beta CD)_2Gl$ at 447 nm is shown in Fig. 3.15.

$$(\beta CD)_2Gl + TNS^- \overset{K_1}{\rightleftharpoons} (\beta CD)_2Gl{\cdot}TNS^- \qquad (3.8)$$

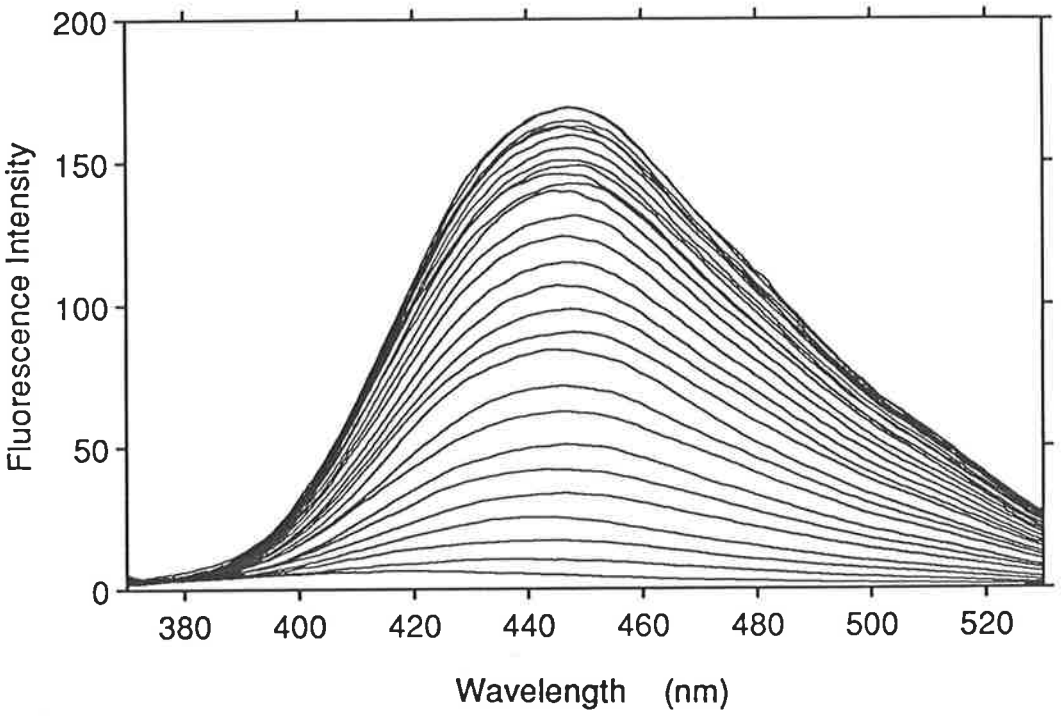

Figure 3.14 *Emission of TNS^- (1.01×10^{-6} mol dm^{-3}) alone and in the presence of increasing concentrations of $(\beta CD)_2Gl$ (ranging from 3.08×10^{-6} to 8.95×10^{-4} mol dm^{-3}) in aqueous phosphate buffer (pH 7.0, $I = 0.10$ mol dm^{-3}) at 298.2 K, as a function of wavelength when excited at 355 nm with excitation and emission slit widths of 5 and 10 nm, respectively. The emission of TNS^- alone is the lowest intensity curve in the montage.*

The fluorescence enhancement upon addition of $(\beta CD)_2Gl$ (Fig. 3.15) is greater than expected from the difference in absorption of free and complexed TNS^- at the excitation wavelength (Section 6.2.3), and the saturation of fluorescence intensity is

consistent with complex formation. The normalised fluorescence of the $(\beta CD)_2Gl{\cdot}TNS^-$ complex is 47 times greater than that of TNS^- in buffer alone under the same conditions, and its maximal emission occurs at 447 nm. This λ_{max} is very similar to that of $(\beta CD)_2{\cdot}TNS^-$ (446 nm, Section 3.3.4), and these observations can be explained in the same way as those discussed in Section 3.3.4.

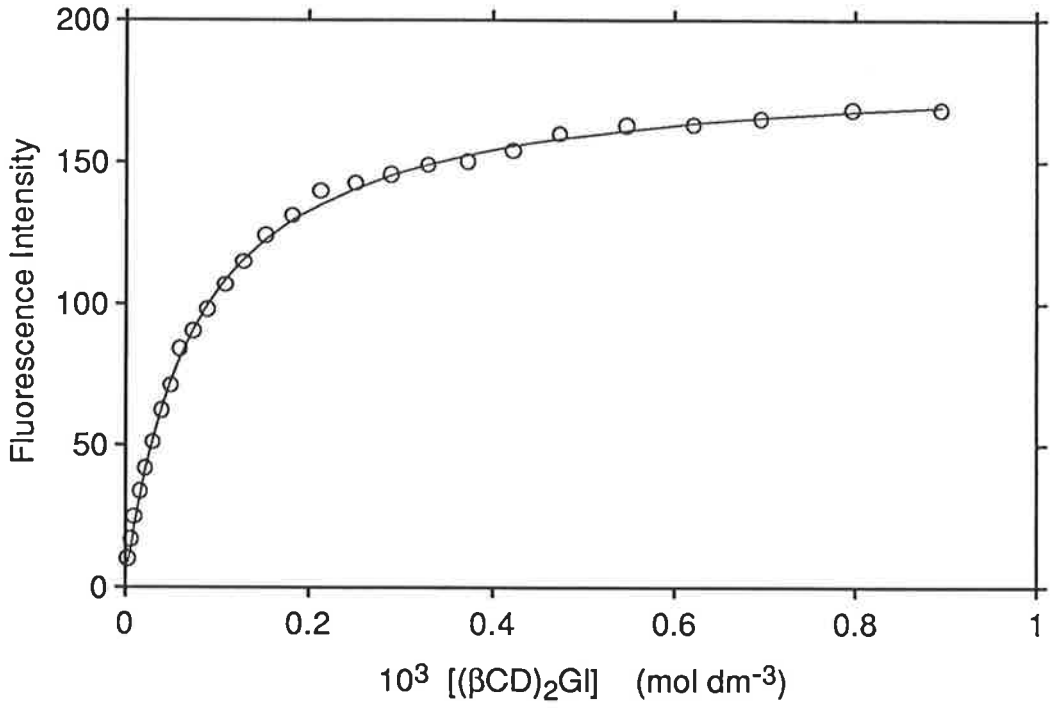

Figure 3.15 *Emission of TNS^- (1.01×10^{-6} mol dm^{-3}) at 447 nm in the presence of increasing concentrations of $(\beta CD)_2Gl$ (ranging from 3.08×10^{-6} to 8.95×10^{-4} mol dm^{-3}) in aqueous phosphate buffer (pH 7.0, I = 0.10 mol dm^{-3}) at 298.2 K, when excited at 355 nm with excitation and emission slit widths of 5 and 10 nm, respectively. The circles represent data points and the solid line represents the best fit to the algorithm arising from the equilibrium shown in Eqn. 3.8.*

The quantum yield of the $(\beta CD)_2Gl{\cdot}TNS^-$ complex was determined to be 0.047. This is approximately double the quantum yield of the $\beta CD{\cdot}TNS^-$ complex (0.024, Section 3.3.4). A more hydrophobic environment surrounding TNS^-, greater protection

from solvent quenching and more restricted movement of TNS^-, are expected upon encapsulation of both aromatic groups by $(\beta CD)_2Gl$.

3.4.6 Complexation of TNS^- by Other Linked Cyclodextrin Dimers

The complexation of TNS^- by a variety of linked cyclodextrin dimers has been studied and the corresponding stability constants of the (host)·TNS^- complexes formed are outlined in Table 3.2. For simplicity and ease of comparison between linked cyclodextrin dimers, the linking group is listed first followed by the linking mode and the type of cyclodextrin, as outlined in Section 3.1.

The complexation of TNS^- by diamide-2°,2°-linked-βCDs leads to stability constants which increase, with a change in host, in the order: oxalamide-2°,2°-linked-βCD (Appendix, (6)) < sebacamide-2°,2°-linked-βCD (Appendix, (8)) < succinamide-2°,2°-linked-βCD (Appendix, (7)). The tether length increases in the order: oxalamide-2°,2°-linked-βCD < succinamide-2°,2°-linked-βCD < sebacamide-2°,2°-linked-βCD. The slightly greater stability constant for sebacamide-2°,2°-linked-βCD compared with oxalamide-2°,2°-linked-βCD (Table 3.2) is possibly due to the longer tether allowing the second annulus to turn in such a way as to allow dipole alignment. Indeed, a similar turning of cyclodextrin annuli connected by long tethers has previously been suggested.[38] Interestingly, the succinamide-1°,2°-linked-βCD (Appendix, (13)), in which the cyclodextrin dipoles are aligned, binds TNS^- more strongly than the analogous 2°,2°-linked-βCD.

The stability constant for the complexation of TNS^- by succinate-2°,2°-linked-βCD (Appendix, (9)) is the same order of magnitude as that of succinamide-2°,2°-linked-βCD. It may therefore be concluded that there is not a large difference in binding properties when amide bonds are used instead of ester bonds for connecting the secondary rims.[39] The addition of more hydrophobic binding sites has no significant effect on the binding of TNS^-, as evidenced by the similarity of the glutarate-2°,2°-linked-βCD (Appendix, (10))

Table 3.2 *Literature stability constants for complexation of TNS^- by various linked cyclodextrin dimers and polymeric cyclodextrin.*

Host	Appendix Structure No.	K ($dm^3\ mol^{-1}$)
disulfide-1°,1°-linked-βCD[a]	(15)	87,000
disulfide-1°,1°-linked-βCD[b]	(15)	28,000
ethanedithiol-1°,1°-linked-βCD[b]	(16)	74,000
glutarate-2°,2°-linked-βCD[c]	(10)	8,300
succinate-2°,2°-linked-βCD[c]	(9)	16,700
succinamide-2°,2°-linked-βCD[d]	(7)	10,500
succinamide-2°,2°-linked-βCD[e]	(7)	8,800
succinamide-1°,2°-linked-βCD[e]	(13)	11,050
succinamide-2°,2°-linked-α-βCD[f]	—	2,800
oxalamide-2°,2°-linked-βCD[e]	(6)	5,500
sebacamide-2°,2°-linked-βCD[d]	(8)	6,700
sebacamide-2°,2°-linked-α-βCD[f]	—	600
3,5-di(thiomethyl)pyridine-2°,2°-linked-βCD[g]	(11)	20,000
poly(acryloyl-βCD)[h]	(14)	10,000

[a] Ref. 19 (carbonate buffer, pH 10.60, I = 0.05 mol dm^{-3}, 298.2 K). [b] Refs. 5 and 40 ($[TNS^-]$ = (0.33 or 3.33) x 10^{-6} mol dm^{-3}, 0.01 mol dm^{-3} phosphate buffer, pH 7.0, 296.2 K). [c] Ref. 20 ($[TNS^-]$ = 1.0 x 10^{-5} mol dm^{-3}, [CD] ≤ *ca.* 2.5 x 10^{-3} mol dm^{-3}, 0.1 mol dm^{-3} phosphate buffer, pH 5.9) [d] Ref. 39 ($[TNS^-]$ = 1 x 10^{-5} mol dm^{-3}, [CD] ≤ 2 x 10^{-4} mol dm^{-3}, 0.1 mol dm^{-3} phosphate buffer, pH 7.0). [e] Ref. 41 ($[TNS^-]$ = 1.0 x 10^{-6} mol dm^{-3}, [CD] ≤ 1.0 x 10^{-3} mol dm^{-3}, phosphate buffer, pH 6.9, I = 0.1 mol dm^{-3}, 298.2 K). [f] Ref. 22 ($[TNS^-]$ = 1 x 10^{-5} mol dm^{-3}, [CD] ≤ 5 x 10^{-4} mol dm^{-3}, 0.1 mol dm^{-3} phosphate buffer, pH 7.0, 298.2 K). [g] Ref. 42 ($[TNS^-]$ = 1 x 10^{-6} mol dm^{-3}, [CD] < 2 x 10^{-3} mol dm^{-3}, 0.2 mol dm^{-3} phosphate buffer, pH 7.0, 298.2 K). [h] Refs. 13 and 20 ($[TNS^-]$ = 1.0 x 10^{-5} mol dm^{-3}, [CD] ≤ *ca.* 5.0 x 10^{-3} mol dm^{-3}, 0.1 mol dm^{-3} phosphate buffer, pH 5.9)

and poly(acryloyl-βCD) (Appendix, (14)) stability constants. In the heterodimer complexes the αCD unit appears to inhibit complexation of TNS^- by βCD.[22]

For all linked βCD dimers (homodimers) and poly(acryloyl-βCD) the stability constants of the complexes formed with TNS^- are greater than that for βCD·TNS^- under similar conditions (Table 3.1). Although βCD exhibits a two-step binding process with TNS^-, poly(acryloyl-βCD) shows only homogeneous binding of TNS^- between two cyclodextrin units on the polymer chain, as revealed by the continuous variation method.[13]

The difference between the stability constant for the succinamide-2°,2°-linked-βCD complex of TNS^- (K = 8,800 dm^3 mol^{-1}) and that of βCD·TNS^- obtained under similar conditions in this study (K = 3,140 dm^3 mol^{-1}, Table 3.1), is more than the statistical increase anticipated for the two cyclodextrin annuli in the linked species, indicating some cooperativity. However, when the statistical factor is taken into account in the corresponding complex of oxalamide-2°,2°-linked-βCD (K = 5,500 dm^3 mol^{-1}) this indicates that the presence of the second annulus disrupts binding. The stability of the succinamide-1°,2°-linked-βCD complex (K = 11,050 dm^3 mol^{-1}) indicates that there is cooperative binding by the cyclodextrin annuli of this species.

Increased binding in linked cyclodextrin dimer systems is probably not due to a more favourable entropy contribution, commonly expected from the chelate effect (Section 1.3.4). This has been demonstrated by BNS^- (Appendix, (23)), which binds βCD with a positive entropy change and disulfide-1°,1°-linked-βCD (Appendix, (15)) with a substantial negative entropy change.[37] The unfavourable entropy contribution may arise from rotational entropy lost on formation of the linked cyclodextrin dimer complex.

The emission maximum of TNS^- (λ_{max}) provides information on the polarity of the environment of the fluorophore. For the linked cyclodextrin dimers in Table 3.2, the TNS^- complexes exhibit the following (λ_{max}/nm): disulfide-1°,1°-linked-βCD (436),[19] succinate- and glutarate-2°,2°-linked-βCD (447),[19,20] succinamide-2°,2°-linked-βCD (440),[39] succinamide-2°,2°-linked-α-βCD (453),[22] sebacamide-2°,2°-linked-βCD (436),[39] sebacamide-2°,2°-linked-α-βCD (453),[22] poly(acryloyl-βCD) polymer (438).[13,20] In each case the emission maximum is at a shorter wavelength than that of βCD·TNS^- (463 nm,

Section 3.3.4), showing an increased hydrophobicity of the TNS^- environment due to binding by a second βCD annulus and possibly interaction with the tether. Duplex-βCD (Appendix, (1)) exhibits a λ_{max} at 444 nm, while the related di(2-aminoethylamino)-βCD (Appendix, (18)) complex has a λ_{max} at 452 nm.[21] The shift in λ_{max} of TNS^- included by duplex-βCD is approximately the same as that of $(\beta CD)_2TNS^-$ (446 nm, Section 3.3.4) even at low host concentration where parent βCD, and di(2-aminoethylamino)-βCD form only (host)·TNS^- complexes. This demonstrates that the multiple recognition mechanism of duplex-βCD is operating, with each aromatic moiety of the guest being bound to a hydrophobic binding site of the host. In all of the homodimer complexes listed above, the wavelength of the emission maximum is similar to that of $(\beta CD)_2$·TNS^-, which may indicate that the polarity of the TNS^- environment in the linked cyclodextrin dimer complexes is similar to that in $(\beta CD)_2$·TNS^-.[20,21] The higher λ_{max} exhibited by the heterodimers, succinamide-2°,2°-linked-α-βCD and sebacamide-2°,2°-linked-α-βCD, indicate that only one cyclodextrin unit is significantly involved in the complexation of TNS^-, which is consistent with the low stability constants (Table 3.2).[22]

The TNS^- complexes of the linked cyclodextrin dimers, succinate-2°,2°-linked-βCD and glutarate-2°,2°-linked-βCD, fluoresce 9 and 8 times more strongly, respectively, than the βCD·TNS^- complex.[20] The polymer, poly(acryloyl-βCD) contains cyclodextrin units which are separated by the same distance as those in glutarate-2°,2°-linked-βCD, and the TNS^- complex of this polymer fluoresces 20 times more strongly than the βCD·TNS^- complex.[13] When both the toluidinyl and naphthyl groups are included in cyclodextrin cavities, this probably produces a more hydrophobic TNS^- environment, greater protection from collisional quenching, and more restricted intramolecular rotation of TNS^- around the -NH- group, all of which hinder nonradiative deactivation of the excited state (Section 3.3.4) and thus enhance fluorescence.

3.5 Summary and Conclusions

All diamide-1°,1°-linked-βCDs studied show a cooperative binding effect with TNS^-, and the stability constants for the $(\beta CD)_2X{\cdot}TNS^-$ complexes formed (X = Ur, Ox, Ma, Sc, Gl) are summarised in Table 3.3. The strongest binding is achieved with $(\beta CD)_2Ur$, which binds TNS^- over 14 times more strongly than βCD.

Table 3.3 *Stability constants for the inclusion complexes of TNS^- with βCD and diamide-1°,1°-linked-βCDs in aqueous phosphate buffer (pH 7.0, I = 0.10 mol dm^{-3}) at 298.2 K.*[a]

Species	K (dm^3 mol^{-1})
$\beta CD{\cdot}TNS^-$ [b]	3,140 ± 20
$(\beta CD)_2{\cdot}TNS^-$ [b]	86 ± 5[c]
$(\beta CD)_2Ur{\cdot}TNS^-$ [d]	45,230 ± 70
$(\beta CD)_2Ox{\cdot}TNS^-$ [e]	32,640 ± 90
$(\beta CD)_2Ma{\cdot}TNS^-$ [f]	11,000 ± 10
$(\beta CD)_2Sc{\cdot}TNS^-$ [g]	16,700 ± 20
$(\beta CD)_2Gl{\cdot}TNS^-$ [h]	13,010 ± 20

[a] Determined by fitting the variation in TNS^- fluorescence with increasing cyclodextrin concentration at 0.5 nm intervals over the wavelength range 410-520 nm,[b] or 400-500 nm,[d,e,f,g,h] to the algorithm arising from the equilibria shown in Eqns. 3.1 and 3.2,[b] Eqn. 3.3,[d] Eqn. 3.5,[e] Eqn. 3.6,[f] Eqn. 3.7,[g] or Eqn. 3.7,[h] using a non-linear least-squares regression routine (Section 6.2.5). Errors quoted represent non-weighted standard deviations. The concentration of TNS^- was fixed at 1.04×10^{-6} mol dm^{-3},[b] 1.00×10^{-6} mol dm^{-3},[d,g] or 1.01×10^{-6} mol dm^{-3}.[e,f,h] The ranges of variation in cyclodextrin concentration for each system were (mol dm^{-3}): βCD (1.50×10^{-6} - 5.50×10^{-3}), $(\beta CD)_2Ur$ (8.32×10^{-7} - 3.07×10^{-4}), $(\beta CD)_2Ox$ (3.98×10^{-6} - 6.03×10^{-4}), $(\beta CD)_2Ma$ (2.51×10^{-6} - 9.00×10^{-4}), $(\beta CD)_2Sc$ (3.00×10^{-6} - 1.00×10^{-3}), and $(\beta CD)_2Gl$ (3.08×10^{-6} - 8.95×10^{-4}). [c] Stepwise stability constant for $(\beta CD)_2{\cdot}TNS^-$ (Eqn. 3.2).

The stability constants of the TNS^- complexes formed with diamide-1°,1°-linked-βCDs are much greater than double that of βCD·TNS^-, indicating that the second hydrophobic recognition site in the linked cyclodextrin dimers is operating cooperatively. The extent of cooperative binding by the cyclodextrin annuli generally increases as the tether connecting them is shortened. This is all the more remarkable because the complexation involves the unfavourable alignment of the opposing dipole moments of the cyclodextrin annuli. A similar trend has recently been reported by Petter *et al.*[5] for the complexation of BNS^- (Appendix, (23)) by dithiol-1°,1°-linked-βCDs. As the length of the tether increases so do the rotational degrees of freedom between the two cavities, permitting a wider range of conformations and reducing the extent of cooperativity. The anomaly of $(\beta CD)_2Ma$ probably arises from the extent of alignment, of the aromatic portions of TNS^- with the hydrophobic βCD cavities and the amine group of TNS^- with the cyclodextrin hydroxyl groups and diamide tether, permitting less hydrophobic and hydrogen bonding interactions, respectively, compared with $(\beta CD)_2Sc$.

The cooperativity exhibited by $(\beta CD)_2X$ (X = Ur, Ox, Ma, Sc, Gl) implies that they are able to exist in a suitable conformation for double binding of TNS^-, and that the binding of the first cyclodextrin does not significantly hinder the binding of the second cyclodextrin. A stabilising interaction may occur between the tether and the guest, as appears to be the case for the complexation of BNS^- by imidazole-1°,1°-linked-βCD (Appendix, (17)).[43]

A study of CPK space filling models shows that either of the hydrophobic regions of TNS^- fit well into a βCD cavity, and TNS^- is capable of passing through a βCD annulus although the fit is quite tight. Molecular models also show that in all of the linked cyclodextrin dimers studied, the two cyclodextrin annuli can completely close up around the guest. Cooperative binding indicates that the toluidinyl group and the naphthyl group are each included inside a cyclodextrin annulus (Fig. 5.1(b)).[13] Once the first of the aromatic groups is included, the other can follow easily due to the close proximity of the annuli, resulting in the formation of the complex.[13,20] Whether the toluidinyl or naphthalene group is included first has not been determined. Since the two cyclodextrins

are linked together by a tether, the cooperation makes the complex difficult to dissociate and the ratio of the rates of complexation and decomplexation increases, hence the greater stability.[13]

A comparison of the stability constants for the TNS^- complexes of oxalamide-2°,2°-linked-βCD (K = 5,500 $dm^3\ mol^{-1}$, Table 3.2) and succinamide-2°,2°-linked-βCD (K = 8,800 $dm^3\ mol^{-1}$, Table 3.2) with those of their 1°,1°-linked counterparts (Table 3.3), reveals that the primary linked derivatives bind TNS^- more strongly. The succinamide-1°,1°-linked-βCD also binds TNS^- more strongly than succinamide-1°,2°-linked-βCD (K = 11,050 $dm^3\ mol^{-1}$, Table 3.2), despite the dipole alignment in the latter. The extent of cooperative binding by the 2°,2°- and 1°,2°-linked-βCDs is only modest, and is lower than that exhibited by the corresponding 1°,1°-linked-βCDs. At first these results may appear surprising, but are readily accounted for by considering the stereochemistry and flexibility of the tether's point of attachment to the cyclodextrin. Presumably the conformations of the secondary linked cyclodextrin dimer complexes of TNS^- are more strained than those of the primary linked analogues. This strain may be attributed to the stereochemistry of substitution on the secondary rim, where the substituents are thought to point toward the interior of the cyclodextrin annulus. In contrast, substituents on the primary rim are attached to sterically unhindered methylene carbons, and are free to point away from the cyclodextrin cavity, resulting in less strained systems. The greater flexibility of substituents attached to the primary rim, compared with those attached to the secondary rim, may also allow more facile complexation than decomplexation, thus enhancing TNS^- binding. Partial inclusion of one cyclodextrin annulus by the other may also be responsible for the strain in the 2°,2°-linked complexes, as reported for disulfide-2°,2°-linked-βCD (Appendix, (12)) (Section 1.3.4).[44,45]

Ethanedithiol-1°,1°-linked-βCD (K = 74,000 $dm^3\ mol^{-1}$, Table 3.2) binds TNS^- about twice as strongly as the diamide-1°,1°-linked-βCD with a comparable length tether, $(\beta CD)_2Ox$. From this similarity in order of magnitude it is concluded that there is not a large difference in binding properties when amide bonds are used instead of thiol bonds for connecting cyclodextrins by their primary rims. A similar conclusion is drawn for linked

cyclodextrin dimers with amide or ester bonds connecting their secondary rims (Section 3.4.6).

In the presence of cyclodextrins, TNS^- shows an enhanced fluorescence with a blue shift of the emission maximum, induced by interaction with the cyclodextrin cavity. The magnitude of this effect is largest when there is either enhanced hydrophobicity of the TNS^- environment, greater shielding from solvent quenching, more restricted intramolecular rotation of TNS^-, or more than one of these, in the complexes formed. These factors appear to increase with a decrease in tether length, as evidenced by the general increase in TNS^- fluorescence enhancement and blue shift of the emission maximum (Table 3.4).

The effect of the cyclodextrins studied on the emission maximum of TNS^- (λ_{max}) is summarised in Table 3.4. These shifts can be explained in terms of the relative contributions of the three excited states (Section 3.2) to the overall fluorescence spectrum. Upon inclusion, TNS^- is transfered from the hydrophilic aqueous medium to the hydrophobic βCD cavity, resulting in a decrease in intramolecular charge-transfer and a dramatic increase in emission from the $S_{1,np}$ excited state (λ_{max} *ca.* 453 nm, Section 3.2). In each case this leads to a blue shift of λ_{max} for the complex with respect to the 490 nm ($S_{1\text{-}ct,np} \rightarrow S_0$) fluorescence band of TNS^- in buffer alone. The dominance of the $S_{1,np} \rightarrow S_0$ transition is also consistent with a nonplanar orientation of the phenyl and naphthyl rings in the inclusion complexes. Since the geometry about the nitrogen of TNS^- is tetrahedral in this state and free rotation of the aryl groups may occur, the extent of conjugation can vary considerably depending on the conformation. The shift in λ_{max} to wavelengths lower than 453 nm may arise from restricted rotational motion decreasing conjugation in the complexes where TNS^- can be encapsulated by two βCD annuli. Indeed, the similarity in λ_{max} values for $(\beta CD)_2X{\cdot}TNS^-$ (X = Ur, Ox, Ma, Sc, Gl) and $(\beta CD)_2{\cdot}TNS^-$, indicate a similarity in TNS^- environment which is consistent with the TNS^- molecule being bound to two cyclodextrin annuli in both cases.

The blue shift of the emission maximum relative to the 490 nm fluorescence band is generally accepted as a measure of hydrophobicity. This implies that the hydrophobicity of

the environment surrounding complexed TNS^- increases in the order: $\beta CD{\cdot}TNS^-$ < $(\beta CD)_2{\cdot}TNS^-$ ~ $(\beta CD)_2Gl{\cdot}TNS^-$ < $(\beta CD)_2Sc{\cdot}TNS^-$ ~ $(\beta CD)_2Ma{\cdot}TNS^-$ < $(\beta CD)_2Ox{\cdot}TNS^-$ ~ $(\beta CD)_2Ur{\cdot}TNS^-$. However, comparisons between the systems should be treated with caution as different excitation wavelengths were used (see footnote Table 3.4).

Table 3.4 *The fluorescence emission maximum and intensity of TNS^- and the complexes it forms with βCD and diamide-1°,1°-linked-βCDs in aqueous phosphate buffer (pH 7.0, $I = 0.10$ mol dm^{-3}) at 298.2 K.*[a]

Species	λ_{max} (nm)	Relative Intensity[b]	Quantum Yield[c]
TNS^-	408, 489[d]	1.0	0.0008
$\beta CD{\cdot}TNS^-$ [e]	463	12	0.024
$(\beta CD)_2{\cdot}TNS^-$ [e]	446	24	—
$(\beta CD)_2Ur{\cdot}TNS^-$ [f]	434	197	—
$(\beta CD)_2Ox{\cdot}TNS^-$ [f]	433	23	—
$(\beta CD)_2Ma{\cdot}TNS^-$ [g]	441	133	—
$(\beta CD)_2Sc{\cdot}TNS^-$ [g]	440	84	—
$(\beta CD)_2Gl{\cdot}TNS^-$ [g]	447	47	0.047

[a] The excitation wavelengths for each system were (nm): βCD (369), $(\beta CD)_2Ur$ (354), $(\beta CD)_2Ox$ (346), $(\beta CD)_2Ma$ (357), $(\beta CD)_2Sc$ (353), $(\beta CD)_2Gl$ (355). Excitation and emission slit widths were 5 and 10 nm, respectively, for all systems except $(\beta CD)_2Ur$, for which the emission slit width was 5 nm. [b] Integrated area under the emission spectrum derived for the complex relative to that of free TNS^- under the same conditions, over the wavelength ranges recorded: 385-550,[e] 370-550,[f] and 370-530.[g] The values listed have been normalised to take into account the differences in absorbance at the excitation wavelength (Section 6.2.3). [c] The excitation wavelength was 366 nm, and emission range was 390-600 nm. Excitation and emission slit widths were 5 and 10 nm, respectively. [d] From fitting two gaussian curves to the emission spectrum of TNS^- (Fig. 3.3).

Preliminary measurements on the effect of βCD and diamide-1°,1°-linked-βCDs on the fluorescence emission intensity of TNS^- are also listed in Table 3.4. The relative intensities and quantum yields show that the fluorescence of TNS^- is enhanced significantly more in $(\beta CD)_2X \cdot TNS^-$ than in $\beta CD \cdot TNS^-$, which supports cooperative binding of TNS^- by $(\beta CD)_2X$.

The quantum yield of TNS^- in the absence of cyclodextrin is negligible compared with the quantum yields of its cyclodextrin complexes (Table 3.4). A 30-fold enhancement of fluorescence is observed upon formation of $\beta CD \cdot TNS^-$ and a 60-fold enhancement is observed for $(\beta CD)_2Gl \cdot TNS^-$.

In each system the emission spectrum derived for the complex and that of TNS^-, previously determined under the same conditions, were compared by integrating the areas under the emission spectra over the range of wavelengths recorded. Any difference in absorption of complexed and free TNS^- at the the excitation wavelength was corrected for (Section 6.2.3) to yield the relative intensity values (Table 3.4). Since the entire emission spectrum of each species present was not encompassed within the wavelength range recorded, these values are only semi-quantitative, and appear to be lower than the actual quantum yield values. As different excitation wavelengths were used this may also have an effect, and comparisons are made with caution.

Although the semi-quantitative relative intensity values are low, they indicate the trend in fluorescence enhancement. These values are consistent with a more hydrophobic TNS^- environment and a greater reduction in solvent quenching of the TNS^- fluorescence in $(\beta CD)_2X \cdot TNS^-$ than in $(\beta CD)_2 \cdot TNS^-$. The general increase in fluorescence enhancement with a decrease in tether length implies that these effects increase as the distance between the βCD annuli of $(\beta CD)_2X$ is decreased. The tether of the linked cyclodextrin dimer restricts the movement of one annulus with respect to the other, leading to a reduction in the rotational degrees of freedom of TNS^- in $(\beta CD)_2X \cdot TNS^-$ by comparison with that in $(\beta CD)_2 \cdot TNS^-$. Any decrease in flexibility of the linked cyclodextrin dimer with a decrease in tether length, may also enhance the fluorescence by restricting the rotational motion of TNS^- to a greater extent. The linked cyclodextrin

dimer containing the shortest link, $(\beta CD)_2Ur$, produces the greatest increase in TNS^- fluorescence, which is consistent with formation of a more rigid complex and a more hydrophobic TNS^- environment with water quenching being limited by the close proximity of the annuli. The linked cyclodextrin dimer containing conjugation in the tether, $(\beta CD)_2Ox$, produces a decreased TNS^- fluorescence enhancement by comparison with that of the other linked cyclodextrin dimers. This may arise from the rigidity of the conjugated tether imposing stereochemical constraints on the complex. Alternatively, the luminescence properties of the tether and its interactions with TNS^- may produce the observed anomaly. The conjugated system in the tether may behave similarly to 2,3-butanedione or glyoxal, which exhibit phosphorescence.[46]

The succinate-2°,2°-linked-βCD (Appendix, (9)) and glutarate-2°,2°-linked-βCD (Appendix, (10)) studied by Harada *et al.*[20] exhibited 3 and 2.7 times stronger fluorescence than $(\beta CD)_2 \cdot TNS^-$, respectively. The hydrophobicity of the TNS^- environment and the degree of protection from solvent quenching, may be influenced by the widths of the cyclodextrin rims which are held adjacent to each other. As mentioned above, secondary linked derivatives are less flexible than primary linked derivatives, and hence, would be expected to restrict rotational motion of the guest more efficiently. However, the fluorescence enhancements reported by Harada *et al.* are similar to those of succinamide-1°,1°-linked-βCD and glutaramide-1°,1°-linked-βCD (Table 3.4). Any interaction of TNS^- with the tether itself may also influence the level of fluorescence enhancement in the linked cyclodextrin dimer complexes.

These studies show that linked cyclodextrin dimers bind TNS^- more strongly than monomeric βCD, and the extent to which the second cyclodextrin annulus enhances binding is dependent on the length of the tether group and the rims of the cyclodextrins which are connected. A comparison of the stability constants listed in Tables 3.2 and 3.3 indicates the extent of cooperative binding by the cyclodextrin annuli is greatest when they are joined by a short tether connecting their primary rims. Larger guests may be more effectively bound by dimers which are linked by their wider ends, and longer guests by those with longer tethers. Although studies on variation of the guest structure have been

made, none of these have extended over a series of hosts such as the diamide-1°,1°-linked βCDs discussed here. The following chapter reports the variation in binding observed for three of these diamide-1°,1°-linked βCDs with two guests of related structure.

References

1. J. H. Coates, C. J. Easton, S. J. van Eyk, S. F. Lincoln, B. L. May, C. B. Whalland and M. L. Williams, *J. Chem. Soc., Perkin Trans. 1*, 1990, 2619.

2. H. Kondo, H. Nakatani and K. Hiromi, *J. Biochem.*, 1976, **79**, 393.

3. M. D. Johnson and V. C. Reinsborough, *Aust. J. Chem.*, 1992, **45**, 1961.

4. V. Crescenzi, A. Gamini, A. Palleschi, and R. Rizzo, *Gazz. Chim. Ital.*, 1986, **116**, 435.

5. C. T. Sikorski and R. C. Petter, *Tetrahedron Lett.*, 1994, **35**, 4275.

6. W. O. M^{c}Clure and G. M. Edelman, *Biochem.*, 1966, **5**, 1908.

7. K. K. Karukstis, D. A. Krekel, D. A. Weinberger, R. A. Bittker, N. R. Naito and S. H. Bloch, *J. Phys. Chem.*, 1995, **99**, 449.

8. U. P. Andley, J. N. Liang and B. Chakrabarti, *Biochem.*, 1982, **21**, 1853.

9. J. R. Lakowicz, *Principles of Fluorescence Spectroscopy*, Plenum Press, New York, 1983.

10. J. R. Lakowics and D. Hogen, *Biochem.*, 1981, **20**, 1366.

11. E. M. Kosower, H. Dodiuk and H. Kanety, *J. Am. Chem. Soc.*, 1978, **100**, 4179.

12. E. M. Kosower and K. Tanizawa, *Chem. Phys. Lett.*, 1972, **16**, 419.

13. A. Harada, M. Furue and S. Nozakura, *Macromolec.*, 1977, **10**, 676.

14. C. J. Seliskar and L. Brand, *Science*, 1971, **171**, 799.

15. M. J. Kamlet, C. Dickinson and R. W. Taft, *Chem. Phys. Lett.*, 1981, **77**, 69.

16. N. Sarkar, K. Das, D. Nath and K. Bhattacharyya, *Chem. Phys. Lett.*, 1992, **196**, 491.

17. M. Adachi, Y. Murata and S. Nakamura, *J. Am. Chem. Soc.*, 1993, **115**, 4331.

18. N. I. Nijegorodov and W. S. Downey, *J. Phys. Chem.*, 1994, **98**, 5639.

19. K. Fujita, S. Ejima and T. Imoto, *J. Chem. Soc., Chem. Commun.*, 1984, 1277.

20. A. Harada, M. Furue and S-I. Nozakura, *Polymer J.*, 1980, **12**, 29.

21. I. Tabushi, Y. Kuroda and K. Shimokawa, *J. Am. Chem. Soc.*, 1979, **101**, 1614.

22. F. Venema, C. M. Baselier, M. C. Feiters and R. J. M. Nolte, *Tetrahedron Lett.*, 1994, **35**, 8661.

23. G. C. Catena and F. V. Bright, *Anal. Chem.*, 1989, **61**, 905.

24. H-J. Schneider, T. Blatter and S. Simova, *J. Am. Chem. Soc.*, 1991, **113**, 1996.

25. D. J. Jobe, R. E. Verrall, R. Palepu and V. C. Reinsborough, *J. Phys. Chem.*, 1988, **92**, 3582.

26. A. Nakamura, K. Saitoh and F. Toda, *Chem. Phys. Lett.*, 1991, **187**, 110.

27. A. Hersey, B. H. Robinson and H. C. Kelly, *J. Chem. Soc., Faraday Trans. 1*, 1986, **82**, 1271.

28. F. V. Bright, G. C. Catena and J. Huang, *J. Am. Chem. Soc.*, 1990, **112**, 1343.

29. A. Muñoz de la Peña, F. Salinas, M. J. Gómez, M. I. Acedo and M. Sánchez Peña, *J. Inclusion Phenom. Mol. Recognit. Chem.*, 1993, **15**, 131.

30. N. J. Turro, T. Okubo and C. -J. Chung, *J. Am. Chem. Soc.*, 1982, **104**, 1789.

31. J. Nishijo, M. Yasuda, M. Nagai and M. Sugiura, *Bull. Chem. Soc. Jpn.*, 1992, **65**, 2869.

32. Y. Inoue, T. Hakushi, Y. Liu, L.-H. Tong, B.-J. Shen and D.-S. Jin, *J. Am. Chem. Soc.*, 1993, **115**, 475.

33. K. Pitchumani and M. Vellayappan, *J. Inclusion Phenom. Mol. Recognit. Chem.*, 1992, **14**, 157.

34. M. Hoshino, M. Imamura, K. Ikehara and Y. Hama, *J. Phys. Chem.*, 1981, **85**, 1820.

35. B.-L. Poh and Y. M. Chow, *J. Inclusion Phenom. Mol. Recognit. Chem.*, 1992, **14**, 85.

36. J. Huang and F. V. Bright, *J. Phys. Chem.*, 1990, **94**, 8457.

37. B. Zhang and R. Breslow, *J. Am. Chem. Soc.*, 1993, **115**, 9353.

38. W. Xu, J. N. Demas, B. A. DeGraff and M. Whaley, *J. Phys. Chem.*, 1993, **97**, 6546.

39. F. Venema, C. M. Baselier, E. van Dienst, B. H. M. Ruël, M. C. Feiters, J. F. J. Engbersen, D. N. Reinhoudt and R. J. M. Nolte, *Tetrahedron Lett.*, 1994, **35**, 1773.

40. R. C. Petter, C. T. Sikorski and D. H. Waldeck, *J. Am. Chem. Soc.*, 1991, **113**, 2325.

41. J. Papageorgiou, Ph.D. Thesis, The University of Adelaide, 1995.

42. T. Jiang, D. K. Sukumaran, S. Soni and D. S. Lawrence, *J. Org. Chem.*, 1994, **59**, 5149.

43. R. Breslow and S. Halfon, *Proc. Natl. Acad. Sci. USA*, 1992, **89**, 6916.

44. R. Breslow, *Israel J. Chem.*, 1992, **32**, 23.

45. R. Breslow, N. Greenspoon, T. Guo and R. Zarzycki, *J. Am. Chem. Soc.*, 1989, **111**, 8296.

46. B. Stevens and J. T. Dubois, *J. Chem. Soc.*, 1962, **2**, 2813; J. C. D. Brand, *J. Chem. Soc., Faraday Trans.*, 1954, **50**, 431.

CHAPTER 4

Complexation of Methyl Orange and Tropaeolin 000 No. 2 by Linked Cyclodextrin Dimers

4.1 Introduction

In the previous chapter the binding of a number of linked cyclodextrin dimer hosts to a particular guest, TNS^-, was considered and the effect of variation in the length of the tether connecting two βCD annuli by their primary rims was discussed. Following from this, the effect of variation in the guest's structure is now considered.

Three of the previously used linked cyclodextrin dimers, $(\beta CD)_2Ur$, $(\beta CD)_2Ox$ and $(\beta CD)_2Sc$ (Fig. 3.1), were selected for this study. The dye molecules, methyl orange (MO) and tropaeolin 000 no. 2 (TR) were selected because of their strong absorption properties and related structures (Fig. 4.1). A structural comparison of the monoanion forms, MO^- and TR^-, shows that in the case of TR^- the dimethylaniline moiety of MO^- is replaced by a β-naphthol moiety. Both dyes have two hydrophobic recognition elements. The structure of MO^- incorporates two phenyl rings, while that of TR^- incorporates one phenyl and one naphthyl ring. Both phenyl and naphthyl groups are capable of inclusion within a βCD cavity.[1]

Since both MO^- and TR^- show negligible spectral changes in the presence of high concentrations of glucose,[2] it is reasonable to attribute the relatively large spectral changes observed upon addition of cyclodextrins, to the formation of inclusion complexes.

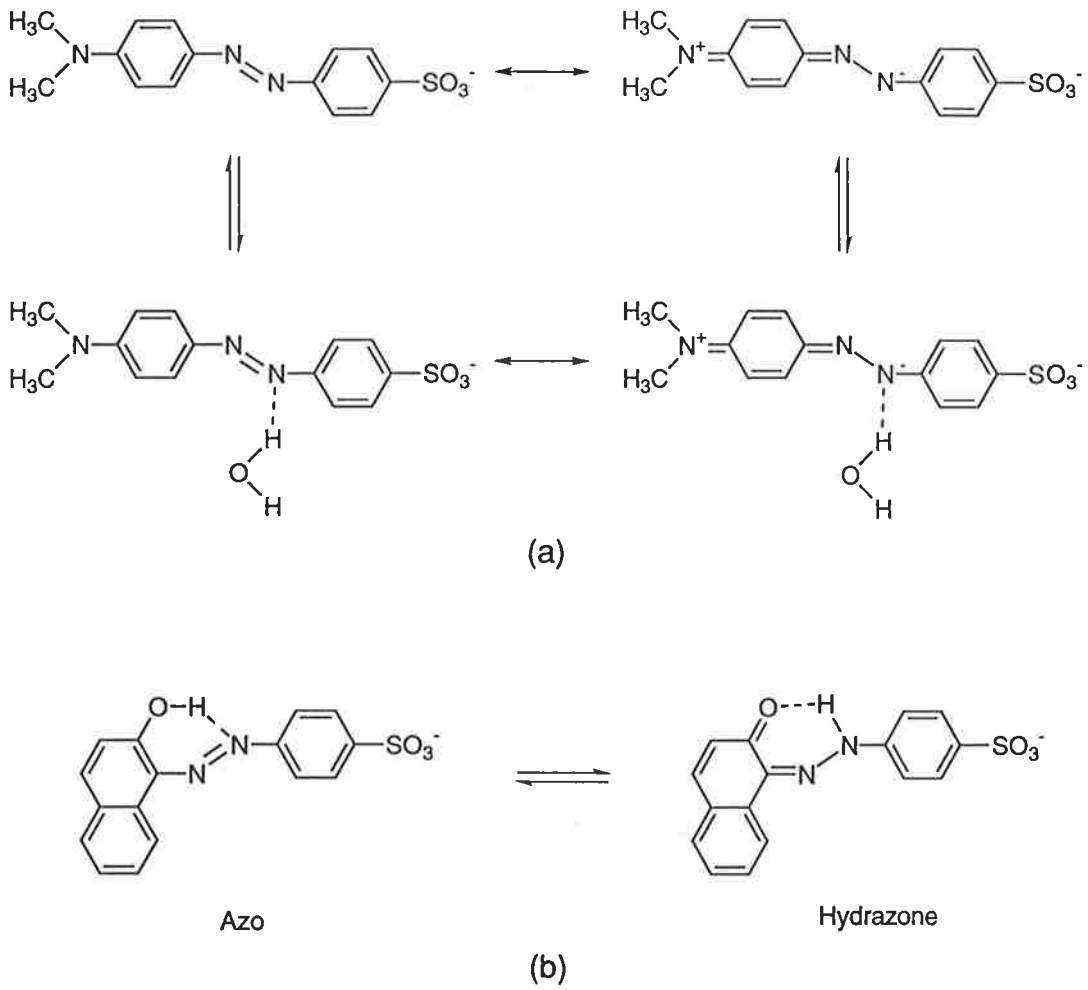

Figure 4.1 *The structure of (a) MO^-, showing its resonance contributors and the hydrogen bonding interaction of water with the azo nitrogens, and (b) TR^-, showing the equilibrium between its azo and hydrazone tautomers.*

The complexation of MO^- is considered first. After discussing the origin of the MO^- absorbance spectrum, the spectral changes, stoichiometry, stability and structure of the complexes formed with βCD are examined. The spectral changes, stoichiometry and stability of the MO^- complexes formed with $(\beta CD)_2Ur$, $(\beta CD)_2Ox$ and $(\beta CD)_2Sc$ are then reported. Comparisons are made with the βCD system and structures are proposed for the linked cyclodextrin dimer complexes. A similar discussion follows for TR^-, and finally comparisons are made between these two guests and the complexes they form in Section 4.4.

4.2 Complexation of Methyl Orange

4.2.1 Properties of the Methyl Orange Anion

The pK_a of methyl orange is 3.38,[3] and the results presented in the following sections correspond to the basic monoanion form, MO^-, in which both the azo and sulfonate groups are deprotonated (Fig. 4.1). In principle, the azo group of MO^- is capable of *cis-trans* isomerism (the *cis* isomer is restricted to a nonplanar geometry, because of steric crowding, while the almost linear *trans* isomer can exist in a planar geometry). However, *cis-trans* isomerism in aqueous media is improbable, and the *trans* isomer predominates.[4-6] In aqueous solution MO^- is known to aggregate, with a resultant decrease in absorption and a departure from Beer's Law.[7] However, at the dye concentration used in this study (3.8-4.0 x 10^{-5} mol dm^{-3}) any such deviations are negligible.[7]

In order to explain the effects of cyclodextrins on the MO^- absorbance spectrum (Fig. 4.2) an understanding of the origin of the electronic transitions in the wavelength range studied is required. In principle, one $\pi \rightarrow \pi^*$ and two $n \rightarrow \pi^*$ transitions are associated with the azo group. However, for *trans*-azo compounds with C_{2h} symmetry only the $\pi \rightarrow \pi^*$ ($^1A_g \rightarrow {}^1B_u$) and $n_a \rightarrow \pi^*$ ($^1A_g \rightarrow {}^1A_u$) transitions are allowed due to symmetry selection rules.[8] The electronic transitions of MO^- in the visible region have previously been attributed to the overlap of the $\pi \rightarrow \pi^*$ transition with the $n_a \rightarrow \pi^*$ transition, causing intense absorption spectra and facilitating its use as a dye.[9,10] Although temperature and solvent variation studies confirm the presence of two high-intensity overlapping absorption bands[4] (Fig. 4.2), the second band does not appear to result from the $n_a \rightarrow \pi^*$ transition.

By reference to the character table for the C_{2h} point group it can be seen that the expected transition moment directions for the $\pi \rightarrow \pi^*$ and $n_a \rightarrow \pi^*$ transitions are parallel to, and perpendicular to, the molecular plane, respectively. Linear dichroism

measurements of MO^- in stretched films indicate that the transition moment of the dominant transition is polarised approximately along the line interconnecting the two phenyl groups.[11] It would appear, from the relatively constant dichroic ratio across the absorption curve, that the two high-intensity overlapping absorption bands are both due to $\pi \rightarrow \pi^*$ transitions. However, molecular-orbital calculations on the MO^- π-system suggest that only a single high-intensity transition, polarised approximately along the line connecting the phenyl moieties, occurs in the visible region.[12]

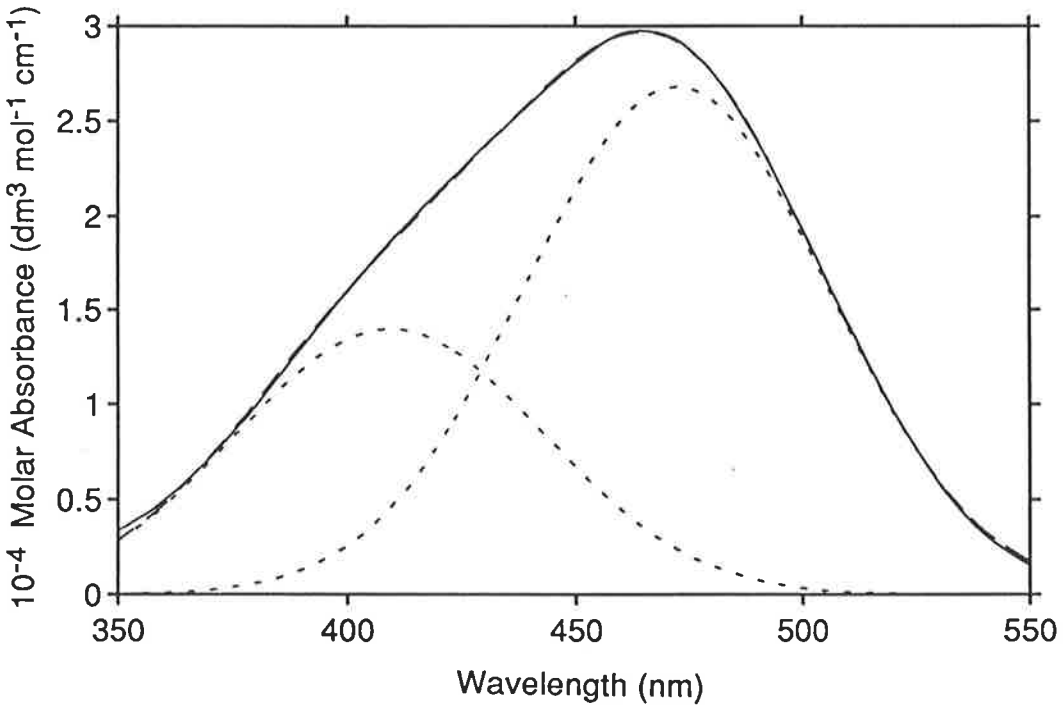

Figure 4.2 *Absorbance spectrum of MO^- (4.0×10^{-5} mol dm^{-3}) in aqueous solution at pH 9.0 and 298.2 K. Dotted lines show the fit to two Gaussians having maxima at 410 and 472 nm.*

Brode[6] suggested the two overlapping bands were due to the presence of two distinct MO^- species in solution. A hydrated species in which water hydrogen bonds to one of the azo nitrogens (Fig. 4.1) would result in a wavelength shift of the absorption maximum. Considering the temperature and solvent dependence of the MO^- spectrum,

Reeves *et al.*[4] attributed the high and low wavelength bands to the $\pi \rightarrow \pi^*$ transitions of the hydrogen-bonded and non-hydrogen-bonded species respectively. The spectral changes observed upon binding of MO^- to various hydrophobic sites may then be interpreted as arising from a shift in the equilibrium between the two species as a result of a decrease in hydrogen bonding with the aqueous solvent.

Although Brodes' hypothesis adequately explains the absorption spectrum of MO^-, the magnitude of this shift (*ca.* 3000 cm^{-1}, 60 nm)[4] is unusually large for a solvent effect on a $\pi \rightarrow \pi^*$ transition. Small shifts (*ca.* 400 cm^{-1}, 10 nm) can be explained in terms of general solvent effects, but larger shifts imply an additional effect is operating.[13] Large spectral shifts have been explained in terms of dye dimerisation, increasing the intensity of the dimer peak relative to that of the monomer peak.[13] Increasing MO^- concentration results in a blue shift and a decrease in intensity of the absorbance spectrum.[7] It may be inferred that dimerisation of MO^- produces these spectral changes, with the absorbance peak at 464 nm being attributed to the overlap of a high wavelength monomer band and a low wavelength dimer band. These explanations show there is still some uncertainty as to the origin of the MO^- absorbance bands.

4.2.2 Complexation of Methyl Orange by βCD

The interaction between βCD and the basic form of methyl orange, MO^-, has been studied by a number of workers[2,5,13-23] and the reported stability constants for the complexes formed are listed in Table 4.1. The induction of circular dichroism in the absorption region of MO^- by the addition of βCD indicates formation of an inclusion complex.[2,17] The pK_a of methyl orange is also found to decrease by approximately one pH unit on inclusion by βCD.[3] This may result from the basic form, MO^-, being included inside the βCD cavity with a greater stability than that of the acidic form, (MO)H, in which one of the nitrogen atoms is protonated. A shift in the tautomeric equilibrium of the acidic form upon inclusion[5,24] may also contribute to the observed decrease in pK_a.[15] A change in the hydrogen bonding interactions of the azo group, upon entering the βCD cavity, may

result in a different *cis-trans* isomer equilibrium distribution of MO^- (Section 4.2.1) in the complexed form.[18,25] However, the *trans* isomer of MO^- probably still dominates,[5] as the nonplanar *cis* isomer is not as suited to deep inclusion in the βCD cavity, and hence, spectral shifts are unlikely to arise from a change in this equilibrium.[5]

The absorbance of MO^- upon addition of βCD increases in the range 400-440 nm, and decreases at wavelengths ≥ 470 nm.[2] Although a red shift in the absorption spectrum of a guest is usually produced upon its inclusion by a cyclodextrin,[26,27] in this case a blue shift of the absorption maximum from 462 to 454 is observed upon complexation of MO^- by βCD.[17] This shift may be interpreted as an increase in the amount of non-hydrogen-bonded species present (Section 4.2.1) as a result of βCD decreasing the dye-solvent hydrogen bonding interactions. The decrease in hydrogen bonding with the solvent appears to outweigh any hydrogen bonding interactions between MO^- and the βCD hydroxyl groups. A similar spectral blue shift is seen for the acidic form, (MO)H, in which the azo group is protonated, and this large shift permits the use of this dye as a pH indicator.[28] As mentioned in Section 4.2.1, a dimerisation phenomenon may account for a blue shift. Dimerisation is usually accompanied by a decrease in intensity (Section 4.2.1), and the similar intensities of the MO^- spectrum in the absence and presence of βCD may arise from the environmental effect of the cyclodextrin cavity.[11] Interestingly, a blue shift and an increase in intensity is observed in the presence of γCD, which is known to form highly stable dimeric MO^- complexes.[11] However, in the case of βCD, the dimeric MO^- complex, $\beta CD\cdot(MO)_2^{2-}$, appears to exist in at most only small amounts, and hence the dimerisation phenomenon does not explain the spectral changes as readily as the presence of hydrogen bonded and non-hydrogen bonded species does.

An isosbestic point is apparent at 396 nm in the absorbance spectrum of MO^- upon addition of βCD. Also observed is a crossover point which moves from 454 to 466 nm with increasing βCD concentration.[2] The shifting crossover point is evidence of more than two absorbing species. This suggests that two complex species are absorbing in addition to free MO^-, however, the isosbestic point implies that two of these species are dominant.

At a given wavelength a satisfactory fit of the data to the algorithm arising from the equilibrium in Eqn. 4.1 alone can be obtained, however, the resultant stability constants show a two-fold variation across the wavelength range of 420-540 nm.[2] This probably indicates the presence of another complex besides βCD·MO^-. The variation in the stability constant is found even if the data are restricted to very low βCD concentrations, which implies that the additional complex may be βCD·$(MO)_2^{2-}$. The formation of $(\beta CD)_2 \cdot MO^-$, as the additional complex, has also been proposed, and the reported stability constants are listed in Table 4.1.[14,19] However, Clarke[2] could not achieve a satisfactory fit of the data to the algorithm arising from the consecutive equilibria of Eqns. 4.1 and 4.2, and the value of K_2 determined by Schneider *et al.*[19] required K_1 to be fixed to a previously determined value. It is possible that this fitting difficulty arises because two of the absorbing species have very similar spectra, or because only small amounts of the additional complex form. The formation of a third complex, $(\beta CD)_2 \cdot (MO)_2^{2-}$, which may occur since the size of the βCD cavity permits inclusion of two phenyl moieties,[1] would also complicate the fitting.

$$\beta CD + MO^- \overset{K_1}{\rightleftharpoons} \beta CD \cdot MO^- \qquad (4.1)$$

$$\beta CD \cdot MO^- + \beta CD \overset{K_2}{\rightleftharpoons} (\beta CD)_2 \cdot MO^- \qquad (4.2)$$

The majority of reported stability constants were determined assuming the presence of a single βCD·MO^- complex (Table 4.1). The reported values of K_1 range from 2,160 to 4,880 $dm^3\ mol^{-1}$ (Table 4.1), a variation which may arise from differences in experimental conditions, measurement methods and data treatments (see footnote Table 4.1). Buffer concentration and inorganic salts added are known to influence the βCD complex stability of a related azo dye, *p*-(4-hydroxy-1-naphthylazo)benzenesulfonate (Appendix, (33)).[29] Increasing ionic strength results in an increase in stability of αCD·MO^-, and a similar effect is expected in the analogous βCD complexes.[15] Variation in pH should have little effect on the stability constants listed in Table 4.1 over the pH range in which the basic form, MO^-, exists exclusively. Many of the stability constants are determined using linear fitting

Table 4.1 *Reported stability constants for the complexes of MO^- with βCD in aqueous solution.*[a]

K_1 ($dm^3\ mol^{-1}$)	K_2 ($dm^3\ mol^{-1}$)
2160[b]	—
2273[c]	—
2630[d]	—
2720[e]	—
2800[f]	—
2820[g]	—
2970[h]	606[h]
3100[i]	600[i]
3850[j]	—
3980[k]	—
4500[l]	—
4880[m]	—

[a] A dash indicates no complex formation detected. [b] Ref. 2 (*nl*, multi λ (408-540 nm), $[MO^-] = 4.0 \times 10^{-5}$ mol dm^{-3}, [βCD] ≤ 1.2×10^{-2} mol dm^{-3}, pH 9.0, 298.2 K). [c] Ref. 16 (*nl*, $[MO^-] = 5.0 \times 10^{-5}$ mol dm^{-3}, [βCD] ≤ 1.0×10^{-3} mol dm^{-3}, 0.02 mol dm^{-3} MES buffer, pH 6.2, 298.2 K). [d] Ref. 15 (*l*, 2λ (507 and 530 nm), $[MO^-] = 2.0 \times 10^{-5}$ mol dm^{-3}, [βCD] ≤ 2.0×10^{-3} mol dm^{-3}, weakly acidic solution, I = 0.5 mol dm^{-3}, 298.2 K). [e] Ref. 23 (*l*). [f] Ref. 16 (*nl*, $[MO^-] = 5.0 \times 10^{-5}$ mol dm^{-3}, [βCD] ≤ 1.0×10^{-3} mol dm^{-3}, 0.02 mol dm^{-3} HEPES buffer, pH 7.0, 298.2 K). [g] Refs. 5, 21 (*l*). [h] Ref. 14 (carbonate buffer, pH 10.60, I = 0.05 mol dm^{-3}, 298.2 K). [i] Ref. 19 (multi λ (490-530 nm), 0.05 mol dm^{-3} carbonate buffer, pH 10.0, 298.2 K. K_1 from fitting a single 1:1 complex at low concentration of βCD: $[MO^-] = (5.52\text{-}2.94) \times 10^{-5}$ mol dm^{-3} and [βCD] = (0-1.41) x 10^{-3} mol dm^{-3}. K_2 from fitting to 1:1 and 1:2 complexes with K_1 = 3100 $dm^3\ mol^{-1}$, at high concentrations of βCD: $[MO^-] = (5.52\text{-}3.03) \times 10^{-5}$ mol dm^{-3} and [βCD] = (0-6.79) x 10^{-3} mol dm^{-3}). [j] Refs. 13, 17 (*l*, $[MO^-] = 5.0 \times 10^{-5}$ mol dm^{-3}, [βCD] ≤ 6.0×10^{-3} mol dm^{-3}, phosphate buffer, pH 7.0, I = 0.1 mol dm^{-3}, 293.2 K). [k] Ref. 20 ($[MO^-] = 1.0 \times 10^{-5}$ mol dm^{-3}, [βCD] ≤ 1.0×10^{-2} mol dm^{-3}, pH 6.08, I = 0.08 mol dm^{-3}, 293.2 K). [l] Ref. 18 (*nl*, $[MO^-] = 3.0 \times 10^{-5}$ mol dm^{-3}, [βCD] ≤ 2.0×10^{-3} mol dm^{-3}, phosphate buffer, pH 7.0, I ≤ 0.02 mol dm^{-3}, 298.2 K). [m] Ref. 22 (*nl*, $[MO^-] = 1.0 \times 10^{-4}$ to 1.0×10^{-3} mol dm^{-3}, [βCD] ≤ 4.2×10^{-3} mol dm^{-3}, pH 6.8, 298.2 K, determined conductometrically).

methods (denoted *l* in Table 4.1 footnote), such as the Hildebrand-Benesi method,[30] which are not as accurate as non-linear regression methods (denoted *nl* in Table 4.1 footnote), as they place more weight on the lower concentration values than on the higher ones.[26,31] The variation in reported values may arise partially from a lack of consideration given to complexes other than a simple βCD·MO^- complex, in some cases. This is probably the main factor contributing to the considerable variation in the values. If an incorrect model has been selected, single wavelength determination can lead to large variations in stability constants determined at different wavelengths. It appears that in most cases the stability constants reported in Table 4.1 have been determined at a single wavelength only.

The βCD/MO^- system was studied by Clarke[2] under experimental conditions which are identical to those used in the following linked cyclodextrin dimer studies. Although the wavelength dependence of K_1 implied the existence of another complex species besides βCD·MO^-, a satisfactory fit of the data to a model incorporating the formation of two complex species could not be achieved. Hence, the βCD·MO^- complex stability constants, determined at 2 nm intervals over the wavelength range 408-540 nm, were averaged to yield a value of (2.16 ± 0.90) x 10^3 dm^3 mol^{-1}.[2] This value is used for making comparisons with the linked cyclodextrin dimer systems (Section 4.2.3).

The thermodynamic quantities for the complexation of MO^- by βCD are $\Delta H° = -19.7$ kJ mol^{-1}, $\Delta S° = +5.0$ J mol^{-1} K^{-1}.[18] The linear shaped molecule allows a more ordered solvent shell while the molecule is in solution. Upon binding, this solvent shell is broken up, leading to the favourable entropy term.[31] The entropy increase for this process is great enough to offset the entropy loss associated with the binding itself.

The stability of αCD·MO^- (*ca.* 9 x 10^3 dm^3 mol^{-1}) is more than double that of βCD·MO^- (*ca.* 3 x 10^3 dm^3 mol^{-1}).[14,15,19,20] This is probably due to a tighter fit of the dye in the smaller αCD cavity. The ability of the larger cavities of βCD and γCD to include two phenyl groups is well established.[1] Both βCD·MO^- and $(\beta CD)_2$·MO^- complexes are proposed to form,[14,19] although formation of a βCD·$(MO)_2^{2-}$ complex can not be ruled out.[2] The wider annulus of γCD results in the formation of γCD·MO^-, γCD·$(MO)_2^{2-}$ and $(\gamma CD)_2$·$(MO)_2^{2-}$ complexes, with stepwise stability constants of 45,

2.2×10^6 and 6.1×10^3 dm^3 mol^{-1}, respectively.[11] In the $(\gamma CD)_2 \cdot (MO)_2^{2-}$ complex the MO^- molecules are considered to be in a parallel-plane head-to-tail arrangement.[11]

The MO^- structure suggests that both the dimethylaniline and phenylsulfonate ends of the molecule may be capable of inclusion, probably from the wider secondary end of the βCD annulus. Space-filling CPK molecular models show that to achieve sufficient penetration of the cavity for complex formation, MO^- must include with its long axis parallel to the βCD C_7 symmetry axis. Since the depth of the cavity is about half the length of the MO^- molecule, only partial inclusion is possible. It also appears that both ends of MO^- fit equally well into the βCD cavity. It is possible that $\beta CD \cdot MO^-$ may not have a single unique structure, but rather two possible structures may exist, in which either the dimethylaniline or the phenylsulfonate end of the dye is included. This is still consistent with the isosbestic and crossover points observed at low βCD concentrations, since the two $\beta CD \cdot MO^-$ complexes would both be in equilibrium with free MO^- and βCD, and hence the ratio of their concentrations would be constant, regardless of the concentration of βCD. However, because of the different shapes and physico-chemical properties of the dimethylamino and sulfonate groups, it is most likely that one end of MO^- is included preferentially.

To determine from which end MO^- is included, stability constants have been measured at pH 9.0 and 13.4, which are above and below the pK_a of the βCD secondary hydroxyl groups.[2] A substantial decrease in stability constant at pH 13.4 would be expected if there was preferential inclusion from the phenylsulfonate end, due to electrostatic repulsion between the negatively charged host and guest. The small change in stability constant detected supports preferential inclusion from the dimethylaniline end. This is probably due to the fact that the localised charge of the sulfonate group results in it being strongly solvated, and hence removal of the solvating water molecules in order to form a complex with βCD is not favoured. Other guests with structures related to MO^- also show preferential inclusion from the uncharged end of the molecule, and increasing solvation of a group appears to decrease complex stability.[32] Preferential inclusion from the dimethylaniline end is also supported by the lack of complex formation between

TR^- (Fig. 4.1) and αCD (Section 4.3.2). The phenylsulfonate moiety of MO^- is also present in TR^-, while the dimethylaniline moiety is replaced by a β-naphthol group which is too large for inclusion in the αCD cavity. This lack of complex formation is consistent with solvation of the sulfonate group inhibiting inclusion of the dyes from the phenylsulfonate end. Interestingly, the stability constant of the complex formed between *N*,*N*-dimethylaniline (Appendix, (34)) and βCD is only 230 $dm^3\ mol^{-1}$,[33] implying that in the βCD·MO^- complex other groups such as the azo group are also involved in complexation, to yield a ten-fold greater stability constant.

The change in the MO^- absorbance spectrum upon addition of αCD is consistent with the formation of both αCD·MO^- and $(\alpha CD)_2 \cdot MO^-$ complexes,[13,34] which may have similar structures to the βCD analogues. X-ray analysis shows that the crystalline complex of αCD and MO^- has the stoichiometry $(\alpha CD)_2 \cdot MO^-$, and the complex structure is unaffected by the cation of the MO^- salt.[35] The X-ray crystal structure reveals that the azo group and one phenyl ring are included within the αCD cavity. The azo group is located nearer the primary rim of the cavity. The dimethylamine group and the charged sulfonate group protrude from the cavity, on the primary and secondary sides, respectively. The dimethylamine group is included at the secondary end of another αCD cavity, and the sulfonate group appears to be hydrogen bonded to the primary hydroxyl groups of yet another αCD, building up a channel-like structure. The dipole moments of MO^- and the threaded αCD are not aligned, however, the negative (secondary) and positive (primary) poles of the other αCDs are aligned with the partial positive charge of the dimethylaniline moiety (Fig. 4.1) and the negative charge of the sulfonate group, respectively. Complex structure in the solid state and in solution may be unrelated. However, 1D ^1H and ^{13}C NMR data suggest that the inclusion of MO^- by either αCD or βCD occurs predominantly from the dimethylaniline end, which passes through the αCD or βCD cavity to a depth which permits inclusion of the azo group, or of the phenylsulfonate end, respectively.[36]

4.2.3 Complexation of Methyl Orange by Linked Cyclodextrin Dimers

Now that background knowledge on MO^- and its interactions with βCD have been established, the more complex linked cyclodextrin dimer systems are discussed. The variation in MO^- absorbance with addition of the linked cyclodextrin dimers: $(\beta CD)_2Ur$, $(\beta CD)_2Ox$ and $(\beta CD)_2Sc$, can be seen in Figs. 4.3, 4.4 and 4.5, respectively. All three systems have spectral changes similar to those observed upon addition of βCD, and are consistent with a change in the local environment of the chromophore upon inclusion by the cyclodextrin.

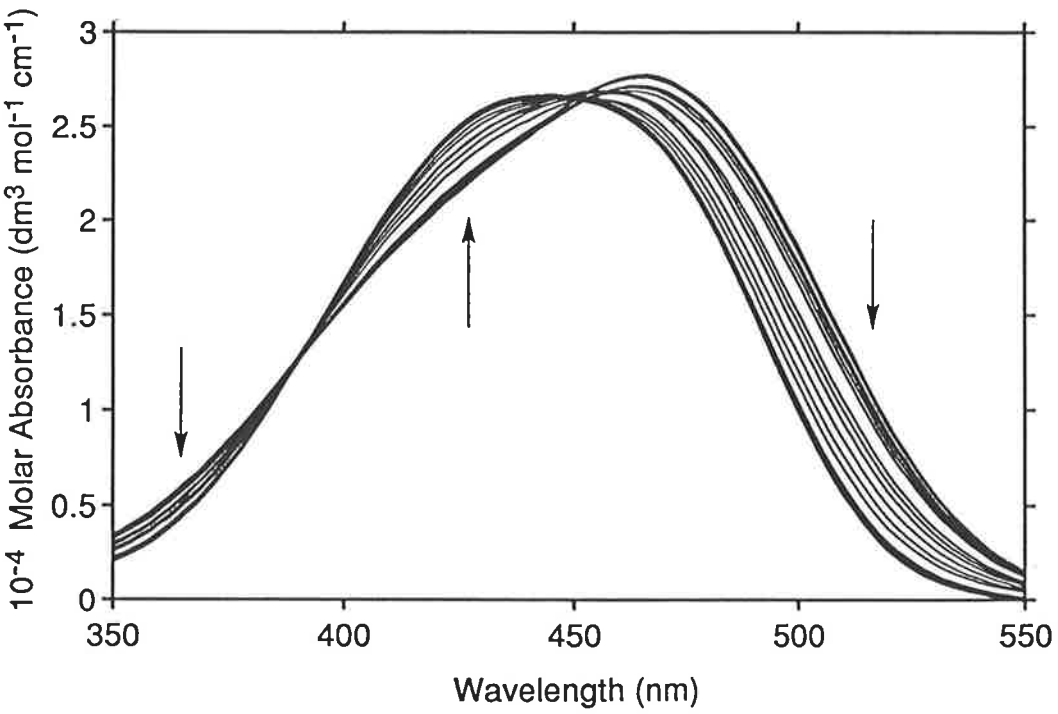

Figure 4.3 *Absorption spectrum of MO^- (3.8×10^{-5} mol dm^{-3}) alone and in the presence of increasing concentrations of $(\beta CD)_2Ur$ (ranging from 1.81×10^{-6} to 2.66×10^{-4} mol dm^{-3}) in aqueous solution at pH 9.0 and 298.2 K. The arrows show the direction of intensity change upon increasing $(\beta CD)_2Ur$ concentration.*

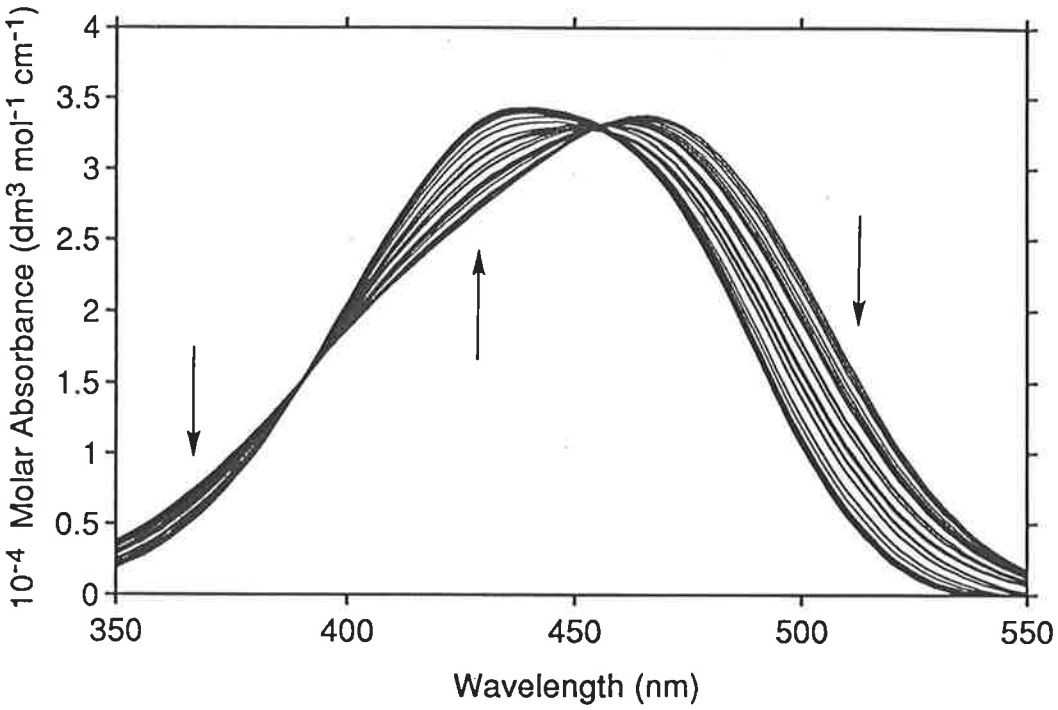

Figure 4.4 *Absorption spectrum of MO (4.0×10^{-5} mol dm^{-3}) alone and in the presence of increasing concentrations of $(\beta CD)_2Ox$ (ranging from 2.80×10^{-6} - 1.00×10^{-2} mol dm^{-3}) in aqueous solution at pH 9.0 and 298.2 K. The arrows show the direction of intensity change upon increasing $(\beta CD)_2Ox$ concentration.*

The isosbestic points observed at 390, 390 and 388 nm in the spectrum of MO^- upon addition of $(\beta CD)_2Ur$, $(\beta CD)_2Ox$ and $(\beta CD)_2Sc$, respectively, are all at slightly lower wavelengths than the isosbestic point observed at 396 nm in the presence of βCD. Crossover points, which shift from 448 to 454, 453 to 457 and 451 to 453 nm with increasing concentrations of $(\beta CD)_2Ur$, $(\beta CD)_2Ox$ and $(\beta CD)_2Sc$, respectively, are also apparent. An isosbestic point implies the presence of two dominant MO^- absorbing species, since the probability of three species absorbing equally at the same wavelength is low. The shift in crossover point may arise either from the presence of another complex species, besides $(\beta CD)_2X{\cdot}MO^-$, or from experimental error. In the case of βCD, the two dominant absorbing species are $\beta CD{\cdot}MO^-$ and MO^- (Section 4.2.2), and the small spectral

change in the 454 nm region has been attributed to a small amount of at least one other complex, probably $(\beta CD)_2 \cdot MO^-$ or $\beta CD \cdot (MO)_2^{2-}$, forming.

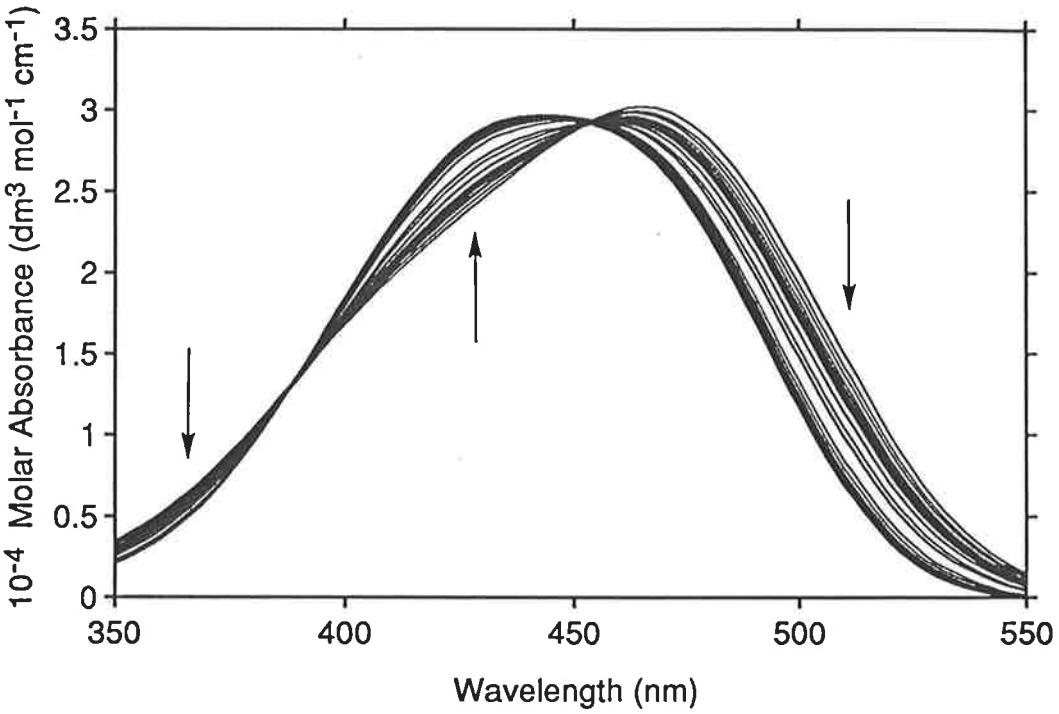

Figure 4.5 *Absorption spectrum of MO^- (4.0×10^{-5} mol dm^{-3}) alone and in the presence of increasing concentrations of $(\beta CD)_2 Sc$ (ranging from 8.12×10^{-6} - 8.01×10^{-3} mol dm^{-3}) in aqueous solution at pH 9.0 and 298.2 K. The arrows show the direction of intensity change upon increasing $(\beta CD)_2 Sc$ concentration.*

In each case the spectral variation was successfully fitted to the algorithm arising from the equilibrium shown in Eqn. 4.3, where $(\beta CD)_2 X$ denotes the linked cyclodextrin dimer host. The values obtained for K_1, by simultaneously fitting the data at wavelengths where significant spectral change occurs (see footnote Table 4.2), are listed in Table 4.2. The data were fitted using a non-linear least-squares routine (Section 6.2.5). Due to the errors involved in spectral measurement and solution preparation, the actual errors on the stability constants are greater than the non-weighted standard deviations quoted (but they

are unlikely to exceed the non-weighted standard deviation by a factor of two in these MO^- systems).

$$(\beta CD)_2X + MO^- \overset{K_1}{\rightleftharpoons} (\beta CD)_2X{\cdot}MO^- \qquad (4.3)$$

The binding curves for the complexation of MO^- by $(\beta CD)_2Ur$, $(\beta CD)_2Ox$ and $(\beta CD)_2Sc$ at one selected wavelength, 500 nm, together with the calculated curves obtained from the best fit of the absorbance data to the algorithm arising from the equilibrium given in Eqn. 4.3, are shown in Figs. 4.6 and 4.7.

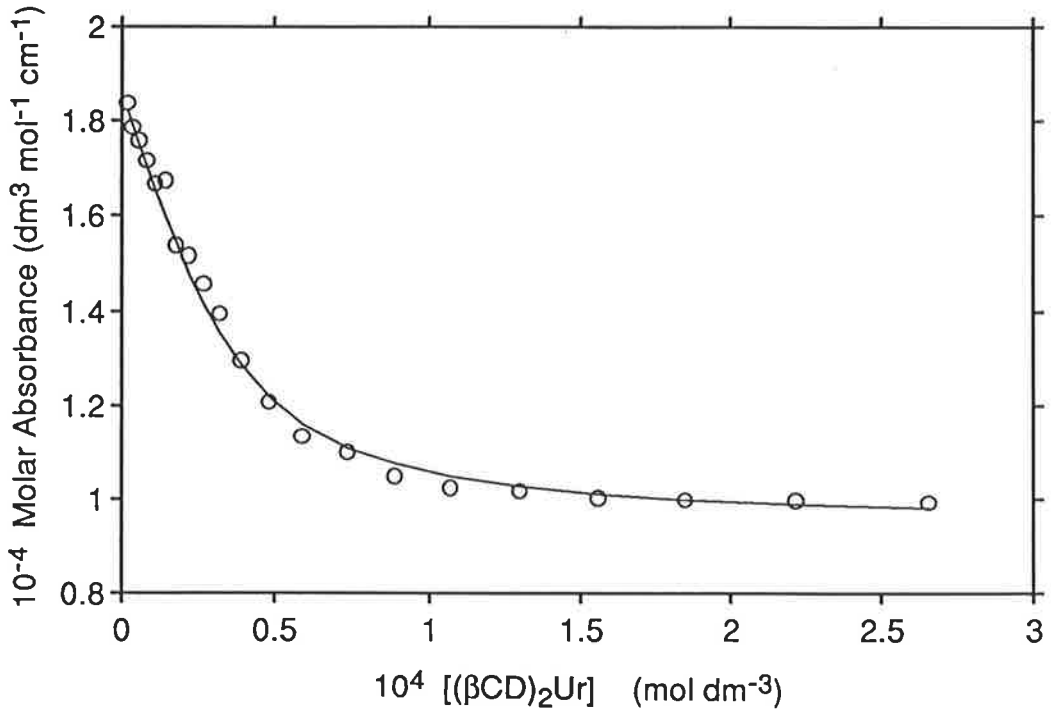

Figure 4.6 *Absorption of MO^- (3.8×10^{-5} mol dm^{-3}) at 500 nm in the presence of increasing concentrations of $(\beta CD)_2Ur$ (ranging from 1.81×10^{-6} to 2.66×10^{-4} mol dm^{-3}) in aqueous solution at pH 9.0 and 298.2 K. The circles represent data points and the solid line represents the best fit to the algorithm arising from the equilibrium shown in Eqn. 4.3.*

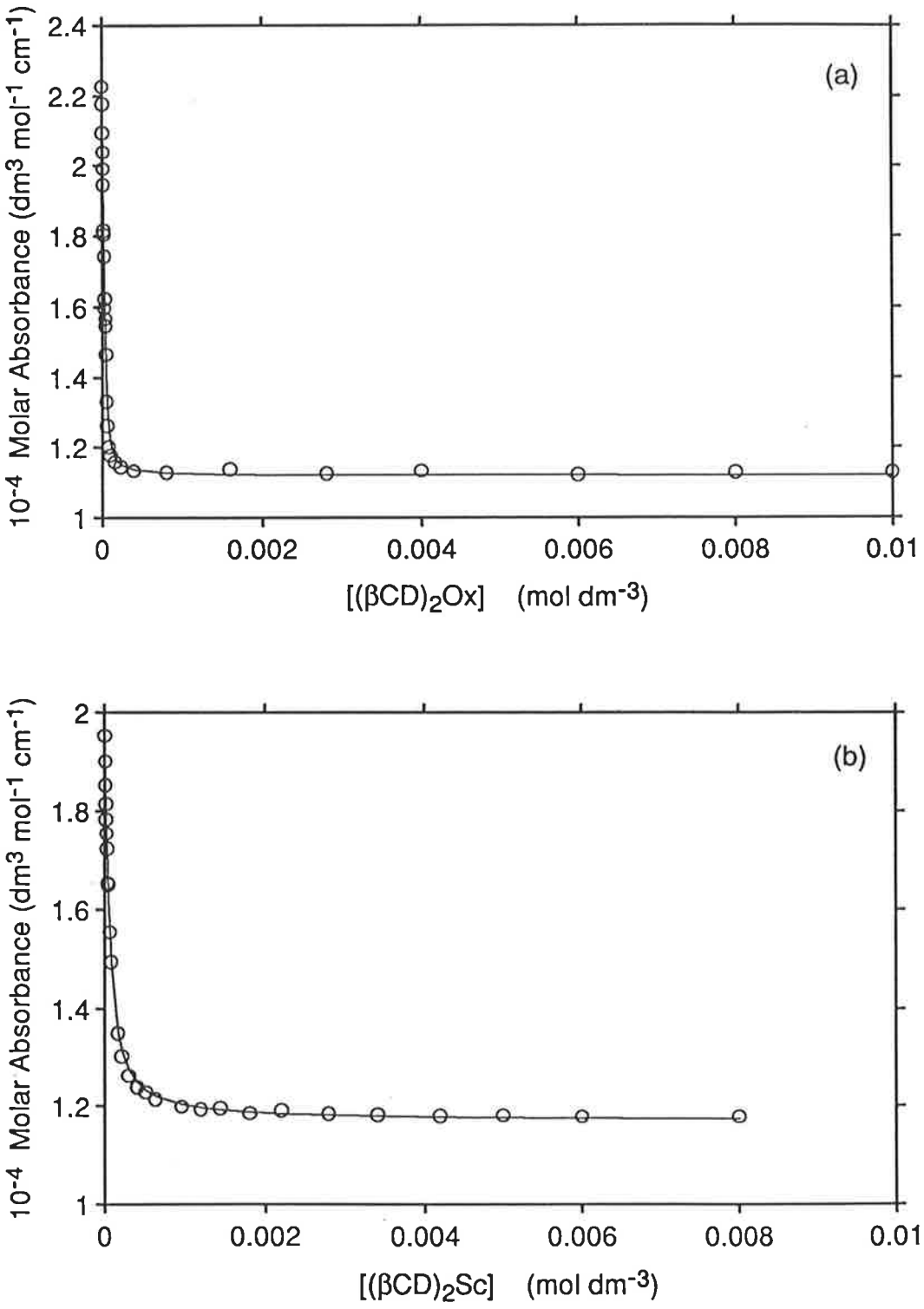

Figure 4.7 *Absorption of MO^- (4.0×10^{-5} mol dm^{-3}) at 500 nm in the presence of increasing concentrations of (a) $(\beta CD)_2Ox$ (ranging from 2.80×10^{-6} - 1.00×10^{-2} mol dm^{-3}) and (b) $(\beta CD)_2Sc$ (ranging from 8.12×10^{-6} - 8.01×10^{-3} mol dm^{-3}), in aqueous solution at pH 9.0 and 298.2 K. The circles represent data points and the solid line represents the best fit to the algorithm arising from the equilibrium shown in Eqn. 4.3.*

Table 4.2 *Stability constants for βCD·MO⁻ and (βCD)₂X·MO⁻ (X = Ur, Ox, Sc) in aqueous solution at pH 9.0 and 298.2 K.*[a]

Host	K_1 ($dm^3\ mol^{-1}$)	SSD[b]
βCD[c]	$(2.16 \pm 0.90) \times 10^3$	—
$(\beta CD)_2Ur$[d]	$(1.05 \pm 0.04) \times 10^5$	5.0×10^3
$(\beta CD)_2Ox$[e]	$(1.92 \pm 0.04) \times 10^5$	5.0×10^3
$(\beta CD)_2Sc$[f]	$(2.50 \pm 0.02) \times 10^4$	1.2×10^3

[a] Determined by fitting the variation in MO^- absorbance with increasing cyclodextrin concentration at 2 nm intervals over the wavelength ranges 408-540 nm,[c] 410-440 and 464-520 nm,[d] 404-446 and 464-520 nm,[e] or 404-444 and 464-520 nm,[f] to the algorithm arising from the equilibrium shown in Eqn. 4.1,[c] or Eqn. 4.3,[d,e,f] using a non-linear least-squares routine. Errors quoted represent non-weighted standard deviations. The concentration of MO^- was fixed at 4×10^{-5} mol dm^{-3},[c] 3.8×10^{-5} mol dm^{-3},[d] or 4.0×10^{-5} mol dm^{-3}.[e,f] The ranges of variation in cyclodextrin concentration for each system were (mol dm^{-3}): βCD (7.5×10^{-5} - 1.2×10^{-2}), $(\beta CD)_2Ur$ (1.81×10^{-6} - 2.66×10^{-4}), $(\beta CD)_2Ox$ (2.80×10^{-6} - 1.00×10^{-2}), and $(\beta CD)_2Sc$ (8.12×10^{-6} - 8.01×10^{-3}). All solutions were prepared in 0.100 mol dm^{-3} Na_2HPO_4 and 0.200 mol dm^{-3} K_2SO_4, adjusted to pH 9.0 with NaOH. [b] Sum of squared deviations. [c] Ref. 2 (Section 4.2.2).

Complex stability increases in the order $\beta CD \cdot MO^- < (\beta CD)_2Sc \cdot MO^- < (\beta CD)_2Ur \cdot MO^- < (\beta CD)_2Ox \cdot MO^-$. If each βCD annulus of $(\beta CD)_2X$ behaves as a separate entity in complexing MO^-, the $(\beta CD)_2X \cdot MO^-$ (X = Ur, Ox, Sc) complex stability constants are expected to be double that of $\beta CD \cdot MO^-$, on statistical grounds. However, the stability constants of $(\beta CD)_2X \cdot MO^-$ (X = Ur, Ox, Sc) are 11 to 88-fold greater than that of $\beta CD \cdot MO^-$ (Table 4.2), indicating that cooperative binding is occurring between the two βCD hydrophobic recognition sites of the linked cyclodextrin dimers.

In the $(\beta CD)_2X \cdot MO^-$ complexes, the aromatic portions of MO^- are likely to maximise their contact with the hydrophobic βCD cavities, and the functional groups of MO^- may be involved in hydrogen bonding interactions with the hydroxyl groups of the βCD annuli and the amide groups of the tether. The relative stabilities of the three linked cyclodextrin dimer complexes imply that these interactions are optimised by the tether

length of $(\beta CD)_2Ox$, which probably allows alignment of the interacting groups. Interestingly, $(\beta CD)_2Ox$ is the only linked cyclodextrin dimer studied which possesses conjugation in the tether, and hence, formation of a more rigid complex is anticipated.

The $(\beta CD)_2X{\cdot}MO^-$ (X = Ur, Ox, Sc) stability constants in Table 4.2, and the directly determined molar absorbances of MO^- and $(\beta CD)_2X$ (X = Ur, Ox, Sc), are used to derive the molar absorbances of the $(\beta CD)_2X{\cdot}MO^-$ (X = Ur, Ox, Sc) complexes formed. These molar absorbances are shown in Figs. 4.8, 4.9 and 4.10 for $(\beta CD)_2Ur{\cdot}MO^-$, $(\beta CD)_2Ox{\cdot}MO^-$ and $(\beta CD)_2Sc{\cdot}MO^-$, respectively, along with the molar absorbance of MO^- itself.

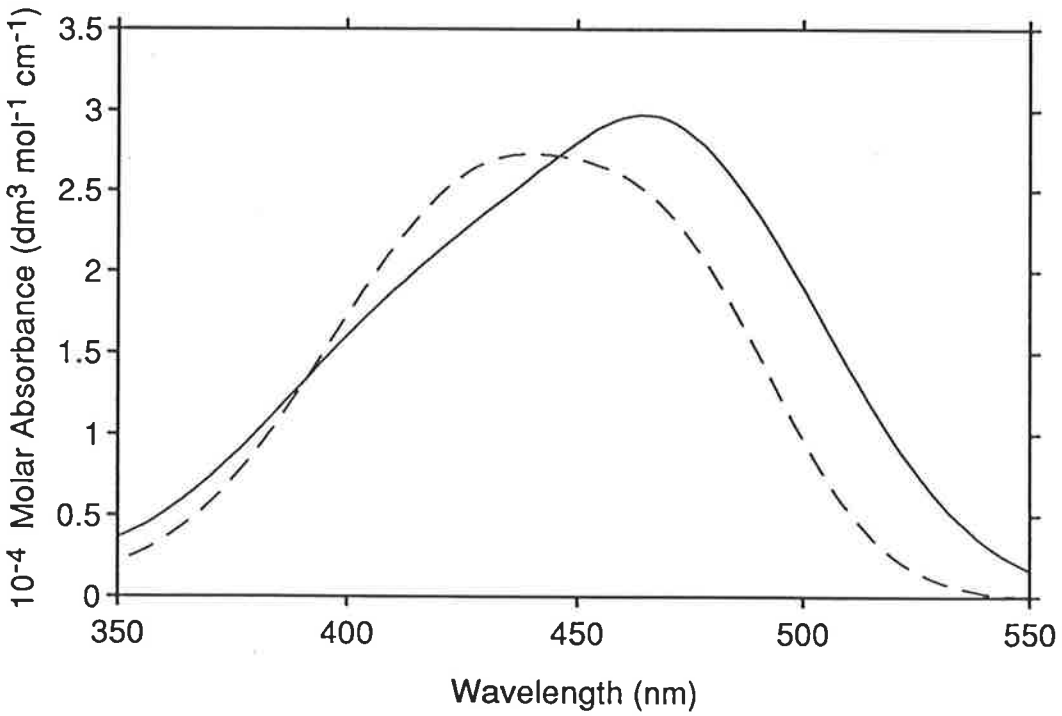

Figure 4.8 *Molar absorbance of MO^- (——) and $(\beta CD)_2Ur{\cdot}MO^-$ (– – –) in aqueous solution at pH 9.0 and 298.2 K. The $(\beta CD)_2Ur{\cdot}MO^-$ spectrum was derived from the best fit of the data in Fig. 4.3, within the wavelength ranges 410-440 and 464-520 nm, to the algorithm arising from the equilibrium shown in Eqn. 4.3.*

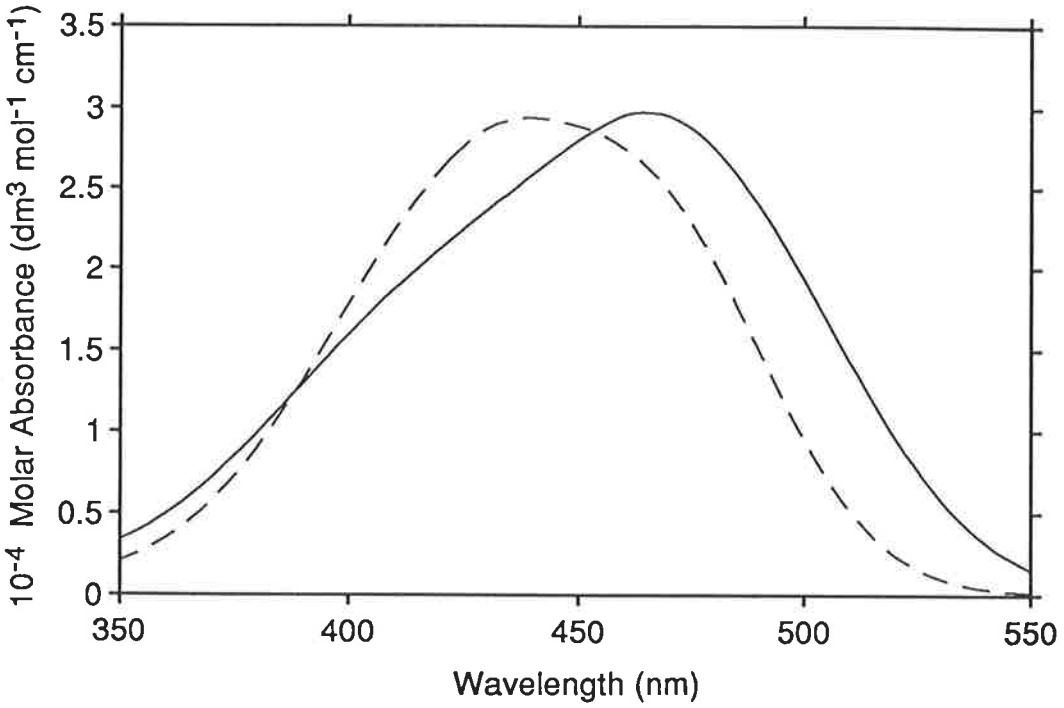

Figure 4.9 *Molar absorbance of MO^- (——) and $(\beta CD)_2Ox{\cdot}MO^-$ (– – –) in aqueous solution at pH 9.0 and 298.2 K. The $(\beta CD)_2Ox{\cdot}MO^-$ spectrum was derived from the best fit of the data in Fig. 4.4, within the wavelength ranges 404-446 and 464-520 nm, to the algorithm arising from the equilibrium shown in Eqn. 4.3.*

In the absence of cyclodextrin, MO^- exhibits an absorption maximum at 464 nm, whereas, upon addition of cyclodextrin a blue shift in the MO^- absorption spectrum is observed. The $(\beta CD)_2Ur{\cdot}MO^-$, $(\beta CD)_2Ox{\cdot}MO^-$ and $(\beta CD)_2Sc{\cdot}MO^-$ complexes exhibit absorbance maxima at 438, 438 and 444 nm, respectively, which are all more blue shifted than the absorbance maximum of $\beta CD{\cdot}MO^-$ at 454 nm (Section 4.2.2). The greater blue shift detected for $(\beta CD)_2Ur{\cdot}MO^-$ and $(\beta CD)_2Ox{\cdot}MO^-$, is coincident with their greater stability, by comparison with that of $(\beta CD)_2Sc{\cdot}MO^-$. The intensity of MO^- absorption in the $(\beta CD)_2X{\cdot}MO^-$ (X = Ur, Ox, Sc) complexes is similar or slightly less than that in the free state, however, the shape of the spectra are significantly different. The derived spectra of $(\beta CD)_2Ox{\cdot}MO^-$ and $(\beta CD)_2Sc{\cdot}MO^-$ are more similar in intensity than that of

$(\beta CD)_2Ur{\cdot}MO^-$. As mentioned in Section 4.2.1, the spectral band may be attributed to the superposition of spectra arising from a hydrogen-bonded and a non-hydrogen-bonded species in equilibrium. Hence, the observed blue shift may correspond to an increase in the amount of non-hydrogen-bonded species. This is consistent with the greater blue shift observed in the presence of linked cyclodextrin dimers, compared with βCD, as they can potentially encapsulate the guest in their hydrophobic cavities, resulting in a more extensive reduction in the interactions with water. The spectral changes are unlikely to arise from an increase in MO^- dimer concentration, as at most only small amounts of the dimeric MO^- complexes, $(\beta CD)_2X{\cdot}(MO)_2^{2-}$ (X = Ur, Ox, Sc), appear to be present, as discussed below.

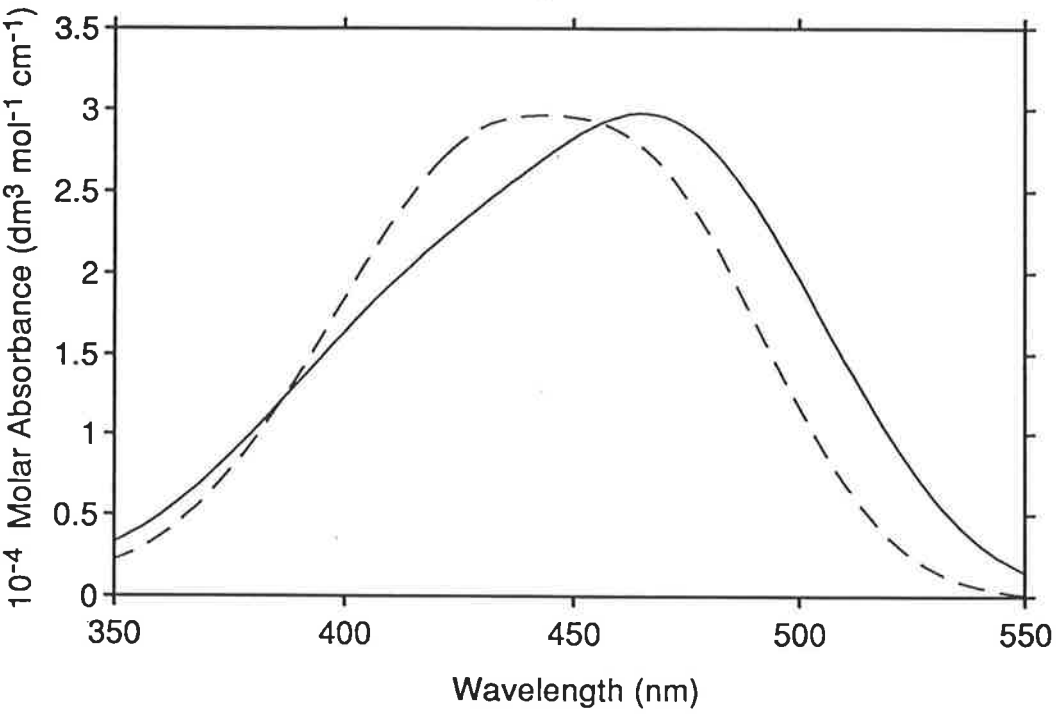

Figure 4.10 *Molar absorbance of MO^- (——) and $(\beta CD)_2Sc{\cdot}MO^-$ (– – –) in aqueous solution at pH 9.0 and 298.2 K. The $(\beta CD)_2Sc{\cdot}MO^-$ spectrum was derived from the best fit of the data in Fig. 4.5, within the wavelength ranges 404-444 and 464-520 nm, to the algorithm arising from the equilibrium shown in Eqn. 4.3.*

Although the experimental data were successfully fitted to the algorithm arising from the equilibrium shown in Eqn. 4.3, they could also be fitted to the algorithm arising from the equilibria shown in Eqn. 4.4, where $(\beta CD)_2X$ denotes the linked cyclodextrin dimer host. The values obtained for K_1 and K_2, by simultaneously fitting the data at wavelengths where significant spectral change occurs (see footnote Table 4.2), are listed in Table 4.3, and good visual fits were generated.

$$(\beta CD)_2X + MO^- \overset{K_1}{\rightleftharpoons} (\beta CD)_2X{\cdot}MO^-$$

$$(\beta CD)_2X{\cdot}MO^- + MO^- \overset{K_2}{\rightleftharpoons} (\beta CD)_2X{\cdot}(MO)_2^{2-} \qquad (4.4)$$

Table 4.3 *Stability constants for $\beta CD{\cdot}MO^-$, $(\beta CD)_2X{\cdot}MO^-$ and $(\beta CD)_2X{\cdot}(MO)_2^{2-}$ (X = Ur, Ox, Sc) in aqueous solution at pH 9.0 and 298.2 K.*[a]

Host	K_1 ($dm^3\ mol^{-1}$)	K_2 ($dm^3\ mol^{-1}$)	SSD[b]
βCD[c]	$(2.16 \pm 0.90) \times 10^3$	—	—
$(\beta CD)_2Ur$	$(1.5 \pm 0.2) \times 10^5$	$(2 \pm 5) \times 10^3$	3.2×10^3
$(\beta CD)_2Ox$	$(2.4 \pm 0.3) \times 10^5$	$(9 \pm 31) \times 10^2$	3.3×10^3
$(\beta CD)_2Sc$	$(4.6 \pm 0.2) \times 10^4$	$(8 \pm 2) \times 10^3$	6.5×10^2

[a] As for Table 4.2, except data were fitted to the algorithm arising from the equilibria shown in Eqn. 4.4 for the $(\beta CD)_2X$ systems. [b] Sum of squared deviations. [c] Ref. 2 (Section 4.2.2).

The sum of squared deviations (SSD) listed in Table 4.3 are decreased, relative to those listed in Table 4.2, however, this decrease is of the size which can be attributed to the introduction of an additional fitting parameter. Although the values of K_1 listed in Table 4.3 are significantly greater than the corresponding K_1 values listed in Table 4.2, the same order of stabilities is observed. Interestingly, the errors on K_1 increase notably upon

incorporation of the additional species, $(\beta CD)_2X\cdot(MO)_2^{2-}$, into the fitting. Nevertheless, the spectra derived for the $(\beta CD)_2X\cdot MO^-$ species (X = Ur, Ox, Sc) are independent of the fitting model (either Eqn. 4.3 or 4.4) used to derive them.

As expected from statistical and entropy factors, K_1 is greater than K_2. No significant difference is detected between the values of K_2 for $(\beta CD)_2X\cdot(MO)_2^{2-}$ (X = Ur, Ox, Sc), due to their large errors. The spectra derived for $(\beta CD)_2Ur\cdot(MO)_2^{2-}$ and $(\beta CD)_2Ox\cdot(MO)_2^{2-}$ are physically unrealistic, having negative intensities within their spectral envelopes. If a low concentration of $(\beta CD)_2X\cdot(MO)_2^{2-}$ (X = Ur, Ox, Sc) exists over the concentration range used, this may prevent a meaningful determination of the species spectra.

The derived stability constants, K_1 and K_2 (Table 4.3), can be used to calculate the percentages of MO^-, $(\beta CD)_2X\cdot MO^-$ and $(\beta CD)_2X\cdot(MO)_2^{2-}$ (X = Ur, Ox, Sc) present under the conditions used in this study. Over the concentration ranges used (Section 6.2.2), the maximal percentages of total MO^- present in the free form are 95.7, 93.5 and 83.7%, and in the $(\beta CD)_2X\cdot MO^-$ form are 96.8, 100.0 and 99.6%, and in the $(\beta CD)_2X\cdot(MO)_2^{2-}$ form are 0.6, 0.4 and 5.7%, for the $(\beta CD)_2Ur$, $(\beta CD)_2Ox$ and $(\beta CD)_2Sc$ systems, respectively. The high uncertainties in K_2 for the $(\beta CD)_2Ur$ and $(\beta CD)_2Ox$ systems, and the physically unacceptable spectra derived for $(\beta CD)_2Ur\cdot(MO)_2^{2-}$ and $(\beta CD)_2Ox\cdot(MO)_2^{2-}$, may arise from the presence of only small amounts of the $(\beta CD)_2X\cdot(MO)_2^{2-}$ complexes (X = Ur, Ox), under these conditions, prohibiting good fits of the spectral data. The low percentages of $(\beta CD)_2X\cdot(MO)_2^{2-}$ (X = Ur, Ox, Sc) are consistent with the presence of two dominant absorbing species, MO^- and $(\beta CD)_2X\cdot MO^-$ (X = Ur, Ox, Sc).

For a number of reasons, the model outlined in Eqn. 4.4 is improbable. Firstly, the presence of at least one isosbestic point in all three systems implies the presence of two absorbing species. Secondly, the change in the sum of squared deviations associated with the fit and the increase in error on K_1, indicate that, for all three systems studied, no significant improvement in the data fit is achieved upon incorporation of the additional fitting parameter. Thirdly, the errors on K_2 exceed the values themselves for the

$(\beta CD)_2Ur$ and $(\beta CD)_2Ox$ systems, and the derived spectra for $(\beta CD)_2X{\cdot}(MO)_2^{2-}$ (X = Ur, Ox) are physically unrealistic. However, the formation of $(\beta CD)_2X{\cdot}(MO)_2^{2-}$ (X = Ur, Ox, Sc) as a minor species cannot be completely ruled out.

No evidence of $((\beta CD)_2X)_2{\cdot}MO^-$ (X = Ur, Ox, Sc) complex formation was detected, probably due to the lower host to guest concentration ratios used for these measurements compared with those in the $(\beta CD)_2Ur/TNS^-$ system (Section 3.4.1).

The spectral variations and derived stability constants for all three systems are consistent with the presence of two dominant species, MO^- and $(\beta CD)_2X{\cdot}MO^-$ (X = Ur, Ox, Sc), over the concentration ranges studied, and possibly also a minor species, $(\beta CD)_2X{\cdot}(MO)_2^{2-}$. The cooperative binding exhibited in all cases implies that in the $(\beta CD)_2X{\cdot}MO^-$ complex hydrophobic interactions are enhanced by the inclusion of each aromatic moiety within a βCD cavity of the linked cyclodextrin dimer (Fig. 5.1(c)). The dimethylaniline group of MO^- may pass through the wider end of the βCD annulus, as proposed for the formation of $\beta CD{\cdot}MO^-$ (Section 4.2.2), and become included through the primary end of the second βCD cavity. Hydrogen bonding interactions between MO^- and the hydroxyl groups of the cyclodextrins and the amide groups of the tether, may also occur.

Cooperative binding of MO^- by a number of linked cyclodextrin dimers is also reported in the literature.[14,19,37,38] ^1H and ^{13}C NMR measurements on the inclusion complex formed between MO^- and 3,5-di(thiomethyl)pyridine-2°,2°-linked-βCD (Appendix, (11)) (nomenclature defined in Section 3.1), imply that each aromatic component of MO^- is encapsulated within a βCD component of the linked cyclodextrin dimer host.[37]

The implications of a change in guest structure (to the more bulky TR^- molecule) on the binding properties of βCD, $(\beta CD)_2Ur$, $(\beta CD)_2Ox$ and $(\beta CD)_2Sc$, are now discussed, after initial consideration is given to the origin of the TR^- absorbance bands.

4.3 Complexation of Tropaeolin 000 No. 2

4.3.1 Properties of the Tropaeolin Anion

The hydroxyl group of tropaeolin is considerably less acidic (pK_a = 11.4) than the hydroxyl groups of either the structural isomer of TR^- in which the hydroxyl group is *para* to the azo group, *p*-(4-hydroxy-1-naphthylazo)benzenesulfonate (Appendix, (33)), (pK_a = 8.2) or 2-naphthol (Appendix, (35)), (pK_a = 9.9).[9] This is due to intramolecular hydrogen bonding between the hydroxyl group and the β-nitrogen of the azo group. The results presented in the following sections correspond to the tropaeolin monoanion, TR^-. The ultraviolet-visible spectrum of tropaeolin is invariant in water within the pH range 2.0-6.0, which indicates that no significant shifts in protonic equilibria occur under these conditions.[39,40]

A tautomeric equilibrium exists between the azo and hydrazone forms of TR^-, as shown in Fig. 4.1.[9] The position of the equilibrium seems to depend on the polarity of the solvent, with the hydrazone form predominating in aqueous solution and the azo form predominating in apolar solutions or microenvironments.[15,41] The hydrazone form stabilises the *trans* form of the azo group.[40] In aqueous solution tropaeolin is known to aggregate, with a resultant decrease in absorption.[42] However, at the dye concentration used in this study (3.7-4.1 x 10^{-5} mol dm^{-3}) any deviations from Beer's Law are negligible. The stability constant for the TR^- dimer is 9.10 x 10^2 dm^3 mol^{-1}.[39]

The linear dichroism of tropaeolin in stretched films,[39,43] in the range 400-550 nm, shows that the absorbance parallel to the direction of stretch is approximately double that perpendicular to the direction of stretch, and the dichroic ratio is relatively constant. These results indicate that the absorption bands in this range are polarised approximately along a line interconnecting the sulfonate group and the more distant ring of the naphthyl residue. The spectrum of tropaeolin in the range 400-550 nm may arise from either

different electronic transitions or a vibronic progression of a single electronic transition. The linear dichroism results do not allow one to distinguish between these possibilities.[39]

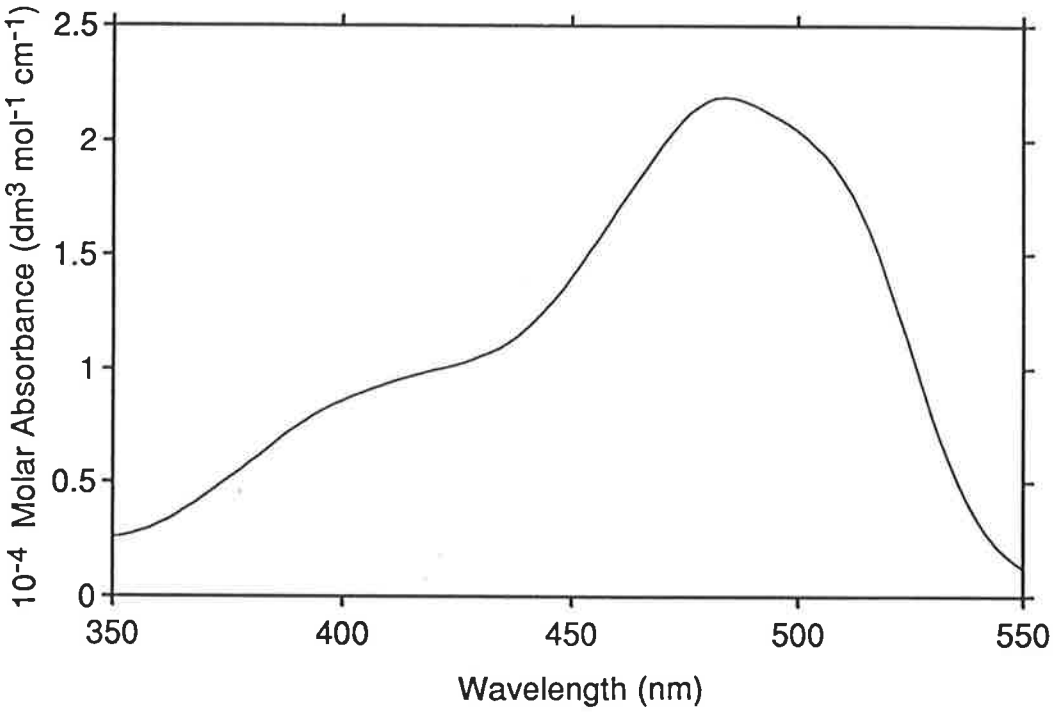

Figure 4.11 *Absorbance spectrum of TR^- (3.7×10^{-5} mol dm^{-3}) in aqueous solution at pH 5.5 and 298.2 K.*

The absorbance in the visible region of the spectrum (Fig. 4.11) has been attributed to the $\pi \rightarrow \pi^*$ transition of the azo group (see Section 4.2.1).[40] The band at 484 nm is usually associated with the hydrazone tautomer[44] and has been assigned to an intramolecular charge-transfer transition directed along the longest conjugated chain in the molecule.[40,43] The shoulder at 420-430 nm is usually associated with the azo form of the dye.[43,44] Although the shoulder at 514 nm has been proposed to arise from the double anion form,[43] it is still apparent at pH 5.5 (Fig. 4.11), where the double anion form is unlikely to be present. This implies that, rather, the shoulder may be part of a vibronic progression. Bands in the ultraviolet region have been attributed to locally excited

transitions of the naphthyl moiety.[43] However, there is still some uncertainty as to the origin of the TR^- absorbance bands.

4.3.2 Complexation of Tropaeolin by βCD

The complexation of TR^- by βCD has been studied by the temperature-jump relaxation method. The kinetics are consistent with dimerisation of the dye within the βCD cavity as outlined in Eqn. 4.5, yielding values of $(7.1 \pm 0.7) \times 10^2$ and $(4 \pm 7) \times 10^6$ $dm^3\ mol^{-1}$ for K_1 and K_2, respectively.[39] The high error associated with K_2 probably arises from the presence of only small amounts of the $\beta CD \cdot (TR)_2^{2-}$ complex, under the conditions used, leading to greater uncertainty.

$$\beta CD + TR^- \overset{K_1}{\rightleftharpoons} \beta CD \cdot TR^-$$

$$\beta CD \cdot TR^- + TR^- \overset{K_2}{\rightleftharpoons} \beta CD \cdot (TR)_2^{2-} \qquad (4.5)$$

Although the linear dichroism of TR^- suggests that the absorption bands in the range 400-550 nm are polarised approximately along the long axis of the molecule,[39,43] the circular dichroic spectrum induced by βCD exhibits both positive and negative signals in that range. This is consistent with dimer formation within the βCD cavity, resulting in the splitting of each monomer absorption band into two bands with mutually perpendicular transition moments due to exciton interactions.

The absorbance spectrum of TR^- shows a red shift from 484 to 487 nm and a decrease in intensity in the region 380-520 nm upon addition of βCD.[2] An isosbestic point is also apparent at 529 nm, suggesting the predominance of two absorbing species, TR^- and $\beta CD \cdot (TR)_2^{2-}$.[39] A decrease in intensity of the 484 nm band is expected from the decrease in intramolecular charge-transfer transition when TR^- moves from the highly polar solvent, which stabilises the charge-transfer state, into the hydrophobic βCD cavity. A similar decrease in absorbance is also observed upon dimerisation of TR^- in the absence

of βCD,[39] as mentioned in Section 4.3.1. If a change in the environmental polarity of the hydroxyl group is encountered upon inclusion, a shift in the tautomeric equilibrium and concomitant spectral change is expected. This is consistent with the colour change from yellow (hydrazone) to orange (azo) observed upon addition of βCD to a solution of TR^-. However, the decrease in intensity of the 420-430 nm shoulder, attributed to the azo form, in addition to that of the 484 nm band, attributed to the hydrazone form, indicates that other effects are also operating.

Absorbance measurements have previously been made under experimental conditions identical to those used in the following linked cyclodextrin dimer studies, thus allowing comparisons to be made between the systems. The absorbance data for the βCD/TR^- system could not be fitted to the model proposed from the temperature-jump results. This situation may arise if one of the three TR^- species does not contribute significantly to the absorption spectrum. For instance one of the species may exist in negligible concentrations across the entire cyclodextrin concentration range or two of the species may have indistinguishable spectra. However, the data were fitted to a one-step model for formation of βCD·$(TR)_2^{2-}$, as outlined in Eqn. 4.6. An overall stability constant of $(2.03 \pm 0.21) \times 10^7$ dm^6 mol^{-2}, for K_{12}, was obtained by averaging the stability constants calculated at 2 nm intervals in the range 440-500 nm.[2,39]

$$\beta CD + 2\ TR^- \overset{K_{12}}{\rightleftharpoons} \beta CD\cdot(TR)_2^{2-} \qquad (4.6)$$

The larger cavity size of γCD, permits formation of a (γCD)$_2$·$(TR)_2^{2-}$ complex. Stepwise stability constants of 4.18×10^2, 1.68×10^6 and 1.77×10^2 dm^3 mol^{-1}, for γCD·TR^-, γCD·$(TR)_2^{2-}$ and (γCD)$_2$·$(TR)_2^{2-}$, respectively, have been determined by temperature-jump relaxation.[39] Equilibrium ultraviolet-visible spectra and circular and linear dichroic spectra suggest a different orientation and penetration of the $(TR)_2^{2-}$ dimer in the βCD·$(TR)_2^{2-}$ and γCD·$(TR)_2^{2-}$ complexes.[39] The naphthalene group of TR^- is too large for inclusion within the αCD cavity. Despite the compatible sizes of the

phenylsulfonate end of TR^- and the αCD cavity, no complex formation is detected by temperature-jump or spectral methods.[2,39]

The cavity of βCD is capable of including two phenyl residues or a phenyl and a naphthyl residue, but not two naphthyl residues.[1] A closely related guest, roccellin (Appendix, (36)), contains two naphthyl groups and forms only a βCD·(roccellin) complex with βCD, $K = 7.20 \times 10^2$ dm^3 mol^{-1}.[45] Preferential encapsulation of the naphthol moiety is suggested by the similarity in binding constants of TR^- and roccellin with βCD. The inclusion of TR^- from the phenylsulfonate end is ruled out by ^{1}H NMR data,[46] indicating that the uncharged naphthyl moiety of TR^- is preferentially included by the βCD cavity. Molecular models show that TR^-, unlike MO^-, is unable to pass through the βCD annulus. The induced circular dichroic spectrum of TR^- in an excess of βCD suggests that the long axis of the naphthyl moiety and the βCD C_7 symmetry axis are aligned upon inclusion.[40,46] Thus, the mode of inclusion of TR^- contrasts that of MO^-, which is included along the long molecular axis. The naphthyl group forms a tight fit in the βCD cavity with the unsubstituted phenyl ring being deeply embedded,[46] while the substituent in the 1-position of the other phenyl moiety, comprising the naphthyl group, permits only partial inclusion of this ring.

The naphthyl group of TR^- is substituted at the 1- and 2-positions (Fig. 4.1). Since inclusion of the long axis of a 1-substituted naphthalene inside the βCD cavity is sterically hindered by comparison with that of a 2-substituted derivative,[26] the stability of βCD·TR^- is expected to be similar to that of the βCD·(1-naphthol) complex (K = 124 dm^3 mol^{-1}) (1-naphthol, Appendix, (37)).[47] However, the stability of βCD·TR^- is greater than that of the βCD·(2-naphthol) complex (K = 556 dm^3 mol^{-1}) (2-naphthol, Appendix, (35)),[47] which may imply that the azo group at the 1-position of TR^- stabilises the βCD·TR^- complex. The isomer of TR^- with the hydroxyl group in the *para* position, *p*-(4-hydroxy-1-naphthylazo)benzenesulfonate (Appendix, (33)), forms an inclusion complex with βCD having a stability of 330-410 dm^3 mol^{-1}.[15,29] This implies that a hydroxyl group in the 1- or 4-position of a naphthyl ring destabilises the complex formed with βCD.

Inclusion of the first TR^- probably occurs from the wider secondary end of βCD. Molecular models show that although inclusion of the second TR^- can occur from either end of the βCD annulus, its depth of inclusion is probably not as great as that of the first TR^-. The structure of the $\beta CD \cdot (TR)_2^{2-}$ complex is proposed to contain one included TR^-, with the other antiparallel but displaced longitudinally and not inside the cavity.[39] The antiparallel arrangement is likely since minimal repulsion between the negatively charged sulfonate groups results. This structure implies that interactions between the dye molecules are primarily responsible for the high stability of the $\beta CD \cdot (TR)_2^{2-}$ complex. Circular dichroism measurements reveal a positive split Cotton effect, which is consistent with an angle of $> 90°$ between the transition moments of the two TR^- molecules.[40] It has been proposed that van der Waals attraction is the most important driving force for the host-guest interaction, and that hydrogen bonding is not significant.[40]

4.3.3 Complexation of Tropaeolin by Linked Cyclodextrin Dimers

Now that background knowledge on TR^- and its interactions with βCD have been established, the more complex linked cyclodextrin dimer systems are discussed. The variation in TR^- absorbance upon addition of the linked cyclodextrin dimers: $(\beta CD)_2Ur$, $(\beta CD)_2Ox$ and $(\beta CD)_2Sc$, can be seen in Figs. 4.12 and 4.13, respectively. All three systems have spectral changes similar to those observed upon addition of βCD, and are consistent with a change in the local environment of the chromophore upon encapsulation by the cyclodextrin.

The isosbestic points observed at 524, 512 and 526 nm in the spectrum of TR^- upon addition of $(\beta CD)_2Ur$, $(\beta CD)_2Ox$ and $(\beta CD)_2Sc$, respectively, are all at slightly lower wavelengths than the isosbestic point observed at 529 nm in the presence of βCD. The presence of an isosbestic point does not eliminate the possibility of more than two species, however, if more than two absorbing species exist in solution, the isosbestic point suggests the predominance of only two absorbing species.[39] This is because the probability of three species absorbing equally at the same wavelength to form an isosbestic

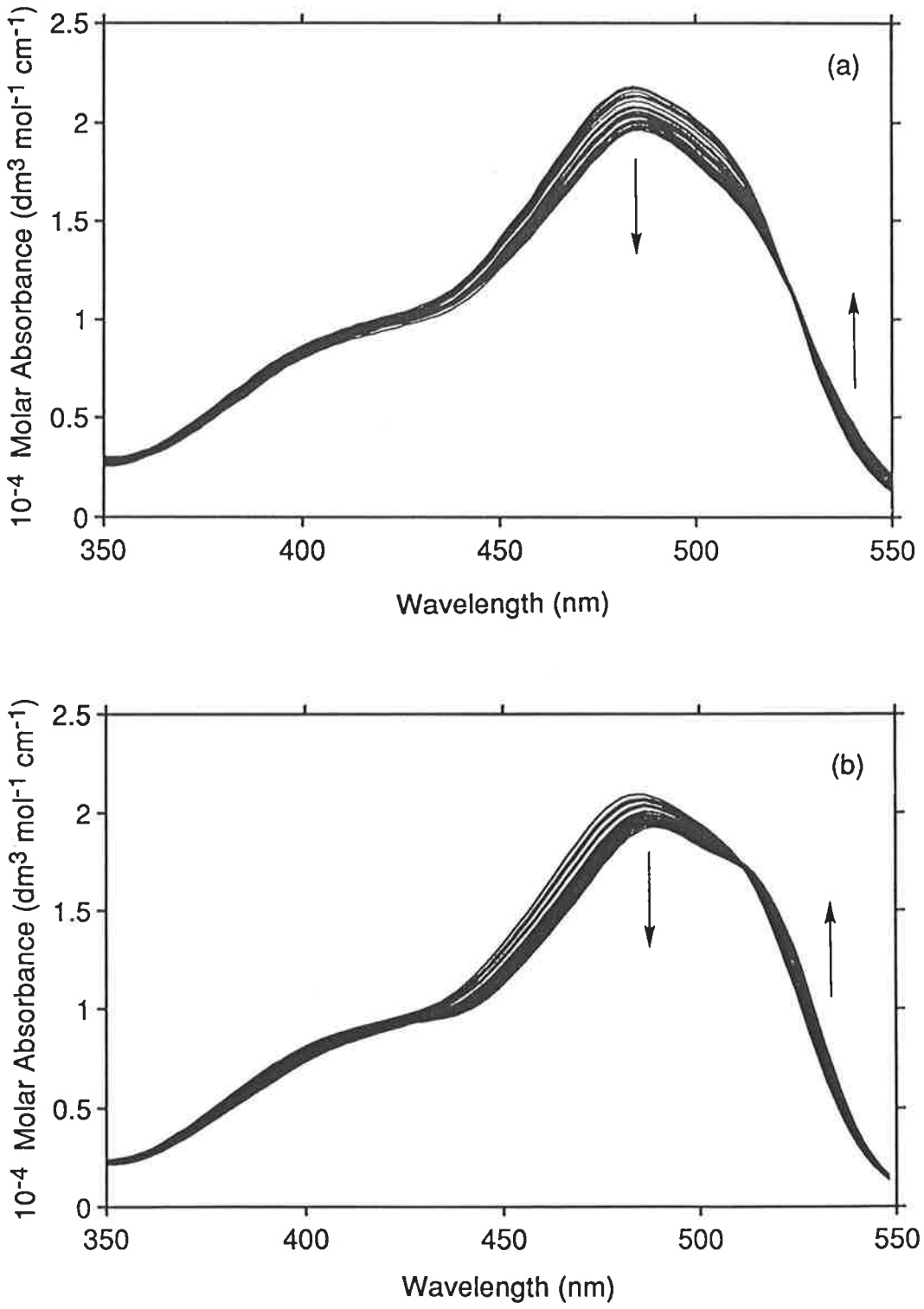

Figure 4.12 *Absorption spectrum of (a) TR^- (4.1×10^{-5} mol dm^{-3}) alone and in the presence of increasing concentrations of $(\beta CD)_2Ur$ (ranging from 3.86×10^{-6} - 3.73×10^{-4} mol dm^{-3}) and (b) TR^- (3.7×10^{-5} mol dm^{-3}) alone and in the presence of increasing concentrations of $(\beta CD)_2Ox$ (ranging from 9.47×10^{-6} - 3.20×10^{-3} mol dm^{-3}), in aqueous solution at pH 5.5 and 298.2 K. The arrows show the direction of intensity change upon increasing the concentration of linked cyclodextrin dimer.*

point is not high. Hence, the spectral variations of Figs. 4.12 and 4.13 are consistent with the presence of two dominant TR^- absorbing species. In the case of βCD, the two dominant absorbing species are $\beta CD{\cdot}(TR)_2^{2-}$ and TR^- (Section 4.3.2).

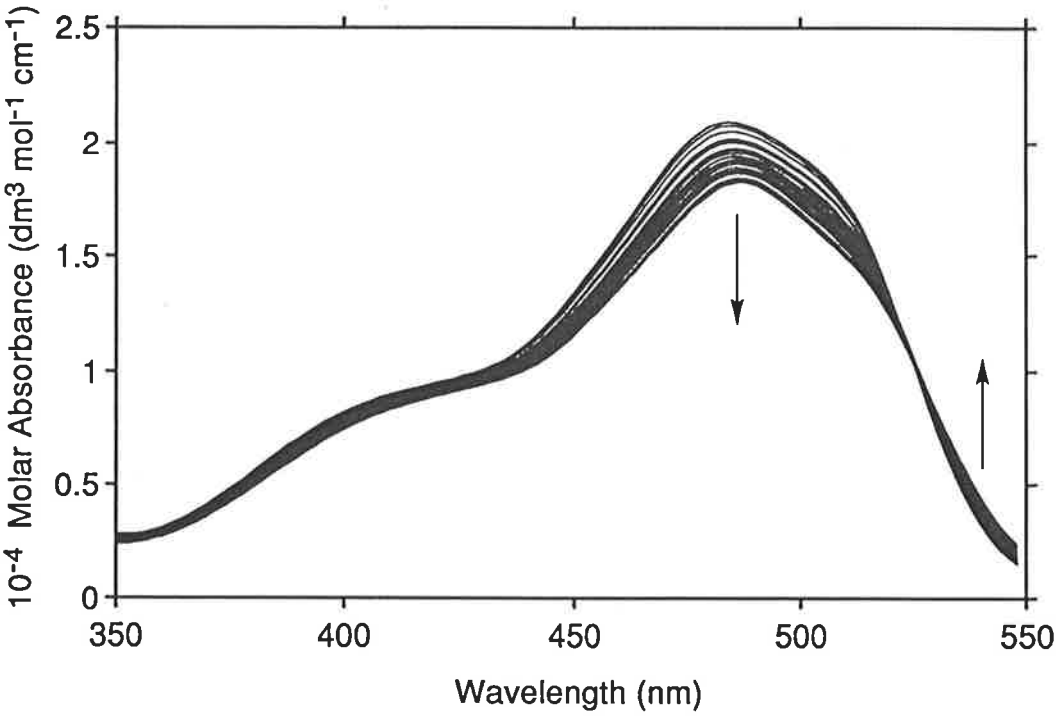

Figure 4.13 *Absorption spectrum of TR^- (4.0×10^{-5} mol dm^{-3}) alone and in the presence of increasing concentrations of $(\beta CD)_2Sc$ (ranging from 2.38×10^{-5} - 4.93×10^{-3} mol dm^{-3}) in aqueous solution at pH 5.5 and 298.2 K. The arrows show the direction of intensity change upon increasing $(\beta CD)_2Sc$ concentration.*

In each case the spectral variation was successfully fitted to the algorithm arising from the equilibrium shown in Eqn. 4.7, where $(\beta CD)_2X$ denotes the linked cyclodextrin dimer host. The values obtained for K_1, by simultaneously fitting the data at wavelengths where significant spectral change occurs (see footnote Table 4.4), are listed in Table 4.4. The data were fitted using a non-linear least-squares routine (Section 6.2.5). Due to the errors involved in spectral measurement and solution preparation, the actual errors on the stability constants are greater than the non-weighted standard deviations quoted (but they

are unlikely to exceed the non-weighted standard deviation by a factor of two in these TR^- systems).

$$(\beta CD)_2X + TR^- \overset{K_1}{\rightleftharpoons} (\beta CD)_2X{\cdot}TR^- \qquad (4.7)$$

The binding curves for the complexation of TR^- by $(\beta CD)_2Ur$ $(\beta CD)_2Ox$ and $(\beta CD)_2Sc$ at one selected wavelength, 480 nm, together with the calculated curves obtained from the best fit of the absorbance data to the algorithm arising from the equilibrium given in Eqn. 4.7, are shown in Figs. 4.14 and 4.15.

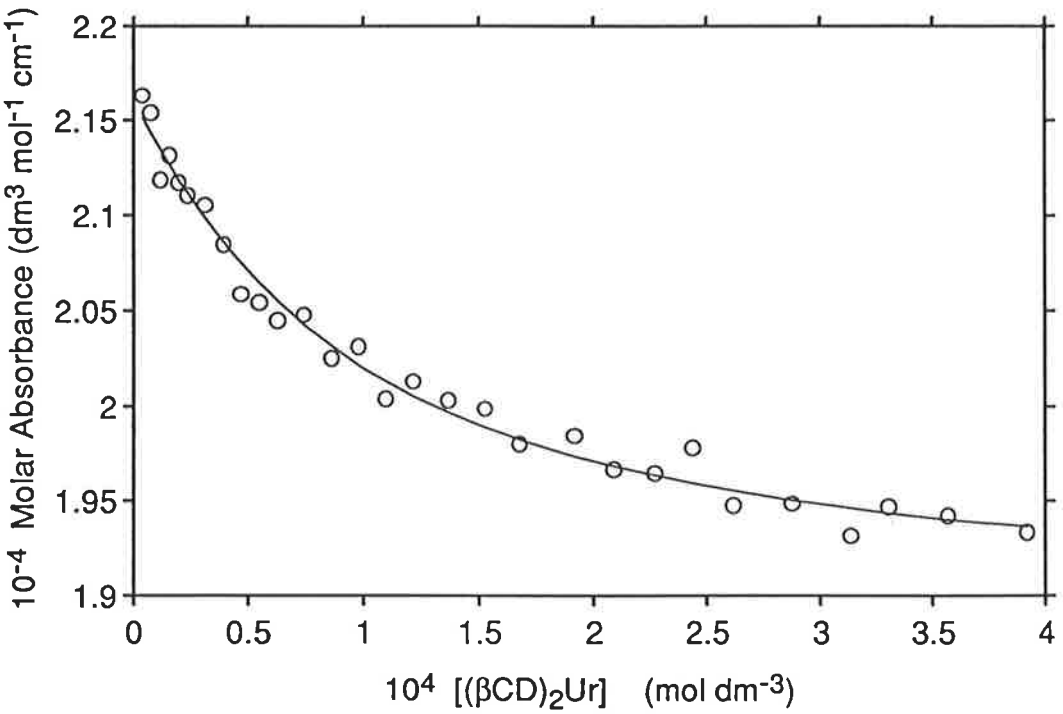

Figure 4.14 *Absorption of TR^- (4.1×10^{-5} mol dm^{-3}) at 480 nm in the presence of increasing concentrations of $(\beta CD)_2Ur$ (ranging from 3.86×10^{-6} - 3.73×10^{-4} mol dm^{-3}) in aqueous solution at pH 5.5 and 298.2 K. The circles represent data points and the solid line represents the best fit to the algorithm arising from the equilibrium shown in Eqn. 4.7.*

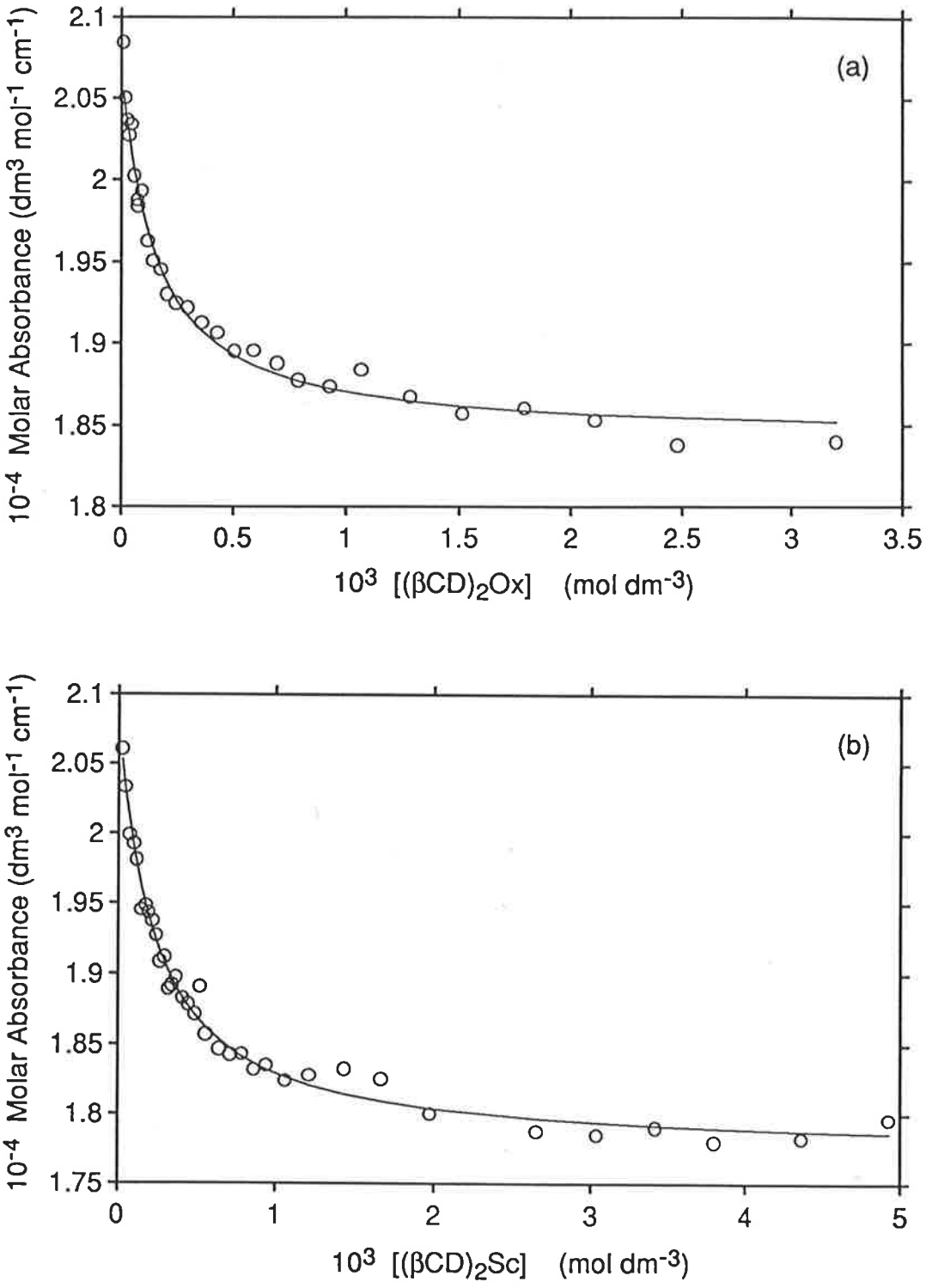

Figure 4.15 *Absorption at 480 nm of (a) TR^- (3.7×10^{-5} mol dm^{-3}) in the presence of increasing concentrations of $(\beta CD)_2Ox$ (ranging from 9.47×10^{-6} - 3.20×10^{-3} mol dm^{-3}) and (b) TR^- (4.0×10^{-5} mol dm^{-3}) in the presence of increasing concentrations of $(\beta CD)_2Sc$ (ranging from 2.38×10^{-5} - 4.93×10^{-3} mol dm^{-3}), in aqueous solution at pH 5.5 and 298.2 K. The circles represent data points and the solid line represents the best fit to the algorithm arising from the equilibrium shown in Eqn. 4.7.*

Table 4.4 *Stability constants for βCD·TR⁻ and (βCD)₂X·TR⁻,[a] (X = Ur, Ox, Sc) in aqueous solution at pH 5.5 and 298.2 K.*

Host	K_1 ($dm^3\ mol^{-1}$)	SSD[b]
βCD[c]	$(7.1 \pm 0.7) \times 10^2$	—
$(\beta CD)_2Ur$[d]	$(1.39 \pm 0.03) \times 10^4$	3.2×10^2
$(\beta CD)_2Ox$[e]	$(7.4 \pm 0.1) \times 10^3$	2.0×10^2
$(\beta CD)_2Sc$[f]	$(4.60 \pm 0.05) \times 10^3$	4.5×10^2

[a] Determined by fitting the variation in TR^- absorbance with increasing cyclodextrin concentration at 2 nm intervals over the wavelength range 450-510 nm,[d,f] or 440-492 nm,[e] to the algorithm arising from the equilibrium shown in Eqn. 4.7,[d,e,f] using a non-linear least-squares routine. Errors quoted represent non-weighted standard deviations. The concentration of TR^- was fixed at 4.1×10^{-5} mol dm^{-3},[d] 3.7×10^{-5} mol dm^{-3},[e] or 4.0×10^{-5} mol dm^{-3}.[f] The ranges of variation in cyclodextrin concentration for each system were (mol dm^{-3}): $(\beta CD)_2Ur$ (3.86×10^{-6} - 3.73×10^{-4}), $(\beta CD)_2Ox$ (9.47×10^{-6} - 3.20×10^{-3}), and $(\beta CD)_2Sc$ (2.38×10^{-5} - 4.93×10^{-3}). All solutions were prepared in 0.100 mol dm^{-3} Na_2HPO_4 and 0.200 mol dm^{-3} K_2SO_4, adjusted to pH 5.5 with H_2SO_4. [b] Sum of squared deviations. [c] Ref. 39. Determined from temperature-jump measurements (Section 4.3.2).

Complex stability increases in the order $\beta CD \cdot TR^-$ < $(\beta CD)_2Sc \cdot TR^-$ < $(\beta CD)_2Ox \cdot TR^-$ < $(\beta CD)_2Ur \cdot TR^-$. If each βCD annulus of $(\beta CD)_2X$ behaves as a separate entity in complexing TR^-, the $(\beta CD)_2X \cdot TR^-$ (X = Ur, Ox, Sc) complex stability constants are expected to be double that of $\beta CD \cdot TR^-$, on statistical grounds. However, the stability constants of $(\beta CD)_2X \cdot TR^-$ (X = Ur, Ox, Sc) are 6 to 19-fold greater than that of $\beta CD \cdot TR^-$ (Table 4.4), indicating that cooperative binding is occurring between the two βCD hydrophobic recognition sites of the linked cyclodextrin dimers.

In the $(\beta CD)_2X \cdot TR^-$ complexes, the aromatic portions of TR^- are likely to maximise their contact with the hydrophobic βCD cavities, and the functional groups of TR^- may be involved in hydrogen bonding interactions with the hydroxyl groups of the βCD annuli and the amide groups of the tether. The relative stabilities of the three linked

cyclodextrin dimer complexes imply that these interactions are optimised by the tether length of $(\beta CD)_2Ur$, which probably allows alignment of the interacting groups.

The $(\beta CD)_2X{\cdot}TR^-$ (X = Ur, Ox, Sc) stability constants in Table 4.4, and the directly determined molar absorbances of TR^- and $(\beta CD)_2X$ (X = Ur, Ox, Sc), are used to derive the molar absorbances of the $(\beta CD)_2X{\cdot}TR^-$ (X = Ur, Ox, Sc) complexes formed. These molar absorbances are shown in Figs. 4.16, 4.17 and 4.18 for $(\beta CD)_2Ur{\cdot}TR^-$, $(\beta CD)_2Ox{\cdot}TR^-$ and $(\beta CD)_2Sc{\cdot}TR^-$, respectively, along with the molar absorbance of TR^- itself.

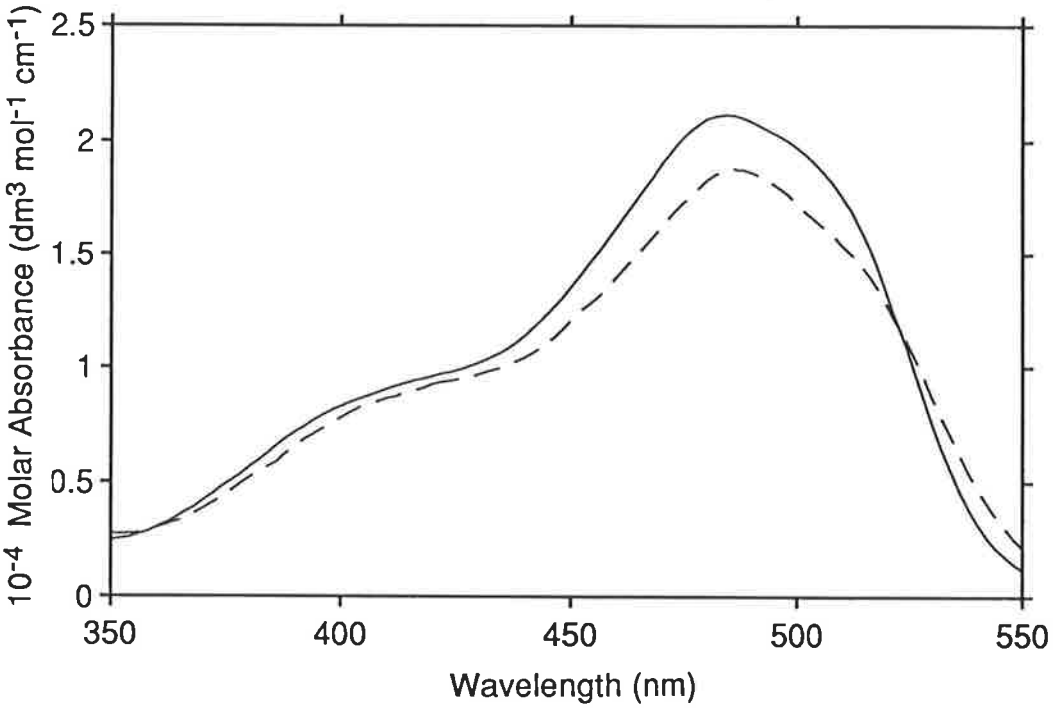

Figure 4.16 *Molar absorbance of TR^- (——) and $(\beta CD)_2Ur{\cdot}TR^-$ (– – –) in aqueous solution at pH 5.5 and 298.2 K. The $(\beta CD)_2Ur{\cdot}TR^-$ spectrum was derived from the best fit of the data in Fig. 4.12 (a), within the wavelength ranges 450-510 nm, to the algorithm arising from the equilibrium shown in Eqn. 4.7.*

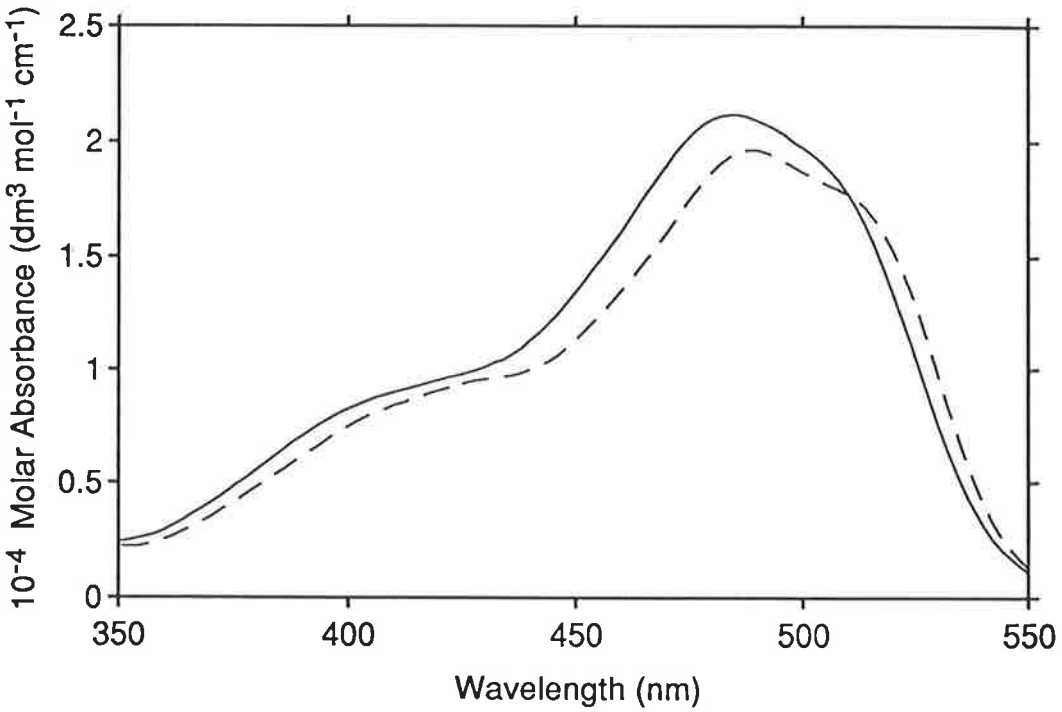

Figure 4.17 *Molar absorbance of TR^- (——) and $(\beta CD)_2Ox{\cdot}TR^-$ (– – –) in aqueous solution at pH 5.5 and 298.2 K. The $(\beta CD)_2Ox{\cdot}TR^-$ spectrum was derived from the best fit of the data in Fig. 4.12 (b), within the wavelength ranges 440-492 nm, to the algorithm arising from the equilibrium shown in Eqn. 4.7.*

In each system the spectrum derived for $(\beta CD)_2X{\cdot}TR^-$ is less intense and slightly broader than that of free TR^-. The spectral shapes of $(\beta CD)_2Ur{\cdot}TR^-$ and $(\beta CD)_2Sc{\cdot}TR^-$ are very similar, while that of $(\beta CD)_2Ox{\cdot}TR^-$ possesses a more intense high wavelength shoulder and exhibits a smaller decrease in intensity relative to the spectrum of TR^-. The progressive decrease in absorbance in the range 380-510 nm with increasing cyclodextrin concentration, is similar to that observed upon dimerisation of TR^- in the absence of cyclodextrin (Section 4.3.1). Upon inclusion, a decrease in intensity of the 484 nm band is expected due to the transfer of TR^- from the hydrophilic aqueous medium into the hydrophobic cyclodextrin cavity, resulting in a decrease in the intramolecular charge-transfer transition (Section 4.3.1). A shift in the tautomeric equilibrium (Section 4.3.1), to

form more of the azo tautomer, may also contribute to the spectral changes.[15] The absorbance maximum of free TR^- is at 484 nm, and the $(\beta CD)_2Ur{\cdot}TR^-$, $(\beta CD)_2Ox{\cdot}TR^-$ and $(\beta CD)_2Sc{\cdot}TR^-$ complexes exhibit absorbance maxima at 486, 488 and 488 nm, respectively, having approximately the same slight red shift as $\beta CD{\cdot}TR^-$, which has an absorbance maximum at 487 nm (Section 4.3.2). A red shift is normally indicative of attractive van der Waals interactions or an increase in planarity of the chromophore, which is consistent with inclusion of the dye within at least one hydrophobic cavity.

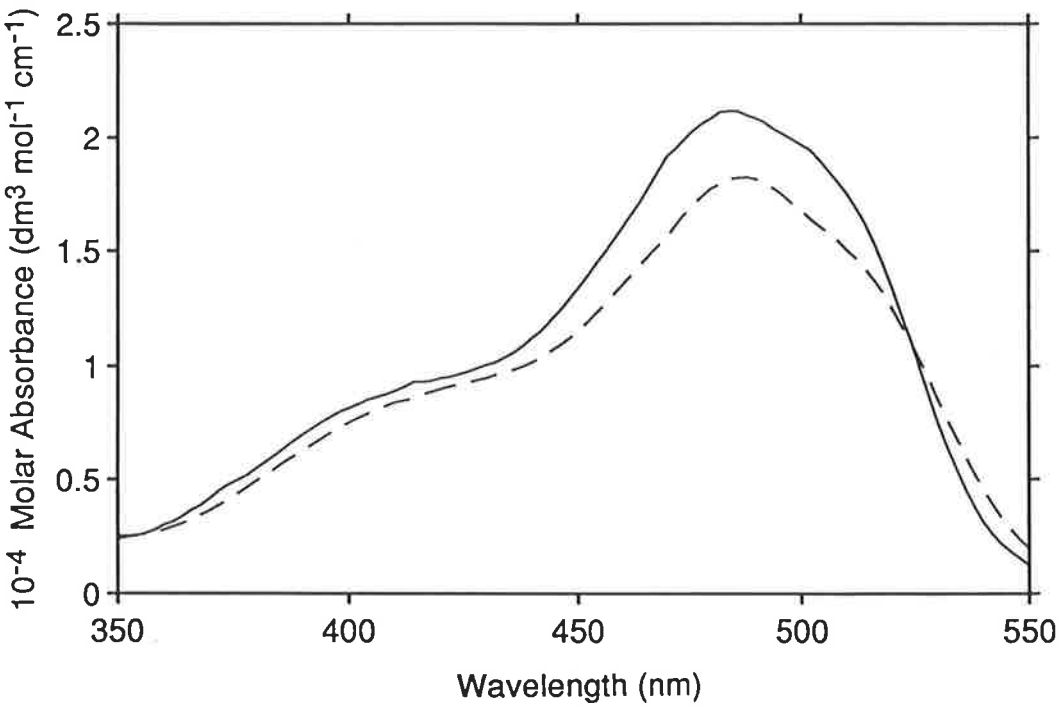

Figure 4.18 *Molar absorbance of TR^- (——) and $(\beta CD)_2Sc{\cdot}TR^-$ (– – –) in aqueous solution at pH 5.5 and 298.2 K. The $(\beta CD)_2Sc{\cdot}TR^-$ spectrum was derived from the best fit of the data in Fig. 4.13, within the wavelength ranges 450-510 nm, to the algorithm arising from the equilibrium shown in Eqn. 4.7.*

The induced circular dichroic spectrum of TR^- in a 17-fold excess of $(\beta CD)_2Sc$ is shown in Fig. 4.19. In the spectral range being considered, 350-550 nm, the circular dichroic spectrum induced by $(\beta CD)_2Sc$ exhibits two positive and one negative signal,

showing that TR^- is in a chiral environment. The sign of the induced circular dichroism is determined by the orientation of the guest's electric transition moment with respect to the principal symmetry axis of the cyclodextrin annulus.[48] The simplest explanation of the spectrum is that the three circular dichroism peaks arise from two $\pi \rightarrow \pi^*$ transitions, which are observed in the absorption spectrum, and one $n \rightarrow \pi^*$ transition, which is not. This spectrum is very similar to that induced by βCD,[39,40] although the negative signal is more intense.

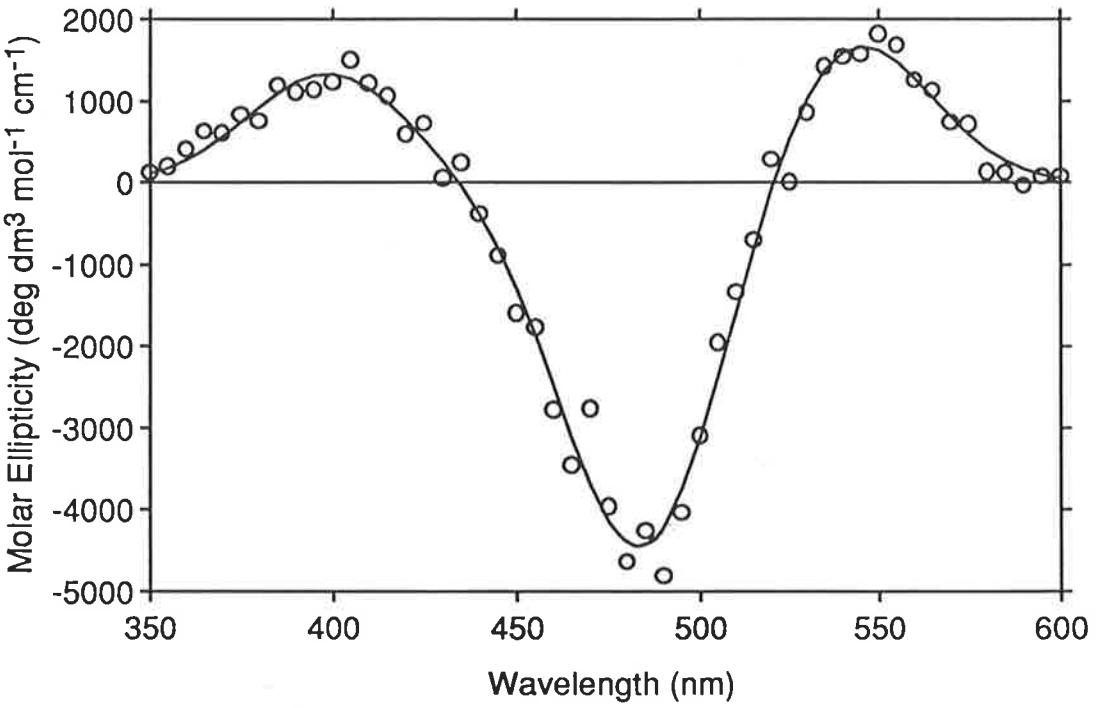

Figure 4.19 *Induced circular dichroic spectrum of TR^- (6.07×10^{-5} mol dm^{-3}) in the presence of $(\beta CD)_2Sc$ (1.04×10^{-3} mol dm^{-3}) in aqueous solution at pH 5.5 and 298.2 K. The circles represent data points and the solid line represents the best fit to three Gaussian curves.*

Although the experimental data were successfully fitted to the algorithm arising from the equilibrium shown in Eqn. 4.7, they could also be fitted to the algorithm arising from the equilibria shown in Eqn. 4.8, where $(\beta CD)_2X$ denotes the linked cyclodextrin

dimer host. The values obtained for K_1 and K_2, by simultaneously fitting the data at wavelengths where significant spectral change occurs (see footnote Table 4.4), are listed in Table 4.5, and good visual fits were generated.

$$(\beta CD)_2X + TR^- \overset{K_1}{\rightleftharpoons} (\beta CD)_2X{\cdot}TR^-$$

$$(\beta CD)_2X{\cdot}TR^- + TR^- \overset{K_2}{\rightleftharpoons} (\beta CD)_2X{\cdot}(TR)_2^{2-} \qquad (4.8)$$

Table 4.5 *Stability constants for* $\beta CD{\cdot}TR^-$, $\beta CD{\cdot}(TR)_2^{2-}$, $(\beta CD)_2X{\cdot}TR^-$,[a] *and* $(\beta CD)_2X{\cdot}(TR)_2^{2-}$,[a] *(X = Ur, Ox, Sc) in aqueous solution at pH 5.5 and 298.2 K.*

Host	K_1 ($dm^3\ mol^{-1}$)	K_2 ($dm^3\ mol^{-1}$)	SSD[b]
βCD[c]	$(7.1 \pm 0.7) \times 10^2$	$(4 \pm 7) \times 10^6$	—
$(\beta CD)_2Ur$	$(5.1 \pm 0.8) \times 10^4$	$(1.6 \pm 0.5) \times 10^5$	2.7×10^2
$(\beta CD)_2Ox$	$(1.4 \pm 0.2) \times 10^5$	$(3.9 \pm 0.8) \times 10^5$	1.2×10^2
$(\beta CD)_2Sc$	$(3.1 \pm 0.6) \times 10^3$	$(6 \pm 2) \times 10^3$	3.8×10^2

[a] As for Table 4.4, except data were fitted to the algorithm arising from the equilibria shown in Eqn. 4.8 for the $(\beta CD)_2X$ systems. [b] Sum of squared deviations. [c] Ref. 39. Determined from temperature-jump measurements (Section 4.3.2).

The sum of squared deviations (SSD) listed in Table 4.5 are decreased, relative to those listed in Table 4.4, however, this decrease is of the size which can be attributed to the introduction of an additional fitting parameter. The K_1 values listed in Table 4.5 differ from those of Table 4.4 by up to an order of magnitude, and a different order of increasing stability: $\beta CD{\cdot}TR^- < (\beta CD)_2Sc{\cdot}TR^- < (\beta CD)_2Ur{\cdot}TR^- < (\beta CD)_2Ox{\cdot}TR^-$, is also apparent. Interestingly, the errors on K_1 increase notably upon incorporation of the additional species, $(\beta CD)_2X{\cdot}(TR)_2^{2-}$. Nevertheless, the spectra derived for the $(\beta CD)_2X{\cdot}TR^-$

species (X = Ur, Ox, Sc) are independent of the fitting model (either Eqn. 4.7 or 4.8) used to derive them.

The surprising feature of the stability constants listed in Table 4.5 is that for all three linked cyclodextrin systems, $K_2 > K_1$. This implies a very pronounced cooperativity for the complexation of a second TR^-, which may be related to interactions between the two dye molecules stabilising the complex and leading to a geometry where both dye molecules are inserted into the linked cyclodextrin dimer host. The preferential inclusion of a dye dimer by comparison with the inclusion of a dye monomer is observed for the γCD/TR^-, γCD/MO^- and γCD/crystal violet systems, and appears to illustrate the increased stability which results from a close matching of the guest and cyclodextrin annular sizes.[39]

The K_2 values increase in the order: $(\beta CD)_2Sc\cdot(MO)_2^{2-} < (\beta CD)_2Ur\cdot(MO)_2^{2-} < (\beta CD)_2Ox\cdot(MO)_2^{2-}$. The overall stability constants of $(\beta CD)_2Ur\cdot(TR)_2^{2-}$, $(\beta CD)_2Ox\cdot(TR)_2^{2-}$ and $(\beta CD)_2Sc\cdot(TR)_2^{2-}$ are 8.16×10^9, 5.46×10^{10} and 1.86×10^7 dm^6 mol^{-2}, respectively. These may be compared with the spectrally determined value of 2.03×10^7 dm^6 mol^{-2} (Section 4.3.2) for the stability of the $\beta CD\cdot(TR)_2^{2-}$ complex. The spectra derived for $(\beta CD)_2Ur\cdot(TR)_2^{2-}$ and $(\beta CD)_2Ox\cdot(TR)_2^{2-}$ are virtually identical to the spectrum of free TR^-, a result that is difficult to rationalise. If a low concentration of $(\beta CD)_2X\cdot(TR)_2^{2-}$ (X = Ur, Ox, Sc) exists over the concentration range used, this may prevent a meaningful determination of the species spectra.

The derived stability constants, K_1 and K_2 (Table 4.5), can be used to calculate the percentages of TR^-, $(\beta CD)_2X\cdot TR^-$ and $(\beta CD)_2X\cdot(TR)_2^{2-}$ (X = Ur, Ox, Sc) present under the conditions used in this study. Over the concentration ranges used (Section 6.2.2), the maximal percentages of total TR^- present in the free form are 84.0, 53.6 and 91.5%, and in the $(\beta CD)_2X\cdot TR^-$ form are 64.9, 94.1 and 91.3%, and in the $(\beta CD)_2X\cdot(TR)_2^{2-}$ form are 31.4, 43.5 and 2.7%, for the $(\beta CD)_2Ur$, $(\beta CD)_2Ox$ and $(\beta CD)_2Sc$ systems, respectively. Although the spectral variations imply the presence of only two dominant species, the derived stability constants of Table 4.5 are consistent with the presence of significant amounts of a third absorbing species in the $(\beta CD)_2Ur$ and $(\beta CD)_2Ox$ systems, over the concentration ranges studied. This would imply that two of the three absorbing species

have very similar spectra, which is an unlikely premise. Although such a spectral similarity was determined for TR^- and $(\beta CD)_2X\cdot(TR)_2^{2-}$ (X = Ur and Ox), as mentioned above, the difference in the local environments of these two species implies that such a spectral similarity seems unlikely to exist. If only small amounts of the $(\beta CD)_2X\cdot(TR)_2^{2-}$ complexes (X = Ur, Ox) were present under the conditions used, this may lead to high uncertainties in the fitted stability constants and associated spectra. In the $(\beta CD)_2Sc$ system, the two dominant absorbing species are TR^- and $(\beta CD)_2Sc\cdot TR^-$, under the conditions of this study, and $(\beta CD)_2Sc\cdot(TR)_2^{2-}$ is only a minor species. As can be seen from the binding curves, the majority of data points are in the region where $(\beta CD)_2X$ is in excess, and the two dominant species are likely to be $(\beta CD)_2X\cdot TR^-$ and TR^- in the other two systems.

For a number of reasons, the model outlined in Eqn. 4.8 is improbable. Firstly, the isosbestic points exhibited by all three systems studied imply the presence of two dominant absorbing species. Conversely, the stability constants derived using this model are consistent with significant amounts of three TR^- absorbing species for the $(\beta CD)_2Ur$ and $(\beta CD)_2Ox$ systems. Secondly, the change in the sum of squared deviations associated with the fit and the increase in error on K_1, indicate that, for all three systems studied, no significant improvement in the data fit is achieved upon incorporation of the additional fitting parameter. Thirdly, the derived spectra for $(\beta CD)_2X\cdot(TR)_2^{2-}$ (X = Ur, Ox) do not appear reasonable. However, the formation of $(\beta CD)_2X\cdot(TR)_2^{2-}$ (X = Ur, Ox, Sc) as a minor species cannot be completely ruled out.

No evidence of $((\beta CD)_2X)_2\cdot TR^-$ (X = Ur, Ox, Sc) complex formation was detected, probably due to the lower host to guest concentration ratios used for these measurements compared with those in the $(\beta CD)_2Ur/TNS^-$ system (Section 3.4.1).

The spectral variations and derived stability constants for all three systems are consistent with the presence of two dominant species, TR^- and $(\beta CD)_2X\cdot TR^-$ (X = Ur, Ox, Sc), over the concentration ranges studied, and possibly also a minor species, $(\beta CD)_2X\cdot(TR)_2^{2-}$. The inclusion of TR^- may occur in a similar way to that proposed for

the formation of βCD·TR$^-$ (Section 4.3.2). The long axis of the naphthyl moiety may be included parallel to the C_7 symmetry axis of one βCD annulus, from the primary end, possibly also permitting some hydrophobic interactions with the primary end of the second βCD annulus (Fig. 5.1(d)). Hydrogen bonding interactions between the naphthyl substituents and the primary hydroxyls of the βCD annuli, or the amide groups of the tether, may assist in stabilising the complex. Alternatively, the extent of cooperative binding observed for the $(\beta CD)_2X\cdot TR^-$ (X = Ur, Ox, Sc) complexes may imply the inclusion of both aromatic moieties (Fig. 5.1(e)), since hydrophobic interactions are the main driving force for inclusion (Section 1.2.4). Charge and steric effects are known to determine which portion of the guest is included.[49] The size of the phenylsulfonate group is better suited to the width of the narrow primary cavity rim, and although the solvating water molecules surrounding the sulfonate group are stripped off as it passes through the βCD cavity, another solvation shell forms as the sulfonate group protrudes from the cavity. The negatively charged sulfonate end of a molecule appears to be capable of inclusion by a cyclodextrin, despite being highly solvated.[40,49] Hence, the inclusion of both phenylsulfonate and napthyl moieties may occur.

4.4 Summary and Conclusions

The spectra of MO$^-$ and TR$^-$ show isosbestic points upon addition of $(\beta CD)_2Ur$, $(\beta CD)_2Ox$ or $(\beta CD)_2Sc$. The spectral variations are consistent with the formation of a $(\beta CD)_2X\cdot(guest)^-$ complex in each case. There is also some evidence for the presence of a $(\beta CD)_2X\cdot(guest)_2^{2-}$ (X = Ur, Ox, Sc) complex existing in small amounts under the conditions used. The stabilities of the complexes formed by MO$^-$ and TR$^-$ upon addition of $(\beta CD)_2Ur$, $(\beta CD)_2Ox$ or $(\beta CD)_2Sc$, are summarised in Table 4.6.

The inclusion of MO$^-$ by βCD occurs preferentially from the dimethylaniline end rather than the strongly solvated sulfonate end, which possesses a localised negative charge. Inclusion probably occurs from the wider secondary end of the annulus. In the $(\beta CD)_2X\cdot MO^-$ complexes, the dimethylaniline end may pass through the first βCD

cavity and interact with the second. The bulkiness of TR^- may result in a different inclusion mode and orientation, by comparison with those of MO^-, and less freedom of motion.[46] While MO^- is included inside βCD with its long molecular axis aligned with the βCD C_7 symmetry axis (Section 4.2.2), TR^- is included with its short (*i.e.* naphthyl) molecular axis aligned (Section 4.3.2). Consequently, although MO^- penetrates the full depth of the βCD cavity, the naphthyl group of TR^- is only partially included because of the steric hindrance of the naphthyl substituents. A similar TR^- inclusion mode in the $(\beta CD)_2X{\cdot}TR^-$ (X = Ur, Ox, Sc) complexes would explain the smaller spectral changes and lower complex stabilities of these complexes, by comparison with the corresponding $(\beta CD)_2X{\cdot}MO^-$ complexes. In the $(\beta CD)_2X{\cdot}TR^-$ complexes, the naphthyl group may be included at the primary end of one βCD annulus, also permitting interactions with the second annulus, or alternatively, inclusion of the phenylsulfonate group and a portion of the naphthyl moiety may occur. Besides optimisation of guest-βCD interactions, guest-tether interactions, and charge and steric effects,[49] may influence the complex structure. Minimisation of the repulsion between the opposed dipoles of the βCD annuli, does not appear to have a strong influence. The linked cyclodextrin dimer may exist in many possible conformations due to the flexibility of the tether. Any misalignment between the cyclodextrin annuli and the aromatic binding sites of the guest induces additional strain energy, and consequently only a few of the many possible complex conformations are stable.[19]

For comparison, the stabilities of the corresponding $(\beta CD)_2X{\cdot}TNS^-$ (X = Ur, Ox, Sc) complexes, discussed in the previous chapter (Section 3.5), are included in Table 4.6. The stability increase in the order: $(\beta CD)_2X{\cdot}TR^- < (\beta CD)_2X{\cdot}TNS^- < (\beta CD)_2X{\cdot}MO^-$, is in accordance with increasing linearity of the guest structure (Figs. 3.1 and 4.1) facilitating complexation compared with decomplexation.

In each case the linked cyclodextrin dimer complex, $(\beta CD)_2X{\cdot}(guest)^-$ (X = Ur, Ox, Sc), is substantially more stable than the corresponding $\beta CD{\cdot}(guest)^-$ complex, indicating that cooperative binding is operating. The $(\beta CD)_2X{\cdot}(guest)^-$ complex stabilities increase with a change in host in the order: $(\beta CD)_2Sc{\cdot}(guest)^- < (\beta CD)_2Ur{\cdot}(guest)^- <$

$(\beta CD)_2Ox\cdot(guest)^-$, for guest = MO, and in the order: $(\beta CD)_2Sc\cdot(guest)^-$ < $(\beta CD)_2Ox\cdot(guest)^-$ < $(\beta CD)_2Ur\cdot(guest)^-$, for guest = TR or TNS. This variation in stability order may arise from differences in the guest structure and inclusion mode. The binding mode of TNS^- is probably similar to that of MO^-, however, the aromatic moieties are separated by two bonds (Fig. 3.1, Section 3.1) rather than three (as for MO^-, Fig. 4.1), and consequently a shorter optimum tether length in $(\beta CD)_2X$ is expected and observed. The tether length in $(\beta CD)_2Ox$ appears most appropriate for the azo group separation between the aromatic moieties of MO^-. If TR^- is bound by inclusion of the naphthyl moiety only, a more stable complex would be expected to form with a linked cyclodextrin dimer possessing a short tether length, as observed.

Table 4.6 *Stability constants for the complexes formed between various cyclodextrins and either MO^-,[a] TR^-,[b] or TNS^-,[c] in aqueous solution at 298.2 K.*

Host	Guest	K_1 ($dm^3\ mol^{-1}$)
βCD	MO^-	$(2.16 \pm 0.90) \times 10^3$
$(\beta CD)_2Ur$	MO^-	$(1.05 \pm 0.04) \times 10^5$
$(\beta CD)_2Ox$	MO^-	$(1.92 \pm 0.04) \times 10^5$
$(\beta CD)_2Sc$	MO^-	$(2.50 \pm 0.02) \times 10^4$
βCD[d]	TR^-	$(7.1 \pm 0.7) \times 10^2$
$(\beta CD)_2Ur$	TR^-	$(1.39 \pm 0.03) \times 10^4$
$(\beta CD)_2Ox$	TR^-	$(7.4 \pm 0.1) \times 10^3$
$(\beta CD)_2Sc$	TR^-	$(4.60 \pm 0.05) \times 10^3$
βCD	TNS^-	$(3.14 \pm 0.02) \times 10^3$
$(\beta CD)_2Ur$	TNS^-	$(4.523 \pm 0.007) \times 10^4$
$(\beta CD)_2Ox$	TNS^-	$(3.264 \pm 0.009) \times 10^4$
$(\beta CD)_2Sc$	TNS^-	$(1.670 \pm 0.002) \times 10^4$

[a] See footnote Table 4.2. [b] See footnote Table 4.4. [c] See footnote Table 3.3.

These studies reveal that the distance between the hydrophobic cavities of the linked cyclodextrin host is just one factor involved in determining the stability of the resultant complex. The distance between the two aromatic moieties of the guest, the size of these aromatic groups and their geometrical arrangement, and the inclusion mode of the guest, also appear to influence complex stability.

Of primary importance to this study was the effect of the second βCD recognition site on binding. The stability constants in Table 4.6 show that cooperative binding is occurring in all cases studied, and that the extent of cooperativity may be varied by the relative distances between the hydrophobic βCD cavities of the linked cyclodextrin dimer host, and the aromatic binding sites of the guest.

References

1. R. J. Clarke, J. H. Coates and S. F. Lincoln, *Adv. Carbohyd. Chem. Biochem.*, 1988, **46**, 244.

2. R. J. Clarke, Ph. D. Thesis, The University of Adelaide, 1985.

3. W. Broser, *Z. Naturforsch.*, 1953, **8b**, 722.

4. R. L. Reeves, R. S. Kaiser, M. S. Maggio, E. A. Sylvestre and W. H. Lawton, *Can. J. Chem.*, 1973, **51**, 628.

5. A. Buvari and L. Barcza, *J. Inclusion Phenom.*, 1989, **7**, 313, and references therein.

6. W. R. Brode, I. L. Seldin, P. E. Spoerri and G. M. Wyman, *J. Am. Chem. Soc.*, 1955, **77**, 2762.

7. F. Quadrifoglio and V. Crescenzi, *J. Colloid Interfac. Sci.*, 1971, **35**, 447.

8. H. Bock, *Angew. Chem. Int. Ed. Engl.*, 1965, **4**, 457; G. Kortüm and H. Rau, *Ber. Bunsenges. Physik. Chem.*, 1964, **68**, 973.

9. H. Zollinger, *Azo and Diazo Chemistry: Aliphatic and Aromatic Compounds*, Interscience, New York, 1961.

10. J. Kroner and H. Bock, *Chem. Ber.*, 1968, **101**, 1922.

11. R. J. Clarke, J. H. Coates and S. F. Lincoln, *Carbohydr. Res.*, 1984, **127**, 181.

12. T. Kurucsev, unpublished results, The University of Adelaide, 1981.

13. H. Hirai, N. Toshima and S. Uenoyama, *Bull. Chem. Soc. Jpn.*, 1985, **58**, 1156.

14. K. Fujita, S. Ejima and T. Imoto, *J. Chem. Soc., Chem. Commun.*, 1984, 1277.

15. Y. Matsui and K. Mochida, *Bull. Chem. Soc. Jpn.*, 1978, **51**, 673.

16. I. Tabushi, Y. Kuroda and T. Mizutani, *Tetrahedron*, 1984, **40**, 545.

17. H. Hirai, N. Toshima and S. Uenoyama, *Polymer J.*, 1981, **13**, 607.

18. R. I. Gelb and L. M. Schwartz, *J. Inclusion Phenom. Mol. Recognit. Chem.*, 1989, **7**, 537.

19. H-J. Schneider and F. Xiao, *J. Chem. Soc. Perkin Trans. 2*, 1992, 387.

20. W. Broser and W. Lautsch, *Z. Naturforsch.*, 1953, **8b**, 711.

21. J. Szejtli, Z. Budai and M. Kajtar, *Magyar Kemiai Folyoirat*, 1978, **84**, 68.

22. K. M. Tawarah and A. A. Wazwaz, *Ber. Bunsenges. Phys. Chem.*, 1993, **97**, 727.

23. H. M. Abu-Shamleh, M. Sc. Thesis, Yarmouk University, 1990.

24. K. M. Tawarah, *J. Inclusion Phenom. Mol. Recognit. Chem.*, 1992, **14**, 195.

25. K. Hamasaki, A. Nakamura, A. Ueno and F. Toda, *J. Inclusion Phenom. Mol. Recognit. Chem.*, 1992, **13**, 349.

26. A. Muñoz de la Peña, F. Salinas, M. J. Gómez, M. I. Acedo and M. Sánchez Peña, *J. Inclusion Phenom. Mol. Recognit. Chem.*, 1993, **15**, 131.

27. S. Li and W. C. Purdy, *Chem. Rev.*, 1992, **92**, 1457 and references therein.

28. J. Szejtli, *Cyclodextrins and Their Inclusion Complexes*, Akadémiai Kiadó, Budapest, 1982, p 164-166.

29. K. Mochida, A. Kagita, Y. Matsui and Y. Date, *Bull. Chem. Soc. Jpn.*, 1973, **46**, 3703.

30. H. A. Benesi and J. H. Hildebrand, *J. Am. Chem. Soc.*, 1949, **71**, 2703.

31. G. C. Catena and F. V. Bright, *Anal. Chem.*, 1989, **61**, 905.

32. J. W. Park and K. H. Park, *J. Inclusion Phenom. Mol. Recognit. Chem.*, 1994, **17**, 277.

33. M. Hoshino, M. Imamura, K. Ikehara and Y. Hama, *J. Phys. Chem.*, 1981, **85**, 1820.

34. F. Cramer, W. Saenger and H.-C. Spatz, *J. Am. Chem. Soc.*, 1967, **89**, 14.

35. K. Harata, *Bull. Chem. Soc. Jpn.*, 1976, **49**, 1493; K. Harata and H. Uedaira, *Nature (London)*, 1975, **253**, 190.

36. M. Suzuki and Y. Sasaki, *Chem. Pharm. Bull.*, 1979, **27**, 609.

37. T. Jiang, D. K. Sukumaran, S. Soni and D. S. Lawrence, *J. Org. Chem.*, 1994, **59**, 5149.

38. I. Tabushi, Y. Kuroda and K. Shimokawa, *J. Am. Chem. Soc.*, 1979, **101**, 1614.

39. R. J. Clarke, J. H. Coates and S. F. Lincoln, *J. Chem. Soc., Faraday Trans. 1*, 1984, **80**, 3119.

40. M. Suzuki, M. Kajtar, J. Szejtli, M. Vikmon and E. Fenyvesi, *Carbohydr. Res.*, 1992, **223**, 71.

41. R. L. Reeves and R. S. Kaiser, *J. Org. Chem.*, 1970, **35**, 3670.

42. B. Milicevic and G. Eigenmann, *Helv. Chim. Acta.*, 1964, **47**, 1039; R. L. Reeves, M. S. Maggio and S. A. Harkaway, *J. Phys. Chem.*, 1979, **83**, 2359.

43. K. R. Popov, *Opt. Spectrosc.*, 1972, **33**, 27.

44. E. Sawicki, *J. Org. Chem.*, 1956, **21**, 605.

45. R. J. Clarke, J. H. Coates and S. F. Lincoln, *J. Chem. Soc., Faraday Trans. 1*, 1986, **82**, 2333.

46. M. Suzuki and Y. Sasaki, *Chem. Pharm. Bull.*, 1979, **27**, 1343.

47. K. Pitchumani and M. Vellayappan, *J. Inclusion Phenom. Mol. Recognit. Chem.*, 1992, **14**, 157.

48. M. Kajtar, C. Horvath-Toro, E. Kuthi and J. Szejtli, *Acta Chim. Acad. Sci. Hung.*, 1982, **110**, 327.

49. N. Yoshida, A. Seiyama and M. Fujimoto, *J. Phys. Chem.*, 1990, **94**, 4246; N. Yoshida and K. Hayashi, *J. Chem. Soc., Perkin Trans. 2*, 1994, 1285.

CHAPTER 5

Summary and Conclusions

5.1 General

The binding and selectivity of modified cyclodextrins, containing essentially two recognition sites, were studied in order to gain information on the requirements for two recognition sites to reinforce each other. The cyclodextrin annulus provides a predominantly hydrophobic recognition site. The metallocyclodextrins discussed in the first section of this thesis (Chapter 2) also incorporate a coordination recognition site which is provided by a metal ion, bound by the coordinating group substituted on the primary rim of the βCD annulus. The linked cyclodextrin dimers discussed in the second section (Chapters 3 and 4) contain two hydrophobic βCD recognition sites which are linked through their primary rims by a tether. There are probably many recognition interactions occurring, but there are two main sites for guest interaction with either the metallocyclodextrin or linked cyclodextrin dimer host. Hence, the modified cyclodextrins studied here are referred to as double recognition hosts. It is possible that interactions occur with the tether in the linked cyclodextrin dimer systems, in which case triple recognition may be occurring.

The stability constants obtained in both the metallocyclodextrin and linked cyclodextrin dimer binding studies, show that in each system the guest simultaneously interacts with both recognition sites of the host, and thus, multiple recognition is achieved by the modified cyclodextrins studied. The selectivity of these modified cyclodextrins and the stability of the complexes formed, depend on the extent to which guests can interact with the two recognition sites of the host. This is influenced by a number of factors, and those involved in the complexation of amino acids by metallocyclodextrins are considered first.

5.2 Metallocyclodextrins

The variation in [Cu(βCDpn)(amino acid)]$^+$ stability with a change in amino acid guest is in the order: phenylalanine < tryptophan < histidine. This reflects the different coordination mode of histidine by comparison with phenylalanine and tryptophan, and the variation in size of the amino acid aromatic side chain. While phenylalanine and tryptophan may coordinate through the carboxylate oxygen and the amine nitrogen, histidine may also coordinate through the imidazole nitrogen. The size and nature of the aromatic amino acid side chain may influence the extent of hydrophobic interaction of the guest within the cyclodextrin cavity.

A comparison of the stability constant for βCDtren·Trp$^-$ with that previously reported for βCDpn·Trp$^-$, suggests that the interactions between the amino acid and the modified cyclodextrin may be influenced substantially by either steric effects, hydrogen bonding, the dipole moment of the modified cyclodextrin, or more than one of these. A similar situation is apparent in the presence of a metal ion. Other factors which appear to influence the stabilities of metallocyclodextrin complexes are: charge-charge interactions, hydration of charged species, the strength of metal binding and the denticity of the coordinating ligands. By changing the substituent on the cyclodextrin from a bidentate coordinating group in βCDpn, to a tetradentate coordinating group in βCDtren, the metallocyclodextrin stability was enhanced substantially. The greater denticity of the coordinating group probably produces a more sterically constrained metallocyclodextrin.

The variation in [M(βCDtren)]$^{2+}$ and [M(βCDtren)Trp]$^+$ stability, with a change in the nature of M^{2+}, follows the Irving-Williams series: $Ni^{2+} < Cu^{2+} > Zn^{2+}$. This is consistent with the M^{2+} ionic radius and d^n electronic configuration exerting a major influence in the complexation of tryptophan. The coordination number of the metal ion in [M(βCDtren)]$^{2+}$ appears to be unchanged in the [M(βCDtren)Trp]$^+$ complex. The binary and ternary metallocyclodextrins appear to be six-coordinate for Ni^{2+} and Zn^{2+}, but five coordinate for Cu^{2+}, probably with cis-diaquo-octahedral and distorted trigonal

bipyramidal geometry, respectively. U/v-visible spectra of $[M(tren)]^{2+}$ and $[M(\beta CDtren)]^{2+}$ show that the presence of the cyclodextrin does perturb the binding ability of the tren substituent. The spectral similarity of $[M(\beta CDtren)]^{2+}$ and $[M(\beta CDtren)Trp]^{+}$ suggest negligible perturbation is induced by the amino acid. The binary and ternary Cu^{2+} metallocyclodextrins of βCDpn probably have six-coordinate tetragonally distorted octahedral geometry around the metal centre. The proposed general structure of these complexes (Fig. 5.1(a)) has the aromatic moiety of the amino acid included inside the cyclodextrin annulus with the chiral centre in the vicinity of the primary hydroxyl groups, where the amino acid donor atoms can coordinate to the metal ion which is anchored at the primary end of the cavity by the amines of the coordinating group attached to the cyclodextrin.

The $[Cu(\beta CDpn)His]^{+}$ and $[M(\beta CDtren)Trp]^{+}$ complexes (M^{2+} = Ni^{2+}, Cu^{2+}, Zn^{2+}) studied are stabilised, relative to the βCDpn·His^{-} and βCDtren·Trp^{-} complexes respectively, by coordination interactions between the guest and the additional recognition site introduced by the metal ion. The stability of the $[Cu(\beta CDpn)His]^{+}$ complex is lower than that of $[Cu(His)]^{2+}$, whereas the stabilities of the $[M(\beta CDtren)Trp]^{+}$ complexes (M^{2+} = Ni^{2+}, Cu^{2+}, Zn^{2+}) are considerably higher than those of the corresponding $[M(Trp)]^{2+}$ complexes. The interaction of the guest's amino acid moiety with the metal ion, and of its aromatic moiety with the cyclodextrin cavity, reinforce each other in the latter case, but not the former. The lower stability of $[Cu(\beta CDpn)His]^{+}$ indicates that the conformation required for optimum metal-histidine interaction cannot be achieved. Interestingly, the relative strengths of the guest-cyclodextrin and guest-metal ion interactions are similar in the tryptophan/M^{2+}/βCDtren system (M^{2+} = Ni^{2+}, Cu^{2+}, Zn^{2+}), but the stability of βCDpn·His^{-} is substantially lower than that of $[Cu(His)]^{2+}$ in the histidine/Cu^{2+}/βCDpn system.

The complexation of His^{-} by $[Cu(\beta CDpn)]^{2+}$ shows no enantioselectivity, despite the fact that this metallocyclodextrin shows slight enantioselectivity for (*R*)-Phe^{-} and (*S*)-Trp^{-}. Enantioselectivity appears to be dependent on the size of the amino acid aromatic side chain, requiring a snug fit of the guests in the βCD cavity.

Enantioselectivity has previously been shown for $[M(\beta CDpn)]^+$ to be very dependent on the metal ion involved. When $M^{2+} = Co^{2+}$, Ni^{2+} and Cu^{2+}, $[M(\beta CDpn)]^+$ binds (*S*)-Trp^- enantioselectively over (*R*)-Trp^-. However, $[M(\beta CDtren)]^{2+}$ ($M^{2+} = Ni^{2+}$, Cu^{2+} and Zn^{2+}) does not bind Trp^- enantioselectively, despite the greater stability of these complexes by comparison with those of βCDpn. This shows that an increase in complex stability does not necessarily induce a corresponding increase in enantioselectivity. The absence of enantioselectivity in the $[M(\beta CDtren)]^{2+}$ complexation of Trp^-, appears to be correlated with the strength of the diastereomeric ternary complexes formed. The existence of thermodynamic enantioselectivity requires the difference in the free energy contributions arising from selective interactions of the (*R*)- and (*S*)- chiral centres of the guests with the homochirality of the metallocyclodextrin to be significant compared with the total free energy for guest binding by the metallocyclodextrin. The enantioselectivity of $[M(\beta CDpn)]^+$ ($M^{2+} = Co^{2+}$, Ni^{2+} and Cu^{2+}) is coincident with the weaker interaction of Trp^- with βCDpn, by comparison with βCDtren, allowing M^{2+} to exert more influence on the binding of Trp^-. These studies imply that the relative strengths of the selective and non-selective interactions play a vital role in determining enantioselectivity.

5.3 Linked Cyclodextrin Dimers

The complexation of guests, which possess two aromatic binding sites, by linked cyclodextrin dimers are now considered. These binding sites vary in size and stereochemistry for the selected guests, MO^-, TNS^-, and TR^-.

In each system studied, the $(\beta CD)_2X\cdot$(guest) stability constant is much greater than double that of the corresponding βCD·(guest) complex, indicating that the two hydrophobic recognition sites of the diamide-1°,1°-linked-βCDs operate cooperatively in guest binding. This cooperativity implies that diamide-1°,1°-linked-βCDs are able to exist in a suitable conformation for double binding of the guest, and that the binding of the first cyclodextrin does not significantly hinder the binding of the second cyclodextrin.

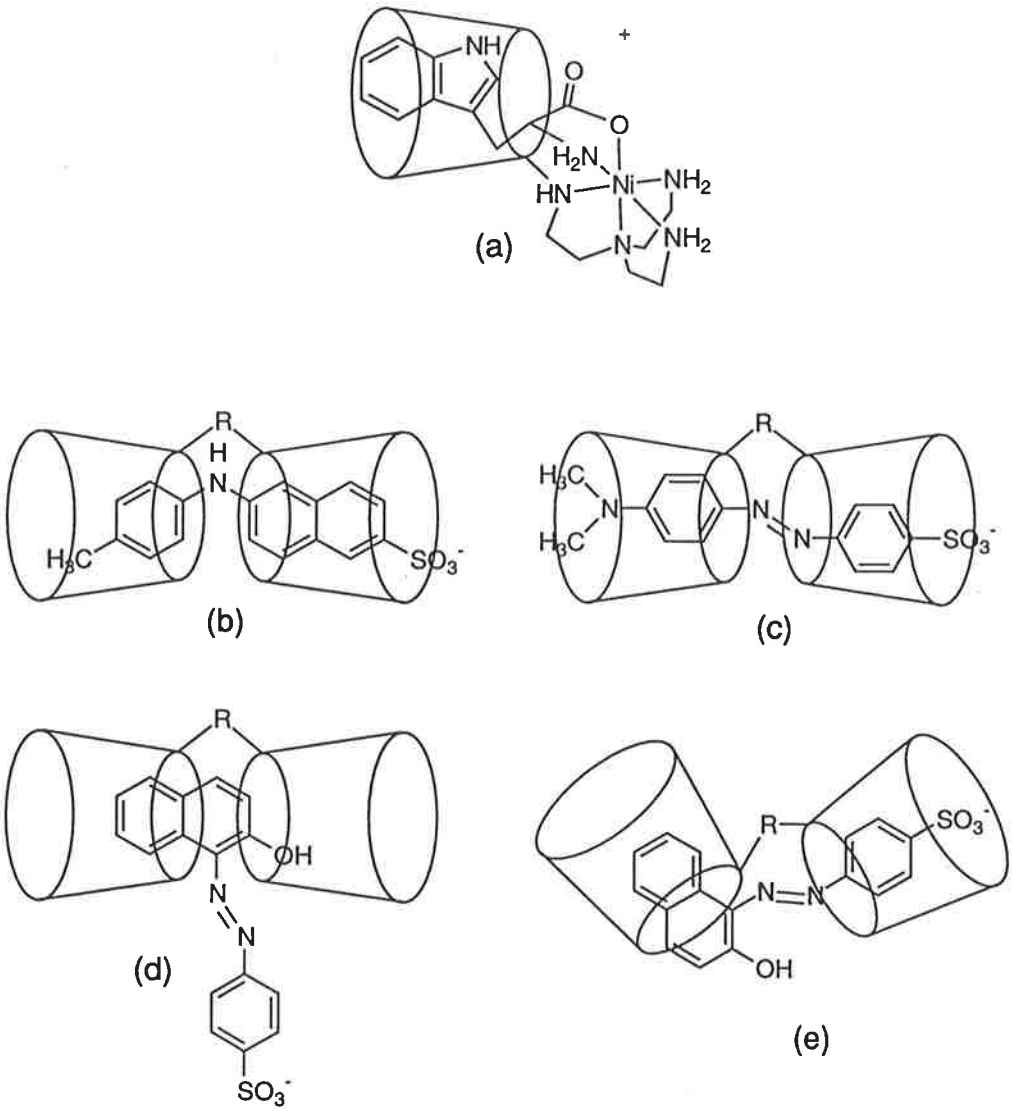

X = Ur R = NHC(O)NH

X = Ox R = NHC(O)-C(O)NH

X = Sc R = NHC(O)-$(CH)_2$-C(O)NH

Figure 5.1 *The proposed structure of (a) [Ni(βCDtren)Trp]$^+$ (b) $(\beta CD)_2X{\cdot}TNS^-$ and (c) $(\beta CD)_2X{\cdot}MO^-$, and the alternative structures of $(\beta CD)_2X{\cdot}TR^-$ are shown in (d) and (e). (The cyclodextrin substituents are exaggerated in size by comparison with the βCD annuli.)*

The extent of cooperative binding by the cyclodextrin annuli generally increases as the tether connecting them is shortened. This is all the more remarkable because the complexation involves the unfavourable alignment of the opposing dipole moments of the cyclodextrin annuli. As the length of the tether increases so do the rotational degrees of freedom between the two cavities, permitting a wider range of conformations and reducing the extent of cooperativity.

The strongest binding of TNS^- by $(\beta CD)_2X$ (X = Ur, Ox, Ma, Sc, Gl) is achieved with $(\beta CD)_2Ur$, which forms a complex that is over 14 times more stable than $\beta CD \cdot TNS^-$. Of the linked cyclodextrin dimers, $(\beta CD)_2X$ (X = Ur, Ox, Sc), $(\beta CD)_2Ox$ binds MO^- most strongly, forming a complex which is over 88 times more stable than $\beta CD \cdot MO^-$, and $(\beta CD)_2Ur$ binds TR^- most strongly, forming a complex which is over 19 times more stable than $\beta CD \cdot TR^-$. The diamide-1°,1°-linked-βCDs show selectivity, forming more stable complexes with the more linear guests. The variation in $(\beta CD)_2X \cdot (guest)$ complex stability increases in the order: $(\beta CD)_2X \cdot TR^- < (\beta CD)_2X \cdot TNS^- < (\beta CD)_2X \cdot MO^-$, for X = Ur, Ox, Sc.

For TNS^- the complex stabilities increase in the order: $(\beta CD)_2Ma \cdot TNS^- < (\beta CD)_2Gl \cdot TNS^- < (\beta CD)_2Sc \cdot TNS^- < (\beta CD)_2Ox \cdot TNS^- < (\beta CD)_2Ur \cdot TNS^-$. For MO^- the complex stabilities increase in the order: $(\beta CD)_2Sc \cdot MO^- < (\beta CD)_2Ur \cdot MO^- < (\beta CD)_2Ox \cdot MO^-$, and for TR^- they increase in the order: $(\beta CD)_2Sc \cdot TR^- < (\beta CD)_2Ox \cdot TR^- < (\beta CD)_2Ur \cdot TR^-$. The slight variations in stability order may arise from differences in guest structure and inclusion mode. The binding modes of TNS^- and MO^- are probably similar, however, optimal binding of TNS^- is achieved by a shorter tether length than that required for optimal binding of MO^-. The change in optimum tether length parallels the change in distance separating the aromatic moieties of the guest, implying that alignment of interacting groups plays an important part in determining complex stability. If TR^- is bound as shown in Fig. 5.1(d), a more stable complex would be expected to form with a linked cyclodextrin dimer possessing a short tether length, as observed. The $(\beta CD)_2Ma \cdot TNS^-$ complex departs from the general increase in stability with a decrease in

tether length, an anomaly which probably arises from the extent of alignment of interacting groups.

Spectral changes reveal that when TNS^- becomes included by $(\beta CD)_2X$ (X = Ur, Ox, Ma, Sc) the hydrophobicity of its environment is greater than that in either $\beta CD \cdot TNS^-$ or $(\beta CD)_2 \cdot TNS^-$, but the hydrophobicity of the TNS^- environment is similar in $(\beta CD)_2Gl \cdot TNS^-$ and $(\beta CD)_2 \cdot TNS^-$. The protection of TNS^- from solvent quenching, and the restriction of intramolecular rotation, also appear to be greater in the $(\beta CD)_2X \cdot TNS^-$ complexes than in either $\beta CD \cdot TNS^-$ or $(\beta CD)_2 \cdot TNS^-$. These factors generally increase with a decrease in tether length, which is coincident with a general increase in stability. An additional effect may be operative in the $(\beta CD)_2Ox \cdot TNS^-$ complex, arising from the conjugation present in the tether of this linked cyclodextrin dimer.

Comparison of the determined $(\beta CD)_2X \cdot TNS^-$ stability constants with those of other linked cyclodextrin dimers reveals that 1°,1°-linked derivatives bind TNS^- more strongly than their 1°,2°-linked and 2°,2°-linked counterparts, despite the dipole alignment in the 1°,2°-linked derivatives. The extent of cooperative binding by the 2°,2°- and 1°,2°-linked-βCDs is only modest by comparison with that of the corresponding 1°,1°-linked-βCDs. These results are readily accounted for by considering the stereochemistry and flexibility of the tether's point of attachment to the cyclodextrin. Substituents on the secondary rim are thought to point toward the interior of the cyclodextrin annulus, whereas those on the primary rim are free to point away from the cyclodextrin cavity as they are attached to sterically unhindered methylene carbons. Consequently, the linked cyclodextrin dimer conformation in the TNS^- complex is probably more strained when the tether is connected to at least one secondary rim. Strain may also be induced by partial inclusion of one cyclodextrin annulus by the other. From the similarity in order of magnitude of the $(\beta CD)_2X \cdot TNS^-$ stability constants for either diamide-1°,1°-linked-βCDs and dithiol-1°,1°-linked-βCDs, or diamide-2°,2°-linked-βCDs and diester-2°,2°-linked-βCDs, it is concluded that the TNS^- binding properties are not strongly dependent on the nature of the tether group.

The proposed general structures for the TNS^- and MO^- complexes (Fig. 5.1(b) and (c), respectively) have each aromatic moiety of the guest included inside a hydrophobic βCD annulus, and the amino or azo groups, respectively, held in the vicinity of the cyclodextrin's primary hydroxyl groups and the tether's diamide groups, where hydrogen bonding interactions can occur. Inclusion probably occurs from the wider secondary end of the annulus. Both MO^- and TNS^- are capable of passing through a βCD annulus, and their long molecular axes are probably aligned approximately along the C_7 symmetry axes of the βCDs in the linked cyclodextrin dimer complexes. In each case, the two cyclodextrin annuli can completely close up around the guest.

The general structure of the TR^- complexes may have either only the naphthyl moiety included (Fig. 5.1(d)), or the phenylsulfonate group and a portion of the naphthyl moiety included (Fig. 5.1(e)). The bulkiness of TR^- may result in a different inclusion mode and orientation, by comparison with those of MO^-, and also less freedom of motion. This is the case in the βCD complexes, where the short molecular axis of TR^- (*i.e.* naphthyl group) is aligned with the C_7 symmetry axis of βCD, and the naphthyl group of TR^- cannot penetrate the full depth of the cavity due to the steric hindrance of the naphthyl substituents. A similar TR^- inclusion mode in the $(\beta CD)_2X{\cdot}TR^-$ (X = Ur, Ox, Sc) complexes would explain the smaller spectral changes and lower complex stabilities of these complexes, by comparison with the corresponding $(\beta CD)_2X{\cdot}MO^-$ complexes. However, the extent of cooperativity supports inclusion of both aromatic moieties.

This work demonstrates the additive contribution of the second hydrophobic recognition site in complexing guests which contain two aromatic binding sites. The extent of cooperative binding is dependent on the distance between the hydrophobic βCD recognition sites, which is determined by the tether length, relative to the aromatic separation in the guest. The extent to which the second cyclodextrin annulus enhances binding is also dependent on the rims of the cyclodextrins which are connected. The inclusion mode of the guest, the size of its aromatic moieties and their stereochemistry also appear to influence complex stability. Cooperative binding is greatest, in the systems discussed here, when the cyclodextrin annuli are joined by a short tether connecting their

primary rims. It is anticipated that longer guests will be more effectively bound by dimers with longer tethers.

Studies of the type discussed within this thesis may assist in the construction of modified cyclodextrins which have a higher degree of molecular recognition for guests. As the number of non-covalent recognition interactions operating are increased, such studies may provide a stepwise approach to understanding the multiple recognition which is very common in biological systems, permitting the geometry of a reactive guest centre to be optimally positioned relative to catalytic groups.

CHAPTER 6

Experimental

6.1 Metallocyclodextrin Studies

6.1.1 Materials

6^A-(3-Aminopropylamino)-6^A-deoxy-β-cyclodextrin, βCDpn, and the trimethylsulfonic acid salt of 6^A-(2-(*N*,*N*-bis(2-aminoethyl)amino)ethylamino)-6^A-deoxy-β-cyclodextrin, $\beta CDtrenH_3(MeSO_3)_3$, were prepared as in the literature.[1,2] Their purity was > 95% as shown by TLC, ^1H and ^{13}C NMR spectroscopy and microanalysis. All cyclodextrins and amino acids were dried to constant weight and stored in the dark over P_2O_5 in a vacuum desiccator.

The ^{13}C NMR of (*S*)-histidine (Sigma) showed no impurities, however, the pK_as obtained by potentiometric titration differed significantly from literature values, and consequently (*R*)-, (*S*)- and (*R*/*S*)-histidine (Sigma) were purified before use by recrystallisation from ethanol/water. (*R*)-, (*S*)- and (*R*/*S*)-tryptophan (Sigma) were used without further purification. The enantiomeric purities of these amino acids were determined to be > 99% by optical rotation measurements for (*R*)- and (*S*)-histidine, and by HPLC analysis (Pirkle covalent (*S*)-phenylglycine column) of the respective esters formed with thionyl chloride pretreated methanol at 348 K for (*R*)- and (*S*)-tryptophan.

Metal perchlorates (Fluka) were twice recrystallised from water, dried and stored over P_2O_5 under vacuum. (**CAUTION**: Anhydrous perchlorate salts are potentially powerful oxidants and should be handled with care.[3])

Deionised water, purified with a MilliQ-Reagent system to produce water with a specific resistance of > 15 MΩ cm, was boiled to remove CO_2, cooled under a drying tube filled with sodalime, and used in the preparation of all solutions. Chemicals used were of analytical reagent grade and all glassware was A-grade.

6.1.2 Solution Preparation and Use

The aqueous 0.100 mol dm^{-3} NaOH burette solution was prepared from a 0.1 mol dm^{-3} ampoule (B.D.H.), and was standardised by titration against a 0.010 mol dm^{-3} KHphthalate (B.D.H.) solution which was prepared by weight. In all titrations, this standardised 0.100 mol dm^{-3} NaOH solution was titrated against the species of interest in solutions 0.090 mol dm^{-3} in $NaClO_4$. Acidified solutions were prepared using $HClO_4$ (70%, M&B). All solutions used in the βCDpn study were 0.010 mol dm^{-3} in $HClO_4$, whereas those used in the βCDtren study were 0.007 mol dm^{-3} in $HClO_4$.

The values of E_0 and pK_w are determined by titration of 0.010 mol dm^{-3} $HClO_4$ (0.090 mol dm^{-3} in $NaClO_4$) against 0.100 mol dm^{-3} NaOH. Protonation constants were determined by titration of 10.00 cm^3 aliquots of 0.002 mol dm^{-3} solutions of the cyclodextrin or amino acid of interest. Stability constants for the formation of amino acid-cyclodextrin complexes, were determined by titration of 5.00 cm^3 each of 0.002 mol dm^{-3} solutions of either amino acid enantiomer and the cyclodextrin.

Stock 0.100 mol dm^{-3} $Ni(ClO_4)_2$, $Cu(ClO_4)_2$ and $Zn(ClO_4)_2$ solutions were standardised by titration against disodium ethylenediaminetetraacetate in the presence of Murexide indicator in the first two cases and Eriochrome Black T in the case of $Zn(ClO_4)_2$.[4] Ion exchange of Co^{2+} on an Amberlite HRC-120 cation-exchange column in the acid form followed by back titration of the liberated acid was used as the standardisation method for the 0.100 mol dm^{-3} $Co(ClO_4)_2$ stock solution.

Stability constants for the formation of Cu^{2+}-histidine complexes were determined by titration of 10.00 cm^3 aliquots of 0.001 mol dm^{-3} histidine to which either 0.033, 0.049 or 0.098 cm^3 of $Cu(ClO_4)_2$ solution had been added. Stability constants for the formation of metal ion-cyclodextrin complexes, in the βCDtren study, were determined by titration of 10.00 cm^3 aliquots of 0.001 mol dm^{-3} βCDtren to which either 0.037, 0.075 or 0.150 cm^3 of $M(ClO_4)_2$ ($M = Co^{2+}$, Ni^{2+}, Cu^{2+} or Zn^{2+}) solution had been added.

The stability constants for the formation of the ternary amino acid-metal ion-cyclodextrin complexes, were determined by titration of 5.00 cm^3 each of 0.002 mol dm^{-3} solutions of either amino acid enantiomer and the cyclodextrin, with 0.098 cm^3 of $Cu(ClO_4)_2$ solution added in the βCDpn study, and 0.075 cm^3 of $M(ClO_4)_2$ solution added in the βCDtren study.

6.1.3 Potentiometric Titration Setup and Data Treatment

Potentiometric titrations[5] were carried out using a Metrohm Dosimat E665 titrimator, an Orion SA 720 potentiometer and an Orion 8172 Ross Sureflow combination pH electrode which was filled with 0.10 mol dm^{-3} $NaClO_4$. All titration solutions were saturated with nitrogen by passing a fine stream of nitrogen bubbles (previously passed through aqueous 0.10 mol dm^{-3} $NaClO_4$) through them for at least 15 min before commencement of the titration. During the titrations a similar stream of nitrogen bubbles was passed through the titration solution that was magnetically stirred and thermostatted at 298.2 ± 0.1 K in a water-jacketted 20 cm^3 titration vessel closed to the atmosphere except for a small exit for the nitrogen stream.

Derivations of the stability constants were carried out using the program SUPERQUAD.[6] At least three runs were performed for each system, and at least two of these runs were averaged; the criterion for selection for this averaging being that χ^2 for each run was < 12.6 at the 95% confidence level.[6]

Titration data were fitted to equilibria containing the minimum number of species required for a good fit, and any newly determined species found to be < 5% of the total cyclodextrin or amino acid concentration was considered insignificant. The stability constants for the (*R*) and (*S*) enantiomers were fitted over approximately the same mV range.

The program, SUPERQUAD, can handle a maximum of 18 specified equilibria, characterising stability constants which are either fixed or to be refined. Consequently, some predetermined species had to be omitted in order to determine the ternary species

present in some systems. Using the predetermined protonation constants and binary stability constants, the species which would be present in negligible amounts (< 1.5%) in the ternary system, if no ternary complexes formed, were determined. When necessary, such species were omitted in the fitting of the ternary system.

6.1.4 Absorbance Spectra of Metal Complexes

An aqueous solution of 0.025 mol dm^{-3} NaPIPES (Calbiochem), adjusted to pH 7.0 by the addition of NaOH, was used as a buffer in the preparation of solutions. An ionic strength of 0.10 mol dm^{-3} was maintained by the addition of $NaClO_4$. All cobalt(II) solutions were prepared in a glove box and their spectra were run under nitrogen.

All spectra were run in duplicate on a Cary 2200 spectrophotometer in 1 cm pathlength matched quartz cuvettes thermostatted at 298.2 ± 0.1 K, against reference solutions containing all components of the solution of interest except the metal salt. In the solutions containing tryptophan, metal ion and βCDtren, the major absorbing species present was $[M(\beta CDtren)Trp]^+$, and contributions from the binary metal species were small.

6.2 Linked Cyclodextrin Dimer Studies

6.2.1 Materials

βCD was a gift from Nihon Shokhuin Kako Co. Ltd. and was used without further purification. The linked cyclodextrin dimers: $(\beta CD)_2Ur$, $(\beta CD)_2Ox$, $(\beta CD)_2Ma$, $(\beta CD)_2Sc$ and $(\beta CD)_2Gl$, were prepared by methods similar to those reported in the literature[7] and were shown to be > 95% pure by microanalysis, TLC, and ^1H and ^{13}C NMR spectroscopy. The minor impurity was βCD. All cyclodextrins were dried to constant weight and stored in the dark over P_2O_5 in a vacuum desiccator.

The potassium salt of TNS^- (Molecular Probes) was used without further purification as TLC revealed only a single spot. Methyl Orange (B.D.H.) was also used without further purification. Tropaeolin 000 No.2 (B.D.H.) was purified by salting out from hot distilled water using sodium acetate, after which it was recrystallised three times from distilled water and then twice from ethanol.[8] These probes were dried to constant weight and stored in the dark over P_2O_5 in a vacuum desiccator.

Phosphate buffer (pH 7.0, I = 0.10 mol dm^{-3}) was prepared from Na_2HPO_4 (B.D.H.) and KH_2PO_4 (Ajax) as described in the literature.[9] The other buffers were prepared by adjusting solutions 0.100 mol dm^{-3} in Na_2HPO_4 and 0.200 mol dm^{-3} in K_2SO_4 (B.D.H.) to pH 9.0 and 5.5 by the addition of NaOH and H_2SO_4, respectively. Deionised water, purified with a MilliQ-Reagent system to produce water with a specific resistance of > 15 Ω cm, was used in the preparation of all solutions. Chemicals used were of analytical reagent grade and all glassware was A-grade.

6.2.2 Solution Preparation

All solutions were freshly prepared prior to measurement. For the TNS^- solutions, exposure to light was kept to a minimum by wrapping the containers in aluminium foil. All solutions were diluted by weight from stock solutions.

Solutions of TNS^- obey the Beer-Lambert law for fluorescence at concentrations of less than 10^{-5} mol dm^{-3}. As the concentration of TNS^- was increased above this value the fluorescence diminished progressively from a linear increase. The concentration of TNS^- was fixed at 1.04 x 10^{-6}, 1.00 x 10^{-6}, 1.01 x 10^{-6}, 1.01 x 10^{-6}, 1.00 x 10^{-6} and 1.01 x 10^{-6} mol dm^{-3} for the βCD, $(βCD)_2Ur$, $(βCD)_2Ox$, $(βCD)_2Ma$, $(βCD)_2Sc$ and $(βCD)_2Gl$ systems, respectively. The cyclodextrin concentrations were varied within the following ranges (mol dm^{-3}): βCD (1.50 x 10^{-6} - 5.50 x 10^{-3}), $(βCD)_2Ur$ (8.32 x 10^{-7} - 3.07 x 10^{-4}), $(βCD)_2Ox$ (3.98 x 10^{-6} - 6.03 x 10^{-4}), $(βCD)_2Ma$ (2.51 x 10^{-6} - 9.00 x 10^{-4}), $(βCD)_2Sc$ (3.00 x 10^{-6} - 1.00 x 10^{-3}), and $(βCD)_2Gl$ (3.08 x 10^{-6} - 8.95 x 10^{-4}). The number of concentrations selected from within these ranges was 46, 22, 24, 26, 29

and 27, for the βCD, $(\beta CD)_2Ur$, $(\beta CD)_2Ox$, $(\beta CD)_2Ma$, $(\beta CD)_2Sc$ and $(\beta CD)_2Gl$ systems, respectively. All solutions were prepared in aqueous phosphate buffer (pH 7.0, $I = 0.10$ mol dm^{-3}).

All methyl orange solutions were prepared in 0.100 mol dm^{-3} Na_2HPO_4 and 0.200 mol dm^{-3} K_2SO_4, adjusted to pH 9.0 using NaOH. The concentration of MO^- was fixed at 3.8 x 10^{-5} mol dm^{-3} for the studies with $(\beta CD)_2Ur$, and at 4.0 x 10^{-5} mol dm^{-3} for the $(\beta CD)_2Ox$ and $(\beta CD)_2Sc$ systems. The cyclodextrin concentrations were varied within the following ranges (mol dm^{-3}): $(\beta CD)_2Ur$ (1.81 x 10^{-6} - 2.66 x 10^{-4}), $(\beta CD)_2Ox$ (2.80 x 10^{-6} - 1.00 x 10^{-2}), and $(\beta CD)_2Sc$ (8.12 x 10^{-6} - 8.01 x 10^{-3}). The number of concentrations selected from within these ranges was 21, 28 and 28, for the $(\beta CD)_2Ur$, $(\beta CD)_2Ox$, and $(\beta CD)_2Sc$ systems, respectively.

All tropaeolin 000 No. 2 solutions were prepared in 0.100 mol dm^{-3} Na_2HPO_4 and 0.200 mol dm^{-3} K_2SO_4, adjusted to pH 5.5 using H_2SO_4. The concentration of TR^- was fixed at 4.1 x 10^{-5}, 3.7 x 10^{-5} and 4.0 x 10^{-5} mol dm^{-3} for the $(\beta CD)_2Ur$, $(\beta CD)_2Ox$ and $(\beta CD)_2Sc$ systems, respectively. The cyclodextrin concentrations were varied within the following ranges (mol dm^{-3}): $(\beta CD)_2Ur$ (3.86 x 10^{-6} - 3.73 x 10^{-4}), $(\beta CD)_2Ox$ (9.47 x 10^{-6} - 3.20 x 10^{-3}), and $(\beta CD)_2Sc$ (2.38 x 10^{-5} - 4.93 x 10^{-3}). The number of concentrations selected from within these ranges was 29, 29 and 36, for the $(\beta CD)_2Ur$, $(\beta CD)_2Ox$, and $(\beta CD)_2Sc$ systems, respectively.

6.2.3 Fluorescence Spectra

Fluorescence spectra were recorded at 0.5 nm intervals in duplicate on a Perkin Elmer LS 50B luminescence spectrometer in a quartz cuvette of pathlength 1 cm thermostatted at 298.2 ± 0.1 K. A baseline was recorded with buffer solution prior to each set of measurements. Following averaging of the duplicate runs and baseline subtraction, the spectral data was ready for treatment (Section 6.2.5).

An excitation slit width of 5 nm and an emission slit width of 10 nm were used for all systems studied, with the exception of the $(\beta CD)_2Ur$ system, for which the emission slit

width was 5 nm. In each system studied, the excitation wavelength was selected from within the longest wavelength absorption band, to reduce the possibility of reabsorption of emission. Excitation was made at the longest wavelength at which only a small change, if any, in the absorbance spectrum of TNS^- occurred upon addition of cyclodextrin. This was designed to keep the number of photons absorbed identical or very similar for TNS^- in the free and complexed states, so that comparisons could be made between their fluorescence intensities. The excitation wavelengths and emission ranges, respectively, for the systems studied were (nm): βCD (369, 385-550), $(\beta CD)_2Ur$ (354, 370-550), $(\beta CD)_2Ox$ (346, 370-550), $(\beta CD)_2Ma$ (357, 370-530), $(\beta CD)_2Sc$ (353, 370-530) and $(\beta CD)_2Gl$ (355, 370-530).

At the excitation wavelengths, the percentage variation in fluorescence of TNS^- upon addition of $(\beta CD)_2Ur$, $(\beta CD)_2Ox$, $(\beta CD)_2Ma$, $(\beta CD)_2Sc$ and $(\beta CD)_2Gl$ was 27, 7, 10, 2 and 3%, respectively, and an isosbestic point occurred at 369 nm in the βCD system. The fluorescence emission of TNS^- in the complexed form, relative to that in the free form, was determined by integrating the areas under the emission spectrum of the complex (derived using the fitted stability constant) and the emission spectrum of free TNS^-, recorded over the same wavelength range and under the same conditions. The ratio of these areas was normalised, to determine the proportion of photons emitted relative to the number absorbed, by correcting for the percentage change in absorption of TNS^- in the free and complexed forms.

The scattering or fluorescence spectra of the cyclodextrins were linearly proportional to the cyclodextrin concentration, and exhibited peaks at 420-430 nm. The fluorescence spectrum of free TNS^- was also determined. The molar fluorescence of each reactant was obtained from the slope of the fluorescence versus concentration plot.

6.2.4 Absorbance Spectra

Absorbance spectra were recorded in duplicate on a Zeiss DMR10 double-beam spectrophotometer in 1 cm pathlength matched quartz cuvettes thermostatted at 298.2 ± 0.1 K, against reference solutions containing all components of the solution of interest except the probe and the cyclodextrin. Measurements were made at 2 nm intervals over the range 350-550 nm, using an integration time of 3.2 seconds at each wavelength. Following averaging of the duplicate runs and baseline subtraction, the spectral data was ready for treatment (Section 6.2.5).

The intensity of the scattering or absorbance of free cyclodextrin was linearly proportional to the cyclodextrin concentration, and increased with a decrease in wavelength. The absorbance spectra of free MO^- and free TR^- were also determined. The molar absorbance of each reactant was obtained from the slope of the absorbance versus concentration plot. The molar absorbances of MO^- and TR^- were determined from each stock solution and weighing errors were corrected for in final spectra.

6.2.5 Data Treatment

When a single (host)·(guest) complex is present in solution, the observed absorbance is given by Eqn. 6.1, where A represents the total absorbance, ε_H, ε_G and $\varepsilon_{H\cdot G}$ represent the molar absorbances of the host, guest and (host)·(guest) complex, and [host], [guest] and [(host)·(guest)] represent the equilibrium host, guest and (host)·(guest) complex concentrations, respectively. When an additional (host)·$(guest)_2$ or $(host)_2$·(guest) complex is present, the observed absorbance is given by Eqn. 6.2 or Eqn. 6.3, respectively. Similar relationships exists for fluorescence.

$$A = \varepsilon_H[\text{host}] + \varepsilon_G[\text{guest}] + \varepsilon_{H\cdot G}[(\text{host})\cdot(\text{guest})] \quad (6.1)$$

$$A = \varepsilon_H[\text{host}] + \varepsilon_G[\text{guest}] + \varepsilon_{H\cdot G}[(\text{host})\cdot(\text{guest})] + \varepsilon_{H\cdot(G)_2}[(\text{host})\cdot(\text{guest})_2] \quad (6.2)$$

$$A = \varepsilon_H[\text{host}] + \varepsilon_G[\text{guest}] + \varepsilon_{H\cdot G}[(\text{host})\cdot(\text{guest})] + \varepsilon_{(H)_2\cdot G}[(\text{host})_2\cdot(\text{guest})] \quad (6.3)$$

Stability constants were determined from a simultaneous fit of the spectral data over a range of wavelengths to one or more of these equations (Eqns. 6.1, 6.2 and 6.3) using a non-linear least-squares regression routine which was based on Method 5 of Pitha and Jones.[10] Physical constraints, such as the fact that neither the stability constants nor the derived complex absorbance or fluorescence could be negative, were incorporated in the fitting process. The data were not weighted.

$$K_{1:1}[\text{guest}]^2 + (K_{1:1}\{[\text{host}]_0 - [\text{guest}]_0\} + 1)[\text{guest}] - [\text{guest}]_0 = 0 \quad (6.4)$$

$$K_{1:1}K_{1:2}[\text{guest}]^3 + K_{1:1}(K_{1:2}\{2[\text{host}]_0 - [\text{guest}]_0\} + 1)[\text{guest}]^2 + (K_{1:1}\{[\text{host}]_0 - [\text{guest}]_0\} + 1)[\text{guest}] - [\text{guest}]_0 = 0 \quad (6.5)$$

$$(4K_{1:1}K_{2:1} - K_{1:1}^2)[\text{guest}]^3 + (K_{1:1}K_{2:1}\{4[\text{host}]_0 - 8[\text{guest}]_0\} - K_{1:1}^2\{[\text{host}]_0 + [\text{guest}]_0\})[\text{guest}]^2 + (K_{1:1}K_{2:1}\{[\text{host}]_0^2 - 4[\text{host}]_0[\text{guest}]_0 + 4[\text{guest}]_0^2\} + K_{1:1}[\text{host}]_0 + 1)[\text{guest}] - [\text{guest}]_0 = 0 \quad (6.6)$$

The polynomials in Eqns. 6.4, 6.5 and 6.6 were derived from the mass balance relationships associated with Eqns. 6.1, 6.2 and 6.3, respectively. The initial (total) concentrations of host and guest are denoted by $[\text{host}]_0$ and $[\text{guest}]_0$, respectively, and $K_{1:1}$, $K_{2:1}$ and $K_{1:2}$ represent the stepwise stability constants for the (host)·(guest), $(\text{host})_2$·(guest) and (host)·$(\text{guest})_2$ complexes. For each successive estimate of the stability constants the physically acceptable root of the corresponding polynomial was

found using the MATLAB® "roots" function.[11] Once the equilibrium concentration of the guest was determined, the equilibrium concentrations of all species could be calculated.

The data at all monitored wavelengths where significant spectral change occurred, were used in determining the appropriate model and corresponding stability constants. The spectral data recorded in the wavelength ranges 410-520 and 400-500 nm were used in determining the stability constants for the TNS^- complexes formed with βCD and the linked cyclodextrin dimers, respectively. The wavelength ranges used in determining the stability constants for the linked cyclodextrin dimer complexes of MO^- were as follows (nm): $(\beta CD)_2Ur$ (410-440 and 464-520), $(\beta CD)_2Ox$ (404-446 and 464-520), and $(\beta CD)_2Sc$ (404-444 and 464-520). The wavelength ranges used in determining the stability constants for the linked cyclodextrin dimer complexes of TR^- were as follows (nm): $(\beta CD)_2Ur$ (450-510), $(\beta CD)_2Ox$ (440-492), and $(\beta CD)_2Sc$ (450-510). Between 780 and 10,170 data points were used in the derivation of each stability constant. All data fitting was carried out in MATLAB®[11] format using an AcerPower 466d computer. The stability constants, together with the directly determined molar absorbance or fluorescence of the reactants, were used to derive the spectra of the complexes that form.

For the spectral variation and binding curve diagrams in the text, fluorescence and absorbance measurements were corrected firstly for any spectral contribution arising from the cyclodextrin itself, and secondly for spectral fluctuations arising from slight variations in the probe concentration. The corrections used are outlined in Eqn. 6.1, where S_{corr} and S_{obs} are the corrected and observed spectral intensities, respectively.

$$S_{corr} = \frac{[\text{guest}]_{av}}{[\text{guest}]_i}(S_{obs} - \varepsilon_H[\text{host}]_i) \qquad (6.1)$$

The total concentrations of host and guest in a particular solution are represented by $[\text{host}]_i$ and $[\text{guest}]_i$, respectively, and $[\text{guest}]_{av}$ is the average total $[\text{guest}]_i$ in all the solutions used. The term ε_H is used to represent molar absorbance or molar fluorescence

of the host, which may arise at least partially from scattering. The initial, rather than the equilibrium, host concentration was used in this correction, since the equilibrium concentration is dependent on the fitted stability constant and, in most cases, the host concentration is in a significant excess.

The cyclodextrin fluorescence was most significant for $(\beta CD)_2Ox$, possibly as a result of the conjugation present in the tether. The fluorescence observed for the linked cyclodextrin dimers was greater than that observed for βCD. The cyclodextrin absorbance was most significant for $(\beta CD)_2Ur$, possibly due to greater scattering, which is characterised by an increase in intensity with a decrease in wavelength.

6.2.6 Circular Dichroism Spectra

Circular dichroism spectra were recorded on a Jasco J40-CS spectropolarimeter. One thousand samples were averaged for each data point, which were obtained at 5 nm intervals. A time constant of 0.25 sec and a sensitivity of 1 $m°cm^{-1}$ was used.

The data were obtained as millivolts, which on multiplication by a conversion factor were re-expressed as ellipticities. The relationship in Eqn. 6.7 was used to convert ellipticity, ψ (deg), into molar ellipticity, [θ] (deg dm^3 mol^{-1} cm^{-1}), where l is cuvette pathlength (cm) and c is probe concentration (6.07×10^{-5} mol dm^{-3}). The concentration of $(\beta CD)_2Sc$ used was 1.04×10^{-3} mol dm^{-3}, and all solutions were prepared in 0.100 mol dm^{-3} Na_2HPO_4 and 0.200 mol dm^{-3} K_2SO_4, adjusted to pH 5.5 using H_2SO_4.

$$[\theta] = \frac{100.\psi}{l.c} \qquad (6.7)$$

The circular dichroism spectrum of $(\beta CD)_2Sc$ alone was subtracted from the circular dichroism spectrum acquired from the $(\beta CD)_2Sc/TR^-$ mixture.

6.2.7 Quantum Yields

The quantum yield of a sample (ϕ_s) was calculated from the observed absorbance (A) at the excitation wavelength, and the area enclosed by the emission spectrum, according to Eqn. 6.8,[12,13] where *s* and *q* refer to the sample and standard respectively. The standard used was quinine sulphate ($\phi_q = 0.55$).[14,15]

$$\phi_s = \phi_q \cdot \frac{(1-10^{-Aq})}{(Area)_q} \cdot \frac{(Area)_s}{(1-10^{-As})} \qquad (6.8)$$

Standard solutions were prepared in aqueous 0.5 mol dm^{-3} H_2SO_4 using analytical reagent grade anhydrous quinine (Fluka). All TNS^- solutions were prepared in aqueous phosphate buffer (pH 7.0, $I = 0.10$ mol dm^{-3}).[9]

Absorbance measurements were made at 366 nm on a Cary 2200 spectrophotometer in 1 cm pathlength matched quartz cuvettes thermostatted at 298.2 ± 0.1 K, against reference solutions containing all components of the solution of interest except the fluorophore. Fluorophore concentrations of *ca.* 5 x 10^{-5} mol dm^{-3} were used and measurements were averaged over at least a 60 s time interval.

Fluorescence spectra were recorded at 0.5 nm intervals in duplicate on a Perkin Elmer LS 50B luminescence spectrometer in a quartz cuvette of pathlength 1 cm thermostatted at 298.2 ± 0.1 K. An excitation wavelength of 366 nm, with excitation and emission slit widths of 5 and 10 nm respectively, was used. All measurements were corrected for solvent contributions. Fluorescence spectra were recorded on a 1.05 x 10^{-7} mol dm^{-3} quinine sulphate solution, a 5.67 x 10^{-6} mol dm^{-3} in TNS^- solution, and a range of solutions containing both TNS^- and cyclodextrin, as described below. These concentrations corresponded to absorbances of < 0.03 for the TNS^- solutions and < 0.0005 for quinine sulfate solution at the 366 nm. Since all absorbances were < 0.1 at the wavelength of excitation, corrections for self-absorption, of incident and emitted light,

on the emission intensities were not made. The area under the emission spectrum between 390 and 600 nm was calculated by computerised integration.

The quantum yield when all TNS^- is present as a (cyclodextrin)·TNS^- complex, $\phi_{s\infty}$, may be calculated from Eqn. 6.9,[13] where K_1 represents the association constant for the (cyclodextrin)·TNS^- complex and $[CD]_o$ represents the total cyclodextrin concentration.

$$\frac{1}{\phi_S} = \frac{1}{K_1.\phi_{S\infty}} \cdot \frac{1}{[CD]_O} + \frac{1}{\phi_{S\infty}} \qquad (6.9)$$

Five solutions containing 5.62×10^{-5} mol dm^{-3} TNS^- and concentrations of βCD ranging from 5.11×10^{-4} to 2.48×10^{-3} mol dm^{-3}, were used for absorbance measurements, and fluorescence spectra were run on solutions which were diluted fifty-fold, in order to calculate $\phi_{S\infty}$ for the βCD·TNS^- complex. The maximum percentage of TNS^- in the $(\beta CD)_2$·TNS^- complex form over this concentration range was 0.22%, which, using the quantum yield values reported by Kondo *et al.*[13] would correspond to a 6.0% contribution to the overall fluorescence level.

Similarly five solutions containing 5.60×10^{-5} mol dm^{-3} TNS^- and concentrations of $(\beta CD)_2$Gl varying between 2.50×10^{-3} and 4.52×10^{-3} mol dm^{-3}, were used together with their fifty-fold more dilute solutions, to calculate $\phi_{S\infty}$ for the $(\beta CD)_2$Gl·TNS^- complex.

References

1. S. E. Brown, J. H. Coates, C. J. Easton, S. J. van Eyk, S. F. Lincoln, B. L. May, M. A. Stile, C. B. Whalland and M. L. Williams, *J. Chem. Soc., Chem. Commun.*, 1994, 47.

2. C. A. Haskard, C. J. Easton, B. L. May and S. F. Lincoln, *Inorg. Chem.*, 1996, in press.

3. *J. Chem. Educ.*, 1978, **55**, A355; *Chem. Eng. News*, 1983, **61**, 4; *Chem. Eng. News*, 1963, **41**, 47.

4. A. I. Vogel, *Quantitative Inorganic Analysis*, 3rd edn., Longmans, London, 1961.

5. A. E. Martell and R. J. Motekaitis, *The Determination and Use of Stability Constants*, VCH, New York, 1988.

6. P. Gans, A. Sabatini and A.Vacca, *J. Chem. Soc., Dalton Trans.*, 1985, 1195.

7. J. H. Coates, C. J. Easton, S. J. van Eyk, S. F. Lincoln, B. L. May, C. B. Whalland and M. L. Williams, *J. Chem. Soc., Perkin Trans. 1*, 1990, 2619.

8. K. Mochida, A. Kagita, Y. Matsui and Y. Date, *Bull. Chem. Soc. Jpn.*, 1973, **46**, 3703.

9. *Biochemists Handbook*, ed. C. Long, E. & F. N. Spon, London, 1961.

10. J. Pitha and R. N. Jones, *Can. J. Chem.*, 1966, **44**, 3031.

11. Copyright © 1984-92 The MathWorks, Inc., Cochituate Place, 24 Prime Park Way, Natick, Mass. 01760, U.S.A.

12. W. O. McClure and G. M. Edelman, *Biochem.*, 1966, **5**, 1908.

13. H. Kondo, H. Nakatani and K. Hiromi, *J. Biochem.*, 1976, **79**, 393.

14. R. F. Chen, *J. Res. Nat. Bur. Stand. (U.S.)*, 1972, **76A**, 593.

15. W. H. Melhuish, *J. Phys. Chem.*, 1961, **65**, 229.

APPENDIX

The structures of molecules referred to in the text are shown here:

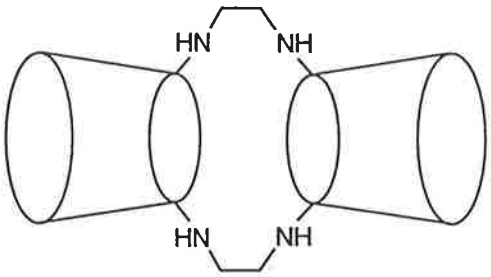

(1)

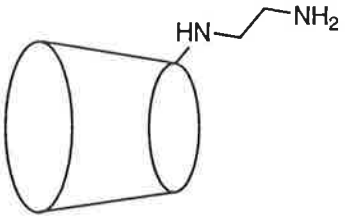

(2)

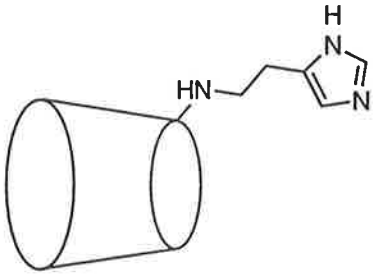

(3)

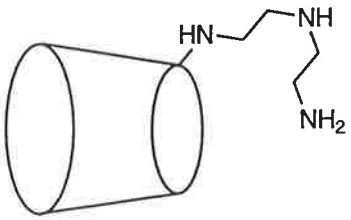

(4)

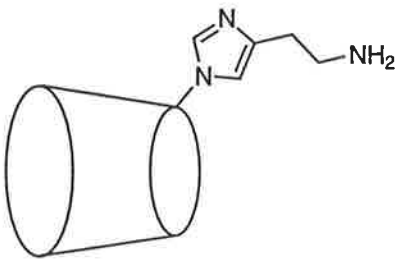

(5)

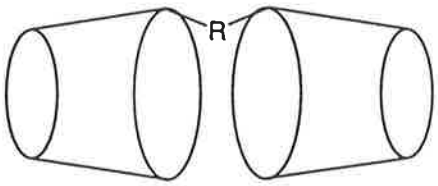

(6) R = -NHC(O)-C(O)NH-
(7) R = -NHC(O)-$(CH_2)_2$-C(O)NH-
(8) R = -NHC(O)-$(CH_2)_8$-C(O)NH-
(9) R = -OC(O)-$(CH_2)_2$-C(O)O-
(10) R = -OC(O)-$(CH_2)_3$-C(O)O-

(11) R =

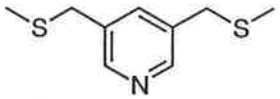

(12) R = -S-S-

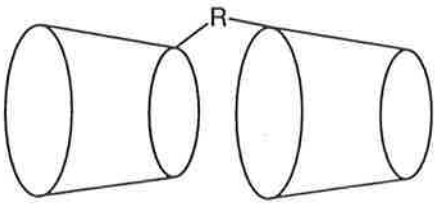

(13) R = -NHC(O)-$(CH_2)_2$-C(O)NH-

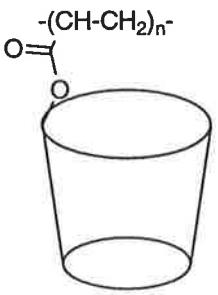

(14)

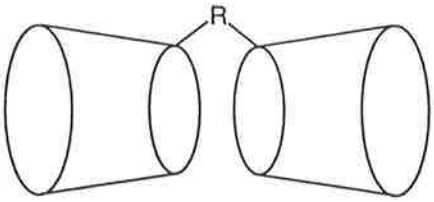

(15) R = -S-S-
(16) R = -S-$(CH_2)_2$-S-
(17) R =

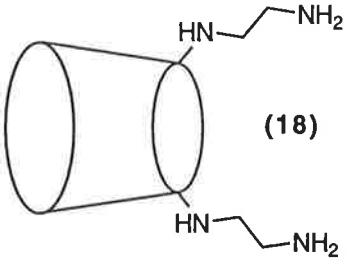

(18)

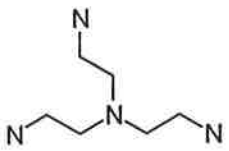

(19)

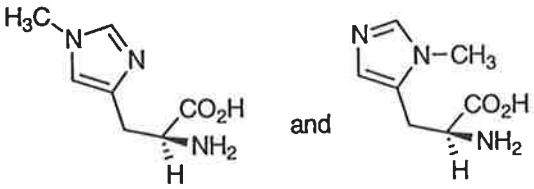

(20)

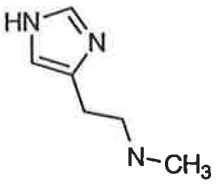

(21)

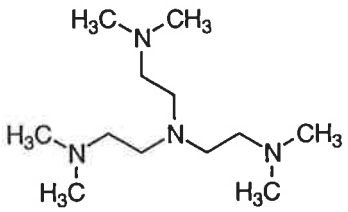

(22)

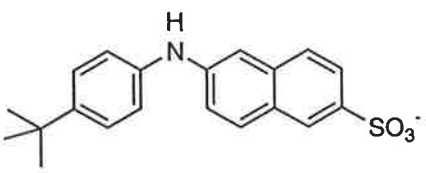

(23)

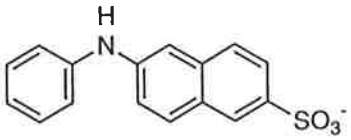

(24)

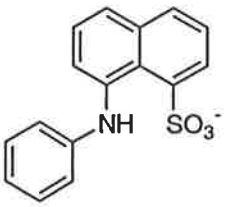

(25)

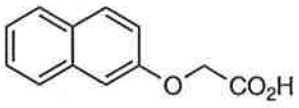

(26)

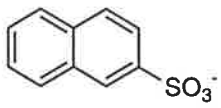

(27)

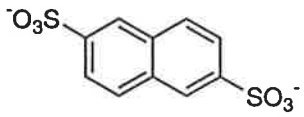

(28)

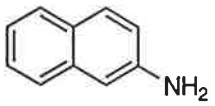

(29)

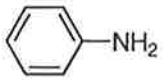

(30)

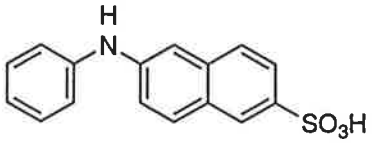

(31)

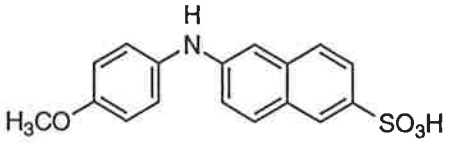

(32)

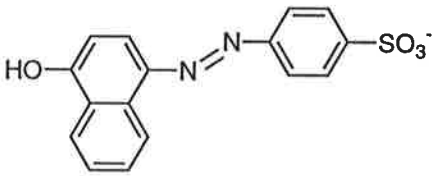

(33)

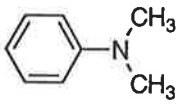

(34)

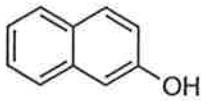

(35)

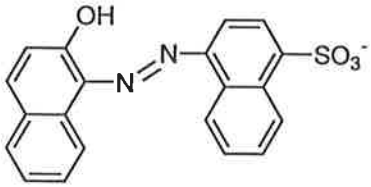

(36)

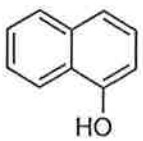

(37)

Publications

1. *"Complexation of Phenylalanine and Histidine by β-Cyclodextrin, 6^A-(3-Amino-propylamino)-6^A-deoxy-β-cyclodextrin and its Metallocyclodextrins in Aqueous Solution"*
   S. E. Brown, C. A. Haskard, C. J. Easton and S. F. Lincoln, *J. Chem. Soc. Faraday Trans.*, 1995, **91**(6), 1013.
   Reprint follows.

2. *"Formation of Metallo-6^A-(2-N,N-bis(2-aminoethyl)amino)ethylamino)-6^A-deoxy-β-cyclodextrins and their Complexation of Tryptophan in Aqueous Solution"*
   C. A. Haskard, C. J. Easton, B. L. May and S. F. Lincoln, *Inorg. Chem.*, 1996, in press.

3. *"Co-operative Binding of 6-(p-Toluidinyl)naphthalene-2-sulfonate by β-Cyclodextrin Dimers"*
   C. A. Haskard, C. J. Easton, B. L. May and S. F. Lincoln.
   Submitted for publication in *J. Phys. Chem.*

4. *"Complexation of Methyl Orange and Tropaeolin 000 No. 2 by β-Cyclodextrin Dimers"*
   C. A. Haskard, C. J. Easton, T. Kurucsev, B. L. May and S. F. Lincoln.
   In preparation.

J. CHEM. SOC. FARADAY TRANS., 1995, 91(6), 1013–1018

Complexation of Phenylalanine and Histidine by β-Cyclodextrin,† 6^A-(3-Aminopropylamino)-6^A-deoxy-β-cyclodextrin and its Metallocyclodextrins in Aqueous Solution

Susan E. Brown, Carolyn A. Haskard, Christopher J. Easton and Stephen F. Lincoln*
Department of Chemistry, University of Adelaide, South Australia 5005, Australia

A pH titration study shows that for the complexation of phenylalanine anion [(*R*)- and (*S*)-Phe$^-$] by β-cyclodextrin (βCD), $\log(K_{1R}/dm^3\ mol^{-1}) = 2.91 \pm 0.08$ and $\log(K_{1S}/dm^3\ mol^{-1}) = 2.83 \pm 0.06$, and that by 6^A-(3-aminopropylamino)-6^A-deoxy-β-cyclodextrin (βCDpn) is characterized by $\log(K_{2R}/dm^3\ mol^{-1}) = 2.51 \pm 0.07$ and $\log(K_{2S}/dm^3\ mol^{-1}) = 2.74 \pm 0.05$. No complexation of histidine (HisH) by βCD was detected, but for the complexation of histidine anion (His$^-$) by βCDpnH$^+$ $\log(K_{3R}/dm^3\ mol^{-1}) = 2.50 \pm 0.02$ and $\log(K_{3S}/dm^3\ mol^{-1}) = 2.37 \pm 0.09$; and for the complexation of HisH by βCDpnH$^+$ $\log(K_{4R}/dm^3\ mol^{-1}) = 2.31 \pm 0.05$ and $\log(K_{4S}/dm^3\ mol^{-1}) = 2.18 \pm 0.05$. For the complexation of Phe$^-$ by the metallocyclodextrin, $[M(\beta CDpn)]^{2+}$, $\log(K_{11R}/dm^3\ mol^{-1})$ and $\log(K_{11S}/dm^3\ mol^{-1}) = 3.6 \pm 0.2$ and 3.69 ± 0.06, <3.6 and 4.4 ± 0.1, 7.2 ± 0.1 and 6.9 ± 0.1, 4.7 ± 0.1 and 4.7 ± 0.2, when $M^{2+} = Co^{2+}$, Ni^{2+}, Cu^{2+} and Zn^{2+}, respectively. For the complexation of His$^-$ by $[Cu(\beta CDpn)]^{2+}$, $\log(K_{11R}/dm^3\ mol^{-1}) = 8.38 \pm 0.04$ and $\log(K_{11S}/dm^3\ mol^{-1}) = 8.42 \pm 0.02$, and for the complexation of a second His$^-$ $\log(K_{12R}/dm^3\ mol^{-1}) = 7.75 \pm 0.05$ and $\log(K_{12S}/dm^3\ mol^{-1}) = 7.6 \pm 0.1$. The roles of the cyclodextrins, divalent metal ions and amino acids affecting complexation are discussed.

Naturally occurring and modified cyclomaltaoses, or cyclodextrins, form host–guest complexes whose structures and thermodynamic stabilities vary with the nature of the cyclodextrin and the guest.[1–5] The most stable complexes are usually formed with guests possessing some aromatic character. When the guest is enantiomeric, two diastereomeric complexes form as a consequence of the single chirality of cyclodextrins and sometimes such complexation is enantioselective as a result of selective interaction of the cyclodextrin with one of the guest enantiomers,[6–11] and a similar phenomenon has been observed with metallocyclodextrins.[12–15] As part of our studies in this area, we have shown that β-cyclodextrin (βCD) and 6^A-(3-aminopropylamino)-6^A-deoxy-β-cyclodextrin (βCDpn) complex the tryptophan anion (Trp$^-$), and that βCDpn forms metallocyclodextrins, $[M(\beta CDpn)]^{2+}$, which are enantioselective for (*S*)-Trp$^-$ over (*R*)-Trp$^-$ in forming $[M(\beta CDpn)(S)\text{-Trp}]^+$ and $[M(\beta CDpn)(R)\text{-Trp}]^+$ when $M^{2+} = Co^{2+}$, Ni^{2+} and Cu^{2+}, but which exhibit no enantioselectivity when $M^{2+} = Zn^{2+}$.[14,15] Several factors affect the stability and enantioselectivity of these cyclodextrin–amino acid complexes and warrant further investigation. Accordingly, we now report a study in which the complexation of phenylalanine and histidine by βCD, βCDpn and $[M(\beta CDpn)]^{2+}$ is explored. These guests promise significant comparisons with the complexation of tryptophan because they are smaller, and phenylalanine retains the phenyl ring of tryptophan, whereas histidine possesses a five-membered polar aromatic ring which resembles that of tryptophan.

Experimental

Preparation of Materials

β-Cyclodextrin (Sigma), 6^A-(3-aminopropylamino)-6^A-deoxy-β-cyclodextrin prepared as in the literature,[14] (*R*)-, (*S*)- and

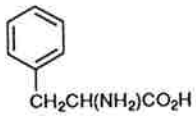

phenylalanine

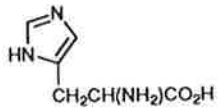

histidine

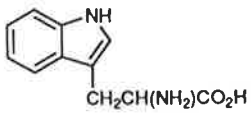

tryptophan

(*RS*)-phenylalanine† (Sigma), and (*R*)-, (*S*)- and (*RS*)-histidine† (Sigma) were dried to constant weight and stored in the dark over P_2O_5 in a vacuum desiccator prior to use. The enantiomeric purities of (*R*)- and (*S*)-PheH were determined to be ⩾99% after HPLC analysis (Pirkle covalent L-phenylglycine column) of their respective *N*-benzoyl methyl esters, and those of (*R*)- and (*S*)-HisH were determined to be ⩾99% from optical rotation determinations. Metal perchlorates (Fluka) were twice recrystallized from water, and were dried and stored over P_2O_5 under vacuum. (Caution: Anhydrous perchlorate salts are potentially powerful oxidants and should be handled with care.) Deionized water purified with a MilliQ-Reagent system to produce water with a resistivity of >15 MΩ cm, which was then boiled to remove CO_2, was used in the preparation of all solutions.

Equilibrium Studies

Titrations were carried out using a Metrohm Dosimat E665 titrimator, an Orion SA 720 potentiometer, and an Orion 8172 Ross Sureflow combination pH electrode which was

† IUPAC recommended name cyclomaltoheptaose.

† Monoprotonated phenylalanine, phenylalanine zwitterion and phenylalanine anion are denoted as $PheH_2^+$, PheH and Phe$^-$, respectively, prefixed by (*R*)- or (*S*)- as appropriate. Diprotonated histidine, monoprotonated histidine, histidine zwitterion and histidine anion are denoted as $HisH_3^{2+}$, $HisH_2^+$, HisH and His$^-$, respectively, prefixed by (*R*)- or (*S*)- as appropriate.

filled with 0.10 mol dm^{-3} $NaClO_4$. During all titrations a stream of fine nitrogen bubbles (previously passed through aqueous 0.10 mol dm^{-3} $NaClO_4$) was passed through the titration solution which was magnetically stirred and maintained at 298.2 ± 0.1 K in a water-jacketted 20 cm^3 titration vessel which was closed to the atmosphere with the exception of a small exit for nitrogen.

The 0.1 mol dm^{-3} $Ni(ClO_4)_2$, $Cu(ClO_4)_2$ and $Zn(ClO_4)_2$ stock solutions were standardized by EDTA (ethylenediaminetetraacetic acid) titration in the presence of Murexide indicator in the first two cases and Eriochrome Black T in the case of $Zn(ClO_4)_2$.[16] Ion exchange of Co^{2+} on an Amberlite HRC-120 cation-exchange column in the acid form followed by back titration of the liberated acid was used as the standardization method for the 0.100 mol dm^{-3} $Co(ClO_4)_2$ stock solution.

In all titrations, standardized 0.100 mol dm^{-3} NaOH was titrated against the species of interest in solutions of 0.010 mol dm^{-3} in $HClO_4$ and 0.090 mol dm^{-3} in $NaClO_4$. Thus the pK_a values of $PheH_2^+$ and $HisH_3^{2+}$ were determined from titrations of 10.00 cm^3 aliquots of their 0.001 and 0.002 mol dm^{-3} solutions, respectively. The stability constants for the formation of the βCD·(*R*)-Phe^- and βCD·(*S*)-Phe^- complexes, and the βCDpn·(*R*)-Phe^- and βCDpn·(*S*)-Phe^- complexes, were determined by titration of 5.00 cm^3 each of 0.001 mol dm^{-3} solutions of either (*R*)-$PheH_2^+$ or (*S*)-$PheH_2^+$ and βCD or $\beta CDpnH_2^{2+}$. Stability constants for the formation of the βCDpn complexes of histidine were similarly determined from 0.002 mol dm^{-3} $HisH_3^{2+}$ and $\beta CDpnH_2^{2+}$ solutions. The stability constants for the formation of the metal amino acid complexes were determined by titration of 10.00 cm^3 aliquots of 0.001 mol dm^{-3} solutions of $PheH_2^+$, with either 0.095 cm^3 or 0.045 cm^3 of 0.1 mol dm^{-3} $M(ClO_4)_2$, and $HisH_3^{2+}$ with 0.098 cm^3 of 0.1 mol dm^{-3} $Cu(ClO_4)_2$ solution added. The stability constants for the formation of [M(βCDpn)(*R*)-Phe]$^+$ and [M(βCDpn)(*S*)-Phe]$^+$ and related complexes were determined by titration of 5.00 mol dm^{-3} each of 0.001 mol dm^{-3} solutions of either (*R*)-$PheH_2^+$ or (*S*)-$PheH_2^+$ and $\beta CDpnH_2^{2+}$ with 0.045 cm^3 of $M(ClO_4)_2$ solution added. Stability constants for the formation of the analogous complexes of histidine were similarly determined from 0.002 mol dm^{-3} $HisH_3^{2+}$ and $\beta CDpnH_2^{2+}$ solutions with 0.098 cm^3 of $Cu(ClO_4)_2$ solution added. E_0 and pK_w values were determined by titration of 0.010 mol dm^{-3} $HClO_4$ (0.090 mol dm^{-3} in $NaClO_4$) against 0.100 mol dm^{-3} NaOH. Derivations of the stability constants were carried out using the program SUPERQUAD.[17] At least three runs were performed for each system, and at least two of these runs were averaged; the criterion for selection for this averaging being that X^2 for each run was <12.6 at the 95% confidence level.[15]

Results

In the 2.0–11.5 pH range, several complexes formed in the aqueous solutions of βCD, βCDpn, M^{2+}, phenylalanine and histidine, and their stabilities were calculated from the differences between the pH profiles arising from titration against NaOH of solutions containing different combinations of the complexing species using the program SUPERQUAD.[17] The sequence of these titrations was: (i) pK_a determinations of the amino acids followed by determination of the stability constants of complexes in solutions of (ii) either βCD or $\beta CDpnH_2^{2+}$ and either (*R*)- or (*S*)-amino acid, (iii) M^{2+} and the amino acid and (iv) M^{2+}, $\beta CDpnH_2^{2+}$ and either (*R*)- or (*S*)-amino acid. The pK_as determined in (i) together with the pK_as of $\beta CDpnH_2^{2+}$ and the stability constants for [M(βCDpn)]$^{2+}$ determined under the same conditions and reported in our earlier studies[14,15] were used as constants in the determination of stability constants in (ii)–(iv). The stability constants determined in (ii) and (iii) were employed as constants in the determination of stability constants in (iv). The titration data were fitted to equilibria containing the minimum number of species required for a good fit, and any newly determined species found to be <5% of the total cyclodextrin or amino acid concentrations were considered to be insignificant. Two such pH titration profiles are shown in Fig. 1. A plot of the major Cu^{2+} species present in the Cu^{2+}–βCDpn–(*S*)-histidine system is shown in Fig. 2. The effect of enantioselectivity on Cu^{2+} species concentration in the Cu^{2+}–βCDpn–(*R*)- or (*S*)-phenylalanine system is shown in Fig. 3. The stability constants of the major M^{2+} complexes

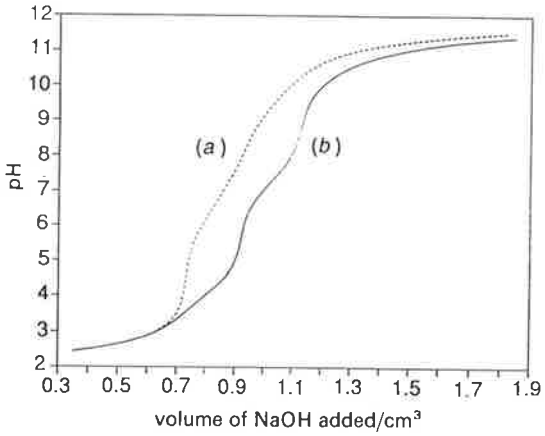

Fig. 1 Titration profiles for (*a*) $\beta CDpnH_2^{2+}$ (1.00×10^{-3} mol dm^{-3}) and (*S*)-$HisH_3^{2+}$ (1.00×10^{-3} mol dm^{-3}), and (*b*) $\beta CDpnH_2^{2+}$ (1.00×10^{-3} mol dm^{-3}), (*S*)-$HisH_3^{2+}$ (1.00×10^{-3} mol dm^{-3}) and $Cu(ClO_4)_2$ (9.98×10^{-4} mol dm^{-3}), each in aqueous 0.010 mol dm^{-3} $HClO_4$ and 0.090 mol dm^{-3} $NaClO_4$ titrated against 0.101 mol dm^{-3} NaOH at 298.2 K

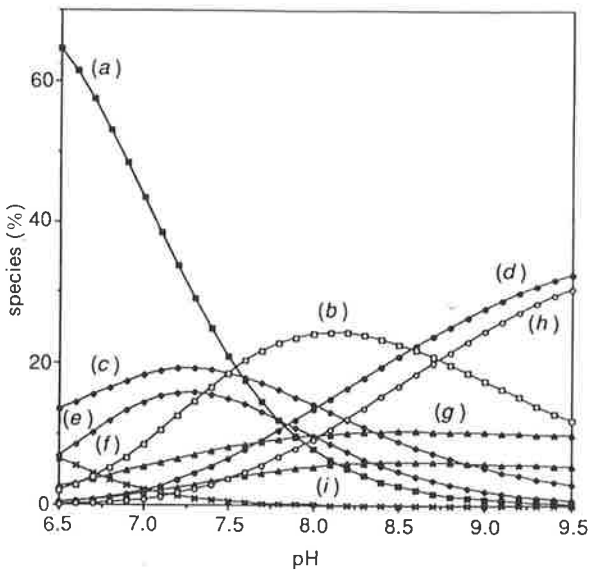

Fig. 2 Percentage of Cu^{2+} species in a solution containing 9.98×10^{-4}, 1.00×10^{-3} and 1.00×10^{-3} mol dm^{-3} total Cu^{2+}, βCDpn and (*S*)-histidine, respectively, plotted relative to $[\beta CDpn]_{total} = [(S)\text{-histidine}]_{total} = 100\%$. (*a*) [Cu{(*S*)-His}]$^+$, (*b*) [Cu(βCDpn)(*S*)-His]$^+$, (*c*) [Cu{(*S*)-His}$_2$], (*d*) [Cu(βCDpn)OH]$^+$, (*e*) [Cu(βCDpn)]$^{2+}$, (*f*) Cu^{2+}, (*g*) [Cu{(*S*)-His}OH], (*h*) [Cu(βCDpn){(*S*)-His}$_2$], (*i*) [Cu{(*S*)-His}OH]$_2$.

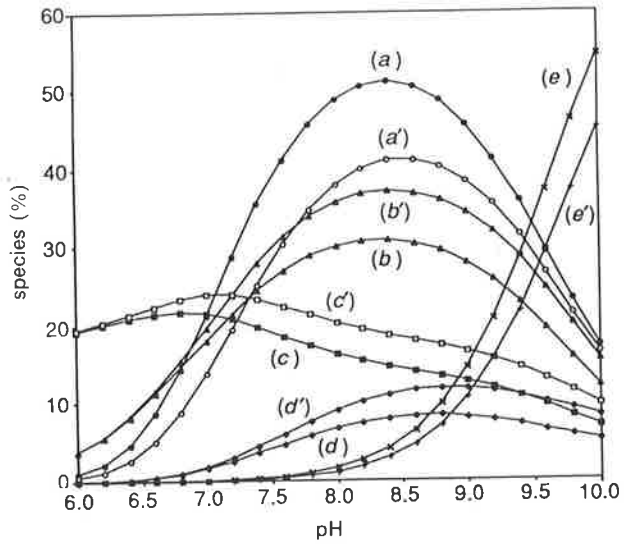

Fig. 3 Percentage of selected species in a solution of 0.000 95, 0.001 and 0.001 mol dm^{-3} total Cu^{2+}, βCDpn and either (*R*)- or (*S*)-PheH (latter indicated by prime on curve labels) concentrations, respectively, plotted relative to $[\beta CDpn]_{total}$ = either $[(R)\text{-PheH}]_{total}$ or $[(S)\text{-PheH}]_{total} = 100\%$. (*a*) $[Cu(\beta CDpn)(R)\text{-Phe}]^+$, (*a'*) $[Cu(\beta CDpn)(S)\text{-Phe}]^+$, (*b*, *b'*) $\beta CDpnH^+$, (*c*) $[Cu\{(R)\text{-Phe}\}_2]$, (*c'*) $[Cu\{(S)\text{-Phe}\}_2]$, (*d*, *d'*) $[Cu(\beta CDpn)OH]^+$, (*e*) $[Cu(\beta CDpn)\{(R)\text{-Phe}\}OH]$ and (*e'*) $[Cu(\beta CDpn)\{(S)\text{-Phe}\}OH]$.

appear in Table 1, and those for other species appear in the text.

For the acid dissociations of $PheH_2^+$, $pK_{a1} = 2.3 \pm 0.2$ and $pK_{a2} = 9.08 \pm 0.08$, and were derived from data obtained in the pH range 2.0–10.5. For $HisH_3^{2+}$, $pK_{a1} = 2.1 \pm 0.2$, $pK_{a2} = 6.04 \pm 0.05$ and $pK_{a3} = 9.07 \pm 0.02$ and were derived from data obtained in the pH range 2.5–11.5. These pK_a values are similar to those in the literature,[18] and may be compared with $pK_{a1} = 2.40 \pm 0.02$ and $pK_{a2} = 9.28 \pm 0.01$ for diprotonated tryptophan, $TrpH_2^+$.[15] For $\beta CDpnH_2^{2+}$, $pK_{a1} = 7.39 \pm 0.04$ and $pK_{a2} = 9.9 \pm 0.1$.[15]

Discussion

Cyclodextrin Equilibria

For the complexation of either (*R*)-Phe^- or (*S*)-Phe^- by βCD:

$$\beta CD + (R)\text{-Phe}^- \overset{K_{1R}}{\rightleftharpoons} \beta CD \cdot (R)\text{-Phe}^- \quad (1)$$

$$\beta CD + (S)\text{-Phe}^- \overset{K_{1S}}{\rightleftharpoons} \beta CD \cdot (S)\text{-Phe}^- \quad (2)$$

$\log(K_{1R}/dm^3\ mol^{-1}) = 2.91 \pm 0.08$ (0.1) and $\log(K_{1S}/dm^3\ mol^{-1}) = 2.83 \pm 0.06$ (0.1) were derived from data in the pH range 8.0–10.0, where the first and second errors are calculated on the basis of phenylalanine being 100 and 99% pure, respectively. These values compare with $\log(K_{1R}/dm^3\ mol^{-1}) = 2.33 \pm 0.06$ (0.2) and $\log(K_{1S}/dm^3\ mol^{-1}) = 2.33 \pm 0.08$ (0.2), for the analogous complexation of tryptophan anion (Trp^-). The phenyl moieties of Phe^- and Trp^- probably reside largely within the hydrophobic region of the βCD annulus in the βCD·Phe^- and βCD·Trp^- complexes as has been shown to be the case for a range of cyclodextrin complexes formed with other aromatic guests.[1–5] The greater stability of βCD·Phe^- by comparison with that of βCD·Trp^- may indicate that the amino acid moiety of Trp^- extends further from the annulus into the aqueous environment than does that of Phe^- such that Trp^- is more hydrated and the stability of βCD·Trp^- is lowered by comparison with that of βCD·Phe^-. No complexation of His^- by βCD was detected. It appears that although the His^- ring is flat and possesses aromatic character, the ability of both the ring and the amino acid function of His^- to hydrogen bond with water, and possibly the smaller size of the ring, engender insufficient stability in βCD·His^- for its detection in this study.

For the complexation of (*R*)-Phe^- and (*S*)-Phe^- by βCDpn:

$$\beta CDpn + (R)\text{-Phe}^- \overset{K_{2R}}{\rightleftharpoons} \beta CDpn \cdot (R)\text{-Phe}^- \quad (3)$$

$$\beta CDpn + (S)\text{-Phe}^- \overset{K_{2S}}{\rightleftharpoons} \beta CDpn \cdot (S)\text{-Phe}^- \quad (4)$$

Table 1 Stability constants $\log(K/dm^3\ mol^{-1})^a$ for metallo-6^A-(3-aminopropylamino)-6^A-deoxy-β-cyclodextrins and related complexes in aqueous solution at 298.2 K and $I = 0.10$ ($NaClO_4$)

	Co^{2+}	Ni^{2+}	Cu^{2+}	Zn^{2+}
K_5[b]	4.22 ± 0.02	5.2 ± 0.1	7.35 ± 0.04	4.96 ± 0.08
K_6[b]	2.5 ± 0.2	3.1 ± 0.1	3.09 ± 0.04	3.0 ± 0.1
			phenylalanine[c]	
K_7	4.19 ± 0.03	5.09 ± 0.05	7.8 ± 0.1	4.59 ± 0.04
K_8	3.38 ± 0.07	4.3 ± 0.1	6.9 ± 0.1	not detected
K_{11R}	3.6 ± 0.2 (0.2)	< 3.6[d]	7.2 ± 0.1 (0.1)	4.7 ± 0.1 (0.1)
K_{11S}	3.69 ± 0.06 (0.1)	4.4 ± 0.1 (0.1)	6.9 ± 0.1 (0.1)	4.7 ± 0.2 (0.2)
			tryptophan[b]	
K_7	4.41 ± 0.05	5.42 ± 0.03	8.11 ± 0.03	4.90 ± 0.04
K_8	4.01 ± 0.08	4.67 ± 0.03	7.20 ± 0.07	not detected
K_{11R}	4.04 ± 0.03 (0.1)	4.1 ± 0.2 (0.2)	7.85 ± 0.07 (0.07)	5.3 ± 0.1 (0.1)
K_{11S}	4.32 ± 0.05 (0.09)	5.1 ± 0.2 (0.2)	8.09 ± 0.05 (0.06)	5.3 ± 0.1 (0.1)
			histidine[c]	
K_7			9.95 ± 0.03	
K_8			8.27 ± 0.04	
K_{11R}			8.38 ± 0.04	
K_{11S}			8.42 ± 0.02	
K_{12R}			7.75 ± 0.05	
K_{12S}			7.6 ± 0.1	

[a] Errors quoted for *K* (mean of *N* runs) represent the standard deviation. Phenylalanine: standard deviation $\sigma = \sqrt{\{[\sum(K_i - K)^2]/(N-1)\}}$ where K_i is a value from a single run for the best fit of the variation of pH with added volume of NaOH titrant obtained through SUPERQUAD and $i = 1, 2, \ldots, N$. When a *K* derived in this way was employed as a constant in the subsequent derivation of another *K*, the error associated with the first *K* was propagated in the derivation of the second *K*. For the diastereomers, the first and second errors quoted are calculated assuming 100 and 99% enantiomeric purity of the amino acid, respectively. [b] Ref. 15. [c] This work. [d] Limit corresponding to the stability constant that would result in the formation of 5–10% of the ternary species $[Ni(\beta CDpn)(R)\text{-Phe}]^+$. This ternary species was not detected at a significant concentration and so, K_{11R} must be less than this value, allowing an upper limit to be placed on the value of K_{11R}.

$\log(K_{2R}/dm^3\ mol^{-1}) = 2.51 \pm 0.07$ (0.2) and $\log(K_{2S}/dm^3\ mol^{-1}) = 2.74 \pm 0.05$ (0.1) were derived from data in the pH range 8.5–11.5, where the errors quoted have the same significance as above. It is seen that βCDpn is slightly enantioselective in complexing (*S*)-Phe$^-$ over (*R*)-Phe$^-$. The corresponding values reported for the complexation of Trp$^-$ by βCDpn are $\log(K_{2R}/dm^3\ mol^{-1}) = 3.41 \pm 0.02$ (0.05) and $\log(K_{2S}/dm^3\ mol^{-1}) = 3.40 \pm 0.07$ (0.1).[15]

The relative stabilities of the βCD and βCDpn complexes decreased in the sequence: βCDpn·(*R*)-Trp$^-$ = βCDpn·(*S*)-Trp$^-$ > βCD·(*R*)-Phe$^-$ = βCD·(*S*)-Phe$^-$ > βCDpn·(*R*)-Phe$^-$ = βCDpn·(*S*)-Phe$^-$ > βCD·(*R*)-Trp$^-$ = βCD·(*S*)-Trp$^-$. The most probable structures for βCDpn·Trp$^-$ and βCDpn·Phe$^-$ place the phenyl group inside the cyclodextrin annulus where hydrophobic interactions occur, and the amino acid moieties in the vicinity of the 3-aminopropylamino substituent of βCDpn where hydrogen-bonding interactions occur. The ten-fold greater stability of βCDpn·Trp$^-$, relative to that of βCD·Trp$^-$, is consistent with these two interactions being additive in stabilizing βCDpn·Trp$^-$. In contrast, βCD·Phe$^-$ is more stable than βCDpn·Phe$^-$ consistent with these interactions not being additive in their contributions to the stability of βCDpn·Phe$^-$. This may be attributed to the greater length of Trp$^-$ allowing an optimization of the two interactions in βCDpn·Trp$^-$ while the shorter Phe$^-$ constrains the interactions in βCDpn·Phe$^-$ to be less favourable.

Although His$^-$ and βCDpn coexist at significant concentrations under the conditions of this study, no βCDpn·His$^-$ complex was detected in the pH range 6.9–11.1. However, βCDpnH·His and βCDpnH·HisH$^+$ were detected and their formation may be expressed through the equilibria:

$$\beta CDpnH^+ + (R)\text{-}His^- \overset{K_{3R}}{\rightleftharpoons} \beta CDpnH\cdot(R)\text{-}His \quad (5)$$

$$\beta CDpnH^+ + (S)\text{-}His^- \overset{K_{3S}}{\rightleftharpoons} \beta CDpnH\cdot(S)\text{-}His \quad (6)$$

$$\beta CDpnH^+ + (R)\text{-}HisH \overset{K_{4R}}{\rightleftharpoons} \beta CDpnH\cdot(R)\text{-}HisH^+ \quad (7)$$

$$\beta CDpnH^+ + (S)\text{-}HisH \overset{K_{4S}}{\rightleftharpoons} \beta CDpnH\cdot(S)\text{-}HisH^+ \quad (8)$$

for which $\log(K_{3R}/dm^3\ mol^{-1}) = 2.50 \pm 0.02$, $\log(K_{3S}/dm^3\ mol^{-1}) = 3.37 \pm 0.09$, $\log(K_{4R}/dm^3\ mol^{-1}) = 2.31 \pm 0.05$ and $\log(K_{4S}/dm^3\ mol^{-1} = 2.18 \pm 0.05$, where all errors are estimated assuming (*R*)- and (*S*)-histidine to be 100% enantiomerically pure. [Equilibria (5) and (6) may be alternatively expressed as between βCDpn and HisH, and equilibria (7) and (8) may be expressed as between either $\beta CDpnH_2^{2+}$ and His$^-$ or βCDpn and $HisH_2^+$.] As $pK_{a2} = 9.9$ for $\beta CDpnH^+$ and $pK_{a3} = 9.07$ for HisH in the free states, it is probable that the aminopropylamino substituent of βCDpn is protonated in both βCDpnH·His and βCDpnH·HisH$^+$. The greater stability of βCDpnH·His over that of βCDpn·His$^-$ may arise from the positive charge on $\beta CDpnH^+$ producing a greater dipole moment (by comparison with that of βCDpn) and providing an increased electrostatic interaction with His$^-$, and the neutralization of charge in the complex decreasing hydration, such that their combined effects stabilize the complex. The stabilization of βCDpnH·HisH$^+$ is less readily rationalized. Complexes analogous to those in equilibria (5)–(8) were not detected in the phenylalanine and tryptophan systems, a difference in behaviour which appears to be at least partially associated with the absence of a phenyl ring in histidine as demonstrated by the βCD complexations discussed above.

Complexation of βCDpn and Amino Acid Ligands by Divalent Metal Ions

The formation of the metallocyclodextrin $[M(\beta CDpn)]^{2+}$:

$$M^{2+} + \beta CDpn \overset{K_5}{\rightleftharpoons} [M(\beta CDpn)]^{2+} \quad (9)$$

has been previously studied,[14,15] and the variation of the magnitude of K_5 in the sequence $Co^{2+} < Ni^{2+} < Cu^{2+} > Zn^{2+}$ (Table 1) is as anticipated from the Irving–Williams series.[19] The formation of $[M(\beta CDpnH)]^{3+}$:

$$M^{2+} + \beta CDpnH^+ \overset{K_6}{\rightleftharpoons} [M(\beta CDpnH)]^{3+} \quad (10)$$

is less favoured (Table 1) as anticipated from the charged and monodentate nature of $\beta CDpnH^+$. The pK_a of $[M(\beta CDpnH)]^{3+}$ is 8.3 ± 0.1, 7.83 ± 0.02, 5.74 ± 0.05 and 8.1 ± 0.1, when $M^{2+} = Co^{2+}$, Ni^{2+}, Cu^{2+} and Zn^{2+}, respectively. These values probably characterize the deprotonation of the monoprotonated aminopropylamino substituents of $\beta CDpnH^+$ in the metallocyclodextrins. A further deprotonation of $[M(\beta CDpn)]^{2+}$ to produce $[M(\beta CDpn)OH]^+$ has been reported for $M^{2+} = Ni^{2+}$ and Cu^{2+} for which $pK_a = 9.20 \pm 0.04$ and 7.84 ± 0.03, respectively.

The formation of $[M(Phe)]^+$ and $[M(Phe)_2]$ also occurs:

$$M^{2+} + Phe^- \overset{K_7}{\rightleftharpoons} [M(Phe)]^+ \quad (11)$$

$$[M(Phe)]^+ + Phe^- \overset{K_8}{\rightleftharpoons} [M(Phe)_2] \quad (12)$$

The stability constants determined in this study (Table 1) are in reasonable agreement with those in the literature,[18] and also exhibit variations anticipated from the Irving–Williams series.[19] A pK_a of 7.46 ± 0.05 was determined for $[Cu(Phe)]^+$ which probably corresponds to the deprotonation of water bound to the metal centre. Similar deprotonations were not reliably detected for the Co^{2+}, Ni^{2+} and Zn^{2+} analogues, because the precipitation of a metal hydroxide species above pH = 8.5, 9.0 and 7.5, respectively, interfered with the titrations. The stability constants K_7 and K_8 were derived from data obtained in the pH ranges 6.5–8.5, 5.5–8.0, 4.0–7.0 and 5.5–7.5 when $M^{2+} = Co^{2+}$, Ni^{2+}, Cu^{2+} and Zn^{2+}, respectively. The analogous formation of $[Cu(His)]^+$ and $[Cu(His)_2]$ is characterized by K_7 and K_8 given in Table 1, and the greater magnitude of K_7 may indicate a different mode of binding of His$^-$ to Cu^{2+} by comparison with that occurring with Phe$^-$ and Trp$^-$. The latter two ligands probably coordinate as a five-membered chelate ring through a carboxylate oxygen and the amine nitrogen. While this may also occur with His$^-$, the alternative coordination as a six-membered chelate ring through the imidazole nitrogen and the amine nitrogen of His$^-$ is more likely.[20] In all three systems $K_7 > K_8$ as anticipated for sequential binding of ligands.

In addition, $[Cu(HisH)]^{2+}$ and $[Cu(HisH)_2]^{2+}$ are formed:

$$Cu^{2+} + HisH \overset{K_9}{\rightleftharpoons} [Cu(HisH)]^{2+} \quad (13)$$

$$[Cu(HisH)]^{2+} + HisH \overset{K_{10}}{\rightleftharpoons} [Cu(HisH)_2]^{2+} \quad (14)$$

for which $\log(K_9/dm^3\ mol^{-1}) = 4.78 \pm 0.04$ and $\log(K_{10}/dm^3\ mol^{-1}) = 4.88 \pm 0.04$, respectively, determined in the pH range 3.5–8.0. The relationship $K_9 < K_{10}$ suggests that the coordination geometry of Cu^{2+} may have changed from a six-coordinated tetragonally distorted stereochemistry in $[Cu(HisH)]^{2+}$ to either a four-coordinate square planar or a tetrahedral stereochemistry in $[Cu(HisH)_2]^{2+}$. The smaller values of K_9 and K_{10} for complexation of HisH by compari-

son with K_7 and K_8, respectively, for complexation of His^- probably reflect the lesser electrostatic interaction between the metal centre and the uncharged HisH. {The proton dissociation of $(Cu(His)H_20]^+$ ($pK_a = 7.92 \pm 0.08$) yields [Cu(His)OH] and the dimerization of this species yields $[Cu(His)OH]_2$ for which log $K_{dim} = 3.8 \pm 0.1$. A minor species, $[Cu(HisH)(His)]^+$ for which log $K = 9.90 \pm 0.03$, also appeared to be formed by the addition of His^- to $[Cu(HisH)]^{2+}$, but it did not exceed 5% of the total species concentration and is not shown in Fig. 2.}

Complexation of (*R*)- and (*S*)-Phe^- and His^- Anions by Divalent Metallocyclodextrins of βCDpn

The stability constants for the complexations shown in equilibria (15) and (16), derived from data obtained in the pH ranges 7.5–8.5, 7.5–9.5, 6.0–10.0 and 6.5–7.5 when $M^{2+} = Co^{2+}$, Ni^{2+}, Cu^{2+} and Zn^{2+}, respectively, show that the complexes formed by $[Cu(\beta CDpn)]^{2+}$ are the most stable. However, $[Ni(\beta CDpn)]^{2+}$ is the most enantioselective complex showing a greater than six-fold enantioselectivity for (*S*)-Phe^- (Table 1) while its Cu^{2+} analogue is less enantioselective. It is also the case that $[Ni(\beta CDpn)]^{2+}$ is the most enantioselective metallocyclodextrin for (*S*)-Trp^-.[14,15] The Co^{2+} and Cu^{2+} analogues show a significant, but lesser, enantioselectivity for (*S*)-Trp^-.

$$[M(\beta CDpn)]^{2+} + (R)\text{-}Phe^- \overset{K_{11R}}{\rightleftharpoons} [M(\beta CDpn)(R)\text{-}Phe]^+ \quad (15)$$

$$[M(\beta CDpn)]^{2+} + (S)\text{-}Phe^- \overset{K_{11S}}{\rightleftharpoons} [M(\beta CDpn)(S)\text{-}Phe]^+ \quad (16)$$

The higher stabilities of $[M(\beta CDpn)(R)\text{-}Phe]^+$ and $[M(\beta CDpn)(S)\text{-}Phe]^+$ (K_{11R} and K_{11S}) by comparison with those of $\beta CDpn \cdot (R)\text{-}Phe^-$ and $\beta CDpn \cdot (S)\text{-}Phe^-$ (K_{2R} and K_{2S}), demonstrate that coordination to M^{2+} strengthens the complexation of Phe^-. Nevertheless, the lower stabilities of $[M(\beta CDpn)(R)\text{-}Phe]^+$ and $[M(\beta CDpn)(S)\text{-}Phe]^+$ by comparison with those of $[M(Phe)]^+$ (K_7) when $M^{2+} = Co^{2+}$, Ni^{2+} and Cu^{2+}, indicate that the factors stabilizing complexation of (*R*)-Phe^- and (*S*)-Phe^- by βCDpn and M^{2+} in $[M(\beta CDpn)(R)\text{-}Phe]^+$ and $[M(\beta CDpn)(S)\text{-}Phe]^+$ do not reinforce each other. A similar situation prevails in the analogous tryptophan systems.[14,15] In contrast, $[Zn(\beta CDpn)(R)\text{-}Phe]^+$, $[Zn(\beta CDpn)(S)\text{-}Phe]^+$ and $[Zn(Phe)]^+$ are of similar stability, and $[Zn(\beta CDpn)(R)\text{-}Trp]^+$ and $[Zn(\beta CDpn)(S)\text{-}Trp]^+$ are more stable than $[Zn(Trp)]^+$ which indicates that Zn^{2+} is more able to accommodate the complex stabilizing effects of βCDpn in the diastereomers.

The influence of M^{2+} and βCDpn on the stabilities of $[M(\beta CDpn)(R)\text{-}Phe]^+$ and $[M(\beta CDpn)(S)\text{-}Phe]^+$ may be rationalized through the structure shown in Fig. 4. The phenyl moiety of Phe^- is inside the cyclodextrin annulus with the Phe^- chiral centre in the vicinity of the primary hydroxy groups of the cyclodextrin, and the Phe^- amine and carboxylate groups coordinated to M^{2+}. The variation of stability with the nature of M^{2+} coincides with the variation of the ionic radii of six-coordinate Co^{2+}, Ni^{2+}, Cu^{2+} and Zn^{2+}, which are 0.745, 0.69, 0.73 and 0.74 Å,[21] respectively, the geometric constraints arising from ligand-field effects in Co^{2+}, Ni^{2+} and Cu^{2+}, and the lack of such constraints arising from d^{10} Zn^{2+}.[22] While $[Ni(\beta CDpn)(R)\text{-}Phe]^+$ and $[Ni(\beta CDpn)(S)\text{-}Phe]^+$ differ substantially in stability, the analogous diastereomers for the other three metals are of similar stability. Evidently the size of Ni^{2+} and its octahedral stereochemistry are particularly appropriate in engendering

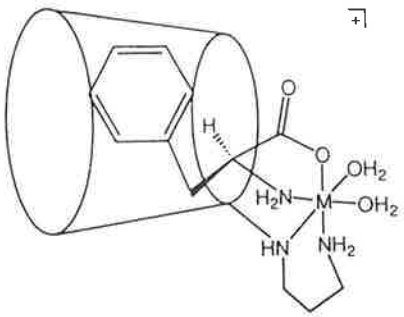

Fig. 4 Structure proposed for $[M(\beta CDpn)(S)\text{-}Phe]^+$. The cyclodextrin annulus is shown as a truncated cone with the narrow and wide ends representing the circles delineated by primary and secondary hydroxy groups, respectively. The two aqua ligands may either occupy the *cis* positions shown, or the aqua ligand *trans* to the secondary amine group of the 3-aminopropylamino substituent may be interchanged with that of the Phe^- carboxylate oxygen.

enantioselectivity for (*S*)-Phe^- over (*R*)-Phe^- and for (*S*)-Trp^- over (*R*)-Trp^- resulting from the interaction of their chiral centres with βCDpn in the metallocyclodextrin. The smaller enantioselectivity observed in the more stable $[Cu(\beta CDpn)(R)\text{-}Phe]^+$ and $[Cu(\beta CDpn)(S)\text{-}Phe]^+$ demonstrates that increasing complex stability does not necessarily induce a corresponding increase in enantioselectivity. The pK_as of 9.56 ± 0.04 (0.05) and 9.6 ± 0.1 (0.2) for deprotonation of $[Cu(\beta CDpn)(R)\text{-}Phe]^+$ and $[Cu(\beta CDpn)(S)\text{-}Phe]^+$, respectively, probably characterize the deprotonation of coordinated water. These reactions were not detected with $M^{2+} = Co^{2+}$, Ni^{2+} and Zn^{2+}.

Studies were limited to complexation of histidine by $[Cu(\beta CDpn)]^+$ because the three titratable protons of $HisH_3^{2+}$ (see Results) generate more protonic and complexation equilibria which result in more minor species than is the case with tryptophan and phenylalanine, and it was considered that the higher metal complex stabilities associated with Cu^{2+} presented the best opportunity for their detection. The K_{11R} and K_{11S}, derived from data in the pH range 6.5–9.5, for the complexation of His^- to form $[Cu(\beta CDpn)(R)\text{-}His]^+$ and $[Cu(\beta CDpn)(S)\text{-}His]^+$ in equilibria analogous to equilibria (15) and (16) are greater than those for the Phe^- and Trp^- complexes (Table 1). This is attributable to bidentate Phe^- and Trp^- coordinating through their carboxylate and amine groups, while bidentate His^- coordinates through a ring nitrogen and an amine group. A second His^- coordinates to form $[Cu(\beta CDpn)\{(R)\text{-}His\}_2]$ and $[Cu(\beta CDpn)\{(S)\text{-}His\}_2]$ (characterized by K_{12R} and K_{12S} in Table 1), but the formation of complexes with analogous stoichiometry was not observed for Phe^- and Trp^-. This probably reflects the smaller size of His^-, its different coordination mode and its weaker interaction with the βCDpn annulus, all of which should favour the coordination of a second His^- over either a second Phe^- or Trp^-.

We gratefully acknowledge the award of Australian Postgraduate Priority Research Awards to S.E.B. and C.A.H. and funding of this research by the University of Adelaide and the Australian Research Council.

References

1 R. J. Clarke, J. H. Coates and S. F. Lincoln, *Adv. Carbohydr. Chem. Biochem.*, 1989, **46**, 205.
2 J. Szejtli, *Cyclodextrin Technology*, Kluwer, Dordrecht, 1988.
3 M. L. Bender and M. Komiyama, *Cyclodextrin Chemistry*, Springer, New York, 1977.
4 W. Saenger, *Inclusion Compounds*, 1984, **2**, 231.

5 K. Harata, *Inclusion Compounds*, 1991, **5**, 311.
6 N. J. Smith, T. M. Spotswood and S. F. Lincoln, *Carbohydr. Res.*, 1989, **192**, 9.
7 S. E. Brown, J. H. Coates, S. F. Lincoln, D. R. Coghlan and C. J. Easton, *J. Chem. Soc., Faraday Trans.*, 1991, **87**, 2699.
8 S. E. Brown, J. H. Coates, P. A. Duckworth, S. F. Lincoln, C. J. Easton and B. L. May, *J. Chem. Soc., Faraday Trans.*, 1993, **89**, 1035.
9 I. Tabushi, Y. Kuroda and T. Mizutani, *J. Am. Chem. Soc.*, 1986, **108**, 4514.
10 I. Tabushi, Y. Kuroda, M. Yamada and T. Sera, *J. Inclusion Phenom. Mol. Recognit. Chem.*, 1988, **6**, 599.
11 D. Greatbanks and R. Pickford, *Mag. Reson. Chem.*, 1987, **25**, 208.
12 G. Impellizzeri, G. Maccarrone, E. Rizzarelli, G. Vecchio, R. Corradini and R. Marchelli, *Angew. Chem., Int. Ed. Engl.*, 1991, **30**, 1348.
13 V. Cucinotta, F. D'Alessandro, G. Impellizzeri, G. Maccarrone and G. Vecchio, *J. Chem. Soc., Chem. Commun.*, 1992, 1743.
14 S. E. Brown, J. H. Coates, C. J. Easton, S. J. van Eyk, S. F. Lincoln, B. L. May, M. A. Stile, C. B. Whalland and M. L. Williams, *J. Chem. Soc., Chem. Commun.*, 1994, 47.
15 S. E. Brown, J. H. Coates, C. J. Easton and S. F. Lincoln, *J. Chem. Soc., Faraday Trans.*, 1994, **90**, 739.
16 A. I. Vogel, *Quantitative Inorganic Analysis*, Longmans, London, 3rd edn., 1961.
17 P. Gans, A. Sabatini and A. Vacca, *J. Chem. Soc., Dalton Trans.*, 1985, 1195.
18 *Critical Stability Constants*, ed., R. M. Smith and A. E. Martell, Plenum Press, New York, 1975, vol. 1.
19 H. Irving and R. J. P. Williams, *J. Chem. Soc.*, 1953, 3192.
20 H. Kozlowski, A. Anouar, T. Kowalik-Jankowska, P. Decock, J. Swiatek-Kozlowska and L. D. Pettit, *Inorg. Chim. Acta*, 1993, **207**, 223.
21 R. D. Shannon, *Acta Crystallogr., Sect. A, Cryst. Phys. Diffr. Theor. Gen. Crystallogr.*, 1976, **32**, 751.
22 A. Cotton and G. Wilkinson, *Advanced Inorganic Chemistry*, New York, 4th edn., 1980.

Paper 4/06240J; *Received* 12*th October* 1994

CORRIGENDUM

Corrigendum to Complexation of Phenylalanine and Histidine by β-Cyclodextrin, 6^A-(3-Aminopropylamino)-6^A-deoxy-β-cyclodextrin and its Metallocyclodextrins in Aqueous Solution

Susan E. Brown, Carolyn A. Haskard, Christopher J. Easton and Stephen F. Lincoln, *Department of Chemistry, University of Adelaide, South Australia 5005, Australia*

J. Chem. Soc., Faraday Trans., 1995, **91**, 1013.

In the third paragraph of page 1016,

$$\log (K_{3S}/\mathrm{dm^3\ mol^{-1}}) = 2.37 \pm 0.09$$

and not 3.37 ± 0.09 as written.